Regulation of Stress-Induced Longevity

by

Hillary A. Miller

A dissertation in partial fulfillment
of the requirements for the degree of
Doctor of Philosophy
(Cellular and Molecular Biology)
in The University of Michigan
2021

Doctoral Committee:

Assistant Professor Scott F. Leiser, Chair
Professor Ursula H. Jakob
Associate Professor Ryan Mills
Professor Scott D. Pletcher

Hillary A. Miller

millhill@umich.edu

ORCID iD: 0000-0002-8204-7990

DEDICATION

To my mother,
my cheerleader and
truest inspiration
to strive and do
something worthwhile.

ACKNOWLEDGEMENTS

Before all else, I need to thank my mentor, Dr. Scott Leiser, for his never-ending support and infectious optimism. I am certain I would not be who I am today without his guidance. And while I am certain most acknowledgment sections start with such a claim, know it is undeniably true. Dr. Leiser has played an integral role in my life for over a decade. We met when I was an excited, naïve undergraduate with little scientific training back in 2010. I began my secondary education pursing a degree in English to become a writer. Everything changed after I took an introductory biology class to fulfill graduation requirements, and a colleague of his presented on their research. They wished to identify the molecular and genetic mechanisms of aging, something I had never realized people could study or understand. I was hooked. I knew from that day on I wanted to be a scientist solving one of life's biggest mysteries.

Despite my lack of knowledge, Dr. Leiser took on the great task of teaching me everything he knew about biogerontology and how to perform experiments. Moreover, he didn't consider his undergraduate students as simply an extra pair of hands to perform experiments for him. He required all those he mentored as a post-doc to present their work at symposiums, volunteer, and, when possible, teach. With his help and support, Dr. Matt Kaeberlein employed me as a technician for two years before applying to PhD programs. These additional years not only allowed me the necessary time to mature in my scientific knowledge, but I also was able to witness Dr. Leiser apply (and re-apply) for K awards and junior faculty positions. Because of his openness, I know better than most trainees the arduous process involved in succeeding in academic science. There were times I believed myself not the ideal candidate, but Dr.

Leiser continuously reminded me I have the two things it takes to succeed at anything: desire and drive. I have learned over the years Dr. Leiser has the great ability to motivate those with a willingness to persevere, and that he meant it when he said his trainees' successes remain his proudest achievement. I can't thank him enough for all his past and future guidance.

As you'd expect, a mentor like Dr. Leiser attracts truly exceptional people. Over the past five years I've been surrounded by incredible scientists that have made the losses more bearable and the successes more enjoyable. More days than not, I woke up excited to get into lab because of its familial atmosphere. In lab I was surrounded by friends who all loved what they were doing. I enjoyed working with them all so much, it's become difficult to imagine myself working anywhere else.

Special thanks to my collaborator Dr. Shijiao Huang who acted as both a mentor and friend throughout most of my time at Michigan. I feel quite lucky I got to work so closely with such an extraordinary scientist. Additionally, I can't say enough nice things about Dr. Safa Beydoun. I owe her an avalanche of thank yous for always being willing to drop whatever she was doing to help me out of a tight spot or be a listening ear. But that's not all! I'd be remiss not to thank Dr. Ajay Bhat for his scientific acumen and joyful presence in lab. Similarly, thank you so much Dr. Rebecca Cox for your insightful edits and being a great conversation buddy. You all have made the experience of writing my thesis and graduating a bitter-sweet experience.

The Leiser lab graduate students who came after me deserve a paragraph all to themselves. What a fun bunch of people to spend lots of time with. Hyo Sub Choi the grey man. Marshall Howington the lab lodestone. Megan Schaller the dynamic dynamo. Elizabeth Dean the green thumbed hacker. Angela Tuckowski the joke-spitting runner. Thank you all for so much more than what can be conveyed here. I've made five life-long friends, and I will cherish all the memories we made while on this journey. I can't wait to see all the great things you accomplish!

I also wish to extend many thanks to my thesis committee members for their input, guidance, and patience. I chose Drs. Ursula Jakob, Ryan Mills, and Scott Pletcher because I wanted to be like them, both as scientists and people, each possessing incredible skillsets I hoped to one day learn and emulate. And while I am still a work-in-progress, I think with their help, I've made great strides towards those goals.

I need to extend my gratitude towards CMB, the Bioinformatics Department, and the Biogerontology group for providing great environments to continue my education surrounded by encouraging and gifted scientists. And special thank yous to the CMB administrative staff, Margarita Bekiares, Pat Ocelnik and Lauren Perl, for answering so many questions about navigating the non-science aspects of being a graduate student.

Outside of the lab, I need to thank my amazing support system of friends I made before and during my time at Michigan. In particular, Amanda Wilber, as one of my oldest friends, I missed you greatly when we moved. It means so much that you've come out to visit me during my time here. Moreover, our walk and talks were a *necessity* this past year. Charlie and Ryan Brink, for the great meals, boardgames and trips to the dog park. I'm so glad we all decided to attend that Meetup! Silvia Dykstra, Jason Cardarelli, Abby, John, and Eva Beals, for the commiseration, runs, and laughs. You all are a perfect example of the amazing people you can meet in Ann Arbor if you're willing to talk to your neighbors. Sadie Marlow, for the being my greatest friend to navigate the trials and tribulations of grad school. I'll never forget meeting you on our first day of orientation.

Finally, I'd like to extend my deepest gratitude to my wonderful family. My mother, Ronda Church, is one of the best people you'd have the pleasure of knowing. I know I'm biased, but you couldn't ask for a better mom. While caring and supportive, she also taught me the power of hard work. Not through lectures, but through her actions. She is the hardest worker I know. She gives 100% into anything she pursues. If I hadn't had such a strong role-model throughout my childhood, I doubt I would have been able to conquer my fears of failure. Thank you for being my greatest advocate through it all!

And I would like to thank my grandfather, Ronald Hutchinson, and step-father, Don Church, for the years I had with them. I miss them both something awful, but I am grateful for the memories and the lessons they taught me.

And, most importantly, thank you to my husband, Steven Warrington Jr, for being here for me through it all. Grad school has been a challenging time, but instead of breaking under the pressure, we've only grown stronger. I have been reflecting on our last six years together and how each year was better than the last. Thank you so much for giving me the emotional support, space, and opportunity to figure out how to balance life's responsibilities. Thank you for convincing me we should adopt Happy. You've taught me that getting older isn't so bad when you're doing it alongside your best friend.

I am forever grateful for you all. I will be giving out a lifetime of thank yous as no amount is sufficient. I hope you get something out of reading my thesis. It was an ultramarathon, but we're closing in on the finish line.

PREFACE

"I tend to live forever, or die trying" – Groucho Marx

This quote holds a special place in my heart as an oddly prescient look into how I'd spend the next decade of my life. Back in 2008 I chose it cavalierly as my senior quote without realizing it would become my credo.

After high school I was unsure of the future, so I stayed at home in Spokane while working towards my associates degree. I wanted to discover that something I could get up and be excited about every day. I knew I enjoyed writing, so I tentatively planned to pursue a degree in English. Like many women, I got the message from my family and community that I should go into a more "nurturing" field, but I just could not shake drive to explore and discover. Fortuitously, my local community college would not let me leave with an Associate's degree until I took a smattering of science courses. I begrudgingly signed up for an introductory biology course, and was struck by how much I enjoyed it. The innovative nature of scientific discovery amazed me and left me with the realization that academic science could provide me with the life of problem solving and intrigue I had been searching for. When I transferred to the University of Washington (UW) I knew I would pursue a career in the biological sciences even though I am the first in my family to pursue a STEM career. At UW I earned a Bachelor of Science degree in Molecular, Cellular and Developmental Biology and the ability to tackle scientific mysteries in the lab. But more importantly, I found inspiration. I wanted to be like my professors. I wanted to feel that enthusiasm I saw in them every time they spoke about their research.

There are hundreds of independent investigators affiliated with UW. How could I choose the right one? Each lab I researched sounded more fascinating than the last. I planned to meet with my favorite professors and fellow students to solicit their opinions, but before I could, the answer appeared in front of me. A postdoctoral fellow from the Kaeberlein lab, Dr. Lara Shamieh, presented a guest lecture to my class on “the mechanism of aging.” I still remember her talk clearly. She performed a forward genetic screen using *C. elegans* to discover genes necessary for longevity induced by dietary restriction (DR). She then isolated homozygous mutants which were longer- and shorter-lived under DR conditions, and went on to characterize the most interesting mutants. I appreciated the simple experimental design to examine a complex, multifaceted subject like aging. I emailed her later that day eager to learn more about aging research and possible openings in the lab. And so begins the saga of my transformation into a proficient, academically trained scientist!

TABLE OF CONTENTS

LIST OF TABLES

LIST OF FIGURES

ABSTRACT

Rapid advances in aging research have identified several stressful stimuli (e.g. food/oxygen availability, temperature) that can enhance health and longevity across taxa. Many of these longevity pathways act through cell non-autonomous signaling mechanisms. These pathways utilize sensory cells, frequently neurons, to signal to peripheral tissues and promote survival during the presence of external stress. Importantly, this neuronal activation of stress response pathways is often sufficient to improve health and longevity in the absence of stress.

Multiple studies, including our own, implicate serotonin (5-HT) as a signal within several longevity pathways. 5-HT is one of the best studied neuromodulators with numerous drugs targeting its actions, yet our understanding of the complex actions of 5-HT signaling is still incomplete. 5-HT is released upon food perception, therefore we posited that a decrease in 5-HT release during dietary restriction (DR) may also result in downstream signaling changes. This hypothesis is bolstered by data showing that the perception of food is sufficient to abrogate DR-mediated longevity. Using an intestinal reporter for a key gene induced by DR but suppressed by attractive smells, we identify three compounds that block food perception, thereby increasing longevity as DR mimetics. These compounds clearly implicate serotonin and dopamine in limiting lifespan in response to food perception.

We further identify an enteric neuron in this pathway that signals through the serotonin receptor 5-HT1A/*ser-4* and dopamine receptor DRD2/*dop-3*, and critically, aspects of this pathway are conserved in the vinegar fly *D. melanogaster* and in mammalian cells. These studies present compelling evidence that reward circuitry is tied to the perception

of food across taxa and may be a viable area of research to discover pro-longevity treatments

Similar to our food availability experiments, we find temperature can modulate longevity interventions outside the laws of thermodynamics. Our data suggest that genetics play a major role in temperature-associated longevity and are consistent with the hypothesis that while aging in *C. elegans* is slowed by decreasing temperature, the major cause(s) of death may also be modified, leading to different genes and pathways becoming more or less important at different temperatures. These data shed light on the complex interplay of stress response signaling and suggest some act in a temperature-dependent manner.

Collectively, the findings in this thesis enhance our understanding of conserved signaling pathways that modify aging while advancing the fields long-term goal to develop therapeutics that increase human health/lifespan.

CHAPTER 1

Cell Non-Autonomous Regulation of Health and Longevity[1]

Abstract

As the demographics of the modern world skew older, understanding and mitigating the effects of aging is increasingly important within biomedical research. Recent studies in model organisms demonstrate that the aging process is frequently modified by an organism's ability to perceive and respond to changes in its environment. Many well-studied pathways that influence aging involve sensory cells, frequently neurons, that signal to peripheral tissues and promote survival during the presence of stress. Importantly, this activation of stress response pathways is often sufficient to improve health and longevity even in the absence of stress. Here we review the current landscape of research highlighting the importance of cell non-autonomous signaling in modulating aging from C. elegans to mammals. We also discuss emerging concepts including retrograde signaling, approaches to mapping these networks, and development of potential therapeutics.

Introduction

It is estimated that by 2050 the number of US citizens over the age of 65 will reach nearly 100 million, more than twice as many as today (1). If this increase occurs without significant fiscal and structural changes, the cost of this aged population could cripple economies across the world. Therefore, deciphering and mitigating the aging process to create a healthier older population has become an increasingly important

1. Originally published in *Elife* (2020 Dec 10;9:e62659) with authors listed as **Miller, H.A.**, Dean, E.S., Pletcher, S.D., and Leiser, S.F.

goal within biomedical research. The benefits of discovering therapeutics that target aging are many, including 1) decreasing the financial burden on our strained healthcare system, 2) increasing the amount of time older adults live free of chronic diseases (often denoted as healthspan), and 3) potentially increasing maximum human lifespan.

Organismal lifespan was first presented as a genetically modifiable trait by groundbreaking publications from the Johnson, Kenyon and Ruvkun labs describing the effects of the FOXO transcription factor DAF-16 on longevity in *C. elegans* (*1-3*). These findings played a critical role in the field's current interest in identifying signals that are crucial regulators of aging across the entire organism. Additional studies have shown that environmental factors, such as food perception or oxygen levels (*4-6*), can also modify longevity in model organisms. While modifying genes or substantially changing environments is not plausible in humans, it is feasible to find anti-aging therapeutics that mimic environmental cues or genetic signaling environments.

Deciphering how cells relay information to one another remains one of the foundational discoveries in biology. It was first posited by John Langley that cells express receptor proteins on the extracellular side of the cell membrane and, when bound by a signaling molecule, initiate a downstream physiological response (*7*). This was validated by a series of discoveries, starting with Rita Levi-Montalcini's finding of nerve growth factor in the 1950s and continuing with the discovery of other growth factors (*8*) before eventually finding the receptors themselves (*9*). These discoveries were pivotal in furthering our understanding of cellular patterning during development (*10*) as well as how organisms adapt to external stimuli. This concept, that cells can relay critical information to other cells in response to an initial signaling cue, allows for genes expressed in one cell or tissue to affect the physiology of other cells and tissues. This ability of genes to affect processes outside of the cells they are expressed in is often referred to as cell non-autonomous action or signaling.

More recently, high profile publications from multiple labs have shown that many signaling pathways reported to improve longevity (e.g. mitochondrial stress, insulin-like signaling, heat shock, and the hypoxic response) act through cell non-autonomous

signaling mechanisms (*11-16*). These pathways originate in sensory cells, often neurons, that signal to peripheral tissues and promote survival during the presence of stress. Importantly, this activation of stress response pathways, either through genetic modification or exposure to environmental stress, is often sufficient to improve health and longevity. Additionally, genetic modification of these pathways can often target the aging process while sparing growth/development/reproduction effects that are often consequences of environmental stress. Understanding how cell non-autonomous signaling influences longevity is a relatively recent concept in aging research and presents a novel opportunity to discover pharmacological interventions that modulate signaling to increase healthspan and longevity.

In this review, we summarize the recent wave of studies investigating the effects of cell non-autonomous signaling on a myriad of canonical aging pathways across taxa. Further, we discuss where the field has excelled and what we can learn from other areas of research that have successfully mapped the neuronal circuitry of behavioral phenotypes.

Caenorhabditis elegans

Utilization of the model organism *C. elegans* has played an integral role in bringing the biology of aging field into prominence. The discovery that mutations in the sole nematode insulin-like growth factor receptor (IGFR), *daf-2*, can double a multicellular organism's lifespan, launched a new field (*1-3*). Their discrete, well-defined somatic cell fate makes them an ideal model system to study how cell non-autonomous signaling influences a complex phenotype like aging. We begin by discussing the extensive studies of different *C. elegans* pathways that protect against stress and modify aging through cell non-autonomous mechanisms.

Energy balance and insulin signaling

Soon after the initial discovery that diminished insulin signaling can extend lifespan, the aging field began exploring where decreased insulin signaling was required to promote longevity. By constructing animals with mosaic expression of *daf-2*, several cell lineages

were identified that require *daf-2* mutations to reproduce the entirety of the *daf-2* lifespan benefit (*17*). This study was the first to clearly define a role for cell non-autonomous activity in aging and validate the significance of inter-tissue signaling during the lifespan of an organism. From here they sought to understand the effects of insulin signaling across tissues and the emergent role of the nervous system in influencing longevity came to the forefront of the field (**Figure 1.1**).

The identification of this role began through epistasis experiments. It was discovered that *daf-2* mutants completely require the class O of forkhead box transcription factors (FOXO) ortholog *daf-16* to extend lifespan (*18*), suggesting that *daf-16* nuclear localization and transcriptional activity is responsible for the longevity benefits. While most of *daf-16*'s pro-longevity effects are thought to be tied to cell-autonomous transcription of target genes in the intestine (*19*), more recent studies show that a subset of target genes, *dod-8, dod-11,* and *hsp12.6*, influence muscle aging cell non-autonomously (*20*). Intestinal expression of *daf-16* leads to elevated induction of target genes in the nervous system and hypodermis. Conversely to *daf-16,* tissue-specific expression of *daf-2* or *age-1* in neurons is sufficient to partially block lifespan extension in mutant animals; whereas, *daf-2* or *age-1* rescue in muscle is sufficient to restore metabolic function (*21*). These studies provide evidence that metabolism and aging are separable, yet interrelated, and that bi-directional signaling from metabolically active tissues to the nervous system occurs. We will expand on this understudied phenomenon in the **emerging concepts** section.

Nematodes have amphid neurons with ciliated projections that relay information about their current environment to the worm. Interestingly, when these projections are genetically knocked out or laser ablated, the animals live longer, often with the requirement of *daf-16* activity (*22, 23*). These data are supported by a recent study analyzing RNA in isolated neurons of *daf-16* and *daf-16; daf-2* mutants that finds *daf-16* target genes exclusively expressed in mechanosensory neurons (*24*). This led to identification of a novel gene, *fkh-9/*FOXL1*,* that, when knocked out, entirely abrogates *daf-2* lifespan. Another transcriptional microarray analysis identified a set of neuronally expressed genes upregulated in animals on *daf-2* RNAi and downregulated in animals

on *daf-16* RNAi (class I) or vice versa (class II) (*25*). The class II hit, *ins-7*, predicted to encode for an insulin-like peptide, is required for *daf-2* RNAi-mediated lifespan extension. *ins-7* may act as a signaling molecule in insulin-mediated cell non-autonomous signaling from the nervous system to the intestine. These data are compelling as *C. elegans* are predicted to have 40 insulin-like peptides that both agonize and antagonize *daf-2,* some of which modify the lifespan of wild-type animals when neuronally overexpressed (*26*).

Foundational work from the Kenyon lab established that signaling from germ cells regulates insulin signaling by decreasing *daf-16* activity throughout the organism (*27*). This means that ablating the germline genetically or physically leads to *daf-16* activation and increased longevity. The absence of germline signals activates a *daf-12*-dependent sterol signaling pathway in somatic reproductive tissues (*28*). This pathway induces the expression of *lips-17/fard-1* and produces an unknown lipophilic signal to increase *sod-3/dod-8* in other somatic tissues (*20*). This signaling pathway is an illustration of cells/tissues signaling to other tissues that “times are good/bad.”

Despite the groundbreaking discovery of microRNAs (miRNAs) in *C. elegans (29)*, their size, abundance across the genome, and evolutionary conservation, little work has investigated their potential role in cell non-autonomous modulation of aging. An intriguing study begins this exploration, interrogating how *mir-71* modulates lifespan (*30*). *mir-71* is necessary for lifespan extension in *glp-1* germline mutants, while *mir-71* overexpression in germline mutants extends lifespan beyond that of germline mutations alone. Rescuing *mir-71* in neurons alone is sufficient to rescue the germline mutant longevity phenotype, and intestinal *daf-16* expression is necessary for *mir-71* overexpression to extend lifespan in germline mutants. While this study presents an incomplete picture, it provides sound evidence for future studies to consider miRNAs as a target for inter-tissue signaling during the aging process.

The absence of gonadal stem cell signaling leads to activation of intestinal transcription factors like *skn-1/*Nrf2 that help to globally remodel the organism’s metabolism (*31*). A lack of gonadal stem cells also increases circulating fatty acids (FAs) that are normally

deposited in this tissue. This increase in circulating lipids may induce *skn-1/*Nrf2 nuclear localization that, in turn, enhances lipid metabolism and increases lifespan. *nhr-49*/HNF4α, a nuclear hormone receptor widely expressed throughout somatic tissues, also regulates both *glp-1*-mediated longevity and lipid metabolism (*32*). Furthermore, *nhr-49* overexpression extends lifespan in a *daf-16*- and *glp-1*-dependent manner. While this work cannot be directly translated to human health, these data provide initial evidence for critical signaling events between stem cells and nearby somatic tissues that influence longevity.

Multiple nutrient sensing pathways that interact with insulin signaling are conserved from worms to mammals including the target of rapamycin (TOR) and AMP-activated protein kinase (AMPK) pathways. The latter nematode ortholog, *aak-2*, has increased activity under low energy conditions and is sufficient to promote longevity when overexpressed (*33*). Follow-up studies show that *aak-2* activity suppresses cAMP-response element binding protein (CREB)/CREB-regulated transcription coactivator 1 (CRTC-1) transcriptional regulation and this ultimately extends lifespan (*34*). *crtc-1* neuron-specific knockout extends lifespan without the undesirable pleiotropic effects that accompany AMPK activation, like decreased growth and fecundity (*35*).

Interestingly, *nhr-49/*HNF4α is activated by AAK-2 (*36*), and its neuronal expression is required for the lifespan extension in AAK-2 overexpressing animals. Furthermore, neuronal CRTC-1 is sufficient to block AMPK-mediated longevity. Neuronal *crtc-1* levels modify intestinal *aak-2* activity through the neurotransmitter octopamine as a mechanism for the nervous system to convey “times are good”. Despite these results, many questions remain involving this signaling pathway. Octopamine is thought to be exclusively synthesized in the RIC head neurons (*37*) and the two known octopamine receptors, *ser-3* and *octr-1,* are expressed throughout inner neurons but not in peripheral tissues (*38, 39*). This suggests that octopamine acts as an initiating signal instead of a direct signal from neurons to downstream tissues. Recent work highlights this point by showing GABAergic signaling and neuron excitability inversely changes throughout the life of short- and long-lived animals (*40*).

TOR and AMPK play antagonistic roles in modulating lifespan and metabolism. Downregulation of TORC1 complex proteins, like *raga-1*, increases lifespan (*41*) but requires neuronal *aak-2* activity (*13*). Moreover, neuronal TORC1 expression is sufficient to shorten lifespan, consistent with a central “times are good” signal modulating longevity. RNA-seq comparisons of wild-type to *raga-1* knockout and neuronal overexpression identified *unc-64/*syntaxin as epistatic to neuronal *raga-1* activity. This work supports neural signaling as responsible for metabolic rearrangements, like increased mitochondrial fragmentation, that occur in peripheral tissues.

Although many of these studies identify the existence of neurosignaling pathways that drive metabolic changes in peripheral tissues, few have identified the signal(s) through which the nervous system transmits information to these tissues. Probing the precise mechanisms of nervous system to intestinal signaling will be an essential next step in furthering our understanding of how cell non-autonomous signaling influences aging.

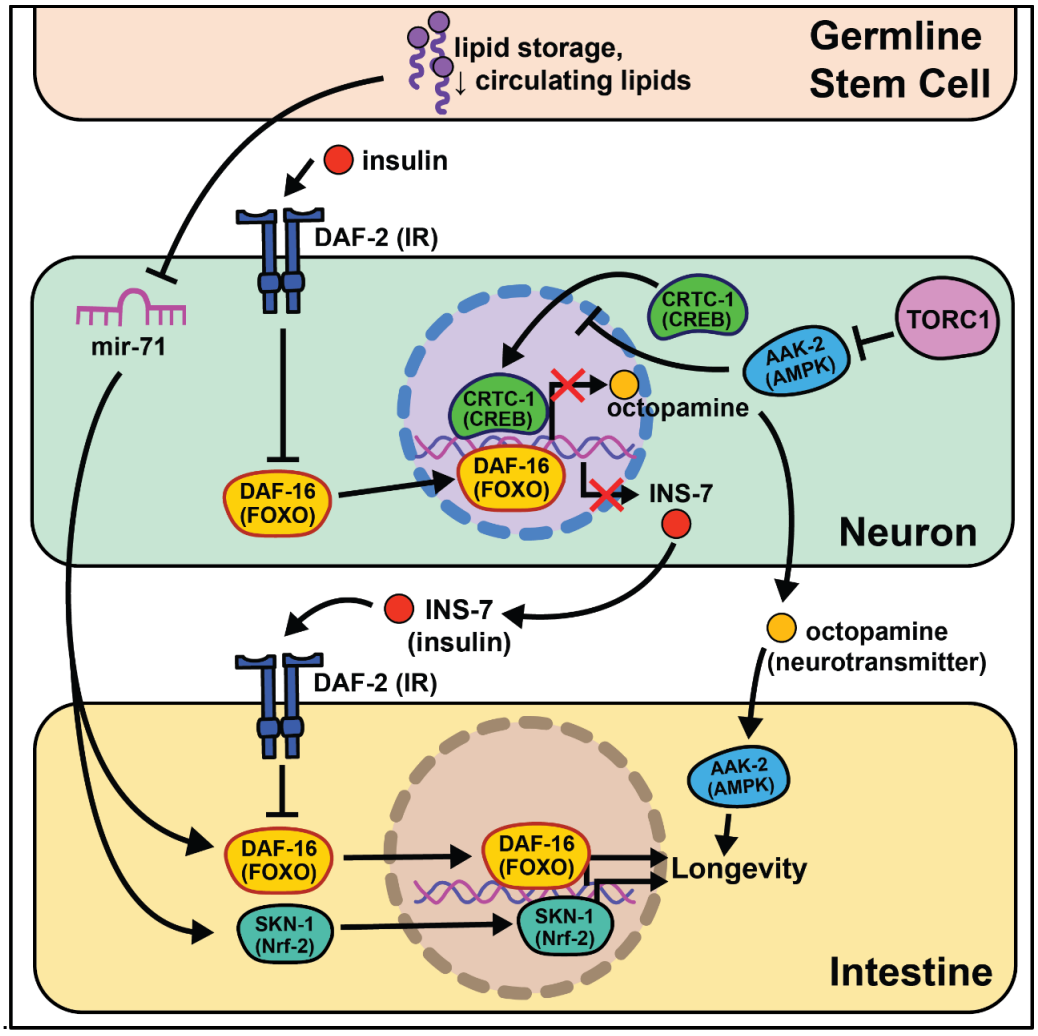

Figure 1.1. Summary of the role energy balance and insulin signaling on cell non-autonomous modulation of longevity in C. elegans.
Mammalian orthologs are listed in parentheses. If there are no parentheses, the name is shared across taxa

Proteostasis signaling pathways

A significant body of literature links increased stress resistance with longevity, leading to the hypothesis that acute moderate stress can trigger hormetic effects that extend lifespan (*42*). Eukaryotic cells have evolved several organelle-specific stress responses that, when induced, extend nematode lifespan.

Knock down of complex IV of the electron transport chain (ETC) with *cco-1* RNAi leads to delayed growth, slowed movement, reduced body length, and increased lifespan. Importantly, *cco-1* knock down exclusively in neurons increases lifespan without

pleiotropic phenotypes by altering mitochondrial homeostasis in peripheral tissues (*43*). Interestingly, this lifespan extension requires the mitochondrial unfolded protein response (mt-UPR), but not *daf-16*/insulin signaling. A follow up study using the heat shock protein-6 (*hsp-6)*p::GFP transcriptional reporter identified *vps-35* as lacking peripheral mt-UPR (*44*). VPS-35 is a highly conserved protein in the retromer complex, involved in recycling Wnt and the Wnt secretion factor MG-4 (*45*). In agreement with this, the Wnt receptor *egl-20* is necessary and sufficient for cell non-autonomous mt-UPR induction and longevity. Interestingly, neuronal serotonin production is necessary for cell non-autonomous mt-UPR even though the loss of each of the four known serotonin receptors (*ser-1, ser-4, ser-7*, and *mod-1*) has no effect. These results clearly define that mitochondrial stress, through reduction of ETC activity or separate activation of the mt-UPR, can be transmitted by neurons cell non-autonomously to modify aging. As with many of these neuronal based networks, however, the central signaling pathways remain largely uncharacterized.

Multiple labs find that neuronal activation of the endoplasmic reticulum unfolded protein response (ER-UPR) is sufficient to enhance stress resistance and extend lifespan (*46-50*). This crucial discovery stems from identifying that the constitutively active spliceoform of X-box binding protein *1* (*xbp-1s)*, a transcription factor activated by the ER-UPR, rescues older animal survival on paraquat (*46*). Expression of *xbp-1s* in the nervous system or intestine extends lifespan, and exclusive *xbp-1s* expression in the neurons is sufficient to increase paraquat stress resistance in young and older animals. It is likely that neuronal ER-UPR releases an activation signal conferring *xbp-1s* upregulation in the intestines that rescues motility in models of proteotoxicity like Aβ, polyglutamine aggregates (Q40), and dynamin (*47*).

More recent work begins to parse out where *xbp-1s* is required in the nervous system to extend lifespan. Surprisingly, expression of *xbp-1s* in glia, helper and insulator cells for neurons, extends lifespan and activates the ER-UPR in peripheral tissues (*48*). This *xbp-1s*-mediated signal requires neuropeptide signaling but not neurotransmission for intestinal induction of *hsp-4,* suggesting a neuropeptide is the intermediate signal from the glia cells to the intestine (*48*). While it is useful to rule-out neurotransmitters as the

causative signaling molecules, there remain hundreds of potential coding regions annotated as “neuropeptides” in *C. elegans* (*51, 52*).

Another open question surrounds whether other transcription factors that respond to the ER-UPR can recapitulate the effects of *xbp-1* activation. Preliminary findings point to *xbp-1* activity, not *pek-1* or *atf-6,* two transcription factors also activated by the ER-UPR (*48*), as key to modifying lifespan. This implies that uncovering the pro-longevity targets of XBP-1 will be of high interest to understand and translate these results. Neuronal activation of *xbp-1s* results in changes in fat metabolism, a build-up in oleic acid (OA), and leaner animals (*50*). It is possible that the pro-longevity phenotypes associated with *xbp-1s* are due to increased expression of lysosomal genes, like *asp-13* and *vha-18*, that enhance acidity and, therefore, protease activity. Furthermore, the lifespan phenotype and expansion of the ER in *xbp-1s* animals requires lipid depletion (*49*). Initial results show enhanced intestinal lipid depletion through *ehbp-1* overexpression modestly extends lifespan and partially recapitulates the effects of *xbp-1s*. Taken together, these data emphasize the significant role metabolically active tissues, like the intestine, play in properly responding to cues from the nervous system (summarized in **Figure 1.2**). While the ER-UPR field is beginning to narrow in on specific neuronal cells and signaling molecules, much is left to delineate in the neuronal circuitry. Understanding how, when and where neuromodulators affect normal and pro-longevity conditions is paramount in translating these results to higher organisms and discovering therapeutic treatments to mimic these phenomena.

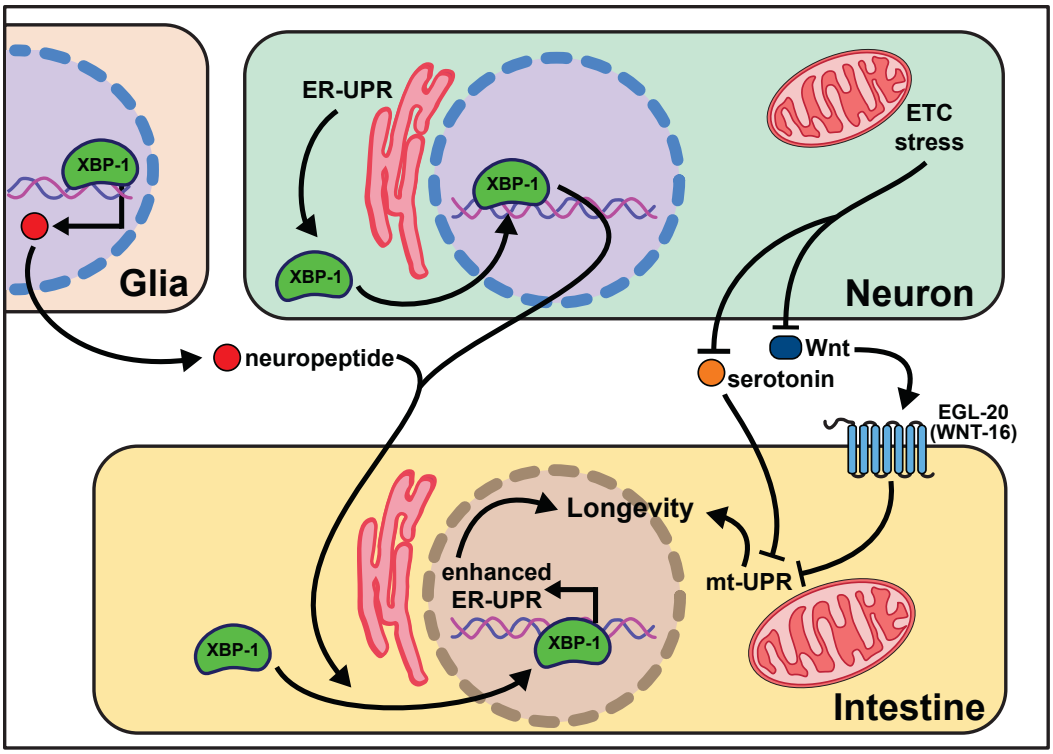

Figure 1.2. Summary of the role of proteostasis in cell non-autonomous modulation of longevity in C. elegans.
Mammalian orthologs are listed in parentheses. If there are no parentheses, the name is shared across taxa.

Perception of external stimuli

An organism's ability to respond to changes in the environment, such as temperature, oxygen levels, and smells, is vital to their survival. In this section, we chronicle research findings linking perception and organismal aging (**Figure 1.3**).

As poikilotherms, *C. elegans* are responsive to heat- and cold-shock. Generally, longevity varies inversely with temperature, where animals housed at lower temperatures (15℃) live longer than those at higher temperatures (25℃). Based on our understanding of thermodynamics this observation seems intuitive, but several papers have challenged this theory and shown changes in lifespan across temperature are genetically modulated. In fact, many pro-longevity genetic mutations have a distinct relationship with temperature, promoting longevity at either cold or warm temperatures but rarely both (*53*). These data are consistent with many genes playing an active role in the physiological response to changes in temperature. Whether by modifying the

perception or response to temperature, this interplay suggests that genes actively influence lifespan at various temperatures, refuting thermodynamics as the sole influence on temperature-mediated lifespan changes.

A robust body of research surrounds activating the heat shock response (HSR) and longevity. In *C. elegans*, post-reproductive adulthood is accompanied by an abrupt decline in protein quality control (*54-56*). Thus, maintaining the ability to effectively respond to heat stress remains a hallmark of long-lived animals. It is important to note that heat shock, described in the literature as >30℃, likely uses partially-distinct genetic mechanisms from warmer conditions (22℃-25℃) that will be addressed separately.

Early studies implicate the nervous system in regulating proteostasis through the HSR. Key signaling components of amphid neurons, *gcy-3* and *ttx-3*, are necessary for proper induction of global HSR during heat shock (*57*). These early studies also implicate an unknown neurotransmitter in signaling from the nervous system to promote survival during heat shock. Optogenetic stimulation of the AFD thermosensory neurons triggers serotonin release from the ADF neurons that activates heat shock factor 1 (HSF-1) in the germline in the absence of heat shock (*58*). In the absence of *ser-1*, a 5-HT2B serotonin receptor ortholog, HSF-1 is not re-localized to the nucleus upon AFD optogenetic excitation or heat shock. This result suggests that *ser-1* is necessary for proper signaling during HSR. It is worth noting there is no predicted synapse or gap junction between AFD and ADF neurons, meaning there is likely an intermediate signaling molecule(s) and/or cells yet to be discovered.

While HSR proteins are necessary for animals to survive warmer temperatures (*59*), it is significant that overexpression of *hsf-1* in neurons is sufficient to increase stress resistance and longevity (*60*). Linking back to earlier work, intact signaling from the AFD/AIY neurons is required for heat stress resistance in worms overexpressing *hsf-1* (*57*). This may be through *pat-4/* integrin-linked kinase (ILK) activity in the AFD/AIY (*61*). Interestingly, intestinal *daf-16* activity is required for the lifespan phenotype but unnecessary for heat stress resistance (*60*), suggesting these phenotypes have distinct signaling events despite their positive correlation.

Less is known about the mechanisms of cold- and warm-sensory signaling and metabolic remodeling that promotes longevity. As with the HSR, the AFD neurons are also thought to play a role in appropriately responding to warmer temperatures as laser ablation and genetic disruption exclusively shortens lifespan at 25℃ (*59*). Mutants lacking functional CNG calcium channels, a *tax-2/tax-4* heterodimer, are also short-lived at 25℃ and thought to be necessary for AFD neuronal activity when exposed to warm temperatures. These results are corroborated in a recent study showing the ASJ sensory neurons also require functional *tax-2/tax-4* channels to sense warm temperatures and activate intestinal *daf-16* to extend lifespan (*62, 63*). Experimental evidence suggests once these thermosensory neurons are activated they deploy *daf-9*, a cytochrome P450 ortholog, which inhibits *daf-12*, a nuclear hormone receptor, allowing worms to live longer at 25℃ (*59*). An important distinction remains between AFD activation during warm- and heat-shock as many heat shock proteins, like hsp-60 and hsp-70, are not upregulated at 25℃ (*59*). These data suggest that perception and response to temperature through thermosensory neurons are sufficient to modulate aging across temperatures. They also refute thermodynamics as the sole mechanism for how poikilotherms live shorter at higher temperatures.

In agreement with neural modulation of aging in warmer temperatures, a transient receptor potential (TRP) channel, TRPA-1, detects cold temperatures in chemosensory neurons. TRPA-1 signals through a protein kinase C (PKC) ortholog, PKC-2, to increase intestinal DAF-16 activity and therefore lifespan (*64*). Loss of *trpa-1* channels in the nervous system prevents the lifespan increase observed in Wild-Type worms at cooler temperatures (15-20°C), but does not change longevity at warmer temperatures (25°C). Interestingly, human transgenic TRPA-1 recapitulates many of these findings, suggesting a conservation in function. An unbiased screen of all sensory neurons showed *trpa-1* expression in the head neuron IL1 is necessary and sufficient to rescue *trpa-1* knockout. Further, genetically knocking out glutamate secretion and uptake prevents IL1 from modifying lifespan (*62*). MGL-1, the glutamate receptor implicated in this study, is only expressed in neurons, indicating there must be another neuron involved in this pathway. Knocking out serotonin signaling blocks the effects of IL1 on

lifespan, and transgenic serotonin expression in the NSM enteric neuron rescues the phenotype. The intestinal GPCR *ser-7* is the likely downstream receptor responding to serotonin release. This study offers a more complete model than is often presented in the field, and suggests it is feasible for other cell non-autonomous signaling pathways to be more explicitly characterized in future studies.

The nervous system in *C. elegans* plays a crucial role in determining nutrient quality and safety as they forage for food, and interestingly, the lack of any perceived signal (i.e. dietary restriction (DR)), can also act as a signal on its own. DR, first reported to increase lifespan in rats in 1935 (*65*), is an intervention that significantly limits food intake without malnutrition, and has been the most consistent intervention to increase longevity across species (*66*). However, since implementation of any dietary intervention for humans at a whole population level is challenging, mapping out the molecular and signaling mechanisms downstream of food perception, where they can be targeted directly, circumvents the challenges of adopting population level-DR protocols.

The first report of DR acting through a sensory, cell non-autonomous signaling mechanism in worms was in 2007. They identify the antioxidant response transcription factor skinhead 1 (SKN-1) in ASI sensory neurons as leading to increased whole-body respiration and extended lifespan (*67*). This report remains foundational in establishing food perception, or lack thereof, as a major driver of the health benefits of DR. More recent studies corroborate the significance of sensory neurons when nematodes are subjected to long- and short-term starvation. A subset of sensory neurons, the ASI and ASJ, shorten lifespan through the expression of insulin-like peptide (ILP) *ins-6* during food perception (*63*). More specifically, *ins-6* is released upon feeding, and ins-6 overexpression exclusively in the ASI or ASJ neurons blocks the longevity effects of *tax-2; tax-4* mutant worms when fasted. This suggests that an unknown inverse signal may suppress *ins-6* expression during fasting.

Sensory cues from food perceived by the nervous system trigger a host of behavioral and metabolic rearrangements that accompany changes in lifespan. Particularly, in the

absence of food, nematodes tend to increase their movement when foraging and stop pharyngeal pumping (*68-70*). Once an attractive odorant is perceived, serotonin is released triggering triglyceride fat catabolism by a predicted acyl-CoA oxidase, *acox-1* (*71*). Surprisingly, this fat catabolism is necessary and sufficient to modulate changes in behavior. *acox-1* mutants do not respond with the canonical behavioral changes observed when animals are exposed to exogenous serotonin (*72*). Additionally, rescuing *acox-1* expression in the intestine alone abrogates the fat accumulation and pumping response to serotonin exposure. *egl-2*, an ether-à-go-go (EAG) K+ channel expressed in the sensory neurons, likely functions as an intermediary neuron signaling back to serotonin neurons communicating satiety from peripheral tissues. Intriguingly, antagonizing serotonin signaling through an atypical antidepressant mianserin extends lifespan and is non-additive with DR (*73*). It is worth exploring whether the changes in metabolism and lifespan when serotonin signaling is antagonized are acting within the same pathway. These results corroborate the hypothesis that a feed-forward signal is released from the intestine back to the nervous system during food perception (**section 5**).

Recognition of low-oxygen conditions or genetic stabilization of the conserved hypoxia-inducible factor-1 (HIF-1) extends nematode longevity (*6, 74*). A single protein, flavin-containing monooxygenase-2 (FMO-2), is necessary and sufficient to provide many of the benefits of HIF-1 activation (*12*). Neuronal stabilization of HIF-1 is sufficient to induce intestinal *fmo-2* and improve health and longevity. Serotonergic signaling is required for HIF-1-mediated longevity and *fmo-2* induction, while FMO-2 overexpression in the intestines is sufficient to increase lifespan. Interestingly, other researchers have found FMO induction in multiple mammalian models with increased lifespan, including DR, consistent with FMOs playing a conserved role in promoting long-term health and increasing the likelihood these results will be translatable to human longevity (*75, 76*).

Together, perception of many environmental signals influence lifespan in *C. elegans*. While the mode of sensory detection varies between these environmental signals, perception of temperature, oxygen, food availability, and mechanosensory cues all activate sensory neuron-initiated signaling pathways. This external perception interacts

with internal cues (e.g. germline signal, proteostasis, and metabolism) to appropriately respond and modify physiology. While we have begun to identify the cells and signals involved in these sensory-driven longevity pathways, many questions remain regarding how information is transmitted and interpreted both within and between tissues.

A

Intervention	Neuron A	Neuron B	Neuron C
Heat Stress	AFD	ADF	NA
Cold Stress	IL1	NSM	unknown
Dietary Restriction	NA	ASI/ASJ	NA
Hypoxia	NA	RIM	NA

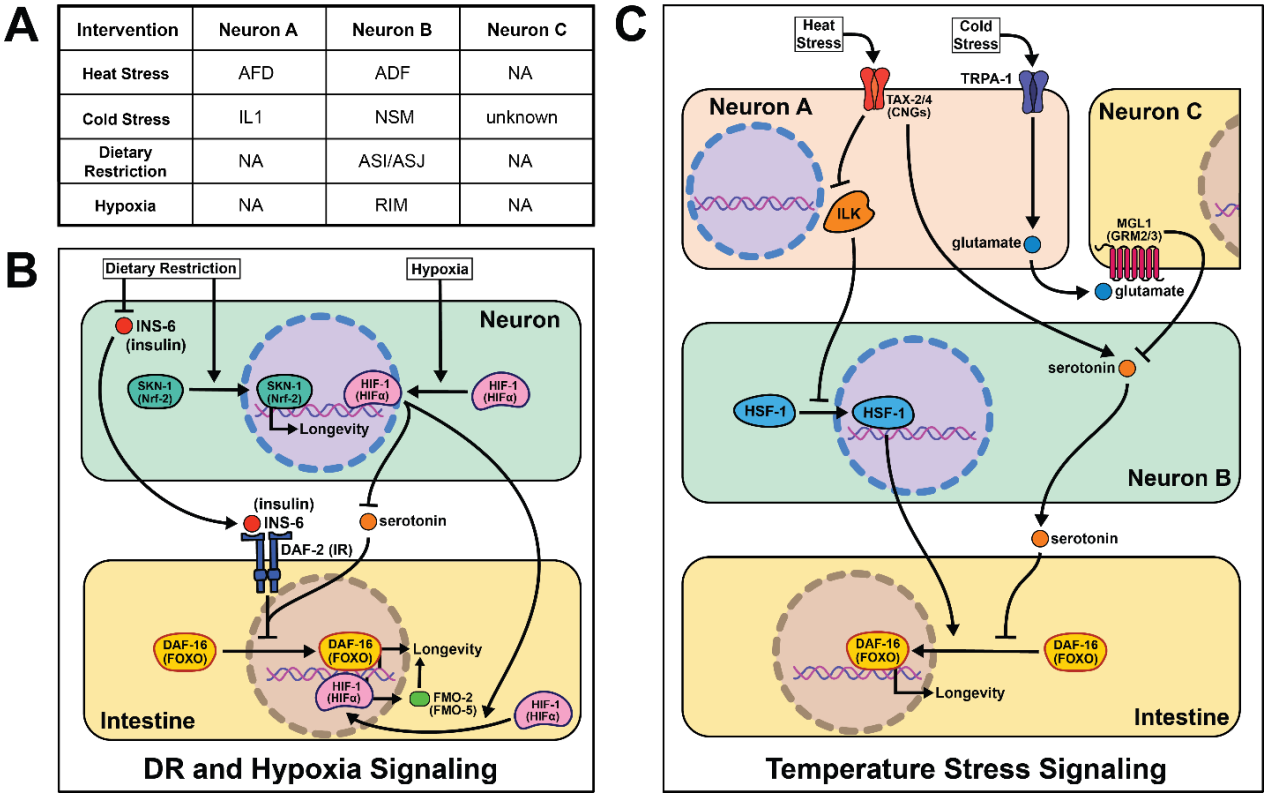

Figure 1.3. Summary of the role of perception on cell non-autonomous modulation of longevity in C. elegans.
Mammalian orthologs are listed in parentheses. If there are no parentheses, the name is shared across taxa.

Drosophila melanogaster

While *C. elegans,* with its simplicity and finite number of cells, is perhaps the most powerful system for identifying genetic mechanisms of aging, it does pose some limitations: its nervous system is rudimentary, precise manipulation of diet and other environmental factors is difficult, and its small behavioral repertoire is restrictive. Conversely, studies of cell non-autonomous modulation of aging in vertebrate animals

are impeded by multiple factors, including but not limited to: 1) the time required for measuring lifespan, 2) challenges in using large-scale genetic modification for pathway discovery, and 3) the difficulty of identifying small subsets of key cells within substantially larger and more complex tissues. Given the remarkable advances in neuroscience, together with its long-standing success as a model for both behavioral neuroscience and aging biology, the vinegar fly, *Drosophila melanogaster*, provides unique strengths to investigate these questions. Conservation of mechanisms of aging, including insulin/FOXO-related signaling and sensory-derived control of longevity, in worms, flies, and mammals suggests that signaling mechanisms likely become more complex in higher organisms but produce similar pro-longevity outcomes. Although the phylogenetic relationship between nematodes, arthropods, and vertebrates is debated, 18S rRNA and mitochondrial rDNA sequencing suggests a greater evolutionary distance between *D. melanogaster* and *C. elegans* than between *D. melanogaster* and *M. musculus* (*77*). Consequently, mechanisms of aging conserved between worms and flies are also likely to span the smaller evolutionary gap between flies and mammals. In the following sections we provide an overview of key cell non-autonomous modulators of fly health and aging (*4, 78*).

Energy balance and insulin signaling

Soon after the foundational discovery that reduced insulin signaling increases nematode lifespan, experiments in *Drosophila* revealed that such results were not worm-specific and that this pathway may be involved in modulating aging across taxa (*79*). Mutations disrupting molecules in this pathway such as the single insulin receptor, *dInR*, or the *fly* homolog of the insulin receptor substrate, *chico*, exert non-autonomous effects on aging, where reduced insulin/IGF-1 signaling (IIS) is associated with extended lifespan (*80, 81*). Genetic manipulations that mimic reduced IIS, such as overexpression of *dFOXO* in the abdominal or pericerebral fat body or overexpression of phosphatase, *dPTEN*, in the pericerebral fat body also extend fly lifespan (*82, 83*). These data indicate that insulin signaling acts cell non-autonomously to control aging and promotes bi-directional signaling between peripheral tissues and neurons like what is seen in *C. elegans*.

The *Drosophila melanogaster* genome encodes several insulin-like peptide genes (*dilps*), which are produced in a handful of neurosecretory cells in the *pars intercerebralis* region of the fly brain. These insulin producing cells, called IPCs, release the signaling molecules into the hemolymph to signal to the rest of the body through a single insulin-like receptor (*InR*) (*84-86*). Among their range of biological functions in development and physiology, *dilps* modulate aging, and in this context the most well studied are *dilp2*, *dilp3*, *dilp5,* and *dilp6* (*86-88*) . Partial ablation of IPCs, the production site of DILPs 2, 3, and 5 reduces IIS and increases lifespan (*89, 90*). Knocking down GABA-B receptors in IPCs decreases DILP secretion in fed and fasted conditions and yields a small but significant decrease in stress resistance and lifespan under starvation (*91*). Mutation of *dilp2*, *dilp3,* and *dilp5 together increases lifespan as does loss of dilp2* alone, although loss of other individual *dilps* does not (*86*). Induction of *dilp6* in fat body tissue promotes longevity. It is unclear whether this is a direct effect of DILP6 or is due to a decrease in the secretion of DILP2 from the IPCs (*87*). Similarly, the extended lifespan observed following increased *dFOXO* expression in pericerebral fat body may also result from a decrease in *dilp2* expression in the IPCs (*92*). More recent work has revealed a role for *dilp1* in promoting lifespan (*93*), potentially through induction of adipokinetic hormone (AKH), which is a functional homolog of mammalian glucagon (*94*) and which increases fly lifespan, fat metabolism, and free fatty acid catabolism (*95, 96*).

The link between lifespan extension from manipulation of neuronal dilps and the insulin-responsive transcription factor FOXO in peripheral tissues are less clear in *Drosophila* as in *C. elegans*, suggesting that IIS extends lifespan, at least partly, through FOXO-independent pathways. Loss of *dilp2* does not influence the expression of known FOXO target genes and interactions with *dilp1* do not modify this result (*93*). Flies lacking IPCs or with loss of dilps 2, 3, and 5 exhibit an abnormal response to diet manipulation (*86, 88*), although *dFOXO* mutation leaves the response largely intact (*97*). Furthermore, loss of *dFOXO* only partially rescues longevity benefits of *chico* mutants (*98*).

Another nutrient-sensing pathway that acts cell non-autonomously in flies, like worms, is AMPK. Neuronal or intestinal activation of AMPK or Atg1 induces autophagy in both the

brain and gut to slow organismal aging and improves numerous healthspan measures (*99*). Dilps are implicated in mediating the inter-tissue response from the nervous system to the intestines and vice versa (*99*). It is interesting that AMPK activation from several tissues causes metabolic remodeling across the whole-body. These data point to a feed-forward mechanism where signaling events occur bi-directionally to modulate the fly response to successfully survive stressful stimuli.

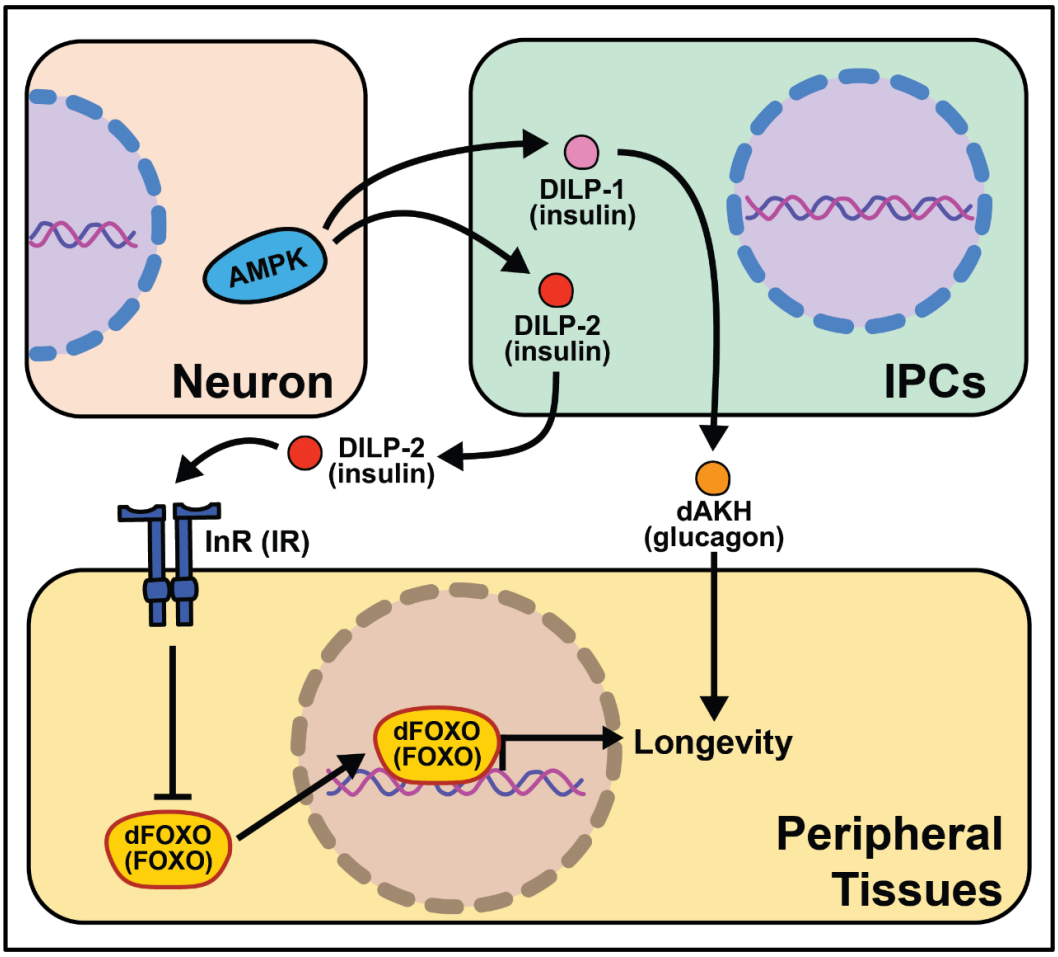

Figure 1.4. Summary of the role energy balance and insulin signaling on cell non-autonomous modulation of longevity in D. melanogaster.
Mammalian orthologs are listed in parentheses. If there are no parentheses, the name is shared across taxa.

Proteostasis signaling pathways

When it was first discovered that knocking-down mitochondrial electron transport chain components in nematodes extends lifespan, it seemed unlikely this phenomenon would

be conserved in higher systems. Surprisingly, research using flies and mice (later discussed in **section 4**) points to a significant role for mitochondrial function in organismal lifespan. Global knockdown of ETC components in complexes I, III, IV, and V extends fly lifespan, but does not inhibit ETC complex formation or ATP production (*100*). Furthermore, knockdown of complexes I and IV in neurons alone is sufficient to extend lifespan. This led researchers to ask how knockdown of the ETC extends lifespan. Follow up studies show that knockdown of ETC complex I using ND75 RNAi in muscle tissue increases reactive oxygen species (ROS) and activates the mito-UPR and ImpL2 (insulin/IGF binding protein) (*101*). Subsequently, upregulation of mito-UPR target genes preserve muscle function while ImpL2 signals to the brain and fat body to decrease global insulin signaling. It is likely both pathways contribute to the longevity phenotype of decreased respiration chain expression, and there are data suggesting that ImpL2 increases lysosomal biogenesis and that autophagy genes are necessary for ND75 knock down animals to live long. Another datapoint that suggests conservation of this pathway is that knock down of ETC ND75 in complex I results in smaller flies, and a similar phenotype is documented in the nematode ortholog *isp-1* mutants (*102*).

Modifying the mitochondrial proton gradient by expressing human uncoupling proteins (hUCPs) modulates fly lifespan. Interestingly, the context of when and where the hUCPs are expressed play a critical role in health and longevity outcomes. hUCP2 targeted to the neurons increases health and longevity while increasing the rate of glycolysis and decreasing ROS production and oxidative damage (*103*). Similarly, moderate pan-neuronal overexpression of hUCP3 leads to a modest lifespan extension exclusively in male flies (*104*). However, use of a stronger driver that targets hUCP3 pan-neuronally or to the median neurosecretory cells (mNSC) significantly decreases their lifespan. These data suggest that lowering uncoupling mitochondria by high expression of hUCP3 alters mNSC function in a way that increases DILP levels in fly heads and leads to a concomitant decrease in lifespan. Much is left to be done to fully understand the relationship between modulating mitochondria ROS levels and lifespan.

An important and robust area of research is focused on muscle maintenance with age. While slightly tangential to this review's primary focus on longevity outcomes, the loss of

muscle mass often precedes other age-related phenotypes like risks of falling. Throughout life, a fly's muscles accumulate protein aggregates that impair function. Maintenance of proteostasis is enhanced in long-lived animals through elevated activity of FOXO target genes like 4E-BP that increase lysosome/autophagy functions (*105*). Interestingly, FOXO signaling through 4E-BP activity in muscle decreases feeding behavior and the release of insulins that delay the age-related accumulation of protein aggregates in other tissues. This result suggests bi-directional cell non-autonomous signaling across tissues with a yet to be discovered signal (*105*).

Overexpression of the gene hedgehog (*hh*), the Hedgehog signaling pathway ligand in *Drosophila,* extends lifespan, while disrupting this pathway shortens lifespan and decreases the number of dopaminergic neurons (*106*). While overexpression of hedgehog signaling components in neurons has little effect on lifespan, overexpression in glia cells is sufficient to extend it. This work parallels nicely with work in *C. elegans* described above in which glial cells modulate aging through the UPR (*48*). Overexpressing *hsp69* and *hsp40* in glia is sufficient to rescue lifespan in *hh* signaling mutants. Overexpression of smoothened (*smo)* and *hsp68* in glia partially rescues the lifespan shortening effects of expressing human Aβ42 plaques in *Drosophila* glia. Hh signaling may increase chaperone protein expression in adult glia, which act to maintain the integrity of dopaminergic neurons, leading to increased longevity (*106*). While such data are compelling, it remains unclear how these neurons contribute to the lifespan extension of enhanced hedgehog signaling. It is also interesting to consider the conserved role glia cells play in neurotransmission, cell non-autonomous signaling, and longevity.

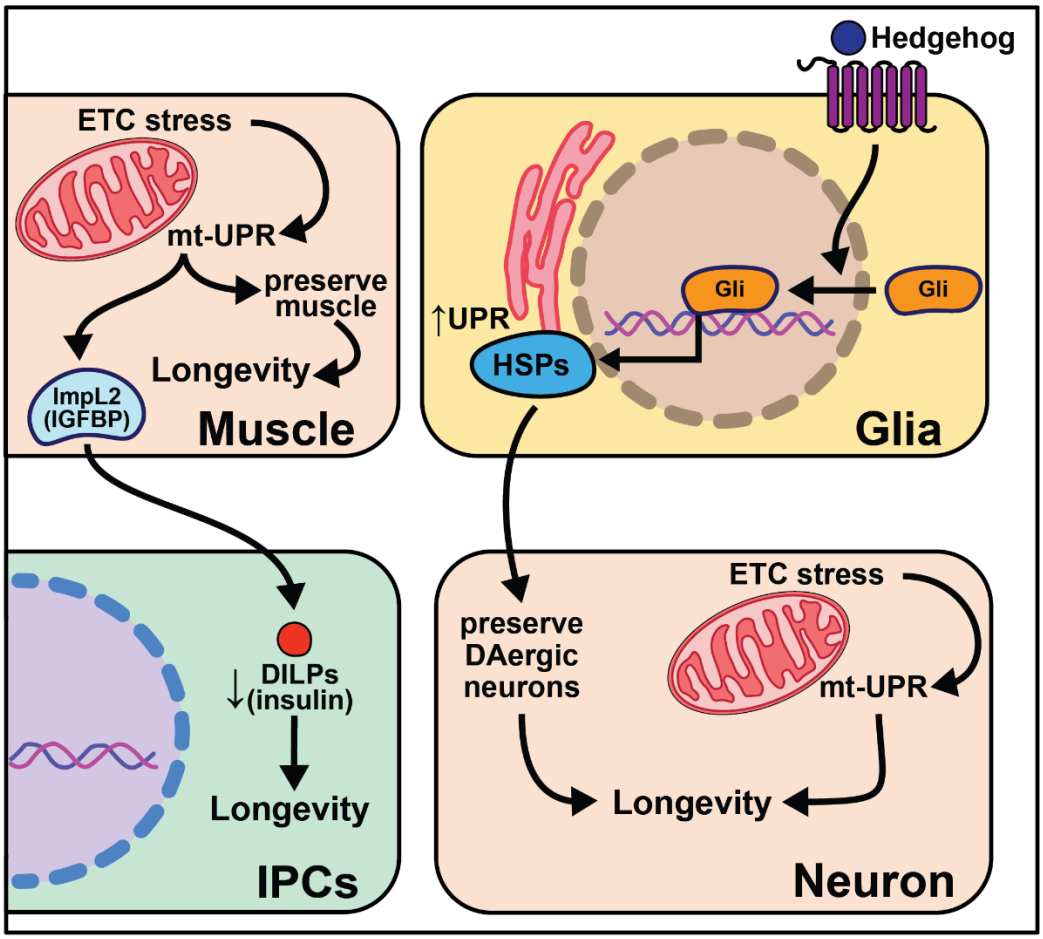

Figure 1.5. Summary of the role of proteostasis in cell non-autonomous modulation of longevity in D. melanogaster.
Mammalian orthologs are listed in parentheses. If there are no parentheses, the name is shared across taxa.

Perception of external stimuli

Research in *Drosophila* has shepherded a significant expansion in our understanding of the effects of sensory perception on aging. Sensory inputs that relate information about nutrition, conspecifics, and danger rapidly initiate changes in fly physiology and patterns of aging, often within a few days. It is known, for example, that a restricted set of olfactory and gustatory neurons influence aging by either promoting or limiting lifespan, fat deposition, or general vigor in old age. Sensory perception of specific sugars and amino acids, as well as social signals such as the health of conspecifics or availability of potential mates, is also important. Conserved neuropeptides and functionally-defined

neuronal populations, some associated with psychological conditions such as reward and hunger, are involved in mediating these effects through new candidate cell-nonautonomous aging mechanisms.

Much of this work is centered around the effects of food perception. Exposure of flies to the odor of an important food source (live yeast) as well as knock-out of a critical co-factor for normal olfactory function (*Or83b*/*Orco*) established food perception is sufficient to partially reverse DR-mediated longevity (Libert et al 2007). Loss of Orco function significantly increases fly lifespan. These effects are independent of food intake, activity, respiration, or early-life reproduction, suggesting a direct effect of sensory perception. Mutation of the water sensor, *ppk28*, extends *Drosophila* lifespan by up to 40%, and this effect requires AKH receptor (*95*). AKH protein levels are higher in *ppk28* mutant animals, and activation of *Akh*-expressing neurons is sufficient to recapitulate the effects of loss of *ppk28* on lifespan. Gustatory perception is necessary for normal stress resistance and lifespan in a low-glucose environment (*107*). Loss of sweet taste receptor *Gr64* produces a sleep-impairment phenotype that is phenocopied by blocking dopamine neurotransmission, and taste-blind flies lived longer than control flies, despite eating more (*108*). Loss of the *Drosophila* trehalose receptor, *Gr5a*, significantly decreases lifespan without altering feeding (*96*), establishing that taste inputs can modulate lifespan in both directions. Similar to some methods of diet restriction in *C. elegans*, loss of labellar taste bristles requires insulin signaling to extend lifespan (*108*).

In *Drosophila,* the effects of dietary restriction on aging are predominantly influenced by dietary composition (mainly protein content) rather than the overall caloric content of the food (*109-112*). Flies exposed to restriction of essential amino acids behaviorally switch from a diet comprised primarily of sugar to one primarily of protein (*113*). This behavioral switch in feeding preference requires both serotonin signaling through the 5-HT2A receptor and plasticity of a dopaminergic circuit (*16, 114*). When the two primary macronutrients in the diet, sugar and protein, are presented separately to flies so that they behaviorally construct the composition of their own diet, they live shorter than when presented with a single, complete diet (*16*); an effect that also requires serotonin

signaling through the serotonin receptor 5-HT2A. This suggests that protein sensing may be mediating this effect. Finally, serotonin, 5-HT2A, and the solute carrier 7-family amino acid transporter, JHL-21, modulate diet-dependent aging by ascribing value to ingested protein. Interestingly, *Jhl-21* is expressed in the reproductive tissues, which are a primary consumer of dietary protein, suggesting an inter-tissue communication.

Outside of a flies' ability to assess food quality, several other sensory cues rely on neuronal signaling to modulate lifespan. Exposure to female sex pheromones in the absence of mating causes rapid and reversible declines in fat stores, stress resistance and longevity in male flies (*115*). Changes in metabolism and lifespan require taste perception through the gustatory receptor, *ppk23,* as well as neuronal signaling involving the conserved neuropeptide NPF/NPY and FOXO. These effects are partially reversed by copulation, suggesting that survival costs of reproduction in male flies are controlled by neural circuits through which reproductive expectation dictates costly precopulatory investment in reproductive success. Related circuits that perceive reproductive reward ameliorate the consequences of this investment if mating is achieved (*116*). Notably, mating decreases both worm and fly lifespan, it's worthwhile to ponder why perception of imminent mating without achieving it causes greater physiological harm to a flies' health. Perhaps upon completing a satisfying activity that is evolutionarily beneficial, like eating or mating, specific neural circuits and signaling peptides reinforce these behaviors, and without these signals only detrimental effects remain.

Cues that putatively signal danger are also important. *Drosophila* can visually perceive dead conspecifics in their environment and this perceptive experience induces both short- and long-term effects on health and longevity. Exposure to dead flies decreases resistance to starvation, depletes lipid storage, and shortens lifespan (*117*). As with protein perception, serotonin signaling via receptor 5-HT2A is required for death perception to influence lifespan. With the advent of new technologies, it would be interesting to test whether the same or different neuron populations require 5-HT2A receptors to influence death and/or food perception. *Gr63a* encodes for one of two proteins which make up a CO_2 receptor, and at low concentrations CO_2 is a known

alarm cue (*118*). Flies with a loss of function mutation in *Gr63a* are long-lived and are additive with ab1C neuronal ablation suggesting DR and alarm sensing act through distinct pathways to influence lifespan (*119*).

A

Intervention	Neuron A	Neuron B	Neuron C
Death Perception	visual neurons, olfactory neurons	unknown	5-HT2A+ neurons
Female Sex Pheromones	leg/wing margin gustatory neurons	NPF+ neurons	NA
Dietary Restriction	gustatory and olfactory neurons	IPCs, DAergic, 5-HT2A+ neurons	NA
CO_2 Perception	ab1C neurons	NA	NA
H_2O Perception	NA	AKH-producing neurons	gustatory neurons

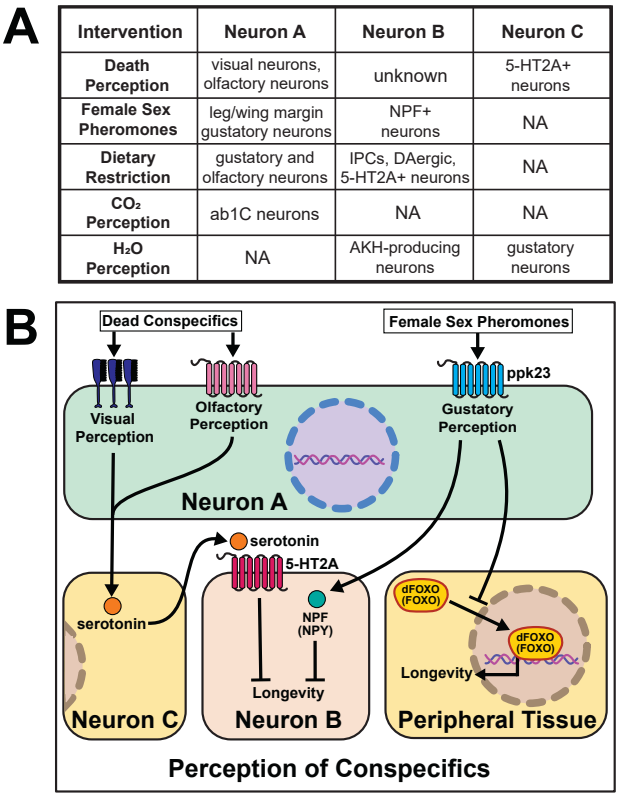

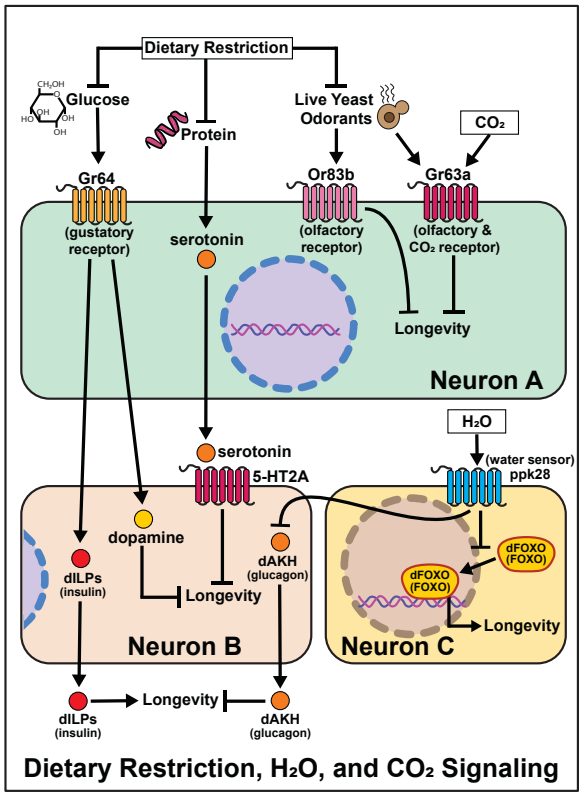

Figure 1.6. Summary of the role of perception on cell non-autonomous modulation of longevity in D. melanogaster.
Mammalian orthologs are listed in parentheses. If there are no parentheses, the name is shared across taxa.

Mammals

Fewer studies have explored the effects of aging and cell non-autonomous signaling in mammals due to the extended amount of time and effort needed to perform these experiments. Despite these considerations, a growing body of literature suggests the types of signaling events seen in invertebrates are conserved from worms to mice. These initial findings portend an increase in the number of studies investigating the effects of the nervous system on aging. In this section we will discuss the individual

studies performed in mice and compelling evidence that suggests this phenomenon may be conserved in humans (**Figure 1.7**).

Similar to the effects observed in worms and flies, reduced insulin and growth hormone signaling also significantly increase mouse lifespan (*120*). Ames dwarf mice, and the similar Snell dwarf mice, each have a single-gene mutation, Prop1 and Pit1, respectively, that impairs anterior pituitary development leading to decreased growth hormone, thyroid stimulating hormone, and prolactin levels. These mice live 40% longer than controls and have decreased plasma IGF-1 (*121*). However, dwarf mice do become obese in old age, showing that pituitary modulation of aging is independent of body weight regulation. Interestingly, grafting a control pituitary gland in adulthood does not rescue control lifespan in Snell dwarf mice (*122*). The mechanism for longevity likely involves IGF-1, because similar results have been obtained using the knockout for growth-hormone receptor binding protein (GHR-KO) (*123*), a heterozygous null mutation of the IGF-I receptor (*124*), and the knockout of growth hormone releasing hormone (lit/lit mice, mutant for Ghrhr) (*122*). Similarly, partial loss of function of IGF-1R in neurons during development leads to reduced growth and lifespan extension (*125*). These mice gain slightly more weight with age than WT controls and have higher levels of subcutaneous adipose tissue, higher circulating leptin, and higher circulating lipids. These studies show decreased insulin signaling can alter global metabolism and extend lifespan in mammals. While they do not directly test the effects of other types of neural signaling, it does confirm that insulin signaling influences lifespan in mice.

Related work in humans suggests insulin regulation, sensitivity, and neuronal excitability all positively correlate with longevity. A transcriptome analysis of cerebral cortex tissue compared >85 year old humans to the <80 year old group. One transcriptional repressor, REST, negatively regulates neural excitation and FOXO1 expression, and its expression positively correlates with longevity (*126*). In *C. elegans* REST orthologues *spr-3* and *spr-4* are required for *daf-2*/IGFR knockout lifespan extension. The signaling mechanisms between neuronal REST activity and FOXO1 expression in peripheral tissues are not known, but these data provide ample evidence of conserved cell non-autonomous modulation of long-term health.

Similarly, genetic studies of centenarians have identified the locus encoding for tyrosine hydroxylase (TH), insulin (INS), and Insulin Growth Factor 2 (IGF2) as correlative with longevity (*127*). TH is the rate-limiting enzyme responsible for producing the neurotransmitter dopamine (*128*). This study looks more closely at the association of specific INS and IGF2 polymorphisms with longevity in humans. Polymorphisms in the subregion spanning TH and INS were significantly associated with lifespan in females, while polymorphisms in the region spanning TH and IGF2 were significant in males. These data support the role of insulin and dopamine signaling in human lifespan, and the gender difference observed may be explained by variations in metabolism between the sexes in old age. Supporting these findings, another research group genotyped a cohort of 90-109 year-olds and compared them to ancestry-matched younger people (ages 7-45). The 90+ cohort had a 66% higher incidence of a specific allele of the dopamine D4 receptor (DRD4 7R) which correlated with higher physical activity (*129*). Additionally, DRD4 knockout in mice leads to an ~8% decrease in lifespan. It's unclear what changes in dopaminergic signaling occur in these two populations and whether the increased physical activity is directly linked with the DRD4 allele.

Mice heterozygous at the insulin receptor substrate 2 (Irs2) locus do not differ from their control counterparts in food intake or body weight, but have significantly increased insulin sensitivity and live ~25% longer (*130*). Knocking out Irs2 in neurons (bIrs2) is sufficient to phenocopy the lifespan extension in the global knockout, and leads to decreased mRNA expression of superoxide dismutase 2 (Sod2) and Foxo1. These results support previous hypotheses that reduced insulin signaling in neurons modulates lifespan by enhanced protection from oxidative stress. It will be interesting to test whether enhanced Irs2 expression in the nervous system shortens mice lifespan.

Recent studies address questions about initiation and duration of a longevity intervention. Most studies introduce dietary or therapeutic interventions while the mice are young adults (*131*). This method is not entirely translatable to humans as we would likely be middle-aged or elderly before adopting a pro-longevity treatment regimen. Many labs are beginning to address this concern by testing the effects of longevity treatments after reaching midlife (*132, 133*). Applying these principles, supplementing

middle-age and elderly mice with intranasally administered recombinant human Hsp70 extends lifespan by ~10% and improves learning and memory during old age (*134*). Interestingly, Hsp70-treated mice had higher neuronal density in the temporal cortex and the hippocampus and immunostaining of the cerebral cortex for ribosomal proteins reveals more accumulation of proteasomal subunits in the Hsp70-treated mice. This suggests that Hsp70 promotes proteasomal activity and can extend lifespan in mammals, presumably through both cell autonomous and cell non-autonomous mechanisms.

The hypothalamus is a key producer of neuropeptides and hormones. It is likely many signals from the hypothalamus are important to relay information from neurosignaling pathways to the rest of the body. Additionally, the hypothalamus is key to maintaining homeostasis in energy balance, blood pressure, oxygenation, body temp, circadian rhythm, etc (*135*). Therefore, any perturbations in environment/environmental stressors are likely transmitted from sensory neurons to the hypothalamus. Overexpressing uncoupling protein 2 (UCP2) in mouse hypocretin neurons (Hcrt) increases body temperature specifically in the hypothalamus and leads to a decrease of 0.3-0.5ºC in core body temperature (*136*). These transgenic Hcrt-UCP2 mice have the same calorie intake relative to WT controls, but live 12-20% longer (*136*). These data suggest that neuronal regulation of core body temperature influences lifespan independently of DR and supports cell non-autonomous modulation of aging in mice.

The significant role the hypothalamus plays in cell non-autonomous modulation of aging is further supported by experiments modulating neuronal NF-kB levels in middle-aged mice. NF-kB is a well-studied transcription factor involved with inflammation and the immune response (*137*). As aging is correlated with increased inflammation, this study asked whether changes in NF-kB expression with age lead to pro- or anti-aging phenotypes. Middle-aged mice with activated NF-kB in the hypothalamus have slightly shorter lifespan whereas NF-kB inhibition extends lifespan by ~15% (*14*). NF-kB inhibition improves maze-learning, muscle endurance, and bone mass while NF-kB knockout in hypothalamic microglia is sufficient to phenocopy the lifespan extension from neural inhibition of NF-kB. Both neuronal and glial hypothalamic NF-kB

knockdown also leads to increased gonadotropin-releasing hormone (GnRH) mRNA expression in old mice. GnRH neurons are hypothalamic cells that regulate fertility through pulsatile GnRH release, and importantly, increases in GnRH expression or treatment of mice with GnRH injection correlates with improved neurogenesis and lifespan. The implication of this study is that increased inflammation from NF-kB expression during aging leads to loss of GnRH release and subsequent diminished health, and that restoring GnRH levels can reverse this effect. These data not only support a role for the hypothalamus in cell non-autonomous modulation of aging, but suggest a plausible signaling mechanism (GnRH release) for this role.

Recent work further explores the role of the brain in influencing health and longevity in mice. Brain-specific Sirt1 OE (BRASTO) mice live 10-15% longer than controls and have decreased cancer incidence (*138*). Middle-aged (20 month) BRASTO mice also exhibit improved healthspan parameters when compared to their aged matched controls; they are more physically active, have higher core body temperature, consume more oxygen, and have more non-REM sleep. Similar traits are often correlated with increased quality of life in elderly humans (*139-141*). While the causative mechanisms behind the improved health and longevity of BRASTO mice are not fully characterized, they show an increase in skeletal muscle mitochondria and mitochondrial functional gene expression in addition to higher mRNA expression of markers of neuronal activity in hypothalamic neurons. Further studies will hopefully identify how SIRT1 expression in the brain changes downstream physiology to improve health and longevity. This will likely involve modulation of neuronal signaling, perhaps due to improved health of neurons in the brain. It will also be interesting to find whether and how these changes are distinct from and overlap with pathways such as insulin-like signaling, that also emanate from the brain. This study further supports the role of neurons, and hypothalamic neurons in particular, as key modulators of cell non-autonomous aging.

Cellular senescence is a process characterized by permanent cessation of cellular proliferation. There is a large body of evidence supporting the hypothesis that the proliferation of senescent cells throughout an animal’s lifetime will accelerate their aging via pro-inflammatory secreted compounds. Plasminogen activator inhibitor-1 (PAI-1), a

neuronally expressed protein, regulates cellular senescence in mammals (*142, 143*). Klotho is an “aging-suppressor” gene and klotho knockout mice exhibit an accelerated aging phenotype and increased plasma PAI-1 levels when compared to age-matched controls (*144*). Knocking out PAI-1 in klotho mutant mice reduces senescence, normalizes telomere length, preserves organ function, and completely rescues their lifespan. These mice are likely short-lived due to accumulation of pro-inflammatory molecules from the “senescence messaging secretome” (SMS) that influences aging through cell non-autonomous signaling. In support of this hypothesis, there is mounting correlative data suggesting elevated PAI-1 levels in humans is strongly associated with aging disease states (*145*). While these data are intriguing, more experiments are needed to test whether neuronal SMS mechanistically accelerates aging.

Cell non-autonomous signaling from senescent cells is another likely mechanism of influencing aging. Mammals accumulate senescent cells throughout life, and when chronically present, senescent cells exacerbate age-dependent tissue deterioration due to inflammatory signals dubbed the senescence-associated secretory phenotype (SASP) (*146*). However, when transiently present, senescent cells can promote healthy outcomes like optimal wound healing (*147*). While the local effects of these signals have been well-studied, their systemic effects remain unclear (*148*). Much work is left to parse out the efficacious effects of senescent cells from SASP, but it is compelling that many anti-aging therapeutics shown to extend mouse lifespan seem to target and kill senescent cells (*149*). Whether the lack of these senescent cells is responsible for the pro-longevity effects from these drugs remains unclear. Senolytic compounds have recently entered clinical trials to test their efficacy in treating age-associated diseases (*150*) and represent a local and possibly systemic mechanism for cell non-autonomous modulation of aging.

The process of identifying pro- and anti-aging signaling events such as SASP is accelerated by the use of heterochronic (differently aged) animals sharing a circulatory system either through parabiosis or serum transfer. Incredibly, circulating factors in the blood of young mice can restore cellular function in older mice. Specifically, old mice exposed to young serum show enhanced Notch signaling in satellite cells, increased

hepatocyte proliferation, enhanced neurogenesis, decreased incidence of cardiac hypertrophy, and a reduced SASP response (*151-155*). Follow-up studies show the TGF-β superfamily member protein GDF11 decreases with age and restoring its levels-alone is sufficient to reverse age-related dysfunction in the skeletal system (*156*) as well as restoration of the neurogenic niche (*153*). Despite the observed benefits of young serum in older mice, an initial study found that young plasma is not able to extend lifespan in aged mice (*157*). Together, these results provide the basis for ongoing work identifying the mechanisms of these observations with the hope of showing that defined "youth factors" can improve human healthspan, lifespan, or both. These data highlight the significant role circulating proteins and secreted compounds likely play in modulating aging cell non-autonomously.

Labs with a previous invertebrate focus have begun to explore whether cell non-autonomous signaling pathways are conserved from invertebrates to mammals. To that end, globally knocking out the capsaicin receptor TRPV1 in mice causes no change in body weight or circulating growth hormone (GH)/IGF-1, but increases metabolic activity and energy expenditure and increases lifespan by 10-20% (*15*). In worms, knocking out the TRPV-1 orthologues, *osm-9* and *ocr-2*, requires the transcription factor CRTC-1 to influence lifespan. In mouse dorsal root ganglion (DRG) primary neuron cultures, TRPV-1 is also necessary for nuclear translocation of CRTC-1. CRTC-1 interacts with CREB in DRG neurons to regulate secretion of the neuropeptides CGRP and substance P at pancreatic beta cells. The model suggests TRPV-1 knockout mice have reduced CRTC-1 activity which reduces calcitonin gene-related peptide (CGRP) expression and increases pancreatic insulin secretion leading to better glucose tolerance and longevity. It is likely this type of translational study will become more common in the future, establishing which cell non-autonomous pathways of aging are conserved from invertebrates to mammals.

Together, mammalian aging studies show a clear role for cell non-autonomous signaling, but with less detail than in invertebrate organisms. Similar to invertebrates, insulin-like signaling represents the best studied pathway, but additional details are continuously emerging. Whether emanating from whole brain (SIRT1), regions of the brain (e.g. hypothalamic NF-kB

and UCP), or from individual tissues throughout the body (SASP, parabiosis), cell non-autonomous modification of systemic aging plays a role in mammals. For many of these pathways, the field is very new and more exciting data will likely come in the future.

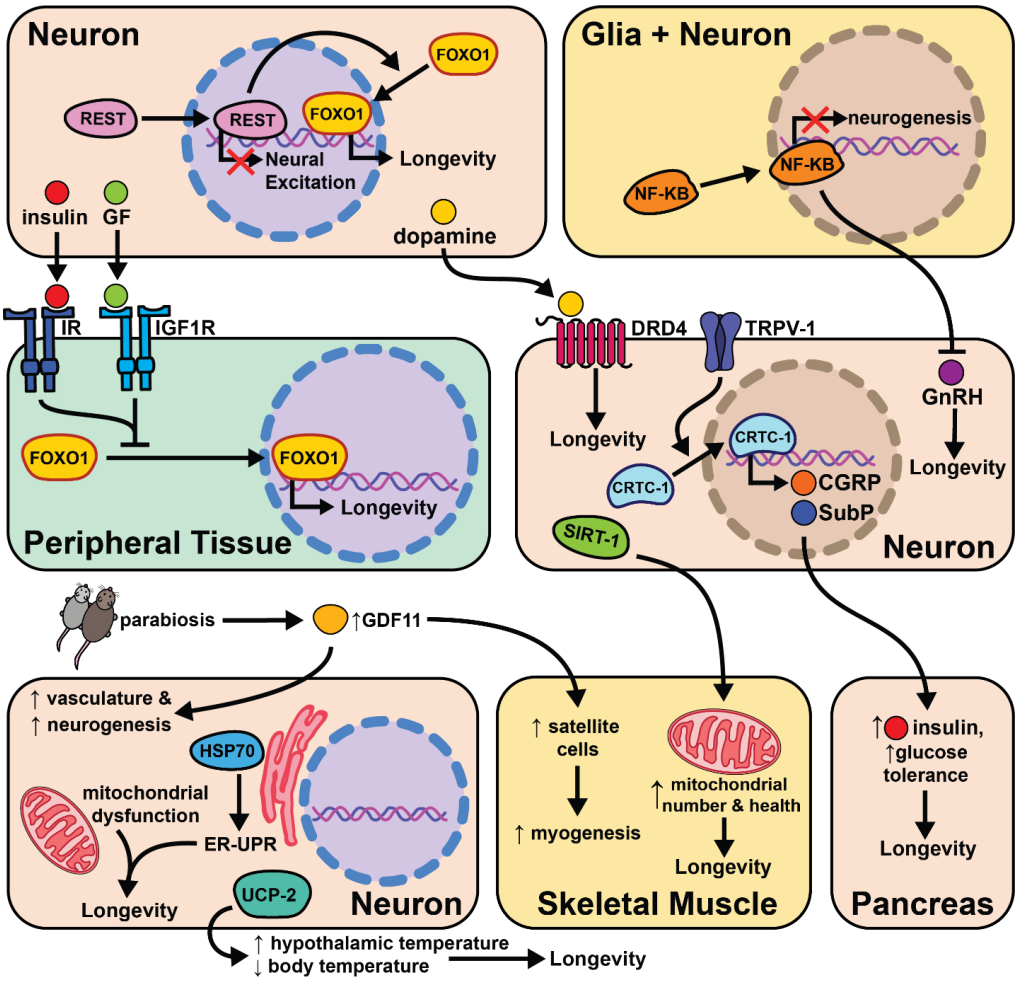

Figure 1.7. The intersection of cell non-autonomous signaling and aging in mammals.

Emerging Concepts

The work reviewed here (summarized in **Figure 1.8**) represents a small sliver of the extensive discoveries the aging field has made in three decades. Despite cell non-autonomous signaling being a relatively new concept to the field, the critical role the nervous system plays in promoting healthy aging is well established. Moreover, by understanding how key signaling tissues evaluate and appropriately integrate large amounts of internal (energy stores and the allocation of resources) and external

(availability of food/sexual partners and quality) stimuli, we can target the decision-making processes to mimic pro-longevity stimuli.

Despite the clear role that cell signaling plays in maintaining proteostasis, oxygen homeostasis, food regulation, and overall physiology, there is much we don't know about these areas. All fields, but invertebrate research in particular, could follow the lead of the behavior field, where there is convincing data establishing neural circuits and signaling molecules that regulate aspects of behavior. The aging field has occasionally completed similar work, but much less is understood about how cells recognize and relay signals about different types of internal and external environmental stimuli. This is to be expected, as behavioral outcomes are often measurable in seconds or minutes, whereas long-term health and lifespans require weeks or months (for invertebrates) or years (for mammals). Due to time constraints, this is an area where invertebrate research will likely need to lead, but once established the translatability of the networks should be measured. A subset of invertebrate studies do establish key aspects of these circuits, and if more effort was put into this endeavor, we may also find whether behavior and long-term health interact or are controlled by entirely distinct pathways.

With the establishment of cell non-autonomous regulation of aging in multiple pathways and organisms, there is immense therapeutic potential for this area going forward. Most therapeutics logically target the tissues where physiological change is important, while understanding signaling networks provides a unique opportunity to use the natural signaling network to "trick" key tissues into improving long-term health. This will not necessarily be easy, as targeting neural circuits using broad drugs (e.g. SSRIs) often have pleiotropic effects, but the better we understand the signaling networks the more specifically we could, in theory, mimic the signal(s). Using a signaling approach to anti-aging therapeutics would allow for induction of hormetic effects without the need for an acute stress, and has great potential to mimic well established longevity interventions such as dietary restriction. It will be of paramount importance, as the field continues to mature, that we test the conservation of these networks from simple worms to complex mammals. It is probable, however, that like the first discovered cell non-autonomous

network to influence aging (insulin-like signaling), other pathways will be partially or largely conserved.

To that end, drug screens in *C. elegans* for pro-longevity therapeutics have found neuromodulators that extend lifespan. More specifically, it is intriguing that serotonin antagonism can extend adult neuroplasticity and lifespan (*73, 158*). It is interesting that antagonizing serotonin signaling or other reward circuitry can lead to the same physiological changes that occur under hormetic stress. Using drug combinations to simultaneously target multiple aging pathways has also shown promise in *C. elegans* and *D. melanogaster*. For example, Admasu *et. al* identified two drug combinations that synergistically improve lifespan and healthspan. The synergistic effects of both drug combinations required TGF-B signaling and increased levels of monounsaturated fatty acids (*159*). Combining multiple anti-aging pharmaceuticals in flies has also proved efficacious. Simultaneous inhibition of mitogen-activated protein kinase kinase, mTOR complex 1, and glycogen synthase kinase-3 acted additively to increase *Drosophila* lifespan by 48% (*160*). These data suggest it may be possible to co-opt these pathways with small molecules to slow mammalian aging. This is crucial since it is likely humans will not change their environment (e.g. dietary restriction) in spite of potential benefits. By better understanding the molecular and signaling mechanisms of these pathways, these processes can be targeted directly, attaining benefits to human health while circumventing the challenges of implementing population-scale environmental perturbations.

Much of the work reviewed here investigates how the nervous system communicates with peripheral tissues to influence aging. This can be thought of as canonical cell non-autonomous signaling. However, recent data from invertebrates supports the idea of non-canonical cell non-autonomous mechanisms where the peripheral tissues use a retrograde signal back to the nervous system to maintain or further modify physiology (*105, 161-163*). This type of signaling is logical, as organisms require feedback from individual tissues to monitor homeostasis, but the role of retrograde signaling in regulation of aging is not well understood. This concept presents an interesting case for future studies to investigate the circuitry events that occur from the downstream

metabolic tissues back to the nervous system. It also provides an opportunity to better understand how cells at the interface of forward and retrograde signaling (i.e. the hypothalamus) make decisions that affect both upstream and downstream physiology.

Another area that will be crucial in future studies will be the identification of epigenetic regulation of these cell non-autonomous networks. While sentinel-like cells such as neurons signal to peripheral tissues to modify stress resistance and longevity, how these pathways maintain their benefits over time is not well understood. Studies show that just a day of hypoxia (*6*), for example, can extend lifespan in a worm, but whether that is just due to the persistent benefits of physiological changes made during that day or due to lasting epigenetic changes in peripheral tissues is an open question. The answer will give clues as to whether we could develop therapeutics that are only taken intermittently or whether more continuous treatment is necessary to extend healthspan. Additionally, studies in this area could separate how organisms respond to acute and chronic stress, and whether a series of acute activations of stress responses bring about long-term benefits.

Together, cell non-autonomous regulation of aging represents an exciting area of study that is well-established with lots of excited but open questions. The future of this area has great potential to both improve our understanding of the aging process and lead to useful therapeutic advances to improve human health.

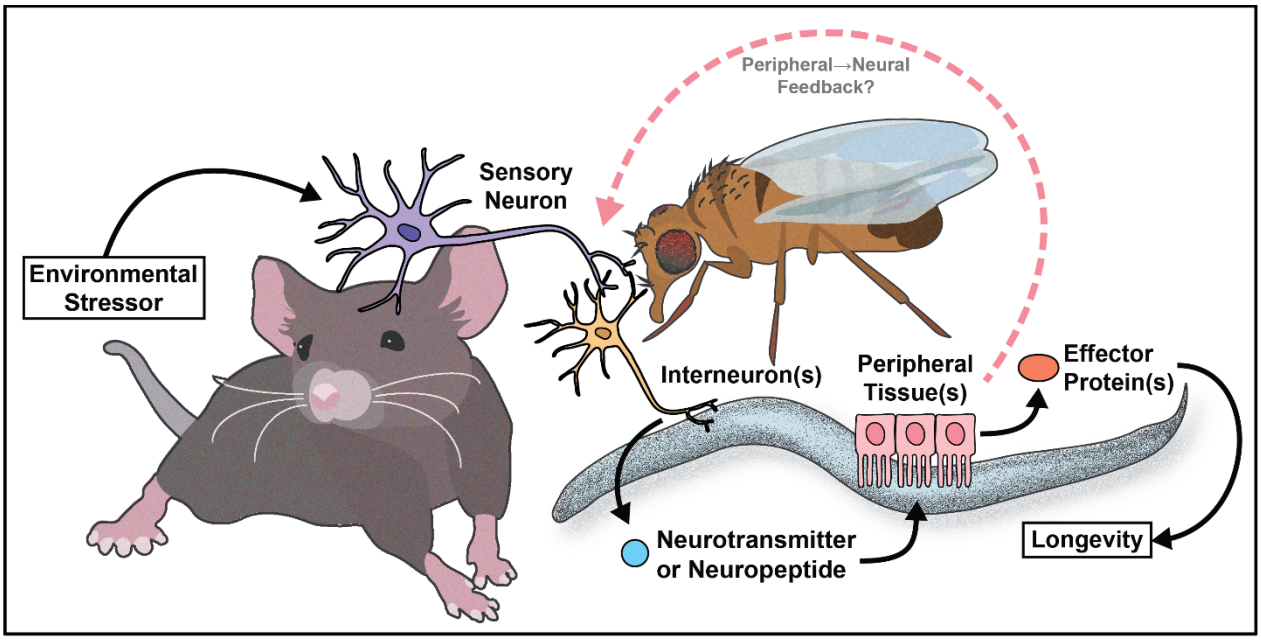

Figure 1.8. Summary model.

CHAPTER 2

Serotonin and Dopamine Modulate Aging in Response to Food Perception and Availability

Foreword

This chapter is the culmination of my primary thesis research exploring the neuronal circuitry necessary for *C. elegans* to properly respond to dietary restriction. Much of this work builds off the post-doctoral research performed by my mentor Dr. Scott Leiser who identified a novel pro-longevity gene *fmo-2* that acts downstream of hypoxic and DR signaling. Having shown the necessity of serotonin signaling during HIF-1 stabilization and the heat-shock response (HSR), I asked whether serotonin was involved in DR-mediated longevity. With substantial help from my co-author, Dr. Shijiao Huang, and direction from Dr. Leiser, we have begun to unravel the neuronal circuitry and signals nematodes use in the presence or absence of food. While much is yet to be uncovered (see chapter 5 for the beginnings of follow-up studies), I believe this project does a good job laying out the significant role the nervous system plays in regulating lifespan.
Note: this chapter is currently undergoing peer-review at *Nature Communications*.

Abstract

An organism's ability to perceive and respond to changes in its environment is crucial for its health and survival. Here we reveal how the most well-studied longevity intervention, dietary restriction (DR), acts in-part through a cell non-autonomous signaling pathway that is inhibited by the perception of attractive smells. Using an intestinal reporter for a key gene induced by DR but suppressed by attractive smells, we identify three compounds that block food perception in *C. elegans*, thereby increasing longevity as DR mimetics. These compounds clearly implicate serotonin and dopamine

in limiting lifespan in response to food perception. We further identify an enteric neuron in this pathway that signals through the serotonin receptor 5-HT1A/ser-4 and dopamine receptor DRD2/dop-3. Aspects of this pathway are conserved in D. melanogaster and mammalian cells. Thus, blocking food perception through antagonism of serotonin or dopamine receptors is a plausible approach to mimic the benefits of dietary restriction.

Introduction

Rapid advances in aging research have identified several conserved signaling pathways that influence aging in organisms across taxa(*164*). Recent work shows that many of these “longevity pathways” act through cell non-autonomous signaling mechanisms(*165, 166*). These pathways utilize sensory cells—frequently neurons—to signal to peripheral tissues and promote survival during the presence of external stress. Importantly, this neuronal activation of stress response pathways, through either genetic modification or exposure to environmental stress, is often sufficient to improve health and longevity. Despite mounting evidence that neuronal signaling can influence multiple longevity pathways, less is known about which specific cells and molecules propagate these signals.

Biogenic amines are among the most well-studied and conserved neuronal signaling molecules(*167*),(*168*). Specifically, serotonin and dopamine play well-defined roles in behavior and physiology. However, their role in aging is less well understood. Several recent studies implicate serotonin, but not dopamine, as an important signal in multiple *C. elegans* longevity pathways including the response to heat shock and hypoxia(*12, 58*). Dopaminergic signaling is associated with physical activity in humans and loss of this signaling decreases lifespan in mice(*129*) and blocks lifespan extension in nematodes(*169*). Serotonin and dopamine levels both decrease with age across species(*170, 171*), consistent with these signaling pathways promoting healthy aging. Despite rigorous study and clinical use of drugs that modify serotonin and dopamine signaling, our understanding of their complex actions and potential interaction is far from complete.

Dietary restriction (DR) is the most well-studied and consistent intervention known to improve health and longevity in organisms ranging from single-celled yeast to primates(*172*). DR leads to improved cell survival and stress resistance, complex intracellular signaling events, metabolic changes, and increased activity in multiple organisms. Nematode flavin-containing monooxygenase-2 (*fmo-2*) is necessary and sufficient to increase health and longevity downstream of DR. FMOs are highly conserved proteins that are also induced in multiple mammalian models with increased lifespan(*75, 76*). Having previously identified a role for *fmo-2* in aging, we wondered whether DR cell non-autonomously regulates *fmo-2* induction and whether perception of food through biogenic amines could be involved in the subsequent signaling pathway.

Results

Attractant food perception represses *fmo-2* to limit longevity.

We developed an integrated single-copy *mCherry* reporter driven by the *fmo-2* promoter to measure *fmo-2* induction. The reporter is primarily expressed in the intestine and responds to stimuli previously reported to induce *fmo-2*, including DR. As an intestinal protein(*173*), we expected that *fmo-2* would likely be induced cell autonomously by the change in nutrient intake under DR. To test this hypothesis, we asked whether the perception of food smell by worms in the absence of eating can abrogate the induction of *fmo-2.* Using a “sandwich plate” assay as described in **Figure 2.1A**, we were surprised to find a significant reduction in *fmo-2* induction when worms could smell but not eat food (**Figure 2.1B-C**). This reduction is consistent with a model in which increased *fmo-2* mediates the increase in longevity from DR, as food smell completely abrogates this lifespan extension (**Figure 2.1D**, lifespan statistics in Table 2.2)(*5*). We also find that active bacterial metabolism is required to abrogate *fmo-2* induction, as the “smell” of bacteria metabolically killed with 0.5% paraformaldehyde does not prevent DR from inducing *fmo-2* expression (Figure 2.2A-B). Since intestinal cells are not known to perceive external environmental cues such as smell, these results suggest that *fmo-2* expression is suppressed when food is present through cell non-autonomous signaling.

We next wondered what types of odorant compounds worms sense in this pathway. Bacteria are known to secrete hundreds of volatile compounds that are classified in three categories based on how they promote chemotaxis: attractants, repellants, and neutral compounds(*174-176*). We tested whether exposure to any volatile compound secreted from bacteria is sufficient to block the lifespan-promoting effects of DR or whether compounds identified as attractants and repellants oppositely regulate *fmo-2* induction. Using compounds derived from studies of the *E. coli* strain HB101 in a range of concentrations (Table 2.3), we find that attractants are more likely to suppress DR-mediated induction of *fmo-2* (**Figure 2.1E-F**) whereas neutral and repellant compounds can induce *fmo-2* under fed conditions (Figure 2.2C-H). We also find that many compounds suppress *fmo-2* expression, consistent with the hypothesis that this pathway is not acting through a single receptor **(Figure 2.1G**, all results in Figure 2.3A-Z). These results support a model in which perception of attractive smells secreted by *E. coli* abrogates the induction of the pro-longevity gene *fmo-2.* This is consistent with these smells preventing the lifespan-promoting effects of DR, possibly through a neural response to external stimuli that leads to physiological changes in peripheral tissues.

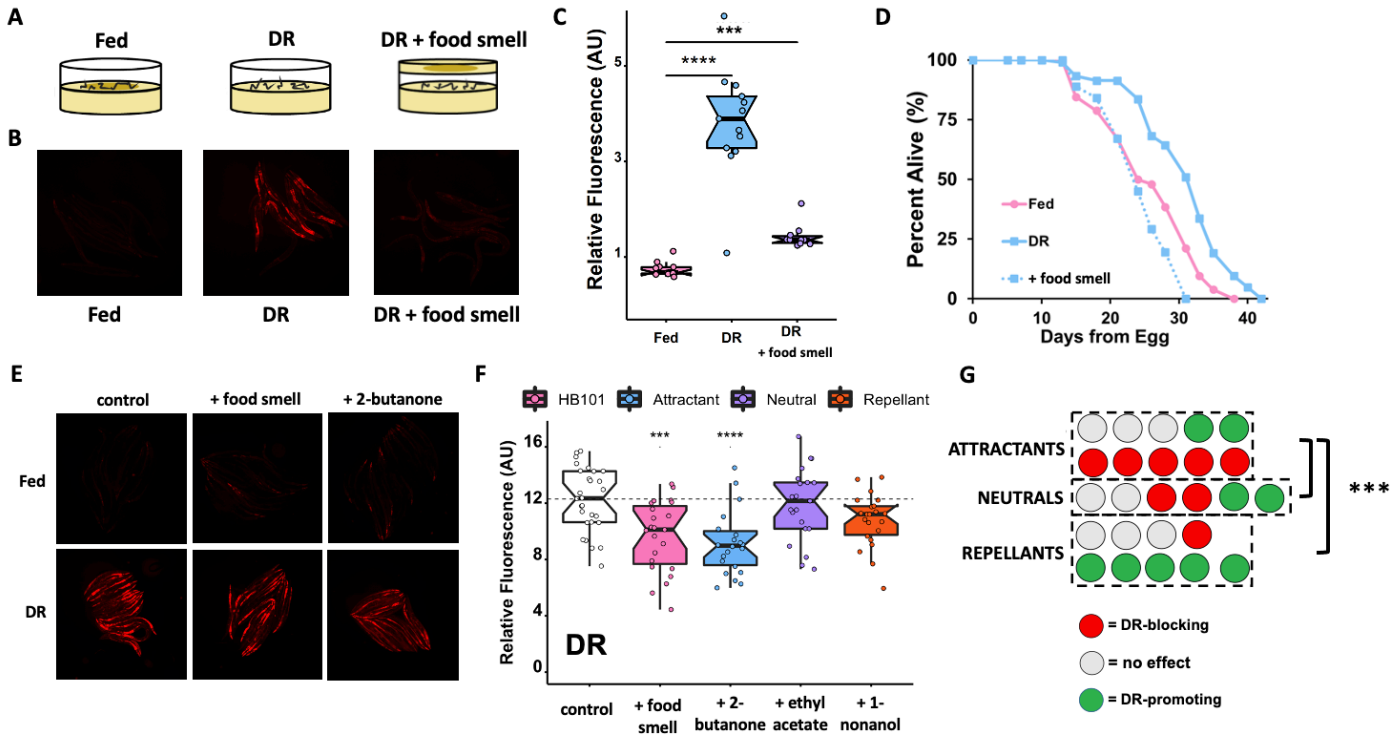

Figure 2.1. Attractive food smell blocks dietary restriction-mediated *fmo-2* induction and longevity.

Diagram of "smell plates" (**A**). Images (**B**) and quantification (**C**) of individual *fmo-2p*::*mCherry* worms on fed (pink), DR (blue) and DR + food smell (OP50) (purple). Survival curves (**D**) of N2 (WT) animals fed (pink) or DR (blue) under normal conditions (solid lines) or subjected to the smell of bacteria (dotted lines). Images (**E**) and quantification (**F**) of individual *fmo-2p*::*mCherry* worms on DR plates exposed to food smell (HB101) (pink) or attractive (2-butanone in blue), neutral (ethyl acetate in purple), or repellant (1-nonanol in orange) odorants. (**G**) Summary of the effects of 26 odorants on *fmo-2* induction during DR. *** denotes P<.001, **** denotes P<.0001 when compared to fed (Tukey's HSD) ### denotes P < 0.001 when compared to neutrals (ANOVA).

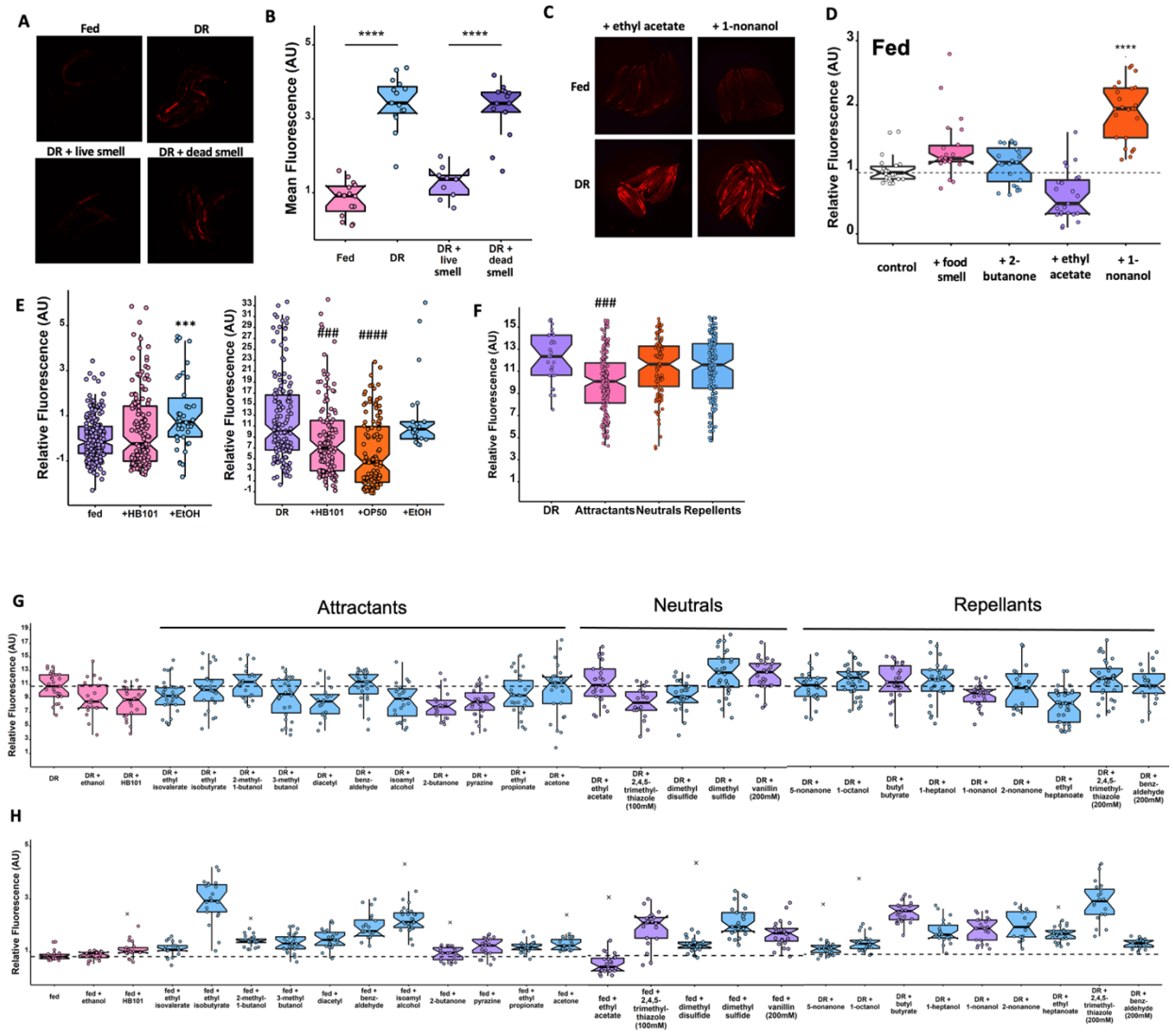

Figure 2.2. Odorant effects on *fmo-2* expression.
Images (A) and quantification (B) of individual *fmo-2p::mCherry* worms on fed (pink), DR (blue), and smell with live OP50 (light purple) or PFA-killed OP50 (dark purple). Additional images (C) and quantification (D) of *individual fmo-2p::mCherry* worms on fed plates exposed to food smell (pink) or attractive (2-butanone in blue), neutral (ethyl acetate in purple), or repellant (1-nonanol in orange) odorants. Summary of controls HB101 (pink), OP50 (orange) and ethanol (blue) effects on fed and DR conditions across experiments (E). Summary of worms treated with attractant (pink), neutral (orange) or repellant (blue) compounds compared to DR (G). All odorants effects on DR (G) and fed (H) conditions. **** denotes P<.0001 when compared to fed (Tukey's HSD). ### denotes P<.001 when compared to Neutrals or Repellants (Tukey's HSD).

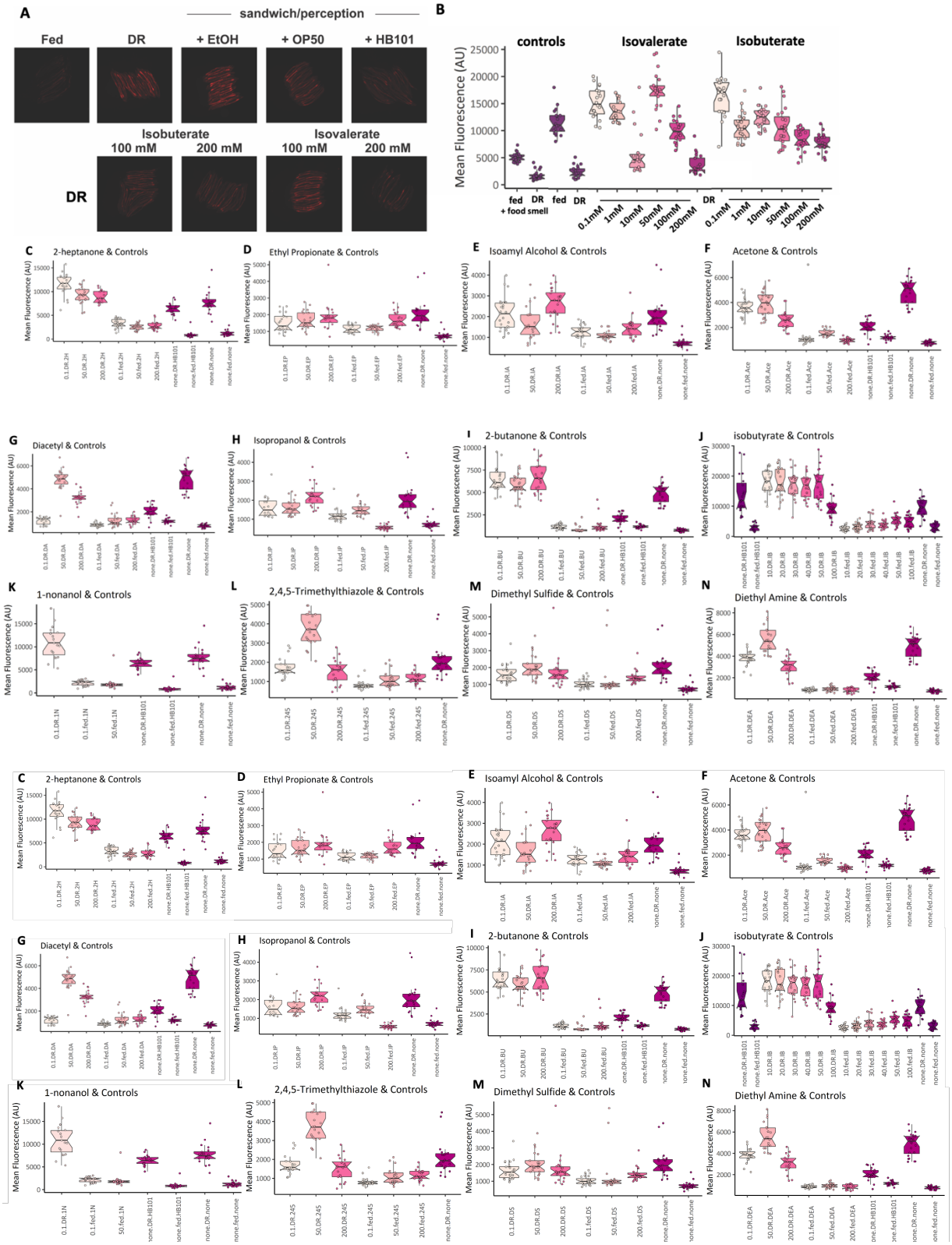

Figure 2.3. Titration experiments of odorants tested.
Panels show representative images (A) and quantification of *fmo-2p::mCherry* under DR (B- Z). Dosing and preparation can be found in Table S2.

Serotonin and dopamine antagonists induce *fmo-2* to mimic DR longevity. Biogenic amines can regulate pro-longevity pathways and are involved in behavioral changes in response to food(*12, 16, 58, 107, 177*). We next asked whether neurotransmitters are involved in the *fmo*-2-mediated food perception pathway. Using a targeted approach focusing on neurotransmitters and their antagonists, we tested for compounds sufficient to prevent the abrogation of *fmo-2* induction in the presence of food smell (Figure 2.4A-D). The biogenic amine neurotransmitter antagonists mianserin (for serotonin) and thioridazine and trifluoperazine (for dopamine) consistently and significantly restore *fmo-2* induction to DR levels in the presence of food smell (Figure 2.4E-F, **Figure 2.5A-C**). Mianserin is a tetracycline serotonin antagonist that is thought to competitively bind to specific serotonergic G protein-coupled receptors (GPCRs)(*178*) while thioridazine and trifluoperazine's mechanism of action involves blocking dopamine receptors(*179*). Importantly, while each compound induces *fmo-2* to a different extent (Figure 2.4G and 2.4I, **Figure 2.5D**), when combined with DR, no antagonist further induced *fmo-2*, suggesting they act in the same pathway (Figure 2.4H-I).

Diphenyleneiodonium chloride (DPI), an inhibitor of NADPH oxidase, acts as a positive control, and further induces *fmo-2* when combined with DR (**Figure 2.5E**). Because thioridazine and trifluoperazine act through similar mechanisms and the effects of thioridazine were more consistent in our studies, we focused further experiments on dopamine antagonism through thioridazine. Together, these results support antagonism of serotonin or dopamine as partial mimetics of DR in their induction of *fmo-2.*

To validate that the induction of *fmo-2* through biogenic amine antagonism is beneficial for longevity, we next asked whether these compounds extend lifespan. We find that both mianserin and thioridazine extend lifespan on agar plates in a dose-dependent manner (**Figure 2.5F-G**)(*180*). Since we identified mianserin and thioridazine through their induction of *fmo-2,* and previously found that *fmo-2* is necessary for DR-mediated lifespan extension, we next asked whether *fmo-2* was necessary for the beneficial longevity effects of mianserin or thioridazine. Our results show that the *fmo-2* loss of

function completely blocks the lifespan effect of mianserin (**Figure 2.5H**) and thioridazine (**Figure 2.5I**). Importantly, we also see that mianserin treatment combined with DR does not further extend lifespan (Figure 2.4J). These results are consistent with these compounds mimicking some aspects of DR-signaling, recapitulating part of the DR lifespan extension effect. Collectively, this supports a model where DR induces *fmo-2* because of decreased biogenic amine signaling and establishes neuromodulators as a useful tool to decipher where in the signaling pathway a cell, signal, or receptor plays a role in DR-mediated longevity.

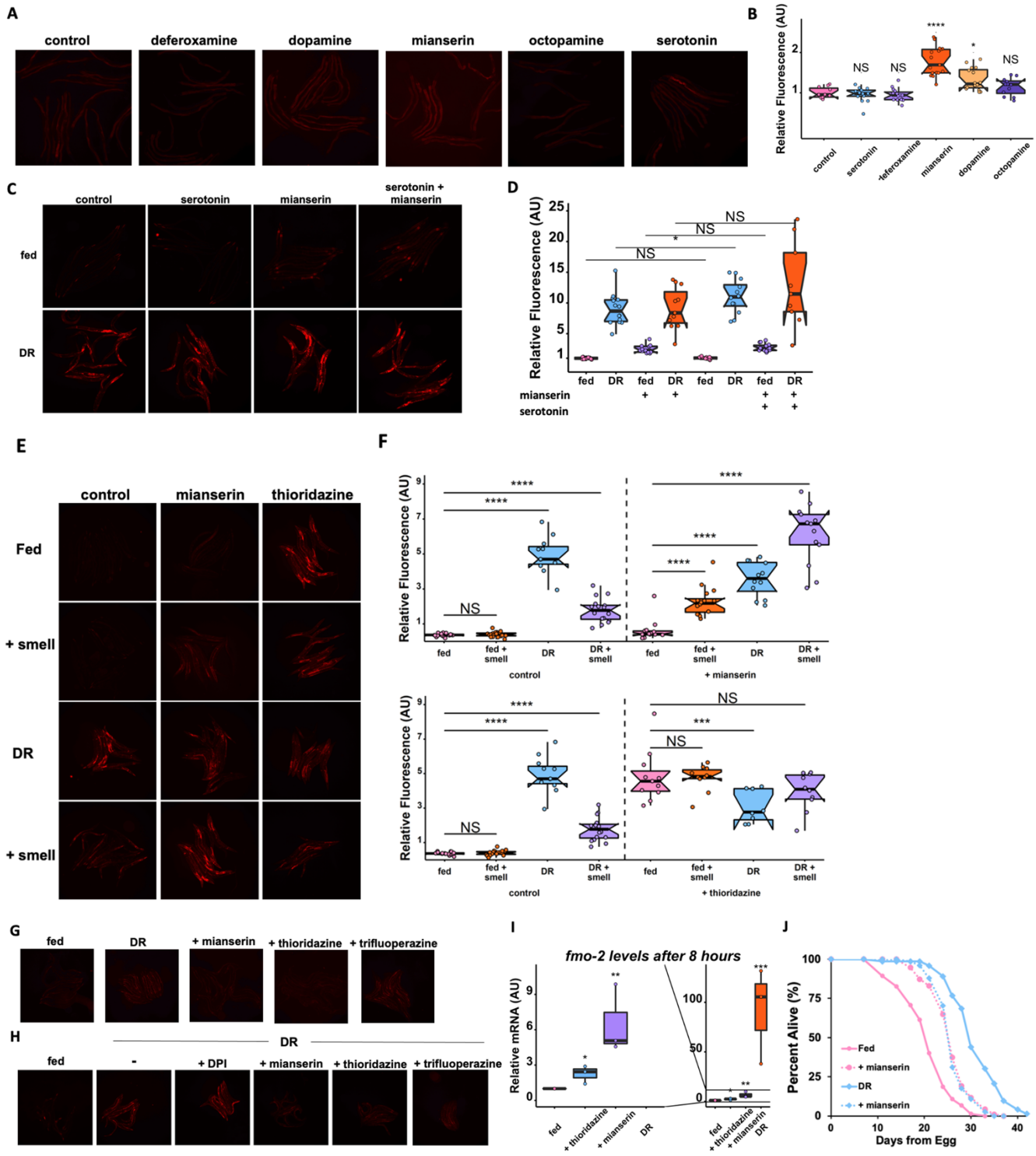

Figure 2.4. Induction of *fmo-2* by neuromodulators.
Images (A) and quantification (B) of *fmo-2p*::*mCherry* worms exposed to water (pink), dopamine (blue), serotonin (purple), mianserin (orange), octopamine (yellow), or deferoxamine (dark purple). Images (C) and quantification (D) of *fmo-2p*::*mCherry* exposed to water (pink), DR (blue), mianserin (purple) or both (orange) in combination with serotonin. Additional control images (E) and quantification (F) from Fig 2A-C. Images (G) quantified in Figure 2d. Images (H)

quantified in Figure 2E. qPCR results (I) for fmo-2 mRNA levels after 8 hours post DR (blue), mianserin (purple) or thioridazine (orange) treatment normalized to water control. Survival curves (J) of WT animals on fed conditions in pink and DR conditions in blue on water (solid lines) or 50μM mianserin (dotted lines). * denotes P<.05, ** denotes P<.01, **** denotes P<.0001 when compared to fed (Tukey's HSD).

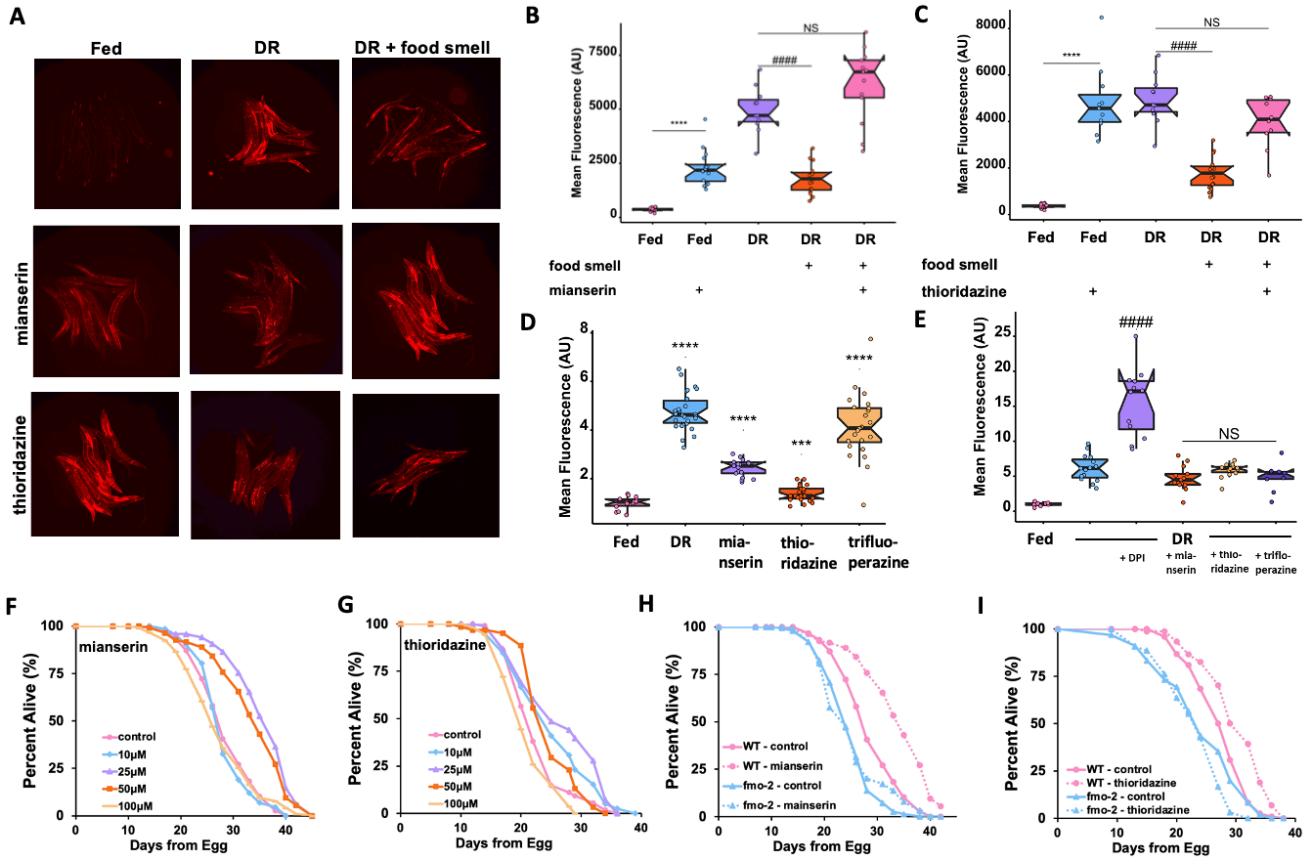

Figure 2.5. Serotonin and dopamine antagonists induce *fmo-2* and extend lifespan. Images (**A**) and quantification of *fmo-2p*::*mCherry* exposed 100μM of mianserin (**B**) or thioridazine (**C**) (blue) in combination with DR (orange) and food smell (pink) compared to DR alone (purple). Quantification (**D**) of *fmo-2p*::*mCherry* exposed to water (pink), DR (blue), 100μM mianserin (purple), thioridazine (orange), or trifluoperazine (yellow). Quantification (**E**) of *fmo-2p*::*mCherry* exposed to water (pink) or DR (blue) in combination with 500μM DPI (purple), 100μM mianserin (orange), 100μM thioridazine (yellow), or 100μM trifluoperazine (dark purple). Survival curves (**F**) of N2 (WT) animals treated with 0μM (water; pink), 10μM (blue), 25μM (purple), 50μM (orange), or 100μM (yellow) mianserin. Survival curves (**G**) of WT animals treated with 0μM (water; pink), 10μM (blue), 25μM (purple), 50μM (orange), or 100μM (yellow) thioridazine. Survival curves (**H**) of WT animals (pink) and *fmo-2* KO animals (blue) on water (solid lines) or 50μM mianserin (dotted lines). Survival curves (**I**) of WT animals (pink) and *fmo-2* KO animals (blue) on water (solid lines) or 25μM thioridazine (dotted lines). *** denotes P<.001, **** denotes P<.0001 when compared to fed (Tukey's HSD). #### denotes P<.0001 when compared to DR (Tukey's HSD).

DR signaling acts through a pair of enteric neurons.

Our initial results establish that antagonizing serotonin and dopamine signaling leads to induction of the longevity promoting *fmo-2* gene and rescue of the negative effects of food smell. Based on this, we hypothesized that the relative lack of food smell during DR leads to increased longevity through induction of intestinal *fmo-2.* Using this framework, we next sought to better understand how the sensing of bacteria (or lack thereof) is communicated to intestinal cells during DR. Our results, knocking down the synaptic vesicle exocytosis gene *unc-13,* support short-range neurotransmitters as necessary for *fmo-2* induction (Figure 2.6A-B).

In *C. elegans,* perception of the external environment is largely regulated by a specialized organ known as the amphid. Since a previous report using a solid-liquid DR approach suggested a pathway originating in the ASI amphid neurons, we first asked whether these cells are required to modulate *fmo-2* activity during DR (*67*). We find that not only are the ASI neurons (as measured by *daf-3* and *daf-7* RNAi) dispensable for food perception-mediated reduction in *fmo-2* expression (Figure 2.6C-D), but proper formation of the amphid (*daf-6*) is also not required (Figure 2.6E-F). This result is consistent with a non-canonical sensory neuron playing a role in food perception-mediated *fmo-2* suppression.

To better map this pathway, we next asked whether the biogenic amine serotonin is involved in the DR-mediated longevity pathway, and if so, where. We tested whether knocking out serotonin signaling would mimic the effects of DR. We subjected animals lacking *tph-1*, the rate-limiting enzyme necessary to produce serotonin, to DR and mianserin. *tph-1* animals are long-lived compared to wild-type(*181*) and not further extended by our DR protocol (**Figure 2.7A**) or mianserin treatment (Figure 2.8A). These data are supported by the abatement of *fmo-2* induction on DR (**Figure 2.7B-C**) and mianserin (Figure 2.8B-C) when animals are subjected to *tph-1(RNAi)*. As post-mitotic animals, *C. elegans* have a finite number of neurons with discrete connectivity and functions. Three neuronal pairs normally express *tph-1(182).* The hermaphrodite

specific motor neurons (HSN) are located along the ventral tail and regulate egg-laying(*183*) whereas two head neuron pairs, the amphid neurons with dual sensory endings (ADF) and the neurosecretory motor (NSM) neurons, are involved in modifying behavioral states(*177, 184, 185*). To investigate the potential role of these neuron pairs, we utilized *tph-1* cell-specific knockout and rescue strains and found that *tph-1* expression in NSM, but not the ADF, neurons (Figure 2.8D-E) is necessary (Figure 2.8F) and sufficient (**Figure 2.7D**) to promote DR-mediated longevity. These results implicate the NSM neurons as two of the primary neurons involved in reversing the effects of DR under food smell.

Recent research posits that NSM neurons function similar to enteric neurons with neural projections that directly communicate with the pharynx through a pair of acid-sensing ion channels (ASICs), DEL-3 and DEL-7. Signaling through these channels informs the worm to slow locomotion upon contact with food(*184*). These data led us to wonder whether the longevity effects of DR also require the ASICs channels to extend lifespan. We find that *del-7* mutants look phenotypically wild type in their induction of *fmo-2* and lifespan extension, in either DR or DR + food smell (Figure 2.9A-C). Interestingly, *del-3* mutant worms show abrogated induction of *fmo-2* under DR, and did not diminish *fmo-2* induction in response to the smell of food (**Figure 3.7E-F**). These *del-3* mutant animals still exhibit lifespan extension under DR, despite the decreased induction of *fmo-2,* which is not abrogated by the smell of food (**Figure 3.7G**). Together, these data support a model whereby the enteric NSM neurons release serotonin in response to food perception and the lack of this release extends longevity. In addition, the ASIC DEL-3 plays a role in the NSM to both behaviorally(*184*) and physiologically respond to food perception signals.

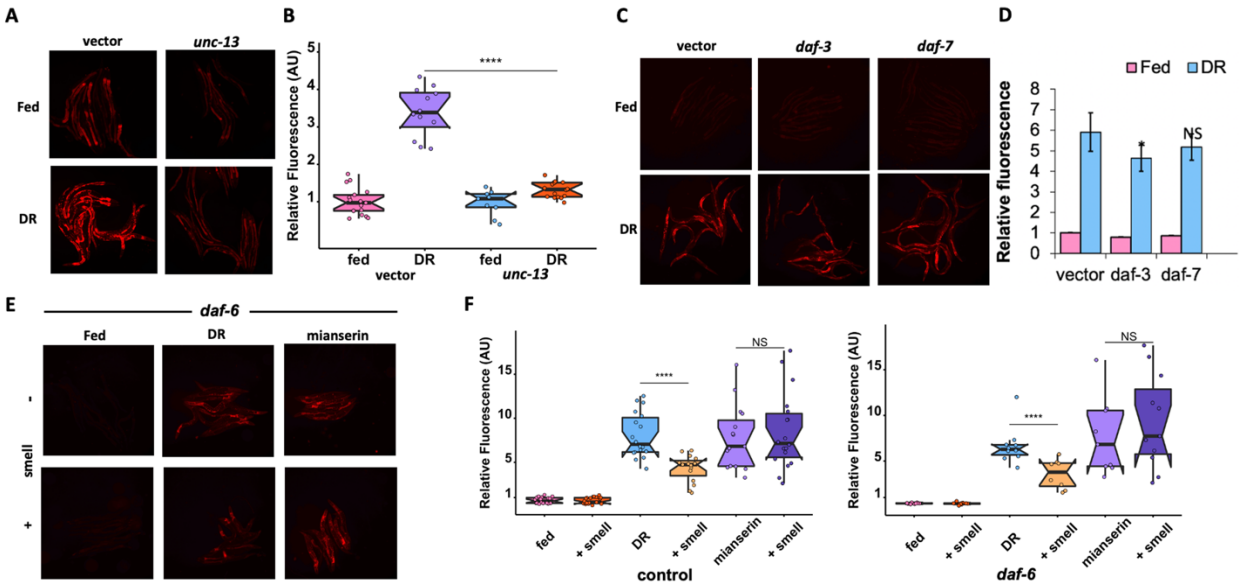

Figure 2.6. Neuronal gene necessity for *fmo-2* induction under DR/food smell/biogenic amin antagonism.
Images (A) and quantification (B) of individual fmo-2p::mCherry worms on fed (pink, blue) and DR (purple, orange) fed vector or unc-13 RNAi, respectively. Images (C) and quantification (D) of individual fmo-2p::mCherry worms on vector, daf-3, and daf-7 RNAi on fed (pink) or DR (blue). Images (E) and quantification (F) of fmo-2p::mCherry in a daf-7 KO background on fed, DR or exposed to mianserin (pink) and food smell (blue). * denotes P<.05, ** denotes P<.01, *** denotes P<.001, **** denotes P<.0001 when compared to DR (Tukey's HSD).

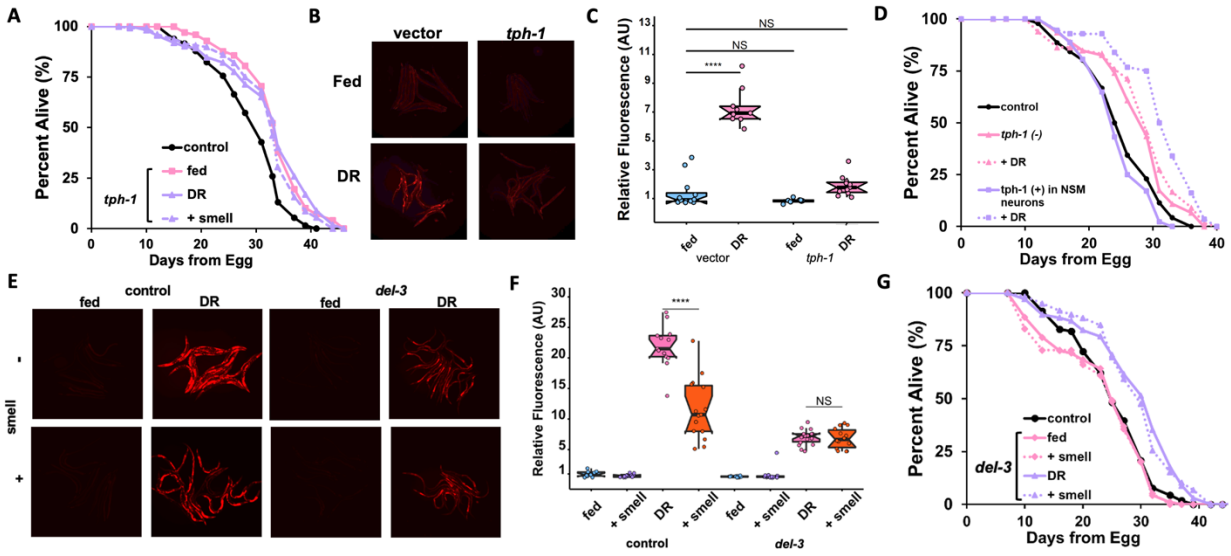

Figure 2.7. Food signals emanate from the NSM neurons.
Survival curves (**A**) of WT animals (black) and *tph-1* KO animals on fed (pink) and DR (purple) conditions exposed to food smell (dotted lines). Images (**B**) and quantification (**C**) of *fmo-2p*::*mCherry* exposed to *tph-1* RNAi on fed (blue) or DR (pink). Survival curves (**D**) comparing control (black), *tph-1* KO (pink), and *tph-1* NSM-specific rescue (purple) animals on fed (solid line) and DR (dotted lines). Images (**E**) and quantification (**F**) of *fmo-2p*::*mCherry* in a WT (control) and *del-3* background on fed (blue) and DR (pink) exposed to food smell (purple and orange, respectively). Survival curves of conditions comparing WT (black) to *del-3* (**G**) on fed (pink) and DR (purple) conditions in combination with food smell (dotted lines). **** denotes P<.0001 when compared to vector RNAi fed (Tukey's HSD).

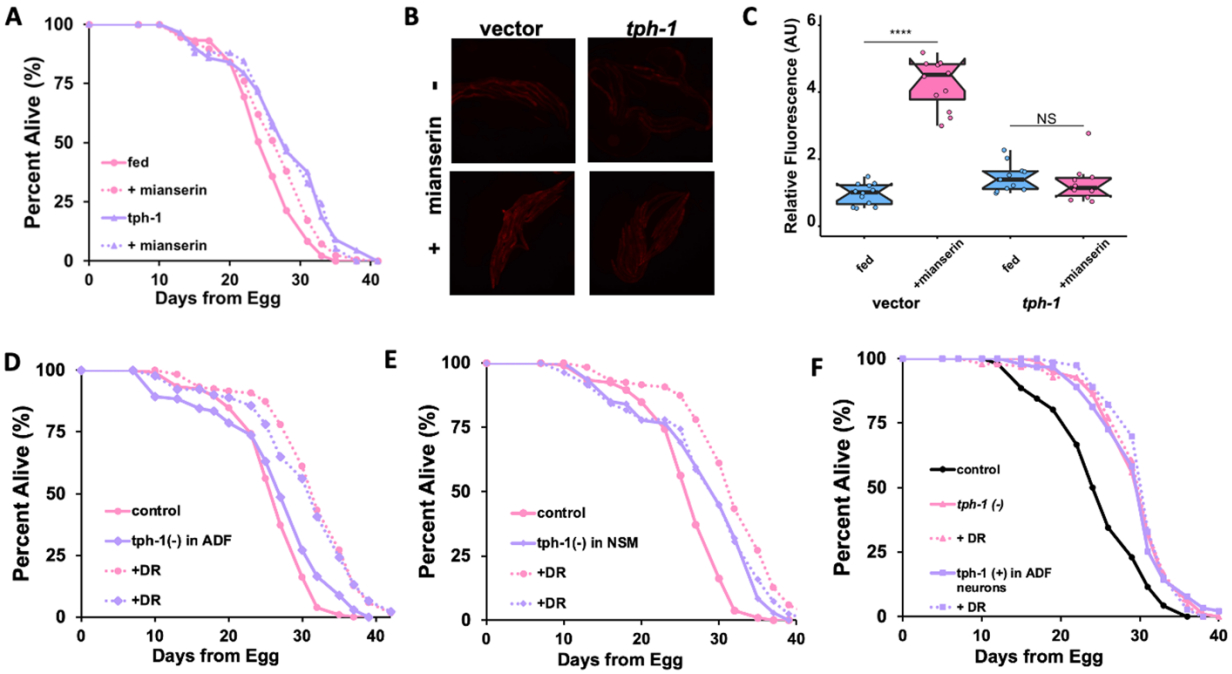

Figure 2.8. Serotonin and serotonergic neuron-regulation of *fmo-2* induction and longevity.

Survival curves (A) of WT animals in pink and *tph-1* KO animals in purple on water (solid lines) or 50μM mianserin (dotted lines). Images (B) and quantification (C) of individual *fmo-2p::mCherry* worms on *tph-1* RNAi exposed to water (pink) or 50μM mianserin (blue) conditions. Survival curves comparing control (pink) and *tph-1* NSM-specific (D) or ADF-specific KO (E) (purple) animals on fed (solid line) and DR (dotted lines). Survival curves (F) comparing control (black), *tph-1* KO (pink), and *tph-1* ADF-specific rescue (purple) animals on fed (solid line) and DR (dotted lines). **** denotes P<.0001 compared to fed (Tukey's HSD).

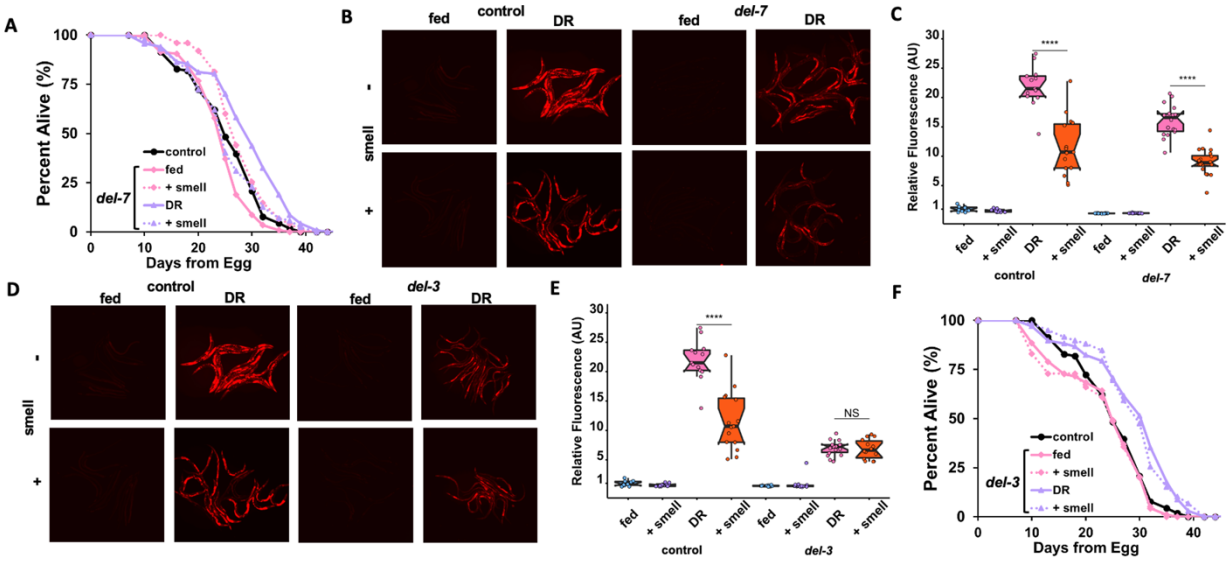

Figure 2.9. ASICs channels modify responses to DR and food smell.
Survival curves of conditions comparing WT (black) to *del-7* (A) on fed (pink) and DR (purple) conditions in combination with food smell (dotted lines). Images (B) and quantification (C) of *fmo-2p*::*mCherry* in a WT (control) and *del-7* background on fed (blue) and DR (pink) exposed to food smell (purple and orange, respectively). Images (D) and quantification (E) of *fmo-2p*::*mCherry* in a WT (control) and *del-3* background on fed (blue) and DR (pink) exposed to food smell (purple and orange, respectively). Survival curves of conditions comparing WT (black) to *del-3* (F) on fed (pink) and DR (purple) conditions in combination with food smell (dotted lines). **** denotes P<.0001 compared to DR (Tukey's HSD).

Mianserin mimics DR by antagonizing the 5-HT1A receptor SER-4.

Prior reports suggest that serotonin receptor orthologs *ser-1* and *ser-4* are necessary for the lifespan benefits of mianserin in *C. elegans*(*73*), and we hypothesized that a subset of the serotonin receptor orthologs will also be necessary for mianserin and DR-mediated *fmo-2* induction. After two generations of RNAi treatment, *ser-1* and *ser-4* were the only two receptors that proved necessary for *fmo-2* induction on mianserin (**Figure 2.10A**, Figure 2.11A-C) whereas *ser-4* knockdown most robustly abrogated DR-mediated *fmo-2* induction (Figure 2.11D-E). Further, we see that *ser-4(RNAi)* slightly but significantly increases lifespan and prevents DR from extending lifespan (**Figure 2.10B**), supporting the hypothesis that mianserin acts as a DR mimetic by antagonizing serotonin signaling that occurs during feeding. Finally, to investigate whether this effect is mediated by neuronal signaling or intestinal SER-4 expression, we rescued *ser-4* knockout animals with tissue-specific promoters and found that only neuronal *unc-119p::ser-4* is sufficient to rescue full induction of *fmo-2* under DR (**Figure 2.10C-D**). This is consistent with serotonergic signaling within the nervous system, and not directly to the intestine, regulating the response to food and food smell.

Thioridazine induces *fmo-2* and extends lifespan through Dopamine receptor DOP-3/DRD2.

Thioridazine is a compound that antagonizes dopamine receptor D2 (DRD2) in mammals(*186*), and induces *fmo-2* and mimics DR to increase longevity in nematodes (**Figure 2.4**). Based on its role in mammals, we tested whether nematode DRD2 is involved in DR and mianserin-related *fmo-2* induction and longevity. When the DRD2 ortholog *dop-3* is knocked down by RNAi, *fmo-2* induction is not affected in fed conditions but its induction by DR is diminished, while its induction by thioridazine is completely abrogated (**Figure 2.10E**, Figure 2.13A). This result is consistent with *dop-3* being required for dopaminergic induction of *fmo-2*. To demonstrate the epistasis of DOP-3 and SER-4 in the signaling pathway, we combined *ser-4* RNAi with mianserin and thioridazine treatment. The results show that *ser-4* depletion blocks *fmo-2* induction by thioridazine as well as suppresses *fmo-2* induction by mianserin, as expected (**Figure 2.10A**). Similarly, depletion of *dop-3* blocks both mianserin and thioridazine from inducing *fmo-2* (**Figure 2.10E**). These results support a model where both serotonin and dopamine signaling are epistatic to each other and are each required for full induction of *fmo-2* under DR. Interestingly, when *ser-4* or *dop-3* receptors are completely absent, via null mutation, the mutant animals show dysregulation of *fmo-2* induction, suggesting that the lack of biogenic amine signaling increases variability in responding to environmental changes (Figure 2.11F-G, 2.12B-D). To test whether DOP-3/DRD2 is necessary for lifespan extension by DR and mianserin, we depleted *dop-3* with RNAi under DR and found that *dop-3* depletion increases lifespan but is not further extended by DR (**Figure 2.10F**). Together, these results suggest that dopamine and serotonin signaling interactively induce *fmo-2* and extend lifespan under DR.

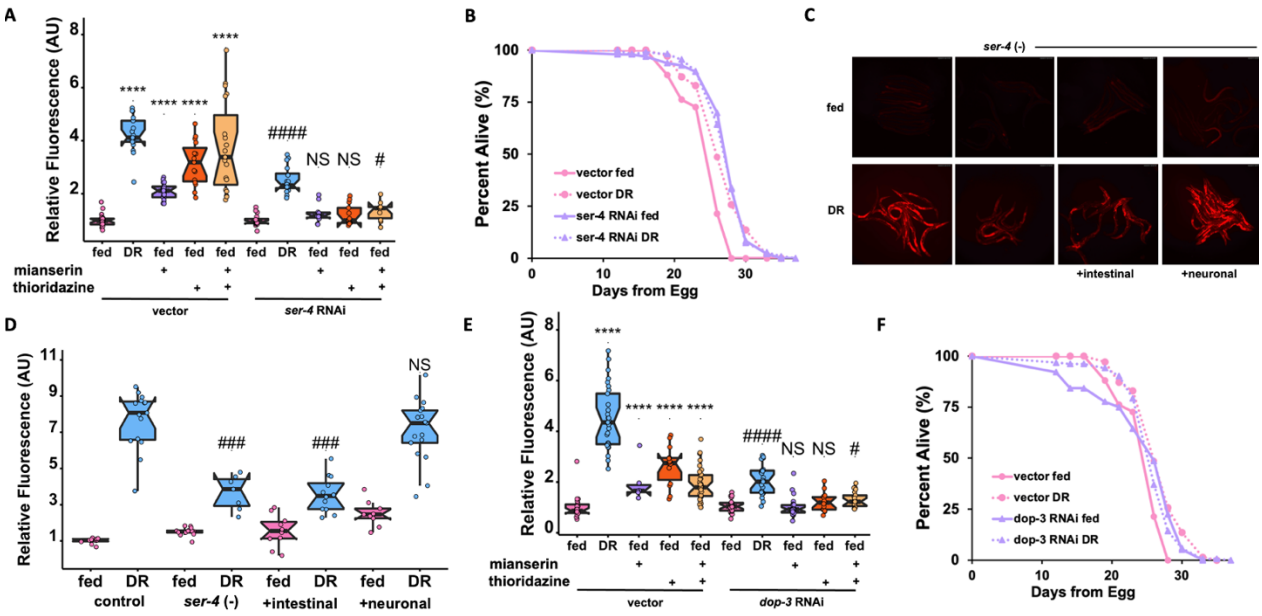

Figure 2.10. 5-HT1A receptor *ser-4* and DRD2 receptor *dop-3* act downstream of food perception.

Quantification (A) of individual fmo-2p::mCherry worms on fed (pink), and DR (blue) treated with 100μM mianserin (purple), 100 μM thioridazine (orange), or combined (orange) worms fed vector or ser-4 RNAi. Survival curves (B) of WT animals on vector RNAi in pink and ser-4 RNAi in purple on fed (solid lines) or DR (dotted lines) conditions. Images (C) and quantification (D) of fmo-2p::mCherry or ser-4 with tissue-specific rescues added back on fed (pink) and DR (blue). Quantification (E) of individual fmo-2p::mCherry worms on fed (pink), and DR (blue) treated with 100μM mianserin (purple), 100 μM thioridazine (orange), or combined (orange) worms fed vector or dop-3 RNAi. Survival curves (F) of WT animals on vector RNAi in pink and dop-3 RNAi in purple on fed (solid lines) or DR (dotted lines) conditions. **** denotes P<.0001 when compared to vector RNAi fed (Tukey's HSD). # denotes P<.05, #### denotes P<.0001 when compared to ser-4/dop-3 RNAi fed (Tukey's HSD).

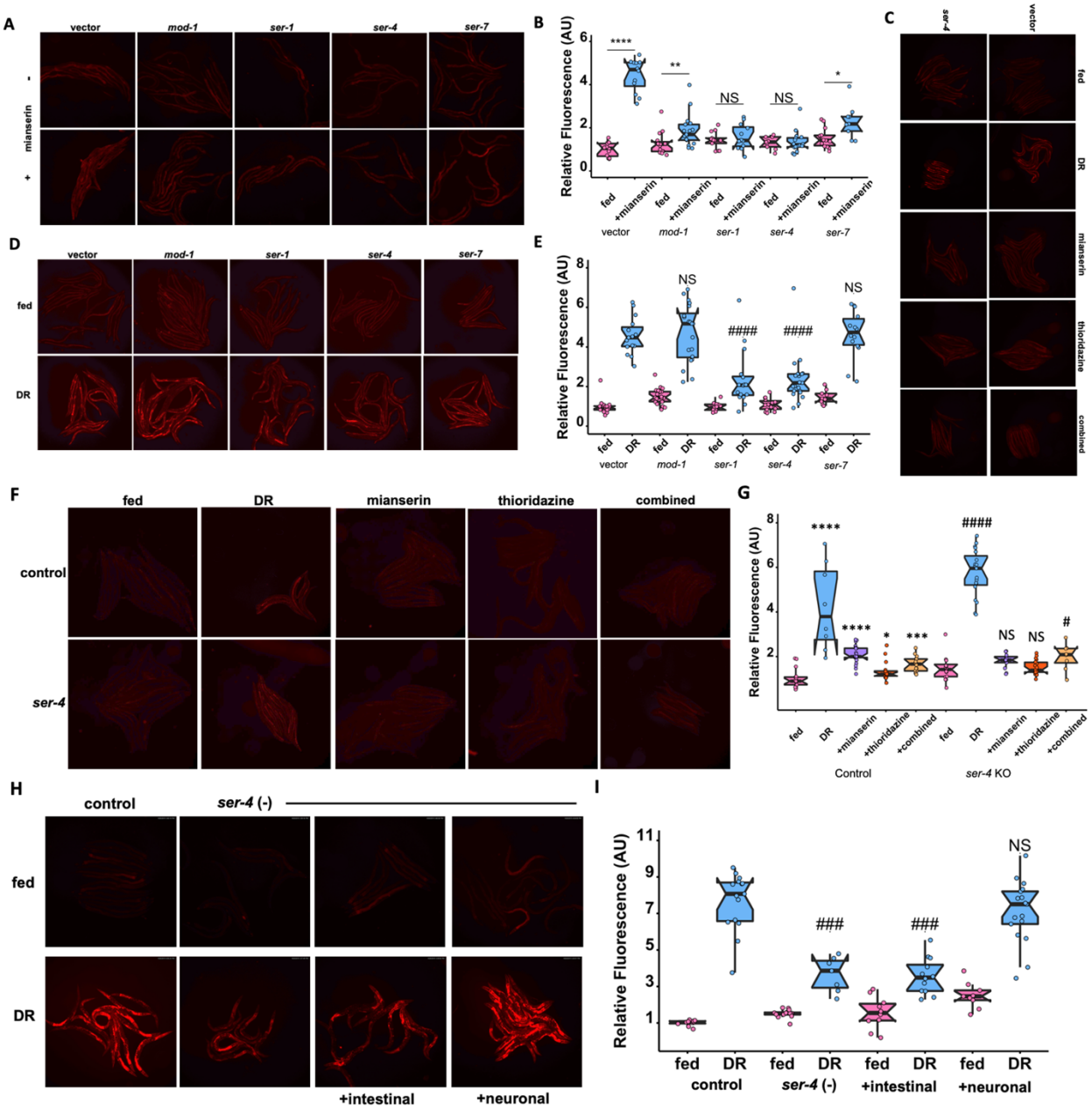

Figure 2.11. The role of serotonergic receptor signaling in *fmo-2* induction by DR and DR mimetics.

Images (A) and quantification (B) of *fmo-2p*::*mCherry* grown on serotonin receptor RNAi exposed to water (pink) or 50μM mianserin (blue). Images (C) quantified in Figure 3E. Images (D) and quantification (E) of *fmo-2p*::*mCherry* grown on serotonin receptor RNAi exposed to fed (pink) or DR (blue). Images (F) and quantification (G) of WT *fmo-2p*::*mCherry* or *ser-4* KO on fed (pink), and DR (blue) treated with 100μM mianserin (purple), 100 μM thioridazine (orange), or combined (orange). Images (H) and quantification (I) of *fmo-2p*::*mCherry* or *ser-4* with cell-specific rescues added back on fed (pink) and DR (blue). * denotes P<.05, ** denotes P<.01, **** denotes P<.001 when compared to fed (Tukey's HSD). ### denotes P<.001, #### denotes P< .0001 when compared to DR (Tukey's HSD).

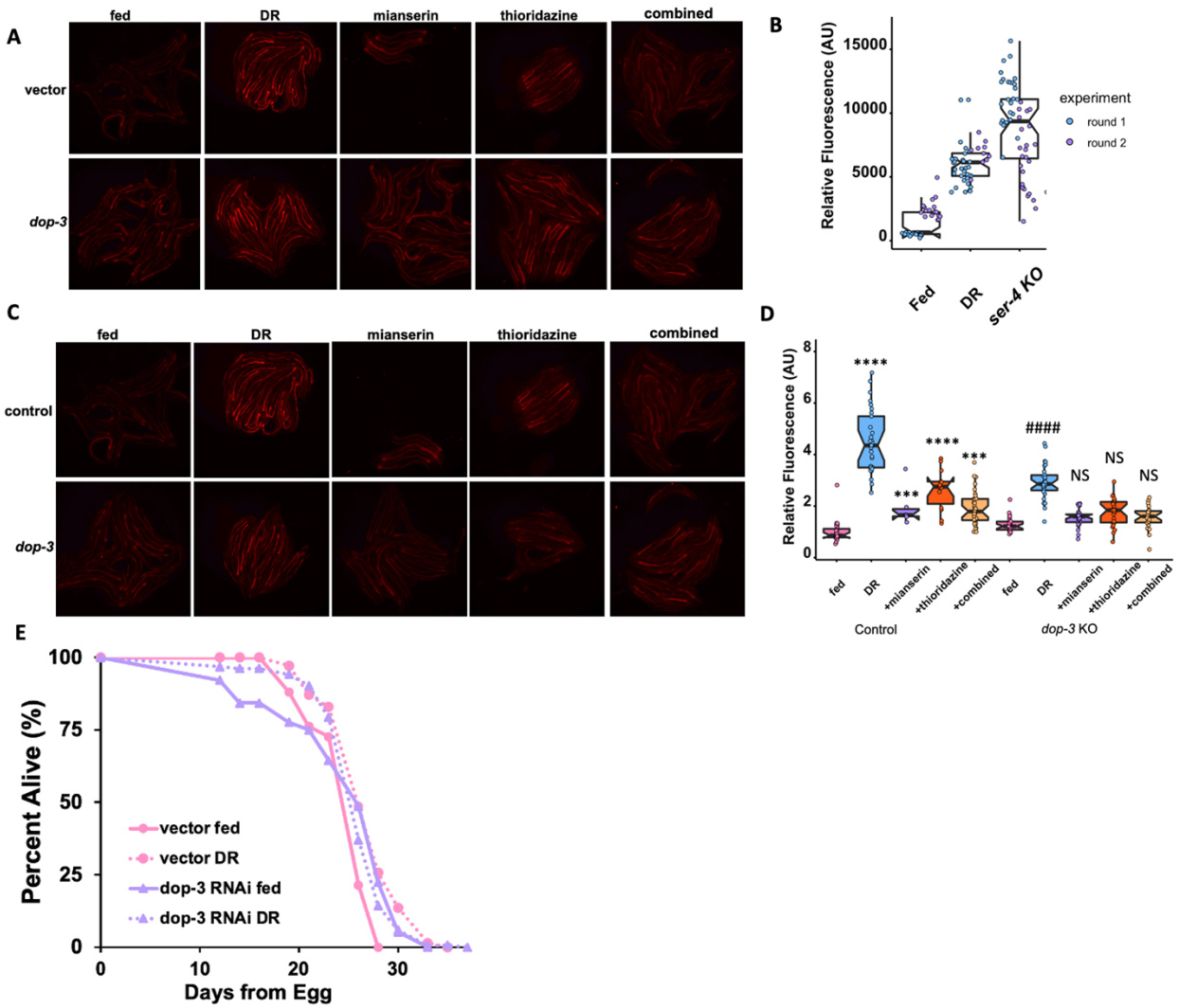

Figure 2.12. The role of dopaminergic receptor signaling in *fmo-2* induction and lifespan extension by DR and DR mimetics.

Images (A) quantified in Figure 3g. Summary (B) of fed and DR conditions of WT and *ser-4* KO animals across multiple experiments. Images (C) and quantification (D) of WT *fmo-2p*::*mCherry* or *dop-3* KO on fed (pink), and DR (blue) treated with 100μM mianserin (purple), 100 μM thioridazine (orange), or combined (orange). Survival curves (E) of WT animals on vector RNAi in pink and *dop-3* RNAi in purple on fed (solid lines) or DR (dotted lines) conditions. * denotes P<.05, ** denotes P<.01, *** denotes P<.001 when compared to fed (Tukey's HSD). ### denotes P<.001 when compared to DR (Tukey's HSD).

Mianserin induces FMOs and promotes stress resistance in mammalian cells. Having identified serotonin and dopamine antagonism upstream of *fmo-2* induction under DR, we were curious whether these relationships might be conserved. In mammals, previous studies show interventions that increase longevity often both induced Fmo genes and increased stress resistance(*76, 187*). Thus we tested whether mianserin and thioridazine are sufficient to induce mammalian Fmo genes and whether this induction could confer stress resistance, as a surrogate for longevity(*188*). Our results, using human liver (HepG2) cells, show that while thioridazine did not lead to any changes (Figure 2.13A), perhaps due to lack of DRD2 receptor expression, mianserin treatment at 2μM increased protein levels of mammalian FMO2 (**Figure 2.14A-B**) and FMO1 (Figure 2.13B-C), while 0.1μM mianserin increased protein levels of FMO4 (Figure 2.13B and 2.13D). FMO3 and FMO5 protein levels are not changed upon mianserin treatment (Figure 2.13B and 2.13E-F). Since stress resistance is often correlated with increased lifespan both within and between species, and *fmo-2* increases stress resistance in *C. elegans,* we next examined whether mianserin also promotes stress resistance(*188*). We treated cells with paraquat, an inducer of mitochondrial oxidative stress through increased production of the reactive oxygen species (ROS) superoxide, and find that 2 μM mianserin, the dose that showed maximal induction of FMOs, slightly but significantly improves the survival of HepG2 cells under an increasing dose of paraquat (Figure S2.14G). These data support serotonin antagonism as a conserved mechanism to induce Fmo expression and improve stress resistance.

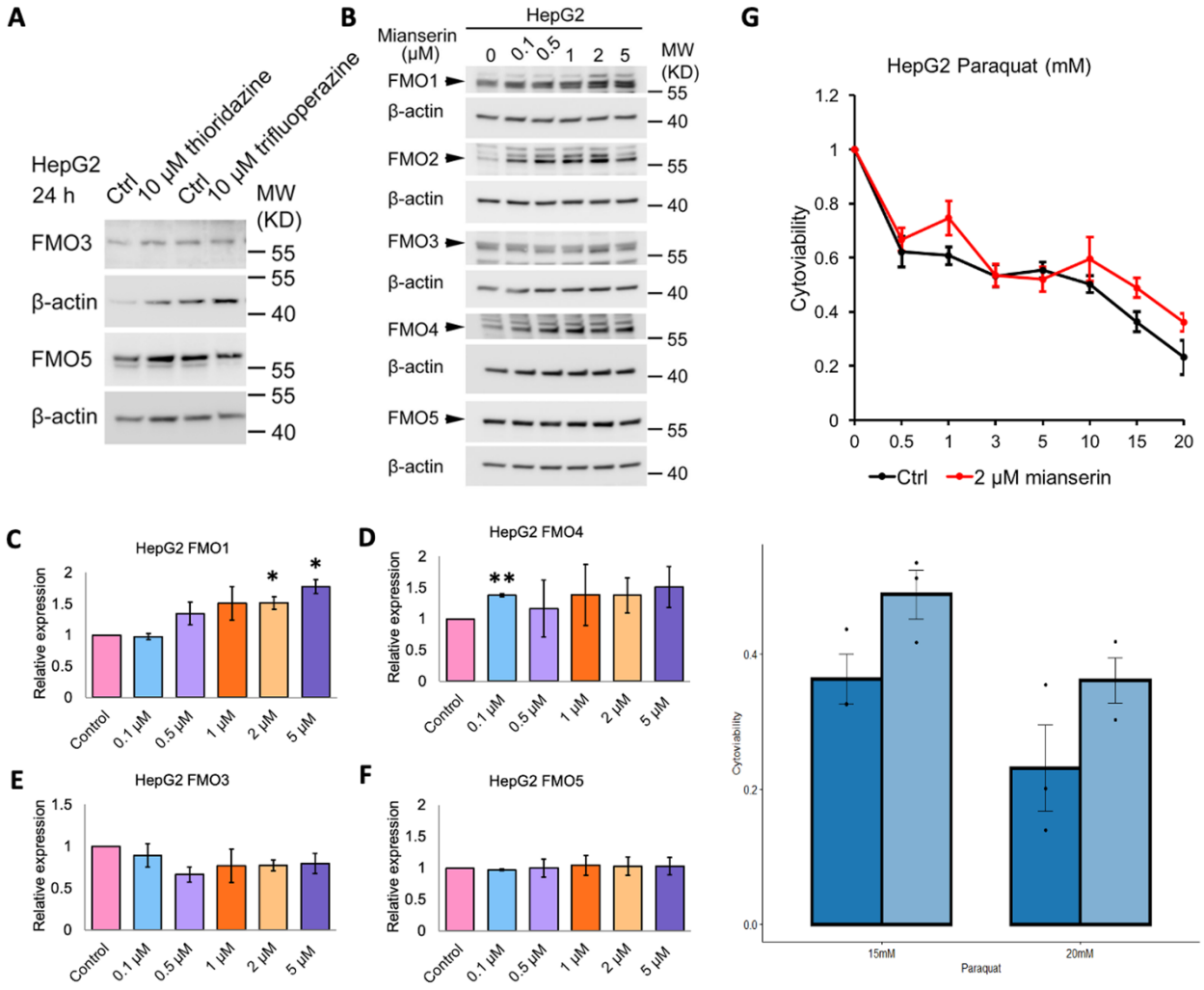

Figure 2.13. Induction of Fmos by biogenic amine antagonists.
Representative western blot image (A) of FMO3 and FMO5 in whole cell lysates from HepG2 cells treated with 10 μM thioridazine or trifluoperazine. Representative western blot image (B) and quantification of FMO2 (C), FMO4 (D), FMO3 (E), and FMO5 (F) in whole cell lysates from HepG2 cells treated with 0.1 μM, 0.5 μM, 1 μM, 2 μM, or 5 μM mianserin. Cell survival percentages of HepG2 cells treated with 2 μM mianserin (light blue) or untreated (dark blue) under 15 mM or 20 mM paraquat (G). * denotes P<.05, ** denotes P<.01 when compared to control (Tukey's HSD).

Mianserin extends *D. melanogaster* lifespan similar to *C. elegans.*

Since mianserin induces mammalian Fmos and promotes survival under paraquat stress, we tested whether it also affects lifespan in evolutionarily distant species. Similar to data in worms, recent data in the vinegar fly *D. melanogaster* show that altered serotonin signaling can change their ability to assess caloric quality and modulate lifespan(*16*). As we found a narrow range of effective doses in worms (**Figure 2.14F**), we tested a slightly higher dose of mianserin in vinegar flies (2 mM) for its effect on Fmo2 induction. The resulting data show that both mianserin and fasting (DR) increase expression of fly *fmo-2* expression (**Figure 2.14C**), but not *fmo-1* (Figure S2.15A). We then asked whether mianserin could also extend lifespan in flies. Using several concentrations, we find a positive correlation between mianserin dosage and increased lifespan until reaching a detrimental level of serotonin antagonism (**Figure 2.14D**, Figure S2.15B-D). We also find a comparable dose response among male and female flies. We note that mianserin treatment does not significantly alter food consumption (Figure S2.15E-F), as measured by the Fly Liquid-Food Interaction Counter (FLIC) assay(*189*). Together, these results are consistent with conserved induction of *fmos* by mianserin and DR, in addition to conserved lifespan extension.

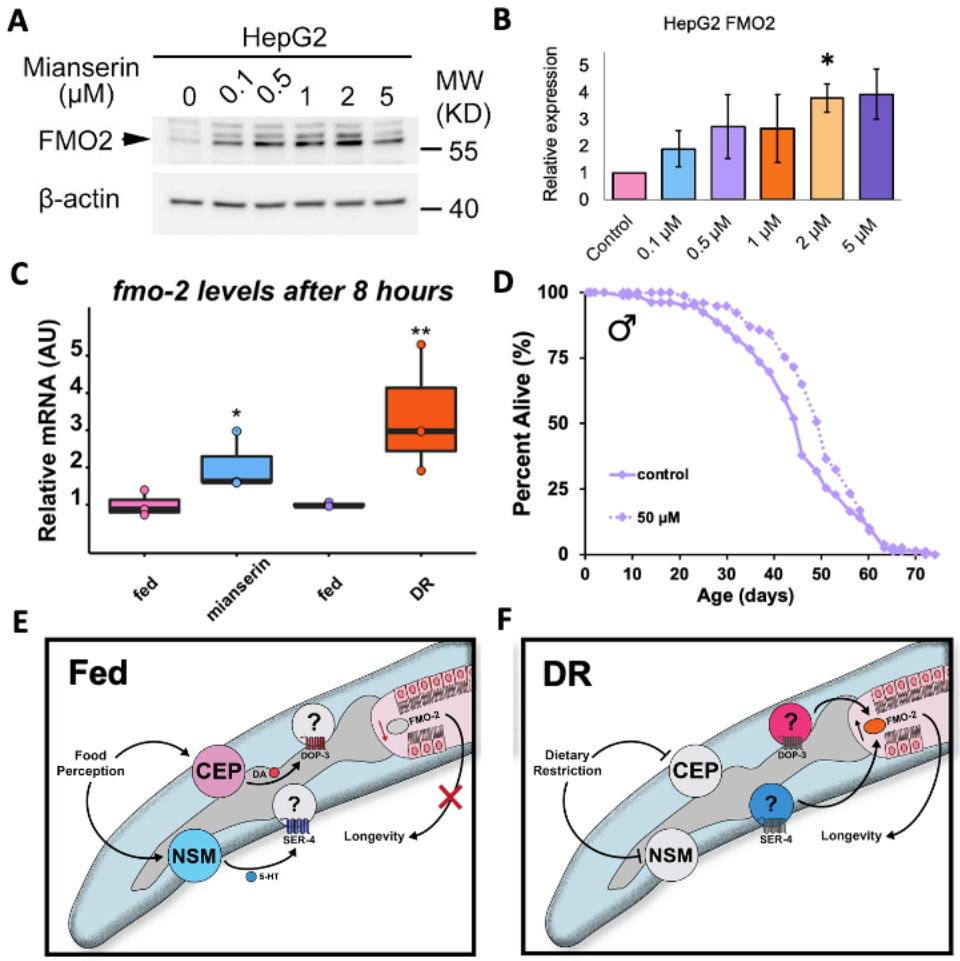

Figure 2.14. Serotonin antagonist mianserin induces FMO and improves health in Drosophila and mammalian cells.
Western blot image (A) and quantification (B) of FMO1 in whole cell lysates from HepG2 cells treated with 0.1 μM, 0.5 μM, 1 μM, 2 μM, or 5 μM mianserin. Fmo-2 mRNA levels (C) after eight hours of 2mM mianserin (blue) or starvation (orange) compared to water controls (pink and purple, respectively). Survival curves of male flies treated with water (solid line) or 50μM (dotted line) mianserin (D). Panels E and F depict the "on/off" state worm's toggle between when perceiving food. * denotes P<.05, ** denotes P<.01 when compared to control or fed (student's t-test).

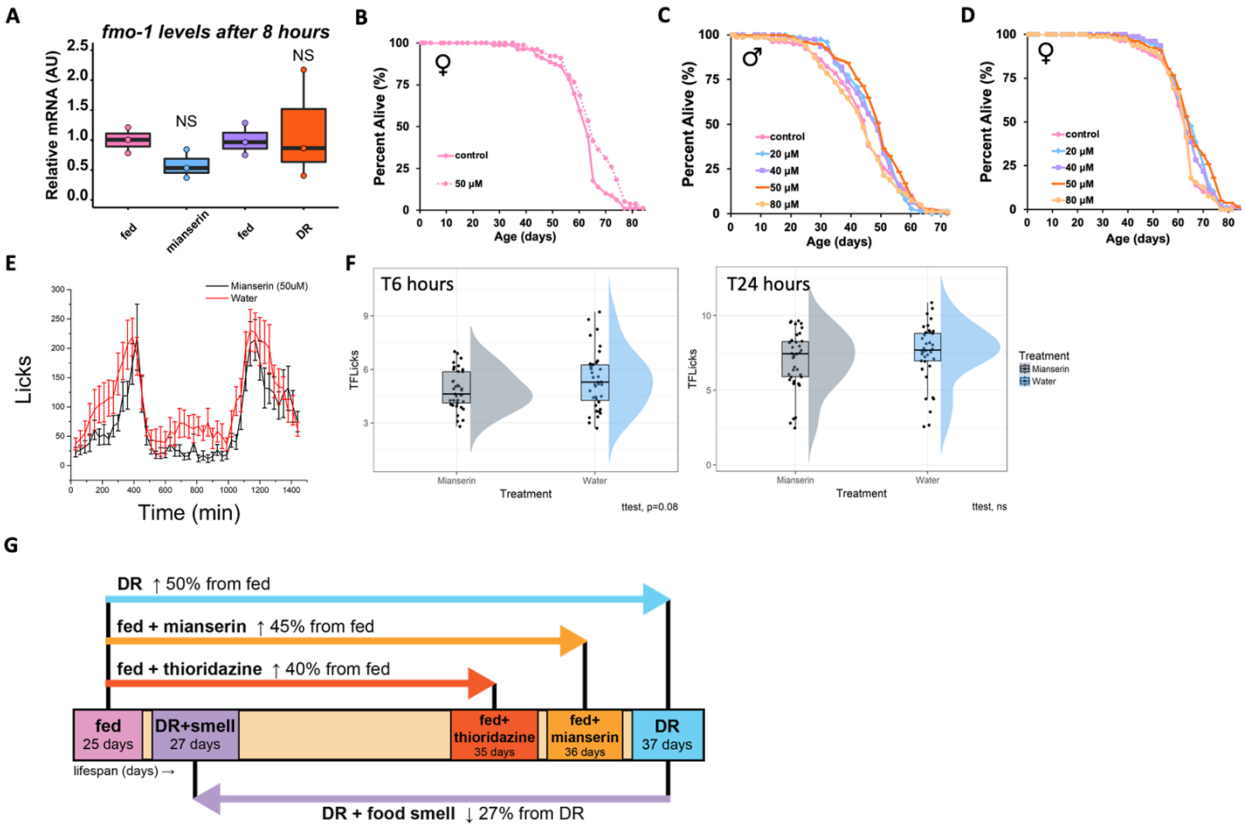

Figure 2.15. Effects of DR mimetic mianserin on Fmo expression, feeding, and lifespan. Fmo-1 mRNA levels (A) after 8 hours of 100μM mianserin (blue) or starvation (orange) compared to water controls (pink and purple, respectively) (red) or starvation (blue) compared to water control (black). Survival curves of female (B) flies dosed with water (solid line) or 50μM (dotted line) of mianserin. Combined survival curves of male (C) and female (D) flies dosed with water (pink), 20μM (blue), 30μM (purple), 40μM (orange), 50μM (yellow), or 80μM (purple) mianserin. 24 hours of FLIC assay data monitoring food intake in control (black) and mianserin (red) treatment (E). Extracted FLIC data (F) at 6 and 24 hours. Summary of the effects of food perception on DR and DR-mimetics longevity (G).

Discussion

Our experimental data in *C. elegans* support a model where the lack of an attractive (food) smell leads to a loss of serotonin release from the enteric NSM neurons and lack of serotonin binding to the SER-4/5-HT1A receptor. This in turn or in combination with other cues leads to a reduction in dopamine signaling to downstream DOP-3/DRD2 receptors. It is notable that both SER-4 and DOP-3 receptors are known to dampen adenylyl cyclase activity when bound, thus the lack of signal will increase the probability of excitement of the cell expressing these receptors. We hypothesize worms toggle their serotonin and dopamine neural activity “on” or “off” depending on the presence or absence of food, respectively (**Figure 2.5E-F**). Based on our ability to rescue DR benefits when food is perceived, we hypothesize that the perception of food during DR prevents the benefits of DR, rather than shortening lifespan through an independent pathway (Figure S2.15G). Critically, these data highlight that understanding how the nervous system evaluates and appropriately integrates large amounts of external stimuli, like the availability of food, allows us to target the decision-making processes to mimic pro-longevity pathways.

It is intriguing that dopamine and serotonin signaling interactively induce *fmo-2* and extend lifespan in a common pathway induced by dietary restriction. In nematodes, slowing locomotion in the presence of food is thought to be distinctly regulated by pharyngeal mechanosensation leading to dopamine release while dwelling behavior is potentiated by serotonin(*190*). Significant scientific effort has identified much of the specific circuitry these neurotransmitters use to promote changes in chemotaxis and egg-laying(*177, 184, 191-193*). The results suggest worms can interpret and implement a diverse set of responses to their changing environment. In mammals, SER-4/5-HT1A receptor activation increases dopamine release throughout the brain(*194, 195*). Similarly, recent work shows release of serotonin and dopamine in the human brain influence non-reward-based aspects of cognition and behavior like decision making(*196*). These findings support a conserved link between these two neurotransmitters in regulating complex phenotypes like aging.

It is also intriguing that one of these drugs, mianserin, successfully induces Fmo genes in both mammals and flies, and leads to increased stress resistance and lifespan, respectively. Since mianserin treatment extends fly lifespan we suspect it acts through a similar mechanism, serotonin antagonism, to mimic DR. This hypothesis is bolstered by *fmo-2* induction under acute mianserin exposure and fasting, analogous to what we see in *C. elegans*. It is not known whether FMOs or 5-HT1A receptors are necessary for mianserin or DR-mediated longevity in flies, but 5-HT2A receptors are necessary for proper food valuation(*16*) suggesting that altering serotonin signaling may prove fruitful in future studies. In cells, the induction of Fmos by mianserin must be direct, suggesting that either serotonergic signaling is more direct in mammalian systems, or more likely, there are other nuances in this signaling in mammals we do not yet understand. Mammals and *C. elegans* share a single common ancestral Fmo(*173*) and mammalian Fmos share similar homology to *C. elegans fmo-2*, with Fmo5 having the highest % identity. It is notable that 5-HT1A expression is detected in hepatocytes (The Human Protein Atlas), supporting a similar mechanism in these cells and suggesting that FMOs can be induced by serotonin antagonism both directly and indirectly. It will be interesting to investigate whether mianserin is beneficial for health and longevity in mammals. To achieve this goal, it is imperative that we understand the causative changes of pro-longevity drugs, such as atypical serotonin antagonists that are known to have pleiotropic effects in humans. In addition to providing the potential for long-term health benefits, this knowledge will benefit our understanding of serotonin and dopamine signaling networks that affect numerous human processes and diseases outside of aging.

Materials and Methods

Strains and growth conditions

Standard procedures for C. elegans strain maintenance(*197*) were used where experiments were performed on animals fed Escherichia coli (OP50) from egg and maintained on solid nematode growth medium (NGM). Additionally, worms were exposed to the smell of OP50 or HB101. Table 2.1 includes a list of the strains and RNAi conditions used in this study. All genotypes were confirmed using PCR.

fmo-2p::mCherry construct

We PCR amplified *mCherry* from pHG8 and the *fmo-2* promoter from the worm gDNA under the *fmo-2* promoter and cloned them into pdonr221 and P4-P1r, respectively. From here, they were combined using Gateway LR cloning (Invitrogen) to create *fmo-2p*::*mCherry*::unc-54 3'UTR on PCFJ150 (pHAM001).

SER-4 rescue constructs

We purchased donor plasmid pPD117.01 from Addgene and used Gibson cloning (NEB) to swap out promoters driving cDNA of *ser-4*::SL2::GFP (on backbone) expression. We used the *unc-119* promoter (pHAM002) to target all neurons and the *vha-6* promoter (pHAM003) to target the intestine. All plasmids were verified via restriction digest and sanger sequencing. ApE files available upon request.

Microinjection

Single-copy integration of pHAM001 using the ttTi5605 (EG6699) Mos allele was performed as previously described(*198*). Overexpression transgenic animals were generated by injecting PureLink (Invitrogen) miniprepped DNA clones (~50ng/µL) with fluorescent co-injection marker *myo-2p*::mNeonGreen (15 ng/µL) and junk DNA (up to 100 ng/µL) into gonads of day 1 gravid adult hermaphrodites. Standard protocols were followed to isolate and obtain stable over-expression mutants(*199*). Because transgene expression can vary substantially, we typically characterized 2-4 independent transgenic lines per experiment.

Lifespan measurements

Lifespans were carried out as previously described with minor modifications (*200*). Briefly, 20 - 30 gravid adult animals were placed on NGM plates for a timed egg-lay. After 12-16 hours, these animals were removed. Once their progeny reached late L4/early adult stage, animals were transferred to plates with 33 µL of 150 mM fluorodeoxyuridine (FUdR) and 100 µL of 50 mg/mL Ampicillin per 100 mL NGM to prevent the development of progeny and growth of bacteria. Roughly 75 worms were placed on each NGM + FUdR plate seeded with concentrated bacteria (10×). A minimum of two plates per strain per condition were used per replicate. Lifespan plates were transferred periodically during early adulthood to prevent starvation and avoid contamination. Animals were scored as dead and removed from the experiment when they did not move in response to prodding under a dissection microscope.

RNAi knockdown

The RNAi feeding bacteria were obtained from the Vidal RNAi library. All RNAi plasmids were sequenced to verify the correct target sequence. Animals were exposed to RNAi plates from egg on plates consisting of NGM supplemented with 1 mM β-D-isothiogalactopyranoside (IPTG) and 25 µg/ml carbenicillin. At late L4 stage of development the animals were transferred to plates containing freshly seeded RNAi bacteria plus FUdR.

PFA treatment

In order to metabolically kill OP50 in food smell assays, bacteria cultures were treated with 0.5% PFA. After 16 hours of shaking, 50 mL of the bacteria were aliquoted into 250 mL Erlenmeyer flasks. 32% PFA was added to the flasks to get the desired final PFA concentration (e.g., 390 µL of PFA was added to get the final concentration of 0.25% PFA). PFA-treated bacteria were shaken at 37^{o}C for 1 hour and then transferred to 50 mL conical tubes, centrifuged and washed with LB five times to remove residual PFA before seeding.

Drug treatments

Recent reports show improved health outcomes and longevity in nematodes treated with mianserin(*73*), but only in liquid culture (*201*). As our studies are on agar plates, we modified previous protocols by adding mianserin, thioridazine or trifluoperazine before pouring NGM agar plates. Without proper dosing, these neurotransmitter antagonists can cause off-target effects like fleeing, especially when combined with DR. All subsequent *C. elegans* experiments were performed at 50 μM of mianserin and 25 μM of thioridazine unless otherwise noted. All drugs were purchased from Sigma-Aldrich and were initially dissolved in milliQ water at 2 mM (mianserin) or 100mM concentration (DRD2 antagonists), aliquoted, and stored at −20 °C.

Dietary restriction (DR) lifespan treatments

Lifespan DR assays were performed like other lifespans until day two of adulthood, when the worms were transferred to plates with 10^9 seeded lawns and transferred every other day four times. This form of DR is termed solid DR (sDR) (Greer et al 2009). For short-term DR assays, worms were starved for eight (real-time PCR) or 20 hours (slide microscopy). We added 100uL of 10mM palmitic acid (Sigma-Aldrich) dissolved in 100% EtOH to the outer rim of the plate to prevent fleeing.

Attractant, repellant, and neutral smell treatments

Fed and DR plates were prepared using NGM plates with palmitic acid. Odorants were chosen from previously published work isolating secreted compounds from the *E. coli* strain HB101(*174, 175*). All concentrations of attractant, repellant, and neutral chemicals were dissolved in 100% ethanol (more details in Table 2.3). A small pad of NGM agar (2 mL) was poured on the lid of each plate and allowed to solidify before 100uL of each smell concentration was added to the agar pads. Plates were prepared the day prior to use to allow the ethanol solutions to dry. Young adult *fmo-2p::mCherry* worms were placed on fed and DR plates and exposed to each smell for 20 h before fluorescent microscopy images were taken.

Slide microscopy

All images in this study were acquired using LASx software and Leica scope with >15 worms/treatment at 6.3x magnification. Worms were paralyzed in 0.5M sodium azide (NaN3). Fluorescence mean comparisons were quantified in ImageJ using the polygon tool and saved as macros.

Real-time PCR

500 N2 worms per biological replicate were transferred at young adulthood, 2.5 days post-hatch, to FuDR plates either seeded with food, DR'ed, or poured with the addition of 50μM mianserin or thioridazine. Worms were harvested in 50uL of M9 and flash frozen in liquid N2 after eight hours of exposure. Samples were freeze-thawed three times in Trizol reagent (Invitrogen) and RNA was extracted following standard phenol-chloroform protocols from the manufacturer. Superscript reverse transcriptase II (Invitrogen) was used to synthesize cDNA. 600ngs of cDNA/sample were used with PowerUp SYBR Green Master Mix (Applied Biosystems) was used in the quantitation with primers:
fmo-2 FWD ACGAAACGAATGAGTCGTCAGT; REV AGAGCAGACAAGAACGCCAT

Canton-S flies were mated and reared on standard food for 2 weeks before separating the flies by sex onto SY10 food with 20 flies/vial. Flies were acclimated to the vials for 24 hours before being transferred to SY10 vials coated with 2mM mianserin or water (control) or vials containing 2% agar to mimic dietary restriction. After 8 hours on these treatments, flies were frozen at -80°C overnight. Fly heads and bodies were then separated by vortexing and dissection by forceps (all samples and materials were kept on dry ice throughout). Each treatment contained 3 biological replicates composed of 10 bodies each. Trizol Reagent (Invitrogen) was used in the RNA extraction, the MultiScribe Reverse Transcriptase kit (Applied Biosystems) was used to synthesize the cDNA, and the real-time PCR analysis used PowerUp SYBR Green Master Mix (Applied Biosystems) and a StepOne Plus Real-time PCR system (Applied Biosystems) primers:
fmo-1 FWD GCGATAGGATGGGCAAACTG; REV CCCGGAAGTGGAGCAAATTC
fmo-2 FWD CGCAACCAGAAGAAAGCACA; REV TGCTCCTGTACGTGTCCAAT

Fly husbandry

The laboratory stock Canton-S was used in the lifespan and molecular experiments. Flies were maintained on standard food and housed at 25°C and 60% relative humidity in a 12:12 hour light-dark cycle.

Fly survival assays

For lifespan measurements, flies were reared under controlled larval density and collected onto standard food within 24 hours of eclosion. Flies were mated for 2-3 days then sorted by sex under light CO_2 onto vials containing standard food used in lifespan experiments (10% sucrose/10% yeast, or SY10), according to well-establish lifespan protocols (*202*). Flies were transferred to fresh food every 2-3 days. At the beginning of the lifespan, mianserin was dissolved in water at a 1mM stock concentration and stored at -20°C. Weekly aliquots were prepared and diluted with water to yield the final concentrations of 20-80μM. 100μL of the drug solution (or water for the control) was added to the top of each vial and kept at room temperature to dry for approximately 2 hours before transferring the flies.

Cell culture and stress resistance assay

HepG2 cells were grown in Dulbecco's modified Eagle's medium (DMEM, GIBCO) supplemented with 10% fetal bovine serum,100 U/ml penicillin, and 100 μg/ml streptomycin. For stress resistance assay, cells were seeded to 96-well microplates with 40,000 cells per well for HepG2 cells. After 16 to 18 h overnight incubation in complete medium, the cells were incubated for 18 to 24 h in serum-free DMEM supplemented with 2% bovine serum albumin (BSA) as described previously(*187*). For stress treatments, cells were exposed to cadmium for 6 h in 2% BSA supplemented DMEM, and then incubated in fresh 2% BSA supplemented DMEM without stressor for 18 h, followed by measurements of cell survival by Cell Proliferation Reagent WST-1 (Sigma 5015944001).

Western blot analysis

10 µg cell lysis samples were separated using SDS–PAGE and transferred to nitrocellulose filters, then blocked with 3% milk in TTBS (20mM Tris–HCl [pH 7.4], 500mM NaCl and 0.1% Tween 20) for 1 h, and incubated with primary antibody overnight at 4°C. After washing three times with TTBS buffer, membrane was incubated with horseradish peroxidase-conjugated secondary antibody (Cell Signaling Technology, diluted 1: 5,000 in 3% milk) for 1 h at room temperature and then washed with TTBS. The filter was developed for visualization by enhanced chemiluminescence (Thermo Scientific Pierce).

Statistical analyses

All box plots show individual data points while the box represents SEM (centered on the mean), and whiskers represent 10%/90%. Comparisons between more than two groups were done using ANOVA. For multiple comparisons, Tukey's multiple comparison test was used, and p values are *$p < 0.05$, **$p < 0.01$, ***$p < 0.001$, and ****$p < 0.0001$. For lifespan assays groupwise and pairwise comparisons among survivorship curves were performed the statistical software R. P values were obtained using the log-rank analysis (select pairwise comparisons and group comparisons or interaction studies) as noted. Interaction P values were calculated using Cox regression when the survival data satisfied the assumption of proportional hazards. All statistics were run in R. Summary lifespan statistics are included in Table 2.2.

Description	Source	Identifier
wild-type	CGC	N2
tph-1(mg280)	CGC	MT15434
ser-4(ok512)	CGC	AQ866
dop-3(vs106)	CGC	LX703
del-3(ok2613)	CGC	RB1979
del-7(ok1187)	CGC	RB1156
fmo-2(ok2147)	CGC	VC1668
daf-6(e1377)	CGC	CB1377
daf-3(e1376)	CGC	CB1376
daf-7(e1372)	CGC	CB1372
LZR1*[(pCF150) (fmo-2p::mCherry + H2B::GFP) + Cbr-unc-119(+)] II	this paper	LZR1
LZR1*[(pCF150) (fmo-2p::mCherry + H2B::GFP) + Cbr-unc-119(+)] II; ser-4(ok512)	this paper	LZR2
LZR1*[(pCF150) (fmo-2p::mCherry + H2B::GFP) + Cbr-unc-119(+)] II; dop-3(vs106)	this paper	LZR3
LZR1*[(pCF150) (fmo-2p::mCherry + H2B::GFP) + Cbr-unc-119(+)] II; daf-6(e1377)	this paper	LZR4
LZR1*[(pCF150) (fmo-2p::mCherry + H2B::GFP) + Cbr-unc-119(+)] II; daf-3(e1376)	this paper	LZR5
LZR1*[(pCF150) (fmo-2p::mCherry + H2B::GFP) + Cbr-unc-119(+)] II; daf-7(e1372)	this paper	LZR6
del-3(ok2613); Lei001*[(pCF150) (fmo-2p::mCherry + H2B::GFP) + Cbr-unc-119(+)] II	this paper	LZR7
LZR1*[(pCF150) (fmo-2p::mCherry + H2B::GFP) + Cbr-unc-119(+)] II; del-7(ok1187)	this paper	LZR8
tph-1(mg280); kySi56 IV; kyEx4077[srh-142::nCre] '' = tph-1(-) in ADF neurons''	Cori Bargmann	CX13571
tph-1(mg280); kySi56 IV; kyEx4057[ceh-2::nCre] '' = tph-1(-) in NSM neurons''	Cori Bargmann	CX13572
tph-1(mg280); pKA805[srh-142p::TPH-1] " = tph-1(+) in ADF neurons"	Kaved Ashrafi (plasmid), this paper	LZR9
tph-1(mg280); pKA807[ceh-2p::TPH-1] " = tph-1(-) in NSM neurons"	Kaved Ashrafi (plasmid), this paper	LZR10
LZR1*[(pCF150) (fmo-2p::mCherry + H2B::GFP) + Cbr-unc-119(+)] II; ser-4(ok512); pHAM002[unc-119p::SER-4] " = + neuronal"	this paper	LZR11
LZR1*[(pCF150) (fmo-2p::mCherry + H2B::GFP) + Cbr-unc-119(+)] II; ser-4(ok512); pHAM003[vha-6p::SER-4] " = + intestinal"	this paper	LZR12

Table 2.1. *C. elegans* strains used in this study.

data	strain	Mean lifespan	comparison	Mean lifespan	p-value
Fig. 1d	DR	30.64	fed	25.77	0.000014
	DR + smell	23.85	DR	30.64	0
Fig. 2f	10µM mianserin	28.22	control (water)	28.5	1
	25µM mianserin	35.61	control (water)	28.5	0
	50µM mianserin	33.97	control (water)	28.5	0
	100µM mianserin	27.66	control (water)	28.5	1
Fig. 2g	10µM thioridazine	25.08	control (water)	20.09	0.0001
	25µM thioridazine	26.54	control (water)	20.09	0
	50µM thioridazine	24.67	control (water)	20.09	0.0000021
	100µM thioridazine	21.11	control (water)	20.09	1
Fig. 2h	WT - 50µM mianserin	33.97	WT - control (water)	28.5	0
	fmo-2 - 50µM mianserin	25.63	fmo-2 - control (water)	24.35	1
Fig. 2i	WT - 50µM thioridazine	30.2	WT - control (water)	26.4	0
	fmo-2 - 50µM thioridazine	23.07	fmo-2 - control (water)	23.07	2.70E-07
Fig. 3a	tph-1 - fed	33.48	WT - fed	30.72	0.000049
	tph-1 - DR	32.35	tph-1 - fed	33.48	1
	tph-1 - DR + smell	32.05	tph-1 - fed	33.48	0.5446
Fig. 3d	tph-1 - fed	28.3	WT - fed	24.98	0.0002
	tph-1 - DR	28.3	tph-1 - fed	29.95	1
	tph-1 (+) in the NSM neurons - fed	24.38	WT - fed	24.98	0.4191
	tph-1 (+) in the NSM neurons - fed	24.38	tph-1 - fed	29.95	0
	tph-1 (+) in the NSM neurons - DR	31.29	WT - DR	28.3	3.10E-07
	tph-1 (+) in the NSM neurons - DR	31.29	tph-1 (+) in the NSM neurons - fed	24.38	0
Fig. 3f	vector RNAi - DR	27.09	vector RNAi - fed	24.89	0
	ser-4 RNAi - fed	27.55	vector RNAi - fed	24.89	0
	ser-4 RNAi - DR	27.55	ser-4 RNAi - fed	27.59	0.5303
Fig. 4d	50µM mianserin [males]	49.28	control (water) [males]	44.66	0.05
Ex Data Fig. 3j	50µM mianserin	26.01	control (water)	20.76	0
	DR	31.15	control (water)	20.76	0
	DR + 50µM mianserin	27.68	control (water)	20.76	0
Ex Data Fig. 5a	tph-1 - fed	28.1	WT - fed	25.21	3.70E-07
	tph-1 - 50µM mianserin	28.1	tph-1 - fed	28.1	1
Ex Data Fig. 5d	WT - DR	31.83	WT - fed	26.13	0
	tph-1 (-) in the NSM neurons - fed	27.43	WT - fed	26.13	0.0027
	tph-1 (-) in the NSM neurons - DR	28.45	WT - DR	31.83	0.000003
	tph-1 (-) in the NSM neurons - DR	28.45	tph-1 (-) in the NSM neurons - fed	27.43	0.000019
Ex Data Fig. 5e	WT - DR	31.83	WT - fed	26.13	0
	tph-1 (-) in the ADF neurons - fed	26.14	WT - fed	26.13	0.3157
	tph-1 (-) in the ADF neurons - DR	30.57	WT - DR	31.83	0.3157
	tph-1 (-) in the ADF neurons - DR	30.57	tph-1 (+) in the ADF neurons - fed	26.14	0.0000075
Ex Data Fig. 5f	tph-1 - fed	29.95	WT - fed	24.98	1.00E-07
	tph-1 - DR	29.93	tph-1 - fed	29.95	1
	tph-1 (+) in the ADF neurons - fed	29.76	WT - fed	24.98	6.00E-07
	tph-1 (+) in the ADF neurons - fed	29.76	tph-1 - fed	29.95	1
	tph-1 (+) in the ADF neurons - DR	30.71	tph-1 (+) in the ADF neurons - fed	29.76	1
Ex Data Fig. 6a	WT - DR	26.1	WT - fed	25.37	6.10E-08
	del-3 - fed	23.86	WT - fed	25.37	1
	del-3 - DR	29.74	WT - fed	25.37	0.000011
	del-3 - DR	29.74	WT - DR	26.1	1
	del-3 - fed + smell	23.41	del-3 - fed	23.86	1
	del-3 - DR + smell	29.75	del-3 - DR	29.74	1
Ex Data Fig. 6f	WT - DR	26.1	WT - fed	25.37	6.10E-08
	del-7 - fed	25.04	WT - fed	25.37	1
	del-7 - DR	28.8	WT - fed	25.37	0.000016
	del-7 - DR	28.8	WT - DR	26.1	1
	del-7 - fed + smell	28.64	del-7 - fed	25.04	1
	del-7 - DR + smell	25.97	del-7 - DR	28.8	0.0626
Ex Data Fig. 8e	vector RNAi - DR	27.09	vector RNAi - fed	24.89	4.90E-07
	dop-3 RNAi - fed	24.62	vector RNAi - fed	24.89	0.0087
	dop-3 RNAi - DR	26.03	dop-3 RNAi - fed	24.62	1
Ex Data Fig. 10c	20µM mianserin [males]	47.82	control (water) [males]	44.66	0.45
	30µM mianserin [males]	46.83	control (water) [males]	44.66	1
	40µM mianserin [males]	47.55	control (water) [males]	44.66	0.68
	50µM mianserin [males]	49.28	control (water) [males]	44.66	0.05
	80µM mianserin [males]	43.69	control (water) [males]	44.66	1
Ex Data Fig. 10d	20µM mianserin [females]	66.98	control (water) [females]	61.25	0.0001
	30µM mianserin [females]	62.07	control (water) [females]	61.25	1
	40µM mianserin [females]	64.23	control (water) [females]	61.25	0.2847
	50µM mianserin [females]	65.18	control (water) [females]	61.25	0.0234
	80µM mianserin [females]	63.89	control (water) [females]	61.25	0.0241

Table 2.2. Lifespan information for this study.

compound	class	attractive (A), neutral (N), or repulsive (R)	source	titrations
2-butanone	ketone	A	Bargmann et al, 1993 Nuttley et al, 2002	0.1mM, 50mM, 200mM
2-heptanone	ketone	A	Worthy et al, 2018	0.1mM, 50mM, 200mM
2-methyl-1-butanol	alcohol	A	Worthy et al, 2018	0.1mM, 1mM, 5 mM, 50mM, 100mM, 200mM
3-methyl butanol	alcohol	A		0.1mM, 1mM, 5 mM, 50mM, 100mM, 200mM
acetone	ketone	A	Nuttley et al, 2002	0.1mM, 50mM, 200mM
diacetyl	ketone	A	Worthy et al, 2018 Bargmann et al, 1993	0.1mM, 50mM, 200mM
ethyl isobutyrate	ester	A	Worthy et al, 2018	0.1mM, 1mM, 5 mM, 50mM, 100mM, 200mM
ethyl isovalerate	ester	A	Worthy et al, 2018	0.1mM, 1mM, 5 mM, 50mM, 100mM, 200mM
ethyl propionate	ester	A	Bargmann et al, 1993	0.1mM, 50mM, 200mM
isoamyl alcohol	alcohol	A	Worthy et al, 2018 Bargmann et al, 1993	0.1mM, 50mM, 200mM
pyrazine	pyrazine	A, variable	Bargmann et al, 1993	0.1mM, 50mM, 200mM
diethylamine	amine	N	Bargmann et al 1993	0.1mM, 50mM, 200mM
dimethyl disulfide	other	N	Worthy et al, 2018 Nuttley et al, 2002	0.1mM, 1mM, 5 mM, 50mM, 100mM, 200mM
dimethyl sulfide	other	N	Worthy et al, 2018	0.1mM, 50mM, 200mM
ethyl acetate	ester	N	Worthy et al, 2018	0.1mM, 50mM, 200mM
hexyl acetate	ester	N	Bargmann et al 1993	0.1mM, 50mM, 200mM
isopropanol	alcohol	N	Bargmann et al 1993	0.1mM, 50mM, 200mM
thiazole	thiazole	N	Bargmann et al 1993	0.1mM, 50mM, 200mM
vanillin	aromatic	N	Bargmann et al 1993	0.1mM, 50mM, 200mM
1-heptanol	alcohol	R		0.1mM, 50mM, 200mM
1-nonanol	alcohol	R		0.1mM, 50mM, 200mM
1-octanol	alcohol	R	Bargmann et al 1993	0.1mM, 50mM, 200mM
2-nonanone	ketone	R		0.1mM, 50mM, 200mM
5-nonanone	ketone	R	Bargmann et al 1993	0.1mM, 50mM, 200mM
butyl butyrate	ester	R	Bargmann et al 1993	0.1mM, 50mM, 200mM
ethyl heptanoate	ester	R		0.1mM, 50mM, 200mM
2,4,5-trimethylthiazole	thiazole	R-high , A or N-low	Bargmann et al, 1993	0.1mM, 50mM, 200mM
benzaldehyde	aromatic	R-high , A-low	Bargmann et al, 1993	0.1mM, 50mM, 200mM

Table 2.3. Odorant classification, identification, and concentrations.

CHAPTER 3

Genetic Interaction with Temperature Is an Important Determinant of Nematode Longevity[2]

Foreword

Before making significant in-roads on my primary thesis project, Dr. Leiser and I wanted to collate a substantial amount of lifespan data we performed in collaboration with members of the Kaeberlein lab. Our goal was to put together a short, discrete story. While a significant portion of the data was collected by my co-authors, the analysis, figure presentation and writing of the manuscript was left to me and Dr. Leiser. I found this methodology to be incredibly helpful going forward in my PhD. It taught me early on how to construct a story and navigate the peer-review process.

2. Originally published in *Aging Cell* (2017 Dec 16;6 1425-1429) with authors listed as **Miller, H.A.**, Fletcher, M., Primitivo, M., Leonard, A., Sutphin, G. L., Rintala, N., Kaeberlein, M., and Leiser, S.F.

Abstract

As in other poikilotherms, longevity in *C. elegans* varies inversely with temperature; worms are longer-lived at lower temperatures. While this observation may seem intuitive based on thermodynamics, the molecular and genetic basis for this phenomenon is not well understood. Several recent reports have argued that lifespan changes across temperatures are genetically controlled by temperature-specific gene regulation. Here, we provide data that both corroborate those studies and suggest that temperature-specific longevity is more the rule than the exception. By measuring the lifespans of

worms with single modifications reported to be important for longevity at 15, 20, or 25°C, we find that the effect of each modification on lifespan is highly dependent on temperature. Our results suggest that genetics play a major role in temperature-associated longevity and are consistent with the hypothesis that while aging in *C. elegans* is slowed by decreasing temperature, the major cause(s) of death may also be modified, leading to different genes and pathways becoming more or less important at different temperatures. These differential mechanisms of age-related death are not unlike what is observed in humans, where environmental conditions lead to development of different diseases of aging.

Results

The aging process has been described as stochastic – a probabilistic degeneration of cellular function that may be explained in sufficient detail by thermodynamic principles (*203*). Thermodynamics and the kinetics of chemical reactions provide the most rudimentary understanding of how physiological processes change as temperature changes. Described most simply, the rates of various chemical reactions increase as temperature increases, resulting in an increased rate of biochemical processes and, possibly, a corresponding increase in the rate of aging. Consistent with this model, lowering the ambient temperature of poikilotherms such as *C. elegans, D. melanogaster and C. bellottii,* and decreasing a mouse's body temperature can increase lifespan (*136, 204-206*).

In *C. elegans*, animals that develop and age at 15°C ("low temperature") are long-lived compared to wild-type animals grown at 20°C (~ room temperature), whereas wild-type worms that develop and age at 25°C ("high temperature") are short-lived compared to wild-type worms grown at 15°C or 20°C (**Figure 3.1**). This "temperature law" has been described as widely accepted, but not tested beyond limited number of strains (*207*).

While the “temperature law” is observed among wild-type organisms, the interplay between genetics and temperature is not well understood. Multiple recent reports suggest that the effects of temperature on longevity are genetically controlled, and that both heat and cold modify transcriptional pathways that effect lifespan (*59, 64, 207-211*). To better understand the interplay between temperature and longevity, we measured the lifespans of worms with genetic manipulations known to affect longevity at 15°C, 20°C, or 25°C. **Figure 3.1** illustrates six examples of how longevity can be impacted across temperatures, representing conditions that:

- robustly increase lifespan at all temperatures (*daf-2* RNAi)
- robustly decrease lifespan at all temperatures (*rhy-1(ok1402)*)
- decrease lifespan at high but not low temperature (*daf-16(mu86)*)
- increase lifespan at high temperature but decrease lifespan at low temperature (*rsks-1(ok1255)*)
- increase lifespan at low temperature but not high temperature (*cep-1(gk138)*)
- do not alter lifespan at any temperature (*cah-4* RNAi)

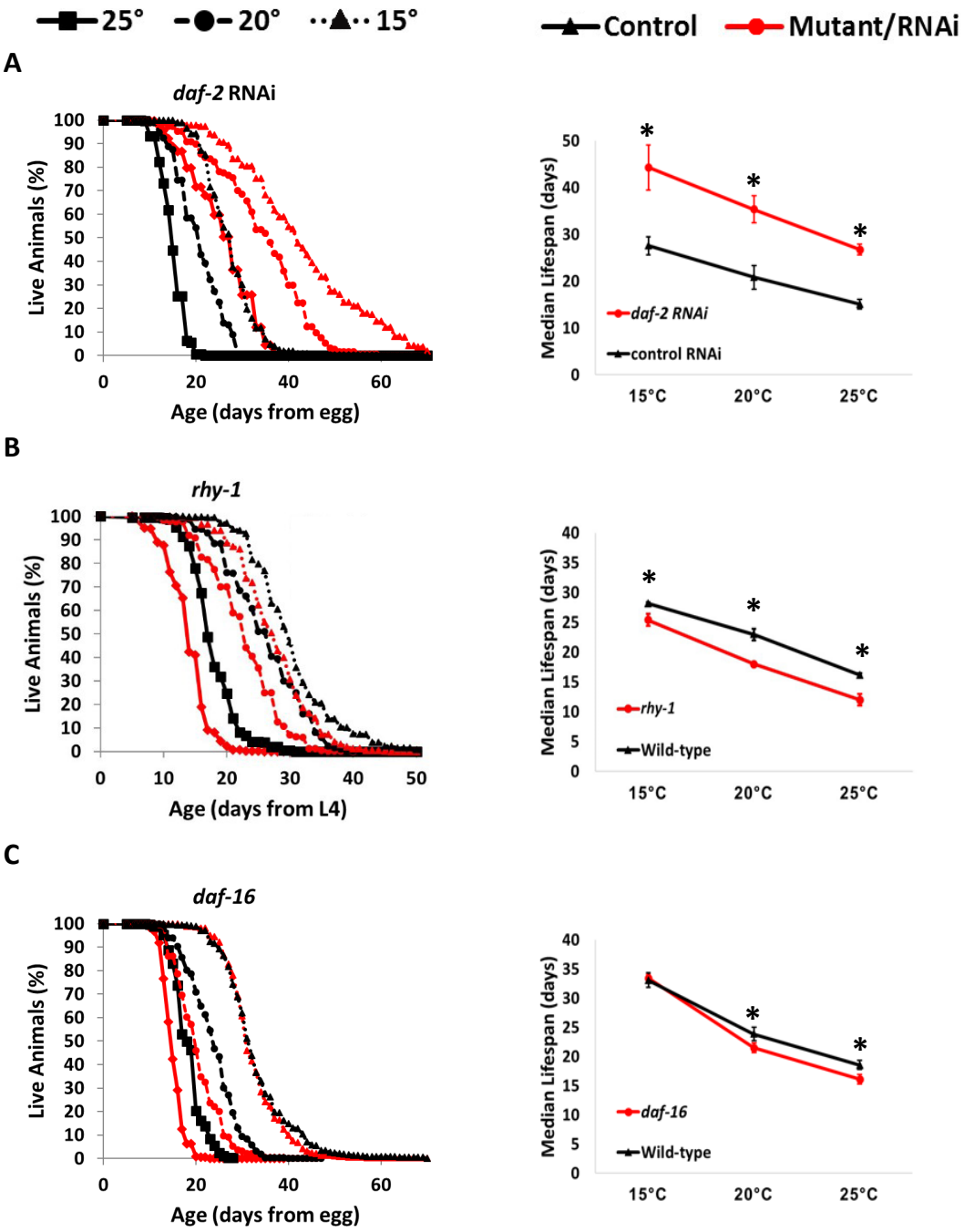

Figure 3.1. Examples of different types of interactions between genotype, temperature, and lifespan.
Panels A-F show survival curves and combined graphs plotting median lifespan vs temperature at 15°, 20°, and 25° for *daf-2* (RNAi), *rhy-1(ok1402), daf-16(mu86), rsks-1(ok1255)*, *cep-1(gk138),* and *cah-4* (RNAi) compared to wild-type (N2). Note that because they are developmentally delayed, *rhy-1* lifespans are shown from L4.

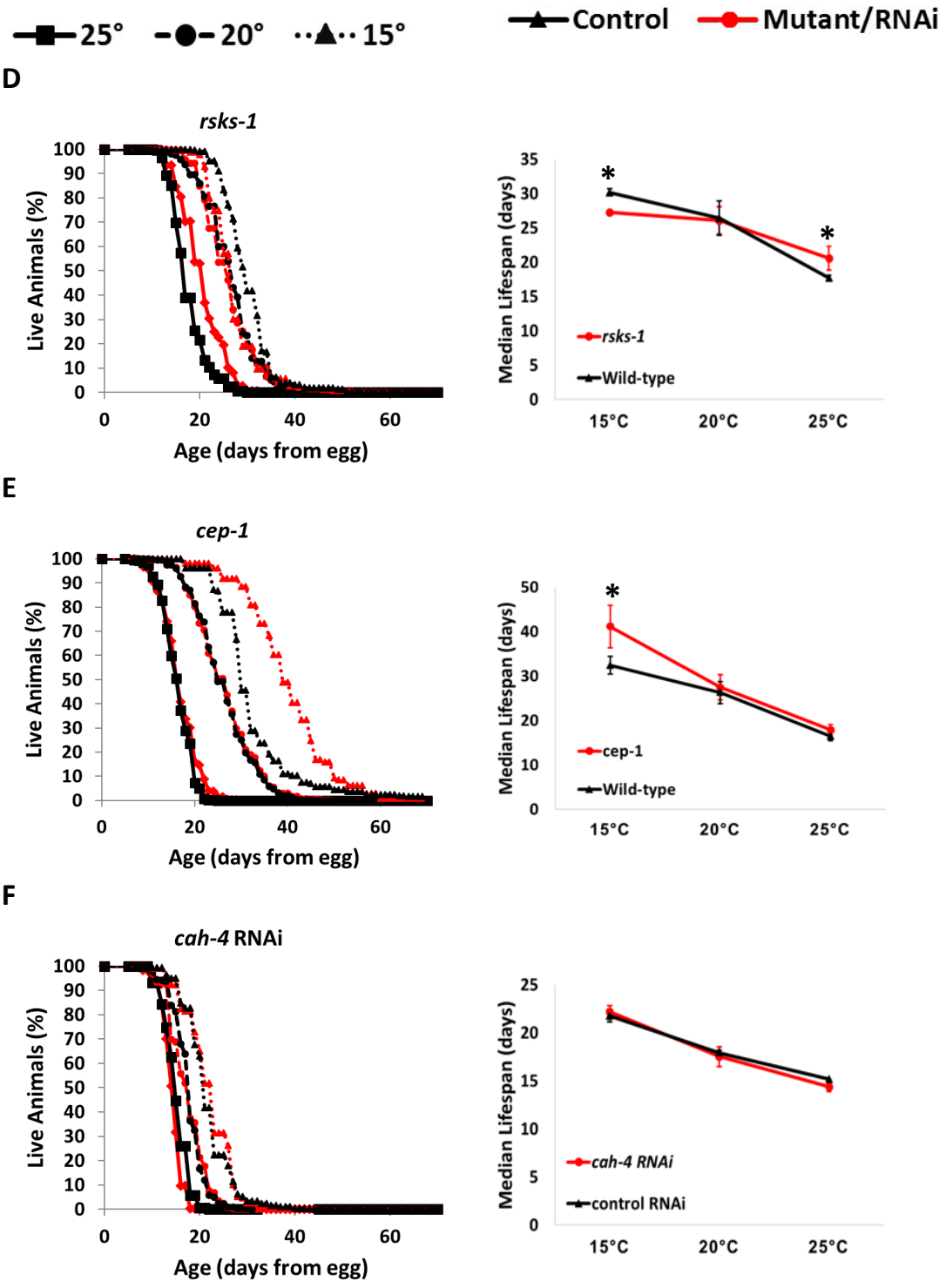

Legend on previous page.

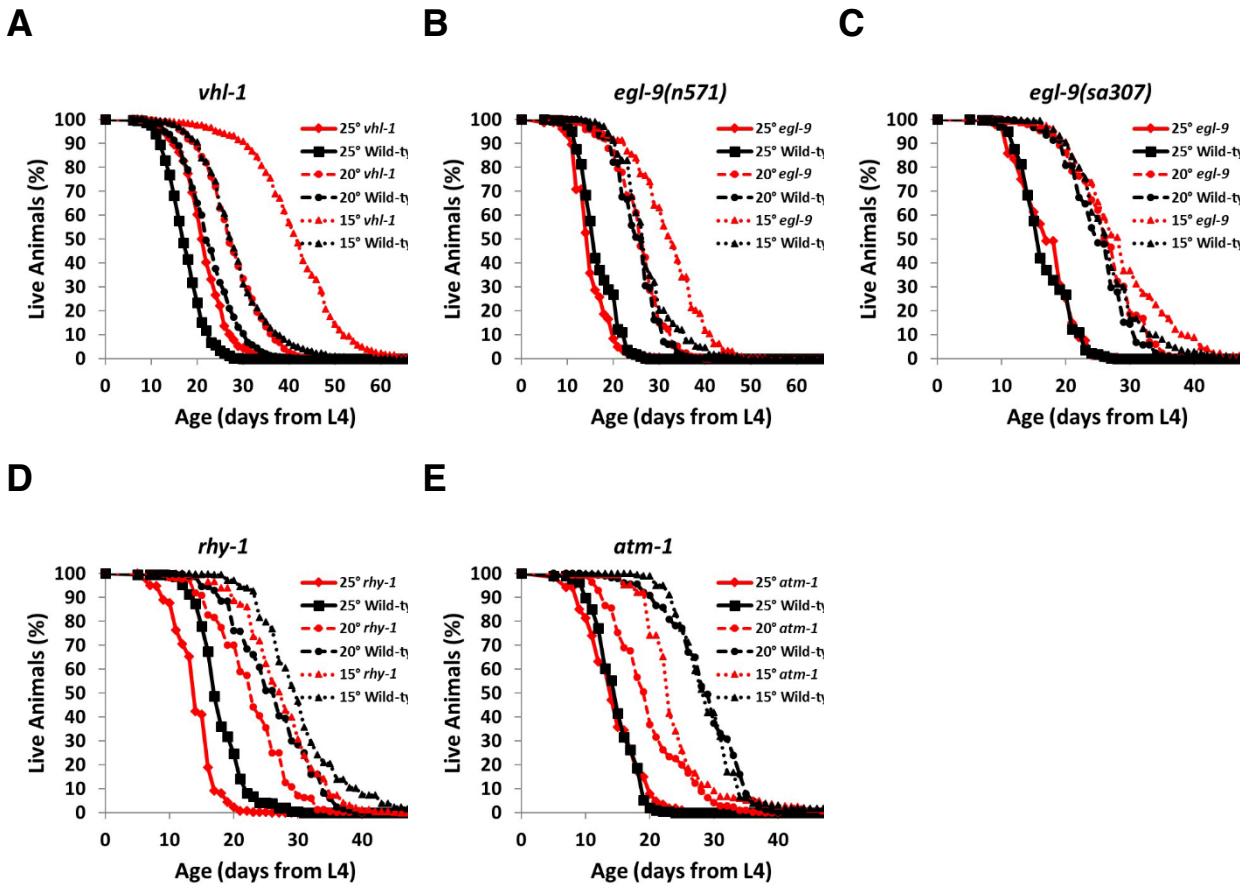

Figure 3.2. Lifespans from L4 for strains with developmental delays.

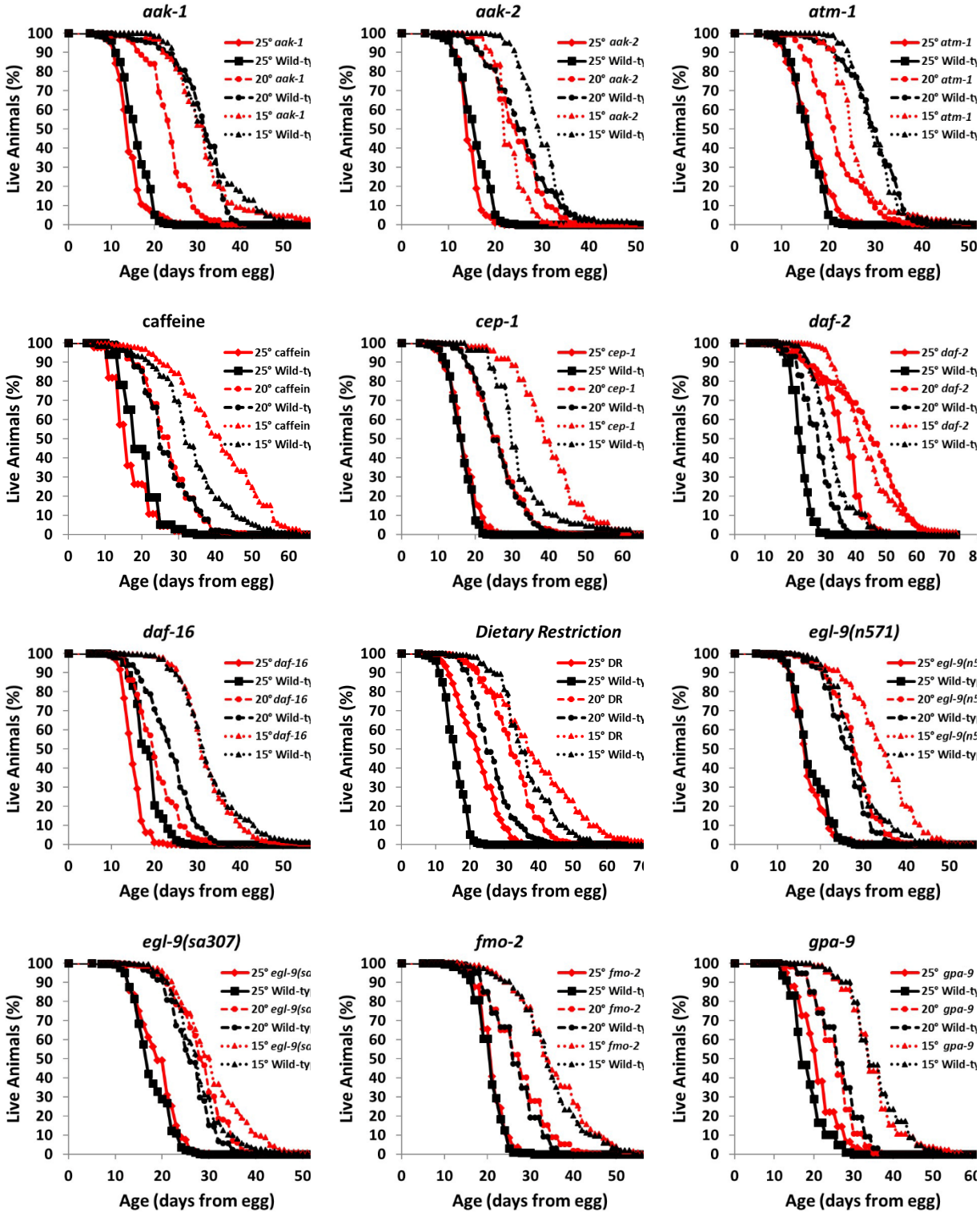

Figure 3.3. Mutant and environmental condition lifespans at 15, 20, and 25°C.

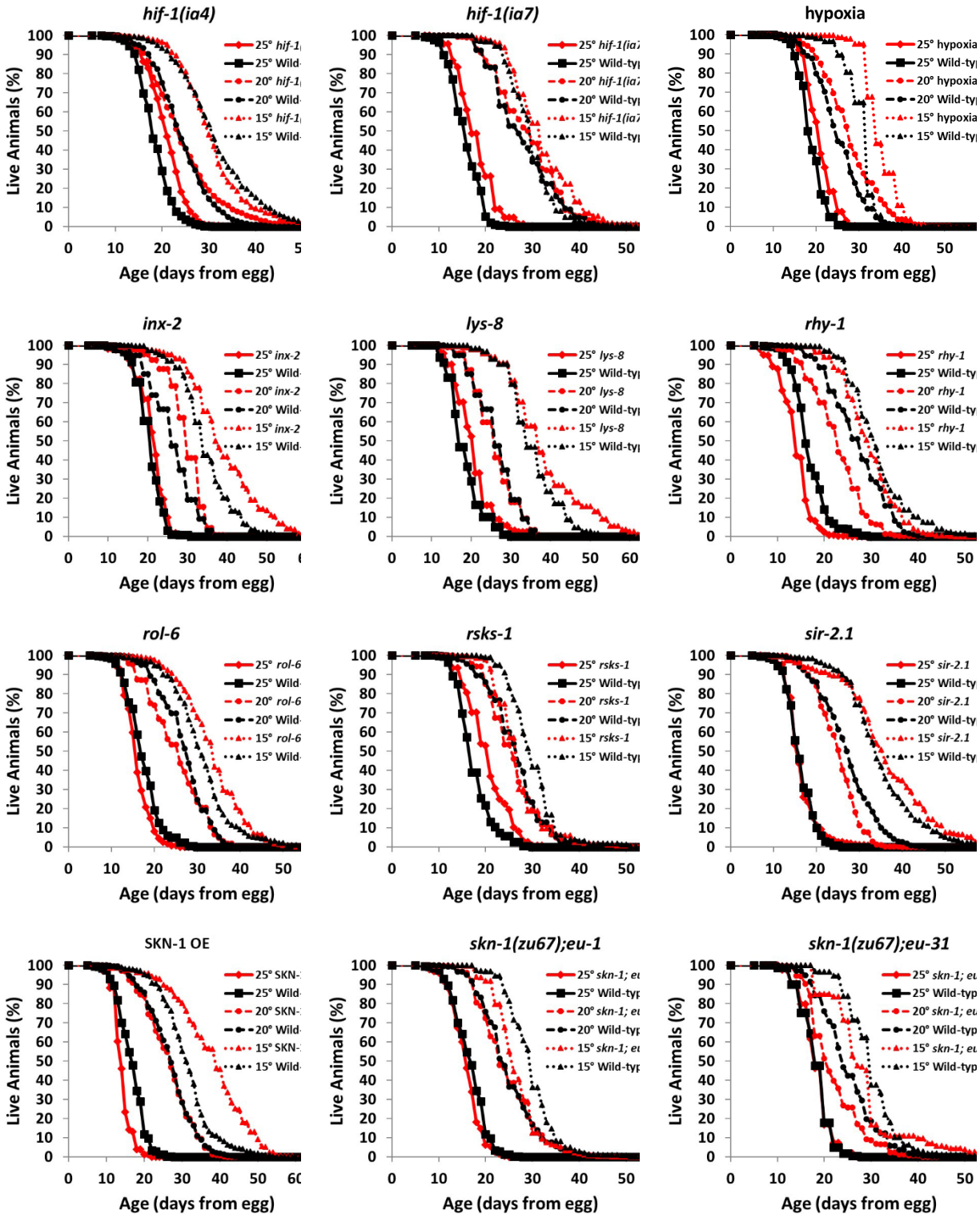

Legend on previous page.

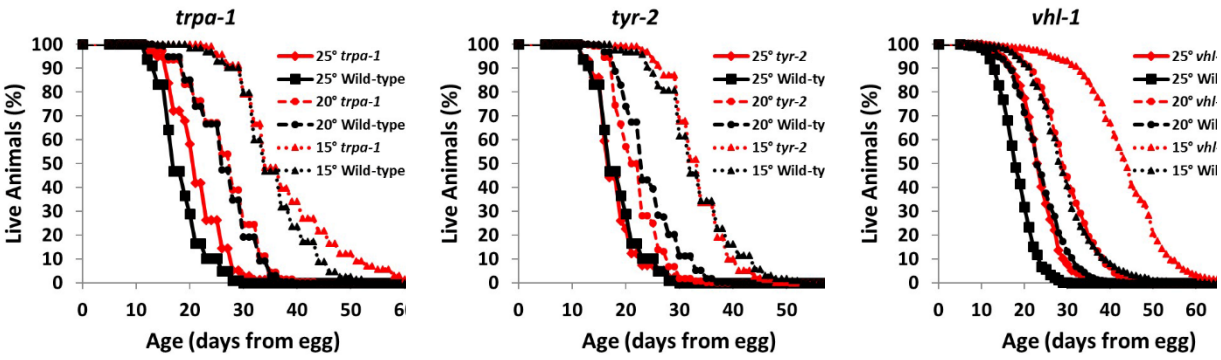

Legend on previous page.

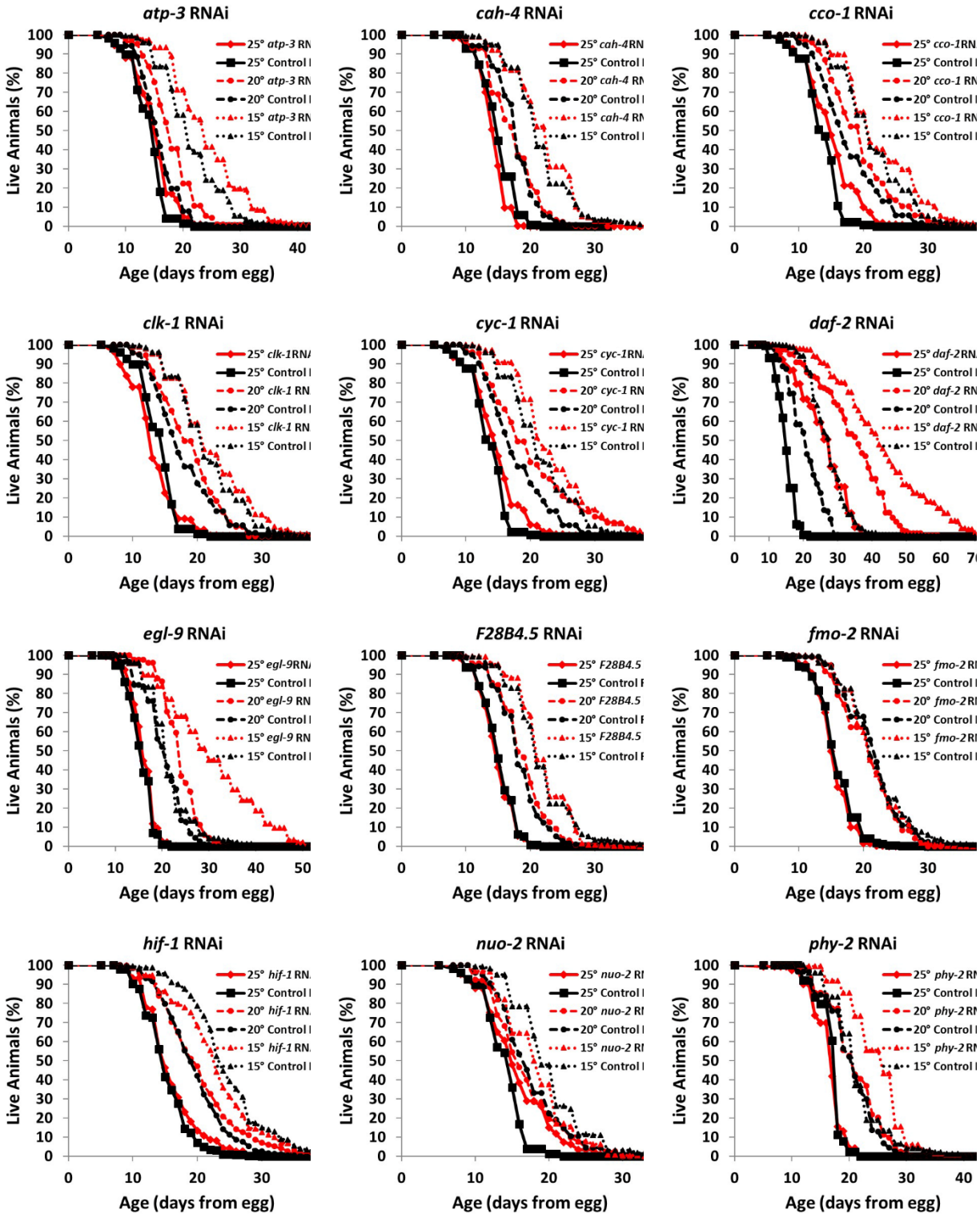

Figure 3.4. RNAi lifespans at 15, 20, and 25°C.

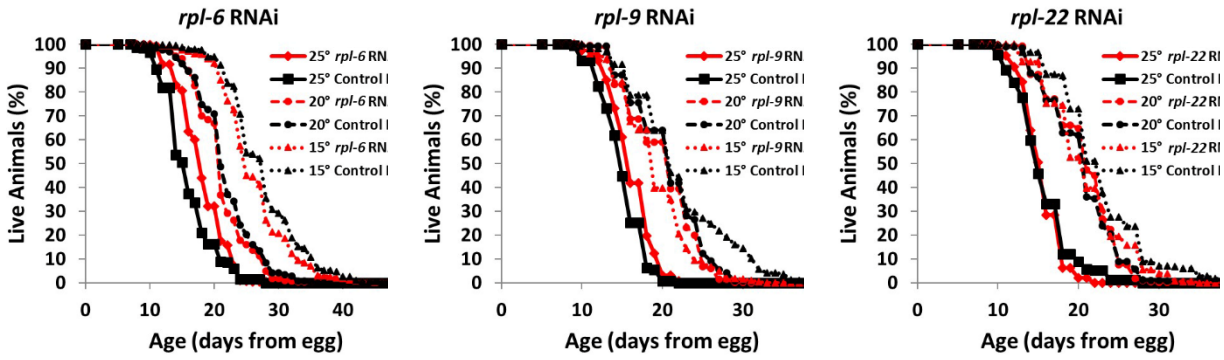

Legend on previous page.

A

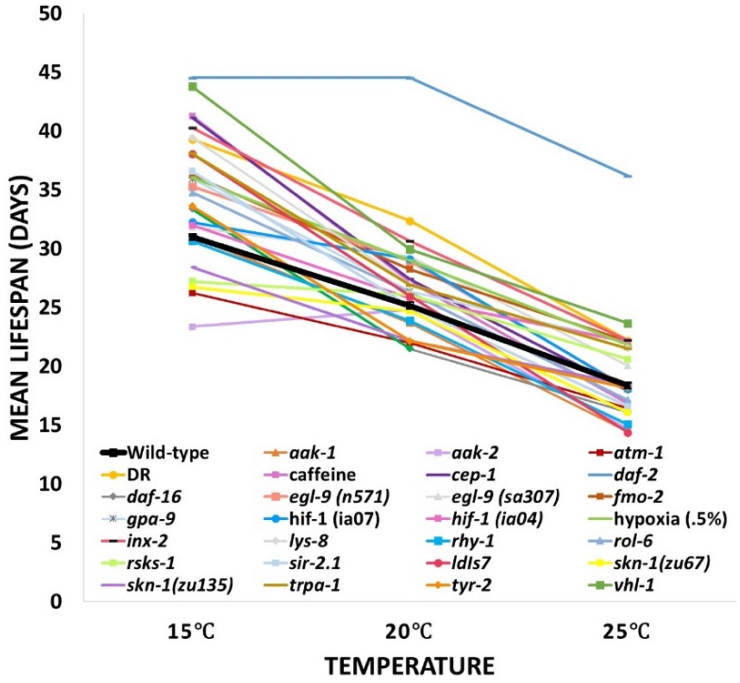

B

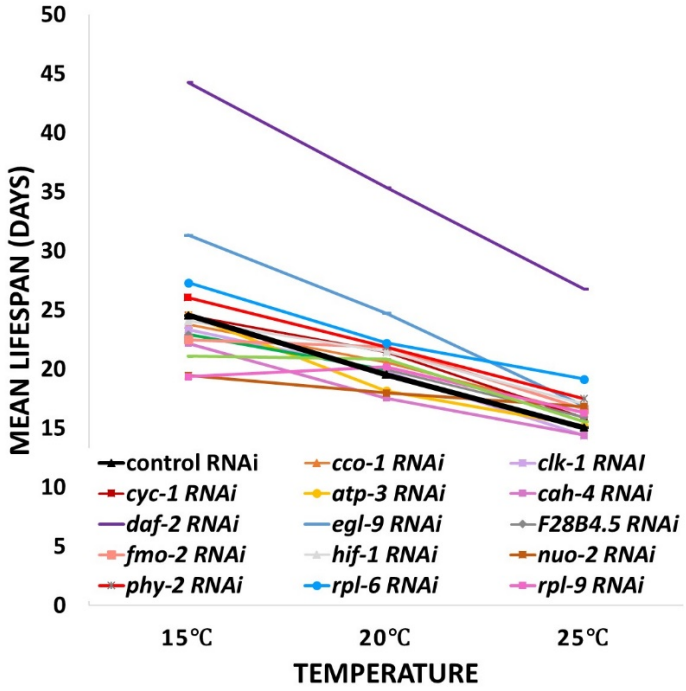

Figure 3.5. Complete graph of median lifespan vs temperature at 15, 20, and 25°C for all lifespan data normalized to wild-type/control.

Having established that relative longevity can vary across temperatures, we next asked whether this variability is common among conditions known to modify longevity. We tested nearly fifty genotypes and interventions previously reported to affect lifespan (Figure 3.2-5 and Table 3.1-2) and found that relative longevity was consistently inconsistent across temperatures. However, there are consistent trends within longevity pathways, where strains/conditions known to have opposing effects are also affected by temperature oppositely (**Figure 3.6A-B**, Figure 3.7A-D). We used Cox regression analysis to assess the interaction between each longevity intervention and temperature. The hazard ratios, which represent the cumulative risk of death throughout a worm's lifespan, confirm the interaction between condition (genotype, RNAi, etc.) and temperature and clearly separate the conditions into three categories: approximately one third (15/43) of the interventions show an increased hazard ratio (significantly "better" at higher temperature), one third (14/43) show a decreased hazard ratio (significantly "better" at lower temperature), and one third (14/43) show no interaction between genetic manipulation and temperature (**Figure 3.6C,D**). The changes in hazard ratio are frequently ~two-fold and are clearly not random, as evidenced by reciprocal results for genes that are known to have opposite effects within the same pathway (e.g. *daf-2(e1370)* vs. *daf-16(mu86)*, *vhl-1(ok161)* vs. *hif-1(ia4)*) (Figure 3.8). Heat-map analysis with hierarchical clustering segregate the tested conditions (Figure 3.9) into the groups described in **Figure 3.1**.

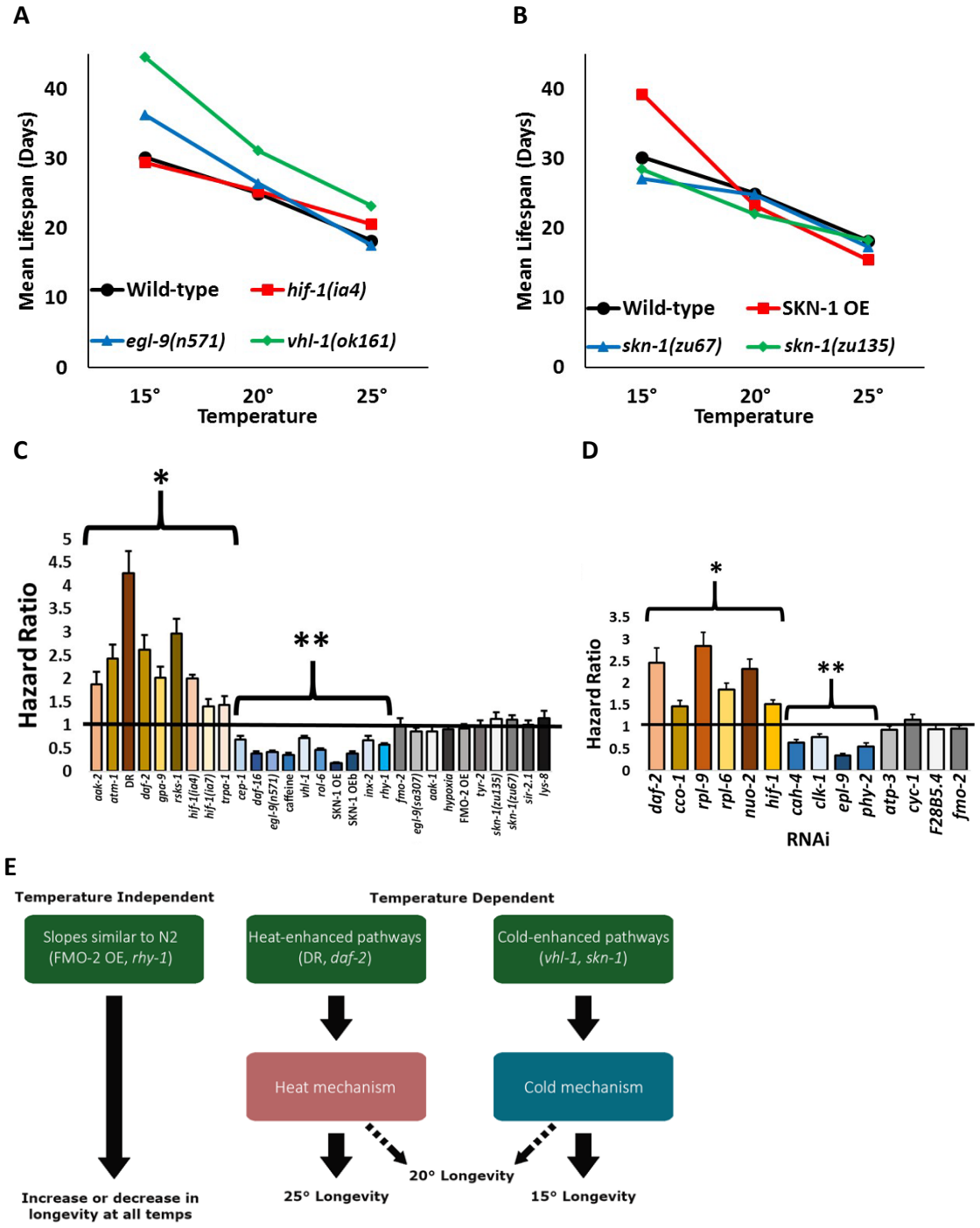

Figure 3.6. Temperature vs. longevity across genotypes.
Panels A-B plot median lifespan vs temperature at 15, 20, and 25°C for opposing genetic conditions in the longevity pathways of hypoxic signaling and antioxidant signaling normalized to wild-type (N2). Panels C-D show the Cox regression-calculated hazard ratios between each condition, separated into UV-killed and RNAi conditions, across temperatures. Panel E depicts a basic model. Significant ($p<0.01$) increased (*) and decreased (**) hazard ratios at 15°C compared to 25°C are denoted.

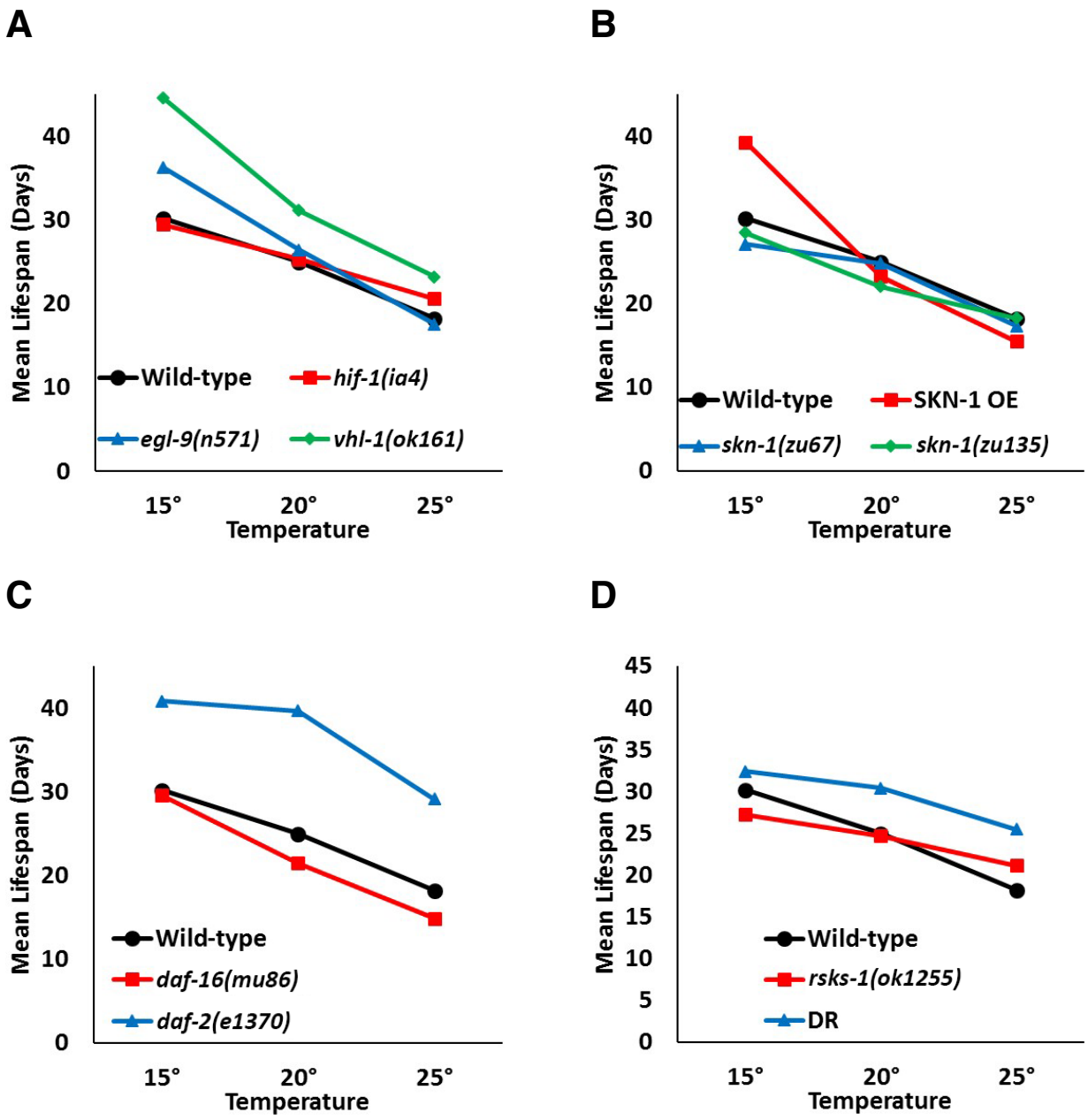

Figure 3.7. Pathway specific lifespans across temperatures by mean lifespan.
Panels A-D plot median lifespan vs temperature at 15, 20, and 25°C for opposing genetic conditions in the longevity pathways of, hypoxic signaling (A), antioxidant signaling (B), insulin signaling (C), and dietary restriction/mTOR (D) normalized to wild-type (N2).

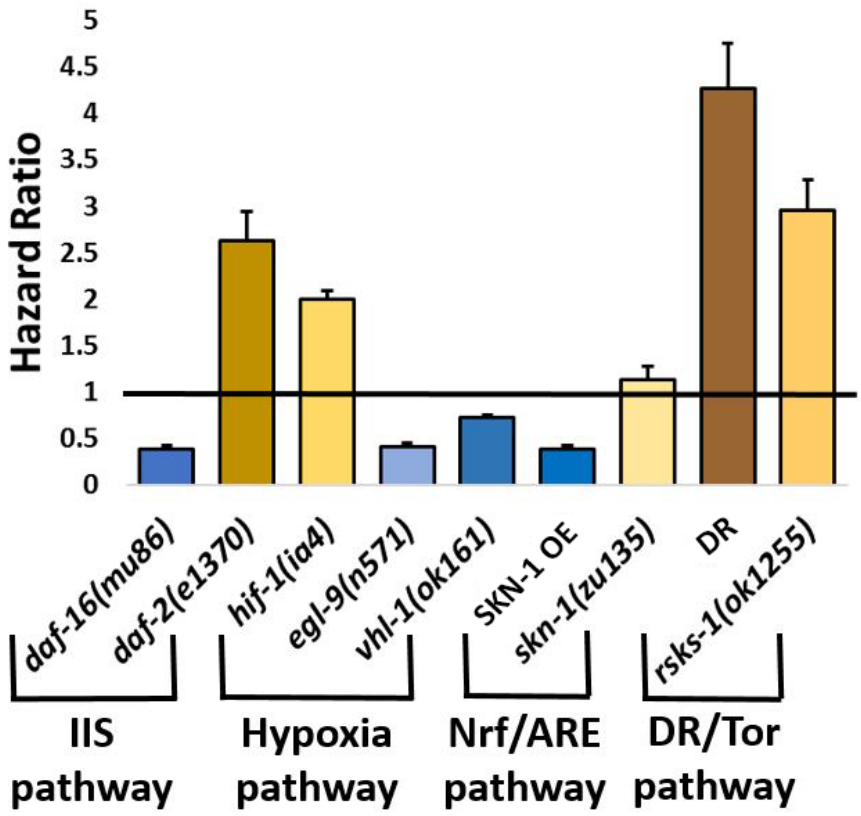

Figure 3.8. Cox regression-calculated hazard ratios between each condition and wild-type across temperatures (25-15°C) for the pathways described in Figure S5.

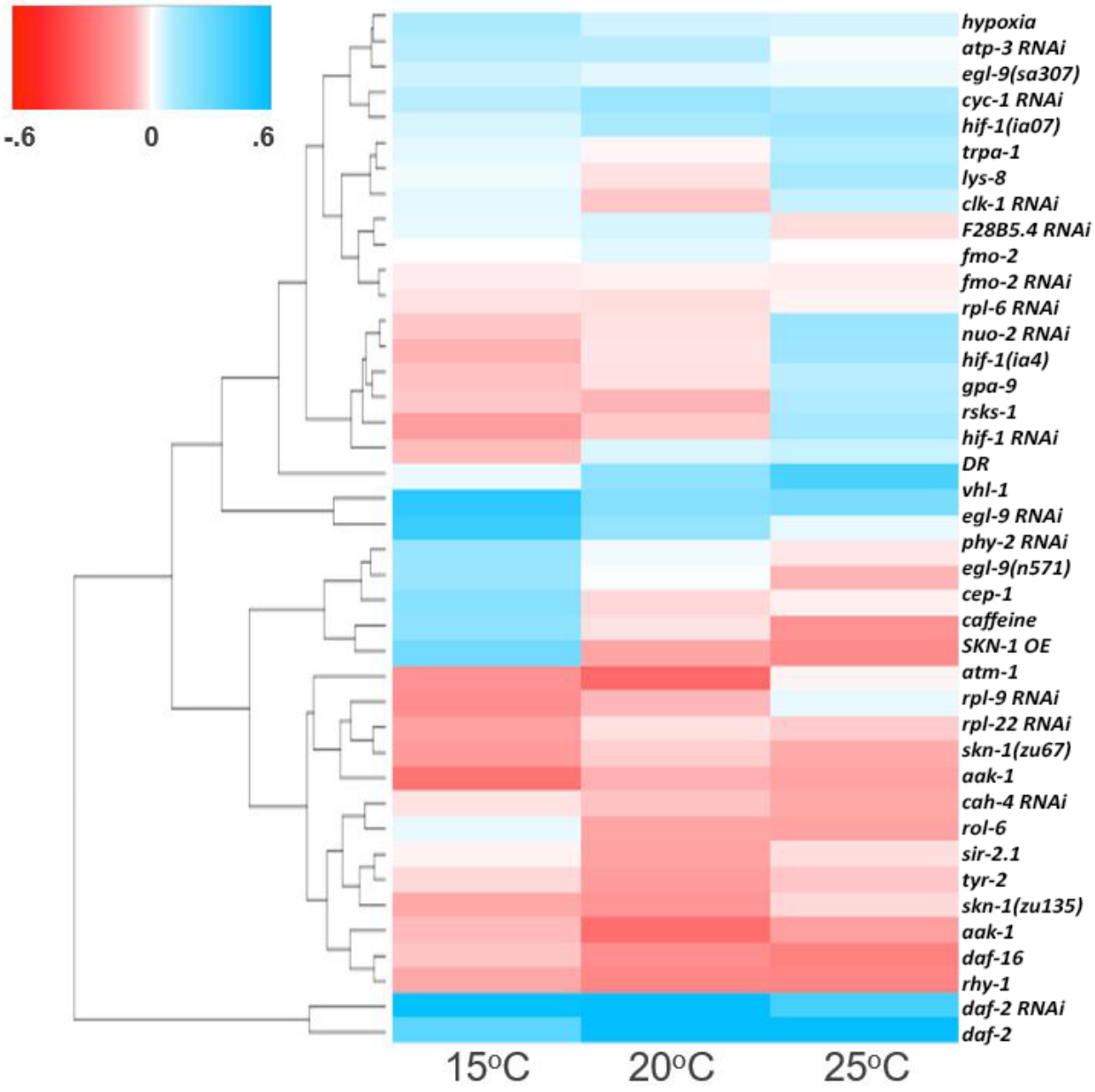

Figure 3.9. Heat map of relative longevity.
A clustered heatmap where red shading depicts longer average lifespan than wild-type and blue shading depicts a shorter average lifespan than wild-type.

Discussion

In summary, we find significant interaction between longevity interventions and environmental temperature in two-thirds (29/43) of the cases examined, indicating that a temperature-independent effect on longevity is more the exception than the rule (**Figure 3.6C-D**). This variation confirms that genetics play a substantive role in temperature-dependent longevity that cannot be explained solely by the rules of thermodynamics and chemical kinetics.

The observed variation in relative longevity with temperature is consistent with the hypothesis that distinct mechanisms determine nematode longevity at different temperatures (**Figure 3.6E**). As shown in the model, there are three distinct types of strains/conditions: those with similar slopes and hazard ratios to N2 (FMO-2 OE, *rhy-1(ok1402)*, etc.), "temperature dependent" strains/conditions that live comparatively longer at higher temperatures (e.g. DR, *rsks-1* (*ok1255)*, *daf-2(e1370)* or RNAi), and "temperature dependent" strains/conditions that live comparatively longer at colder temperatures (*vhl-1(ok161)*, *cep-1(gk138)*, SKN-1 OE). These three categories are further complicated by how they compare to wild-type overall, leading some strains to be consistently long-lived (e.g. *daf-2(e1370)* or RNAi) or short-lived (e.g. *rhy-1 (ok1402)*), whereas other strains vary in relative longevity depending on temperature (e.g. *cep-1(gk138)*). Together, these results suggest that testing strains/conditions at multiple temperature will not only define the robustness of an effect, but may provide clues as to the mechanism.

It has been suggested that protein quality control and the heat stress response are of primary importance for determining nematode longevity at 25°C (*212*). Our data support this model; we find interventions that limit heat stress response (e.g., *daf-16(mu86)*) are detrimental at high, but not low, temperature, while interventions that improve protein homeostasis, such as dietary restriction or reduced expression of translation machinery (e.g. *rsks-1(ok1255), rpl-6* RNAi) show lifespan extension at high temperature. The relevant mechanisms affecting longevity at low temperature are less clear, particularly because relatively few aging studies are conducted at 15°C compared to 20°C or 25°C.

It is possible a combination of a strain's ability to avoid age-associated vulval integrity defects (AVID), a healthspan phenotype primarily observed at colder temperatures (*213*), and to better adapt to temperature-dependent changes to their bacterial food source (growth rate, metabolism, pathogenicity), leads to better outcomes in colder temperatures. We note that a subset of our data (*trpa-1(ok999), daf-16(mu86)* at 15°C) differ from other published works on whether strains are relatively short or long-lived at a given temperature (*64, 209*). While we did not directly test why these differences are observed, we expect that they are due to our lifespans using UV-killed bacteria for a food source and others using live bacteria. It is known that *daf-16* plays an important role in immunity (*214*) in worms and both Xiao *et al* and Chen *et al*.'s reports describe a requirement for *daf-16* in their pathway. Our results agree with these reports on the slopes of the lifespans of these strains, and the differences we observe are consistent with immunity being more important at lower temperature. The difference between studies are similar to differences between live and UV-killed food experiments (which live longer) (*215*), and are worth exploring in future studies as they may explain cold-dependent longevity mechanisms of insulin and *trpa-1(ok999)* signaling.

Our results demonstrate that the impact of temperature on relative lifespan is of greater importance than generally appreciated by the *C. elegans* aging field. The vast majority of published studies report the impact of different interventions on lifespan at a single temperature, usually either 20°C or 25°C. We suggest that studies reporting effects on lifespan should typically be performed at more than one temperature in order to understand the robustness of the effect and the interaction with temperature. As further mechanistic studies on the factors that control differences in the relative lifespan vs. temperature axis are completed, we expect that plausible links will be made between temperature-specific longevity in nematodes and specific diseases of aging in mammals.

Materials and Methods

Strains and Growth Conditions

See chapter 2. Additional information in Table 3.1 includes a list of the strains and RNAi conditions used in this study.

Lifespan measurements

See chapter 2. Additional information in Table 3.2 includes statistics.

RNAi knockdown

See chapter 2.

Dietary restriction (DR) treatment

See chapter 2.

Hypoxia treatment

We followed a protocol as previously described (*216*) to design hypoxia flow chambers to continuously house animals throughout their life at .5% oxygen after development and placement on FUdR.

Caffeine treatment

Solid anhydrous caffeine was added directly to the NGM solution prior to autoclaving and pouring as previously described (*217*). Neither autoclaving nor UV treatment during plate preparation influenced life span in the presence of caffeine.

Statistical analyses

Lifespan data and statistics are included in Table 3.3 provides the results of Cox proportional hazards regression models, which were run in Stata 14. The model includes a categorical variable for temperature, using 25 degrees as the base category, and including two dummy variables for 15 and 20 degrees. It also includes a dummy variable for experimental versus control. The main variables of interest for this paper are the interactions between the experimental dummy and the temperature dummies, which capture the differential effect of temperature on experimental versus control

worms. Hierarchical clustering of the differences between conditions and control median lifespan across temperatures was performed using the heatmap.2 function in the R package “Gplots”. These values were calculated by subtracting the control animal’s median age at death from the condition’s median age at death then dividing by the control animal’s mean age at death. All error bars shown in figures represent the standard error of the mean.

Table 3.1. Descriptions of the 43 conditions included in this study.

Condition	Strain/Dose	Description
aak-1	AGD397	AMPK, downstream of insulin signaling (DAF-16 activation) and energy sensing
aak-2	RB754	AMPK, downstream of insulin signaling (DAF-16 activation) and energy sensing
atm-1	VC381	ATM, DNA damage response
atp-3	RNAi	ATP synthase, regulates mitochondrial ATP production
dietary restriction	bacteria deprivation	Robust intervention to enhance longevity
caffeine	10mM	Commonly used compound, previously reported to be long-lived
cah-4	RNAi	Carbonic anhydrase, downstream of hypoxic response (HIF-1 activation)
cco-1	RNAi	Cytochrome c oxidase, regulates mitochondrial respiration
cep-1	MN1	p53 ortholog, downstream multiple longevity pathways
clk-1	RNAi	COQ7/CAT5 ortholog, regulates mitochondrial respiration
cyc-1	RNAi	Cytochrome c reductase, regulates mitochondrial respiration
daf-2	CB1370	Insulin-like receptor, negative regulator of DAF-16
daf-2	RNAi	Insulin-like receptor, negative regulator of DAF-16
daf-16	CF1038	FOXO homologue, transcription factor downstream of insulin signaling
egl-9	MT1201	Proline hydroxylase, negative regulator of HIF-1
egl-9	JT307	Proline hydroxylase, negative regulator of HIF-1
egl-9	RNAi	Proline hydroxylase, negative regulator of HIF-1
F28B4.5	RNAi	Unknown function, downstream of hypoxic response (HIF-1 activation)
fmo-2	VC1668	Detoxification enzyme, downstream of hypoxic response (HIF-1 activation)
fmo-2	RNAi	Detoxification enzyme, downstream of hypoxic response (HIF-1 activation)
gpa-9	NL793	GTPase, involved in innate immunity
hif-1	ZG31	Hypoxia inducible factor, transcription factor activated by low oxygen (< 1%)
hif-1	ZG596	Hypoxia inducible factor, transcription factor activated by low oxygen (< 1%)
hif-1	RNAi	Hypoxia inducible factor, transcription factor activated by low oxygen (< 1%)
hypoxia	.5%	Intervention to activate HIF-1
inx-2	CX13325	Innexin/gap junction protein, downstream of hypoxic response (HIF-1 activation)
lys-8	RB2528	Lysozyme, involved in innate immunity
nuo-2	RNAi	NDUFS3 ortholog, regulates mitochondrial respiration
phy-2	RNAi	Downstream of the hypoxic response (HIF-1 activation)
rhy-1	RB1297	Negative regulator of HIF-1
rol-6	CB187	Collagen protein, common selection marker for transgenic animals
rpl-6	RNAi	Ribosomal subunit L6, inhibits mRNA translation (improves proteostasis)

rpl-9	RNAi	Ribosomal subunit L9, inhibits mRNA translation (improves proteostasis)
rpl-22	RNAi	Ribosomal subunit L22, inhibits mRNA translation (improves proteostasis)
rsks-1	RB1206	Ribosomal S6 kinase, inhibits mRNA translation (improves proteostasis)
sir-2.1	VC199	NAD-deacetylase, reported to be important for longevity
SKN-1 OE	LD1	Nrf ortholog, antioxidant response, transcription factor activated by ROS
skn-1	EU1	Nrf ortholog, antioxidant response, transcription factor activated by ROS
skn-1	EU31	Nrf ortholog, antioxidant response, transcription factor activated by ROS
trpa-1	RB1052	TRP channel, detects changes in temperature
tyr-2	RB1272	Tyrosinase ortholog, downstream of hypoxic response (HIF-1 activation)
vhl-1	CB5602	E3 ubiquitin ligase, negative regulator of HIF-1

Table 3.2. Lifespan information for this study.

	15oC							
Genotype/ Treatment	**Averaged Mean**	**Exp. Error**	**Rep**	**n**	**Total Mean**	**Total Error**	**Total Median**	**p-value (N2 comparison)**
aak-1 (tm1944)	31.1164	1.4499	3	277	31.805	0.4826	32.00	0.000575
N2 (control)	32.3977	2.7532		350	32.817	0.3840	32.00	
aak-2 (ok524)	23.7323	0.7995	2	166	23.385	0.2544	22.00	3.1E-35
N2 (control)	29.7591	1.3617		227	30.185	0.3346	30.00	
atm-1 (gk186)	26.4768	1.9071	2	283	26.254	0.3479	25.00	4.45E-12
N2 (control)	29.7591	1.3617		227	30.185	0.3346	30.00	
atp-3 (RNAi)	23.8828	1.3261	3	322	24.555	0.3482	24.55	1.9E-16
	21.9532	2.3897		427	21.686	0.2526	21.69	
Dietary Restriction (DR)	38.6467	2.9079	4	608	39.355	0.5305	39.35	1.19E-16
Fed (control)	37.1172	1.1827		432	36.641	0.3858	36.64	
10mM caffeine	39.5129	2.2892	11	670	41.286	0.4421	41.28	1.95E-14
Water (control)	33.8995	1.4479		754	33.836	0.3582	33.84	
cah-4 (RNAi)	22.0451	0.3965	3	325	22.181	0.2704	22.18	0.465556
vector (control)	21.8685	0.2140		484	21.793	0.2223	21.79	
cco-1 (RNAi)	22.9238	2.0090	3	390	22.833	0.2960	22.83	0.000166
vector (control)	21.9532	2.3897		427	21.686	0.2526	21.69	
cep-1 (gk138)	40.9166	4.6852	2	237	40.303	0.5739	39.00	8.56E-19
N2 (control)	33.1881	3.9937		243	32.449	0.5669	30.00	
clk-1 (RNAi)	22.7224	2.3020	3	329	22.431	0.3314	22.43	1.46E-05
vector (control)	21.9532	2.3897		427	21.686	0.2526	21.69	
cyc-1 (RNAi)	23.6866	0.7375	3	325	23.600	0.3425	23.60	0.001109
vector (control)	21.9532	2.3897		427	21.686	0.2526	21.69	
daf-2 (e1370)	43.3146	1.3712	3	354	43.641	0.5002	42.00	8.91E-36
N2 (control)	32.0260	2.3993		336	32.253	0.3546	32.00	

daf-2 (RNAi)	44.3884	4.6223	4	383	43.396	0.7026	43.39	2.51E-35
vector (control)	27.9567	1.6142		474	27.553	0.2579	27.55	
daf-16 (mu86)	32.3871	0.9495	7	899	32.450	0.2057	31.00	5.89E-07
N2 (control)	32.8469	1.4034		775	33.089	0.2692	32.00	
egl-9 (n571)	35.0808	1.9758	4	544	34.373	0.3185	35.00	6.21E-11
N2 (control)	28.7036	0.8776		550	28.573	0.2511	28.00	
egl-9 (RNAi)	30.4919	0.0361	2	236	30.483	0.6498	30.48	1.28E-20
vector (control)	21.6729	0.1503		380	21.666	0.2537	21.67	
egl-9 (sa307)	31.7281	2.2265	5	602	30.895	0.2924	31.00	0.000296
N2 (control)	28.3366	1.6297		586	27.894	0.2320	28.00	
F28B4.5 (RNAi)	22.0068	0.3252	3	371	21.991	0.2058	21.99	0.93052
vector (control)	21.8685	0.2140		484	21.793	0.2223	21.79	
fmo-2 (RNAi)	21.9147	1.3001	4	456	21.535	0.1972	21.53	0.000694
vector (control)	22.3478	1.2185		655	22.119	0.1916	22.12	
fmo-2 (ok2147)	35.6377	0.4584	2	197	35.421	0.5869	34.00	0.442727
N2 (control)	34.4879	1.4879		247	34.494	0.4974	34.00	
gpa-9 (pk438)	35.0242	0.8438	2	277	35.057	0.4069	34.00	0.003043
N2 (control)	35.8475	1.8273		271	35.679	0.3971	34.00	
hif-1 (ia07)	32.5907	0.8500	3	383	32.258	0.3409	32.25	0.001283
N2 (control)	29.5709	0.8084		371	29.801	0.2660	29.80	
hif-1 (ia04)	31.2084	0.6691	19	2446	31.036	0.1437	31.03	1.5E-11
N2 (control)	32.5583	1.1201		2282	31.784	0.1717	31.78	
hif-1 (RNAi)	23.9526	1.6006	10	1097	23.096	0.2000	23.09	2.14E-20
vector (control)	25.2758	1.4691		1070	24.782	0.1852	24.78	
hypoxia (.5%)	35.1186	0.1878	2	329	35.158	0.2089	34.00	1.57E-13
normoxia (21%)	30.9734	1.2266		368	30.647	0.1788	32.00	
inx-2 (ok376)	39.3706	0.8091	3	406	39.384	0.4461	37.50	6.21E-09
N2 (control)	34.8984	1.4191		394	34.843	0.3282	34.00	
lys-8 (ok3504)	38.7615	0.4712	2	197	38.639	0.6904	37.00	5.95E-07
N2 (control)	35.8475	1.8273		271	35.679	0.3971	34.00	
nuo-2 (RNAi)	18.8712	0.7131	5	292	18.534	0.2619	18.53	4.25E-11
vector (control)	19.7298	1.5168		327	20.245	0.2601	20.24	
phy-2 (RNAi)	25.1231	0.4956	2	385	25.093	0.2488	25.09	1.11E-11

vector (control)	21.6729	0.1503		380	21.666	0.2537	21.67	
rhy-1 (ok1402)	29.9563	1.1755	5	742	29.702	0.2090	29.70	0.003236
N2 (control)	31.7757	1.8517		704	31.563	0.2401	31.56	
rol-6 (e187)	33.2982	1.3944	5	657	33.838	0.2750	34.00	6.76E-14
N2 (control)	31.2781	1.4965		619	31.368	0.2826	31.00	
rpl-6 (RNAi)	26.3284	1.1704	9	1166	26.327	0.1576	26.32	0.00139
vector (control)	28.1362	1.2280		740	27.781	0.2097	27.78	
rpl-9 (RNAi)	19.4252	1.0632	3	284	19.350	0.2558	19.35	0.640106
vector (control)	22.8971	3.4709		428	22.474	0.2933	22.47	
rpl-22 (RNAi)	21.7975	2.0328	3	460	21.093	0.2274	21.09	0.000359
vector (control)	23.3280	1.6574		453	23.012	0.2403	23.01	
rsks-1 (ok1255)	27.2270	0.0015	2	238	27.226	0.3593	27.22	0.130964
N2 (control)	29.7591	1.3617		227	30.185	0.3346	30.19	
sir-2.1 (ok434)	37.3703	1.6797	5	355	36.585	0.5622	36.00	4.45E-05
N2 (control)	35.5198	1.3377		414	35.338	0.4272	34.00	
Skn-1 OE (ldIs7)	36.1183	2.4820	5	509	37.242	0.4166	37.24	6.73E-08
***rol-6* (control)**	33.2982	1.3944		657	33.839	0.2751	33.84	
Skn-1 OE (ldIs7)	37.3517	2.3724	6	591	38.081	0.3874	38.08	4.6E-34
N2 (control)	31.8135	1.3341		672	31.615	0.2680	31.61	
skn-1 (zu67); eu-1	26.7325	0.8826	3	520	26.738	0.2188	26.00	8.84E-06
N2 (control)	29.5709	0.8084		371	29.801	0.2660	30.00	
skn-1 (zu135); eu-31	29.9347	4.0856	2	155	28.432	0.6360	28.43	3.82E-07
N2 (control)	30.1576	0.9632		293	30.174	0.3188	30.17	
trpa-1 (ok999)	38.1123	1.4406	2	265	38.101	0.5576	34.00	0.000907
N2 (control)	35.8475	1.8273		271	35.679	0.3971	34.00	
tyr-2 (ok1363)	33.6118	0.0855	3	471	33.612	0.2395	34.00	1.31E-12
N2 (control)	33.6298	2.4558		415	33.429	0.3358	32.00	
vhl-1 (ok161)	43.0419	1.0964	21	1931	43.803	0.2106	43.80	6.5E-152
N2 (control)	30.2526	0.8404		2638	29.649	0.1456	29.65	
	20oC							

Genotype/ Treatment	Averaged Mean	Exp. Error	Rep	n	Total Mean	Total Error	Total Median	p-value (N2 comparison)
aak-1 (tm1944)	23.8208	1.5291	2	88	23.681	0.5066	24.00	9.24E-18
N2 (control)	31.3283	0.4323		196	31.209	0.4138	32.00	
aak-2 (ok524)	23.7868	1.8727	5	475	24.823	0.2584	25.00	0.030651
N2 (control)	24.9216	1.8616		663	25.881	0.2542	25.00	
atm-1 (gk186)	21.9566	1.3013	4	414	21.978	0.2784	22.00	4.78E-27
N2 (control)	29.9752	0.8210		446	29.661	0.2629	30.00	
atp-3 (RNAi)	18.0085	0.9263	2	373	18.150	0.2015	18.15	8.22E-16
vector (control)	16.0026	0.3081		321	16.034	0.1773	16.03	
Dietary Restriction (DR)	31.6880	1.1763	8	933	32.380	0.2400	32.38	5.97E-42
Fed (control)	26.3229	1.1004		973	26.581	0.1968	26.58	
10mM caffeine	27.8220	2.2451	5	490	27.218	0.3143	27.21	6.33E-07
Water (control)	26.7970	1.8349		468	26.776	0.3187	26.78	
cah-4 (RNAi)	17.9257	0.8577	4	508	17.537	0.1678	17.53	0.000153
vector (control)	17.8276	0.5640		514	17.916	0.1463	17.92	
cco-1 (RNAi)	20.6523	2.2853	3	455	19.617	0.2395	19.61	0.036394
vector (control)	18.3823	2.3863		434	17.885	0.2291	17.88	
cep-1 (gk138)	26.1478	1.2837	11	1771	26.431	0.1582	27.00	3.05E-13
N2 (control)	26.2089	1.1179		1637	26.276	0.1544	25.00	
clk-1 (RNAi)	19.0329	1.6065	3	449	18.832	0.2187	18.83	1.97E-10
vector (control)	18.3823	2.3863		434	17.885	0.2291	17.88	
cyc-1 (RNAi)	21.7346	3.5095	3	477	20.454	0.3198	20.45	0.02149
vector (control)	18.3823	2.3863		434	17.885	0.2291	17.88	
daf-2 (e1370)	42.6589	2.5906	5	855	43.568	0.4243	46.00	1.27E-44
N2 (control)	27.9941	1.4160		688	27.410	0.2108	28.00	
daf-2 (RNAi)	33.7672	2.3172	3	187	34.550	0.7295	34.55	6.8E-27
vector (control)	20.7044	1.6324		168	20.815	0.3883	20.82	
daf-16 (mu86)	20.4089	0.8397	8	693	20.537	0.1806	20.00	1.04E-13
N2 (control)	23.4754	0.9090		708	23.838	0.2016	24.00	
egl-9 (n571)	28.1178	0.6664	6	1025	27.983	0.1648	28.00	0.000335
N2 (control)	26.9466	0.6803		829	26.423	0.1667	28.00	

egl-9 (RNAi)	23.7746	0.9940	3	133	23.924	0.3203	23.92	4.62E-10
vector (control)	20.5868	0.9697		117	20.513	0.3979	20.51	
egl-9 (sa307)	28.0807	0.7077	7	947	28.405	0.1715	29.00	2.14E-13
N2 (control)	26.4816	0.7395		897	26.216	0.1617	26.00	
F28B4.5 (RNAi)	19.8677	0.9179	6	506	18.974	0.1683	18.97	0.078974
vector (control)	19.0853	0.9075		558	18.398	0.1531	18.40	
fmo-2 (RNAi)	21.0431	1.3273	3	567	20.915	0.1818	20.91	0.629862
vector (control)	21.3129	1.6868		510	21.614	0.1936	21.61	
fmo-2 (ok2147)	26.9898	1.2637	2	211	27.379	0.4512	28.00	0.012644
N2 (control)	26.4896	0.0046		254	26.488	0.3453	26.00	
gpa-9 (pk438)	25.4859	0.3256	2	269	25.494	0.3052	26.00	0.360287
N2 (control)	26.4896	0.0046		254	26.488	0.3453	26.00	
hif-1 (ia07)	28.5878	2.2847	4	866	29.132	0.2437	29.13	6.33E-07
N2 (control)	28.4840	2.4624		580	28.003	0.2806	28.00	
hif-1 (ia04)	23.6807	0.5972	18	3197	24.827	0.1279	24.82	5.25E-12
N2 (control)	23.8882	0.5073		3058	24.494	0.1043	24.49	
hif-1 (RNAi)	20.6582	0.8761	23	2583	20.494	0.1189	20.49	5.88E-46
vector (control)	19.9860	0.6417		2584	19.674	0.0967	19.67	
hypoxia (.5%)	26.6371	1.3099	9	1104	28.028	0.1962	28.00	0.0007
normoxia (21%)	23.8261	1.1441		1255	25.360	0.1551	25.00	
inx-2 (ok376)	29.8138	0.6271	2	277	29.761	0.2853	30.00	2.99E-06
N2 (control)	26.4896	0.0046		254	26.488	0.3453	26.00	
lys-8 (ok3504)	26.0446	0.6066	2	273	26.113	0.3250	26.00	0.782727
N2 (control)	26.4896	0.0046		254	26.488	0.3453	26.00	
nuo-2 (RNAi)	17.7009	1.9262	4	557	17.007	0.1969	17.00	4.36E-13
vector (control)	17.9691	1.7372		556	17.631	0.1879	17.63	
phy-2 (RNAi)	20.8526	1.9487	3	132	21.030	0.3997	21.03	0.01154
vector (control)	20.5868	0.9697		117	20.513	0.3979	20.51	
rhy-1 (ok1402)	23.0575	0.9883	6	915	22.893	0.1824	22.89	2.53E-09
N2 (control)	27.8723	1.1852		825	27.202	0.2115	27.20	
rol-6 (e187)	25.7377	1.5856	3	427	25.339	0.3120	26.00	1.06E-05
N2 (control)	27.0531	0.5635		415	27.145	0.2646	28.00	
rpl-6 (RNAi)	21.0707	0.7266	8	756	21.247	0.1516	21.24	0.315851

vector (control)	22.3337	1.0605		521	21.904	0.2026	21.90	
rpl-9 (RNAi)	20.2547	0.3132	4	551	20.157	0.1832	20.15	0.3104
vector (control)	21.3416	0.9052		480	20.856	0.2016	20.86	
rpl-22 (RNAi)	21.0665	0.4999	5	583	20.842	0.1714	20.84	0.014073
vector (control)	20.2764	0.4532		589	20.545	0.1737	20.54	
rsks-1 (ok1255)	26.2212	2.1121	2	206	26.077	0.3738	26.07	2.98E-11
N2 (control)	25.7932	2.3869		257	26.397	0.3421	26.40	
sir-2.1 (ok434)	24.9069	0.9283	8	923	25.109	0.1583	26.00	5.4E-36
N2 (control)	26.8938	1.2386		1098	27.287	0.1961	28.00	
Skn-1 OE (ldls7)	26.9298	0.0560	3	430	26.925	0.2554	26.92	2.74E-06
***rol-6* (control)**	25.7377	1.5857		427	25.340	0.3120	25.34	
Skn-1 OE (ldls7)	25.6626	0.8889	11	1837	25.978	0.1422	25.97	2.42E-05
N2 (control)	26.5888	1.0349		1448	27.054	0.1635	27.05	
skn-1 (zu67); eu-1	24.8495	1.5813	7	963	24.689	0.2004	23.00	7.86E-05
N2 (control)	25.0290	1.5262		993	24.863	0.1873	24.00	
skn-1 (zu135); eu-31	21.4625	1.6786	6	767	22.166	0.2009	22.16	3.81E-27
N2 (control)	24.5876	1.4989		953	25.163	0.1939	25.16	
trpa-1 (ok999)	26.9034	0.1034	2	278	26.906	0.3624	28.00	0.535441
N2 (control)	26.4896	0.0046		254	26.488	0.3453	26.00	
tyr-2 (ok1363)	22.4808	1.1152	3	379	22.153	0.2141	23.00	4.81E-07
N2 (control)	24.8820	1.6077		440	24.450	0.2421	23.00	
vhl-1 (ok161)	30.8891	0.7414	28	2931	29.946	0.1198	29.94	9.48E-24
N2 (control)	23.8943	0.5298		2837	24.015	0.1082	24.01	
	25oC							
Genotype/ Treatment	**Averaged Mean**	**Exp. Error**	**Rep**	**n**	**Total Mean**	**Total Error**	**Total Median**	**p-value (N2 comparison)**
aak-1 (tm1944)	14.4258	0.5179	2	330	14.466	0.1801	14.00	2.51E-06
N2 (control)	15.8656	0.6957		308	15.870	0.1852	16.00	
aak-2 (ok524)	14.6095	0.7878	2	280	14.671	0.1394	14.00	0.000138
N2 (control)	15.8656	0.6957		308	15.870	0.1852	16.00	
atm-1 (gk186)	16.7794	0.9669	2	212	16.451	0.2943	16.00	0.147462

N2 (control)	15.8656	0.6957		308	15.870	0.1852	16.00	
atp-3 (RNAi)	15.3811	0.9662	4	644	15.184	0.1381	15.18	0.019101
vector (control)	14.2439	1.0018		721	14.311	0.1041	14.31	
Dietary Restriction (DR)	22.0954	1.4969	2	294	22.197	0.3600	22.19	1.31E-29
Fed (control)	15.8656	0.6957		308	15.870	0.1852	15.87	
10mM caffeine	17.3554	3.7614	2	178	16.848	0.3876	16.84	1.07E-08
Water (control)	19.3120	2.9787		170	19.347	0.3769	19.35	
cah-4 (RNAi)	14.4023	0.0750	2	320	14.400	0.1173	14.40	0.000748
vector (control)	15.1763	0.0375		289	15.176	0.1516	15.18	
cco-1 (RNAi)	15.4544	0.7142	4	566	15.286	0.1641	15.28	0.001286
vector (control)	13.4137	0.8896		638	13.806	0.1073	13.81	
cep-1 (gk138)	17.1625	1.5704	3	453	16.966	0.1859	17.00	0.746163
N2 (control)	16.4714	0.7269		450	16.442	0.1499	17.00	
clk-1 (RNAi)	13.5173	1.2627	5	702	13.377	0.1334	13.37	0.057545
vector (control)	13.9054	0.8466		779	14.180	0.0989	14.18	
cyc-1 (RNAi)	14.8101	0.8309	4	563	14.879	0.1586	14.87	0.108162
vector (control)	13.4137	0.8896		638	13.806	0.1073	13.81	
daf-2 (e1370)	35.3257	1.8097	2	312	35.314	0.4163	35.00	2.2E-50
N2 (control)	21.9517	0.9225		296	22.020	0.1843	22.00	
daf-2 (RNAi)	26.6356	0.8765	3	240	25.895	0.4534	25.89	3.31E-42
vector (control)	14.8038	0.3731		306	15.114	0.1487	15.11	
daf-16 (mu86)	15.3958	0.5247	4	315	15.200	0.1275	15.00	5.79E-16
N2 (control)	18.5590	0.5685		277	18.553	0.2077	18.00	
egl-9 (n571)	17.6966	1.1717	4	408	17.223	0.1876	17.00	0.755425
N2 (control)	18.1461	1.2199		576	17.866	0.1620	17.00	
egl-9 (RNAi)	16.5142	0.5918	4	276	16.174	0.1305	16.17	0.00043
vector (control)	16.0013	0.7256		380	15.632	0.1344	15.63	
egl-9 (sa307)	19.4073	0.5058	4	572	19.141	0.1780	19.00	3.12E-08
N2 (control)	18.1461	1.2199		756	17.866	0.1620	17.00	
F28B4.5 (RNAi)	15.0611	0.1732	3	337	14.997	0.1408	14.99	0.144644
vector (control)	15.2795	0.1054		324	15.210	0.1414	15.21	
fmo-2 (RNAi)	15.6366	0.0942	6	784	15.623	0.0920	15.62	0.213267

vector (control)	15.9761	0.2896		804	15.978	0.1066	15.98	
fmo-2 (ok2147)	21.3042	0.1282	2	162	21.234	0.2319	21.00	0.007665
N2 (control)	20.6394	0.4763		288	20.649	0.1887	21.00	
gpa-9 (pk438)	21.0839	1.0306	2	307	21.107	0.2855	21.00	8.59E-07
N2 (control)	18.4969	0.4908		326	18.497	0.2263	17.00	
hif-1 (ia07)	18.0929	0.2007	2	327	18.088	0.2209	18.08	3.18E-12
N2 (control)	15.8656	0.6957		308	15.870	0.1852	15.87	
hif-1 (ia04)	20.6809	0.2961	11	2306	21.087	0.0835	21.08	9.31E-15
N2 (control)	17.8533	0.3608		2123	18.646	0.0754	18.65	
hif-1 (RNAi)	16.4999	1.1129	8	1072	16.039	0.1280	16.03	0.874266
vector (control)	15.7604	0.6042		1073	15.286	0.1095	15.29	
hypoxia (.5%)	20.8026	0.3776	3	622	20.871	0.1308	21.00	3.69E-06
normoxia (21%)	18.8602	0.5945		545	18.989	0.1239	18.00	
inx-2 (ok376)	21.2884	0.7115	2	171	21.350	0.2746	22.00	0.036735
N2 (control)	20.6394	0.4763		288	20.649	0.1887	21.00	
lys-8 (ok3504)	21.2879	1.7977	2	233	20.618	0.3191	21.00	4.11E-05
N2 (control)	18.4969	0.4908		326	18.497	0.2263	17.00	
nuo-2 (RNAi)	15.4186	1.6212	2	700	15.865	0.1728	15.86	4.57E-09
vector (control)	13.9054	0.8466		779	14.180	0.0989	14.18	
phy-2 (RNAi)	16.8561	1.6532	2	121	16.639	0.2463	16.63	0.57281
vector (control)	16.8262	1.3405		89	17.112	0.2285	17.11	
rhy-1 (ok1402)	14.6166	0.8027	5	980	14.070	0.1037	14.07	1.02E-56
N2 (control)	17.0406	0.6622		839	17.039	0.1242	17.04	
rol-6 (e187)	33.2982	1.3944	5	679	33.838	0.2750	34.00	0.004824
N2 (control)	17.5917	0.7663		771	17.578	0.1393	17.00	
rpl-6 (RNAi)	18.2221	0.2895	4	461	18.199	0.1658	18.19	0.003761
vector (control)	15.6325	0.5989		405	16.054	0.1924	16.05	
rpl-9 (RNAi)	16.6971	0.6527	3	391	16.304	0.1345	16.30	0.003597
vector (control)	14.8038	0.3731		306	15.114	0.1487	15.11	
rpl-22 (RNAi)	15.5370	0.4171	3	281	15.561	0.1428	15.56	0.07451
vector (control)	15.6867	0.5108		521	15.731	0.1637	15.73	
rsks-1 (ok1255)	21.8313	1.4795	4	574	20.588	0.1868	20.58	2.03E-12
N2 (control)	17.6969	0.5400		646	17.704	0.1442	17.70	

sir-2.1 (ok434)	16.8612	0.8868	4	647	16.589	0.1439	16.00	5.63E-11
N2 (control)	16.3812	0.4554		628	16.393	0.1259	16.00	
Skn-1 OE (ldIs7)	14.7445	0.9253	3	402	14.380	0.1186	14.38	0.139615
***rol-6* (control)**	15.3006	1.1411		383	15.504	0.1581	15.50	
Skn-1 OE (ldIs7)	14.7445	0.9253	3	402	14.380	0.1186	14.38	6.98E-08
N2 (control)	16.9883	1.1923		445	16.906	0.1687	16.91	
skn-1 (zu67); eu-1	16.2139	0.8022	3	502	16.069	0.1439	16.00	0.806487
N2 (control)	16.9883	1.1923		445	16.906	0.1687	17.00	
skn-1 (zu135); eu-31	18.2702	0.5827	2	316	18.439	0.1784	18.43	6.25E-05
N2 (control)	18.3412	0.8924		264	18.375	0.1940	18.38	
trpa-1 (ok999)	21.4479	0.3597	2	172	21.523	0.3710	21.00	2.12E-05
N2 (control)	18.4969	0.4908		326	18.497	0.2263	17.00	
tyr-2 (ok1363)	18.7894	1.4156	2	138	18.173	0.3258	17.00	0.084695
N2 (control)	18.4969	0.4908		326	18.497	0.2263	17.00	
vhl-1 (ok161)	23.5363	0.5355	22	1737	23.667	0.1172	23.66	1.11E-23
N2 (control)	18.3044	0.4195		1901	18.567	0.0930	18.57	

Table 3.3. Hazard Ratio calculations for Figure 3.6C-D, Figure 3.8.

Condition	Hazard ratio	Standard Error		p-value	95% confidence interval	
aak-2	1.883359	0.254816	4.68	<0.001	1.444663	2.455272
atm-1	2.423418	0.310277	6.91	<0.001	1.885587	3.114656
Dietary Restriction (DR)	4.271351	0.479679	12.93	<0.001	3.427473	5.323001
daf-2	2.628244	0.313828	8.09	<0.001	2.079826	3.32127
gpa-9	2.013283	0.23811	5.92	<0.001	1.596738	2.538494
rsks-1	2.961879	0.327957	9.81	<0.001	2.384061	3.679742
hif-1 ia4	2.005512	0.084294	16.56	<0.001	1.84692	2.177721
hif-1 ia7	1.405371	0.154761	3.09	0.002	1.132545	1.74392
trpa-1	1.439773	0.188655	2.78	0.005	1.113679	1.86135
cep-1	0.685007	0.07829	-3.31	0.001	0.547533	0.856998
daf-16	0.39232	0.039225	-9.36	<0.001	0.322505	0.477249
egl-9(n571)	0.416451	0.037096	-9.83	<0.001	0.349737	0.495891
Caffeine	0.359499	0.043363	-8.48	<0.001	0.283808	0.455375
vhl-1	0.726289	0.034123	-6.81	<0.001	0.662396	0.796345
rol-6	0.463335	0.036049	-9.89	<0.001	0.397804	0.539661
SKN-1 OX	0.185997	0.017197	-18.19	<0.001	0.155168	0.222951
SKN-1 Oxb	0.394067	0.037374	-9.82	<0.001	0.327221	0.474568
inx-2	0.678473	0.082781	-3.18	0.001	0.534168	0.861763
rhy-1	0.571705	0.04146	-7.71	<0.001	0.495955	0.659023
fmo-2	1.011335	0.139118	0.08	0.935	0.772334	1.324296
egl-9(sa307)	0.863113	0.07188	-1.77	0.077	0.733127	1.016145
aak-1	0.868319	0.099977	-1.23	0.22	0.692904	1.088141
Hypoxia (0.5% O_2)	0.904899	0.088328	-1.02	0.306	0.747333	1.095687

FMO-2 OX	**0.933723**	**0.087696**	**-0.73**	**0.465**	**0.776735**	**1.122441**
tyr-2	**0.978058**	**0.119694**	**-0.18**	**0.856**	**0.769476**	**1.243181**
skn-1 zu135	**1.1333**	**0.148722**	**0.95**	**0.34**	**0.87628**	**1.465706**
skn-1 zu67	**1.109203**	**0.104894**	**1.1**	**0.273**	**0.921543**	**1.335079**
sir2.1	**1.01132**	**0.093278**	**0.12**	**0.903**	**0.84407**	**1.211709**
lys-8	**1.147747**	**0.151666**	**1.04**	**0.297**	**0.885863**	**1.487053**
RNAi	**Hazard ratio**	**Standard Error**		**p-value**	**95% confidence interval**	
daf-2	**2.464961**	**0.342478**	**6.49**	**<0.001**	**1.877351**	**3.236492**
cco-1	**1.469224**	**0.135519**	**4.17**	**<0.001**	**1.226237**	**1.760361**
rpl-9	**2.84442**	**0.314401**	**9.46**	**<0.001**	**2.290383**	**3.532477**
rpl-6	**1.851258**	**0.15362**	**7.42**	**<0.001**	**1.573379**	**2.178215**
nuo-2	**2.318233**	**0.226252**	**8.62**	**<0.001**	**1.91462**	**2.80693**
hif-1	**1.517506**	**0.092637**	**6.83**	**<0.001**	**1.346382**	**1.710381**
cah-4	**0.639755**	**0.069733**	**-4.1**	**<0.001**	**0.516695**	**0.792125**
clk-1	**0.770578**	**0.069769**	**-2.88**	**0.004**	**0.645279**	**0.920206**
egl-9	**0.35076**	**0.041811**	**-8.79**	**<0.001**	**0.27768**	**0.443073**
phy-2	**0.549394**	**0.086731**	**-3.79**	**<0.001**	**0.403189**	**0.748617**
atp-3	**0.928429**	**0.086832**	**-0.79**	**0.427**	**0.772929**	**1.115213**
cyc-1	**1.167516**	**0.110711**	**1.63**	**0.102**	**0.969498**	**1.40598**
F28B5.4	**0.949464**	**0.099172**	**-0.5**	**0.62**	**0.773695**	**1.165163**
fmo-2	**0.954942**	**0.075838**	**-0.58**	**0.562**	**0.817292**	**1.115775**

CHAPTER 4

Using Bioinformatic Tools to Cultivate New Hypotheses

Foreword

The data for this chapter encompasses two independent projects that rely on "omics" exploratory analyses. Since the advent of microarray studies in the 1990s (*218*), bioinformatic analyses of large datasets have played an integral role in advancing our understanding of the complex relationship between genotypes and phenotypes. By employing computer programming and statistical principles to a pleiotropic phenomenon like aging, we can assess similarities and differences amongst pro-longevity conditions in order to uncover the causative changes promoting healthy aging. Using whole-animal transcriptomic profiling (RNA-seq) we developed testable hypotheses to enhance our understanding of *fmo-2* activation (project 1) and activity (project 2).

My role on project 1, as the second author, was to analyze the RNA-seq data, prepare the plots, and provide my interpretation. The data and written portion included here is an excerpt from a published manuscript[3]. Project 2 is an unpublished story exploring the potential role of an understudied family of proteases that are down-regulated during DR and FMO-2 OE. Drs. Scott Lesier and Jason Pitt prepared the RNA-seq samples at the University of Washington I analyzed in both projects. Abrielle Fretz, a master's student turned research technician in the Leiser lab, played an important role in project 2 performing lifespans and imaging experiments throughout the course of this project.

3. Information included here was originally published in *Geroscience* (2020 May 42; 1621–1633) with authors listed as Kruempel, J.K., **Miller, H.A**., Schaller, M.L., Fretz, A., Howington, M., Sarker, M., Huang, S., and Leiser, S.F.

Hypoxic response regulators RHY-1 and EGL-9/PHD promote longevity through a VHL-1-independent transcriptional response

Abstract

HIF-1-mediated adaptation to changes in oxygen availability is a critical aspect of healthy physiology. HIF is regulated by a conserved mechanism whereby EGLN/PHD family members hydroxylate HIF in an oxygen-dependent manner, targeting it for ubiquitination by Von-Hippel-Lindau (VHL) family members, leading to its proteasomal degradation. The activity of the only *C. elegans* PHD family member, EGL-9, is also regulated by a hydrogen sulfide sensing cysteine-synthetase-like protein, CYSL-1, which is, in turn, regulated by RHY-1/acyltransferase. Over the last decade multiple seminal studies have established a role for the hypoxic response in regulating longevity, with mutations in *vhl-1* substantially extending *C. elegans* lifespan through a HIF-1-dependent mechanism. However, studies on other components of the hypoxic signaling pathway that similarly stabilize HIF-1 have shown more mixed results, suggesting that mutations in *egl-9* and *rhy-1* frequently fail to extend lifespan. Here, we show that *egl-9* and *rhy-1* mutants suppress the long-lived phenotype of *vhl-1* mutants. We also show that RNAi of *rhy-1* extends lifespan of wild-type worms while decreasing lifespan of *vhl-1* mutant worms. We further identify VHL-1-independent gene expression changes mediated by EGL-9 and RHY-1 and find that a subset of these genes contributes to longevity regulation. The resulting data suggest that changes in HIF-1 activity derived by interactions with EGL-9 likely contribute greatly to its role in regulation of longevity.

Introduction

Adaptation to changes in oxygen availability is a central requirement for aerobic life. In response to hypoxia, reduced oxygen-dependent hydroxylation of Hypoxia Inducible Factor α (HIFα) transcription factors by members of the EGLN/Proline-Hydroxylase (PHD) family triggers stabilization of HIFα proteins and activation of a transcriptional stress response that promotes survival (*219*). This hypoxic response plays critical roles in a variety of pathological conditions including inflammation and cancer (*220-222*). Constitutive stabilization of the sole *C. elegans* HIFα family member, HIF-1, by deletion

of the Von-Hippel-Lindau ubiquitin ligase, VHL-1, which ubiquitinates HIF-1 and targets it for degradation, results in HIF-1-dependent increases in stress response and longevity (*223-229*).

Genetic studies in *C. elegans* have identified additional players in the hypoxic signaling pathway. Activity of EGL-9, the only known *C. elegans* PHD family member, is inhibited by direct interaction with the H_2S sensing cysteine-synthetase family member CYSL-1 (*230*). CYSL-1 protein levels are in turn reduced through an unknown mechanism by Regulator of Hypoxia-inducible factor-1 (RHY-1), an ER transmembrane protein with predicted acyltransferase activity (*230, 231*). Predicted loss-of-function mutations in *rhy-1* stabilize HIF-1 and produce expression patterns of HIF-1 target genes that are consistent with reduced EGL-9 activity (*231*).

Interestingly, while *vhl-1* mutation extends *C. elegans* lifespan across culture conditions, the role of EGL-9/PHD is more context dependent. While *egl-9(RNAi)* extends lifespan at 20°C, the lifespan phenotypes of partial loss-of-function mutations in *egl-9* are temperature-dependent, extending lifespan in a HIF-1- dependent manner at low temperatures (15°C) but not at higher temperatures (20°C and 25°C) (*225, 226, 232, 233*). The loss-of-function mutant *egl-9(sa307)* also reduces the lifespan of dietary restricted animals and long-lived *rsks-1* mutants when animals are cultured at 25°C, suggesting that EGL-9 activity may promote lifespan in multiple contexts (*234*). Furthermore, recent work from our lab showed that *rhy-1* putative knockout mutants were not long-lived at any temperature, despite their reported robust activation of hypoxic response genes (*231, 233*).

Previous studies on the roles of EGL-9, RHY-1, and VHL-1 show that 1) HIF-1 stabilization when *vhl-1* is mutated leads to robust induction of *egl-9* and *rhy-1*, 2) EGL-9 and RHY-1 have VHL-1-independent effects on transcription of some hypoxic response genes, and 3) EGL-9 and RHY-1 play a VHL-1-independent role in pathogen and hydrogen sulfide resistance (*231, 235-239*). However, the possibility that EGL-9 and RHY-1 modulate longevity through a downstream, VHL-1-independent

transcriptional response has not been addressed. Here we present a genetic study demonstrating that EGL-9 and RHY-1 are necessary for lifespan extension when HIF-1 is stabilized by *vhl-1* mutation. We show that, like EGL-9, RHY-1 has both longevity promoting and inhibiting activities. We further identify genes that are oppositely regulated in *vhl-1* and *egl-9* or *rhy-1* mutants, suggesting that RHY-1 and EGL-9 promote a VHL-1-independent transcriptional response when HIF-1 is stabilized by *vhl-1* mutation. Lastly, we find that RNAi knockdown of four genes downregulated in *vhl-1(ok161)* mutants and upregulated in *egl-9(sa307)* mutants, with likely functions in innate immunity, each partially rescues lifespan extension in *egl-9(sa307);vhl-1(ok161)* mutants. Together, our results suggest that EGL-9 modulates lifespan by regulating a VHL-1-independent transcriptional program.

RHY-1 and EGL-9 control a VHL-1-independent transcriptional response.
Previous studies reported that *egl-9* causes *vhl-1*-independent changes in expression of some transcripts (*231, 235, 236*). We hypothesized that the dominance of the *egl-9(sa307)* and *rhy-1(ok1402)* lifespan phenotypes over the *vhl-1(ok161)* lifespan phenotype might be caused by genes whose transcription is regulated by EGL-9 or RHY-1. Concurrently with our work, Angeles et al. published an analysis of transcriptome profiles from *rhy-1(ok1402)*, *egl-9(sa307)*, *hif-1(ia4)*, *egl-9;hif-1*, and *egl-9;vhl-1* mutants. They identified a class of genes whose transcription is regulated by EGL-9 in a way that is distinct from, and dominant over, their regulation by VHL-1. We will refer to this class as EGL-9/VHL-1 antagonistic genes.

To identify genes that might modulate lifespan downstream of the hypoxic response, we had previously profiled the transcriptomes of *egl-9(sa307)*, *vhl-1(ok161), rhy-1(ok402),* and *hif-1(ia4)* mutants. We reanalyzed our data using the methodology that Angeles et al. reported and an up-to-date bioinformatic pipeline (*240-242*). Our datasets identified a subset of genes that were differentially expressed in the HIF-1 negative regulator mutants relative to wild-type, further confirming that these changes are implicated in the hypoxic response, **(Figure 4.1A**). Conversely, we observed low overlap between the datasets for genes differentially expressed in the *hif-1(ia4)* background, suggesting that differences between *hif-1(ia4)* and wild-type in individual datasets may largely reflect strain-specific effects rather than HIF-1-dependent transcription under normoxia **(Figure 4.1B)**.

We next plotted β coefficients of differentially expressed genes shared between *vhl-1(ok161)* and *egl-9(sa307)* in Leiser and Sternberg datasets **(Figure 4.1C)**. Both datasets produce a similar pattern, with *egl-9(sa307)*, and *vhl-1(ok161)* causing highly correlated changes in expression for most shared differentially expressed genes. Both datasets also contained EGL-9/VHL-1 antagonistic genes, which were either upregulated in *vhl-1(ok161)* and downregulated in *egl-9(sa307)* (**Figure 4.1C**, quadrant II), or upregulated in *egl-9(sa307)* or *rhy-1(ok1402)* and downregulated in *vhl-1(ok161)* (**Figure 4.1C**, quadrant IV). The genes in quadrants II and IV, that we hypothesized

could play a role in different outcomes between *vhl-1(ok161)* and *egl-9(sa307)* or *rhy-1(ok1402)* strains, are listed in **Table 4.1**. Together, our and the Sternberg lab's results show that HIF-1 stabilization through loss of its negative regulators has both many common effects and a smaller number of opposing effects depending on which negative regulator is mutated.

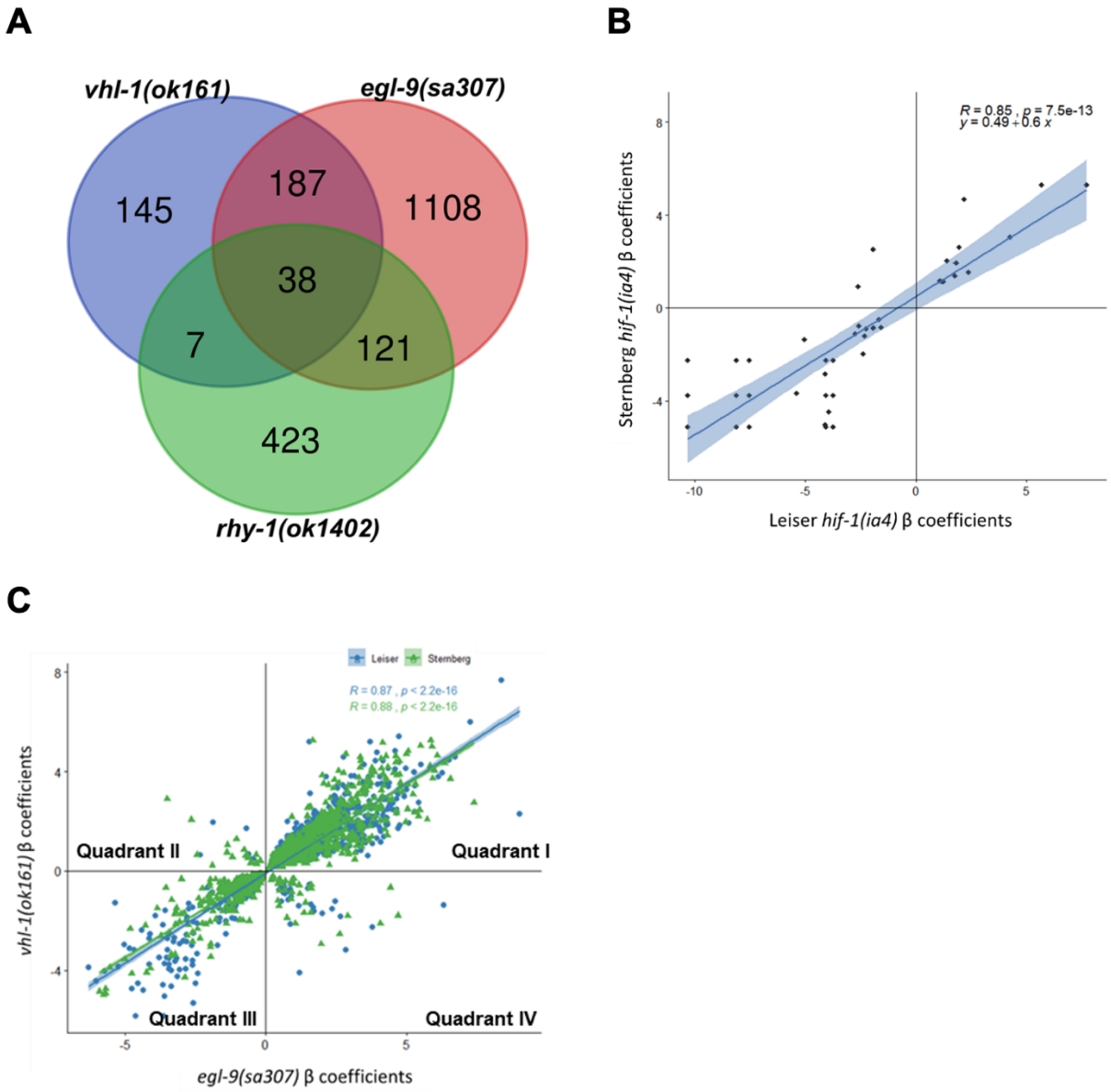

Figure 4.1. A subset of genes are antagonistically regulated by *egl-9* and *vhl-1.*
A) Overlap between genes that are differentially expressed in both Leiser and Sternberg datasets for *vhl-1(ok161)* and *egl-9(sa307)* along with differentially expressed genes from Sternberg *rhy-1(ok1402)*. B) Overlap between differentially expressed genes in *hif-1(ia4)* in Leiser and Sternberg datasets. C) Correlation of expression levels of differentially expressed genes in *egl-9(sa307)* and *vhl-1(ok161)* in Leiser and Sternberg datasets.

ORF	Gene	Description
K08C7.5	*fmo-2*	FMO5 (flavin containing dimethylaniline monoxygenase 5) ortholog
T05B4.2	*nhr-57*	nuclear hormone receptor family transcription factor
C14C6.5	C14C6.5	predicted role in innate immune response
F22D6.10	*col-60*	collagen structural protein in cuticle
F26H9.5	F26H9.5	PSAT1 (phosphoserine aminotransferase 1) ortholog
C08E8.3	C08E8.3	unknown function
K06A4.7	K06A4.7	unknown function
F15B9.1	*far-3*	fatty acid binding protein
F38B2.4	F38B2.4	AK1 (adenylate kinase 1) ortholog
Y37A1B.5	Y37A1B.5	SELENBP1 (selenium binding protein 1) ortholog
F38A3.2	*ram-2*	structural protein in cuticle
F28F8.2	*acs-2*	ACSF2 (acyl-CoA synthetase family member 2) ortholog
F08G5.4	*col-130*	collagen structural protein in cuticle
T10D4.13	*ins-19*	predicted insulin protein
C31C9.2	C31C9.2	PHGDH (phosphoglycerate dehydrogenase) ortholog
F22B5.4	F22B5.4	unknown function
F10D2.9	*fat-7*	SCD5 (stearoyl-CoA desaturase 5) ortholog
R08E5.3	R08E5.3	methyltransferase orthologs
Y22F5A.4	*lys-1*	lysozyme activity, predicted role in innate immune response
C05E7.1	C05E7.1	unknown function
Y58A7A.1	Y58A7A.1	SLC31A1 (solute carrier family 31 member 1) ortholog
M05D6.6	*taap-1*	FAM162A/B (family with sequence similarity 162 member A/B) ortholog
W07A12.7	*rhy-1*	Negative regulator of HIF-1
M199.4	*clec-190*	C-type lectin predicted to have carbohydrate binding activity
B0222.6	*col-144*	collagen structural protein in cuticle
M05D6.5	M05D6.5	HIGD2A/B (HIG1 hypoxia inducible domain family member 2A/B) ortholog
F09A5.9	*ttr-34*	predicted transthyretin-like protein
W07A12.6	*oac-54*	predicted amino-acyl transferase protein
F02H6.5	*sqrd-1*	SQOR (sulfide quinone oxidoreductase) ortholog
ZK637.13	*glb-1*	predicted role in heme/oxygen binding and carrying
F54C9.4	*col-38*	collagen structural protein
Y22F5A.5	*lys-2*	lysozyme activity, predicted role in innate immune response
F37B1.8	*gst-19*	HPGDS (hematopoietic prostaglandin D synthase) ortholog
T03F1.11	T03F1.11	predicted for CIBs (calcium and integrin binding family member) ortholog
VF13D12L.3	VF13D12L.3	predicted oxidoreductase protein
C04G6.2	C04G6.2	unknown function
K10B3.7	*gpd-3*	GAPDH (glyceraldehyde-3-phosphate dehydrogenase) ortholog
R02E4.3	R02E4.3	unknown function

Table 4.1. Core hypoxic response genes.
List of 38 genes that were differentially regulated in *rhy-1(ok1402)* (Sternberg only), *egl-9(sa307)* and *vhl-1(ok161)* mutants in both Leiser and Sternberg RNA-seq datasets.

Knockdown of EGL-9 target genes rescues lifespan of *egl-9; vhl-1* mutants.
We next tested the hypothesis that EGL-9/VHL-1 antagonistic genes regulate longevity. Previous results suggest that individual longevity-pathway-target-genes often have small effects on lifespan, and longevity increases are more likely than longevity decreases to reflect modulation of the aging process as a whole (*243*). Thus, we identified candidate EGL-9/VHL-1 antagonistic genes whose downregulation in *vhl-1(ok161)* mutants was reversed in *egl-9(sa307);vhl-1(ok161)* mutants and determined whether RNAi targeting them could extend life lifespan of *egl-9;vhl-1(ok161)* mutants **(Figure 4.2 A,C,E,G)**.

EGL-9 and VHL-1 have distinct roles in pathogen resistance, with *egl-9(sa307)* mutants exhibiting HIF-1- dependent resistance to fast killing by *Pseudomonas aeruginosa* while *vhl-1(ok161)* mutants do not (*237, 238*). We noticed that our list of EGL-9/VHL-1 antagonistic genes contained several genes with reported or predicted roles in pathogen response, including *nlp-31*, which encodes five neuropeptide-like proteins with functions in defense against fungal pathogens and gram-negative pathogenic bacteria, *lys-7*, which encodes a lysozyme with a reported role in defense against gram-negative bacteria, *lys-10*, which encodes another lysozyme, and *lips-10*, which encodes an enzyme that, like lysozymes, has hydrolase activity (*244-247*). We found that treatment with *lys-10(RNAi), lips-10(RNAi)*, *lys-7(RNAi),* and *nlp-31(RNAi)* each extended longevity of *egl-9;vhl-1* mutants **(Figure 4.2 B,D,F,H)**.

We also tested treatment with RNAi targeting the ferritin genes, *ftn-1* and *ftn-2*, predicted oxidative and heavy metal response genes that have been identified as EGL-9/VHL-1 antagonistic genes in multiple studies (*248, 249*). We found slight but significant increases in lifespan in *egl-9(sa307);vhl-1(ok161)* animals treated with *ftn-1(RNAi)* and *ftn-2(RNAi)*, however the magnitude of these changes was small and they were not consistent across individual replicates (significant in 2 of 4 trials) (Figure 4.3 and Table 4.3). These data are consistent with ferritins playing a minor role in modulation of lifespan by the hypoxic response.

Taken together, these results are consistent with a model in which EGL-9 activity promotes longevity during HIF-1 stabilization through VHL-1-independent inhibition of target genes, including multiple genes with predicted functions in defense against pathogens.

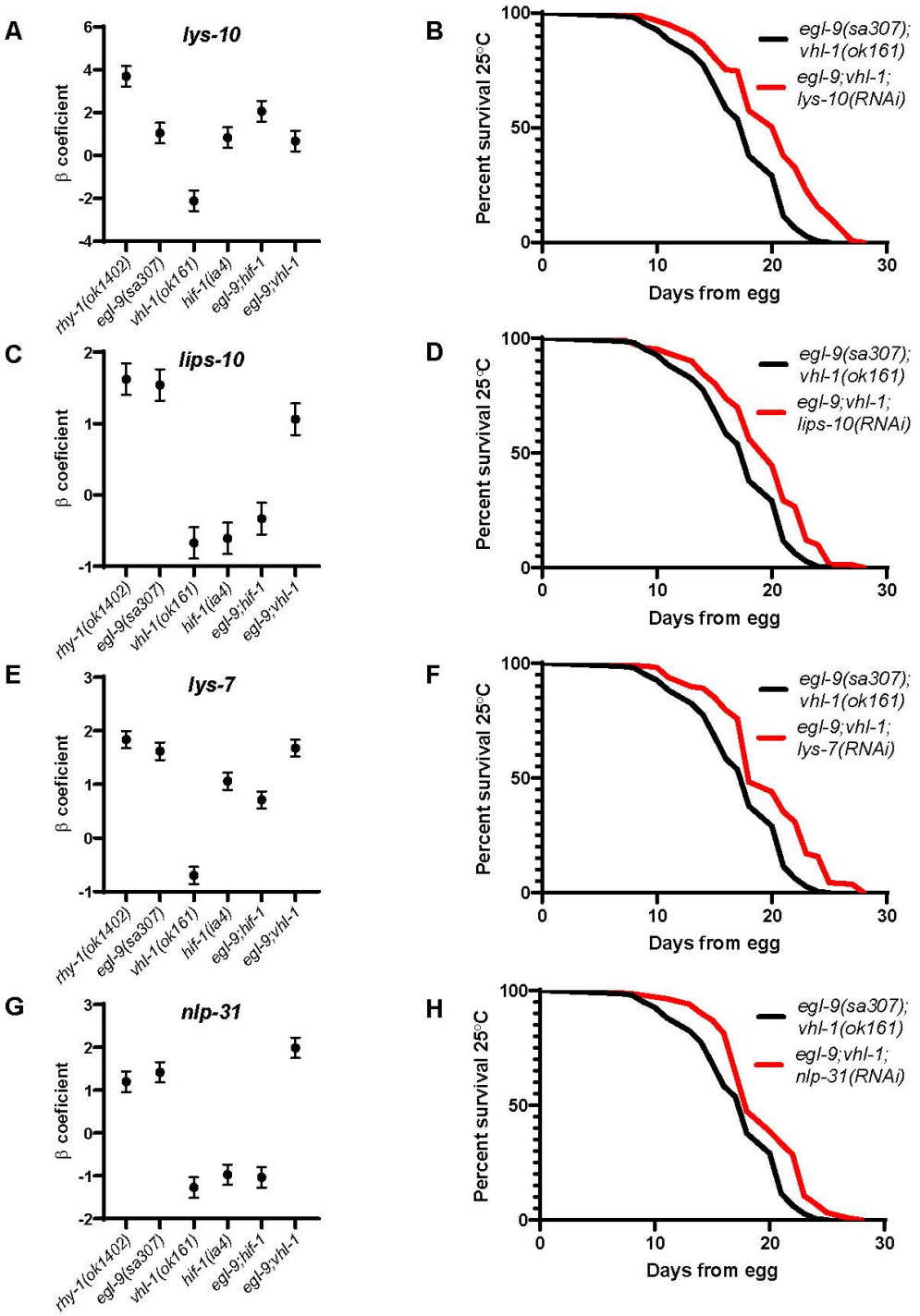

Figure 4.2. VHL-1/EGL-9 antagonistic HIF-1 targets rescue lifespan in egl-9;vhl-1 mutants. A, C, E, G) expression levels of selected transcripts from RNA-seq analyses. B-D-F-H) Treatment with *nlp-31(RNAi)*, *lys-7(RNAi)*, *lys-10(RNAi)* and *lips-10(RNAi)* increases lifespan of *egl-9(sa307);vhl-1(ok161)* mutants ($p<.05$ by log-rank). Lifespan data are aggregated from at least three experiments, and are significant ($p<.05$ by log-rank with Bonferroni correction) in at least 3 of 5 individual trials (Table 4.S1**)**.

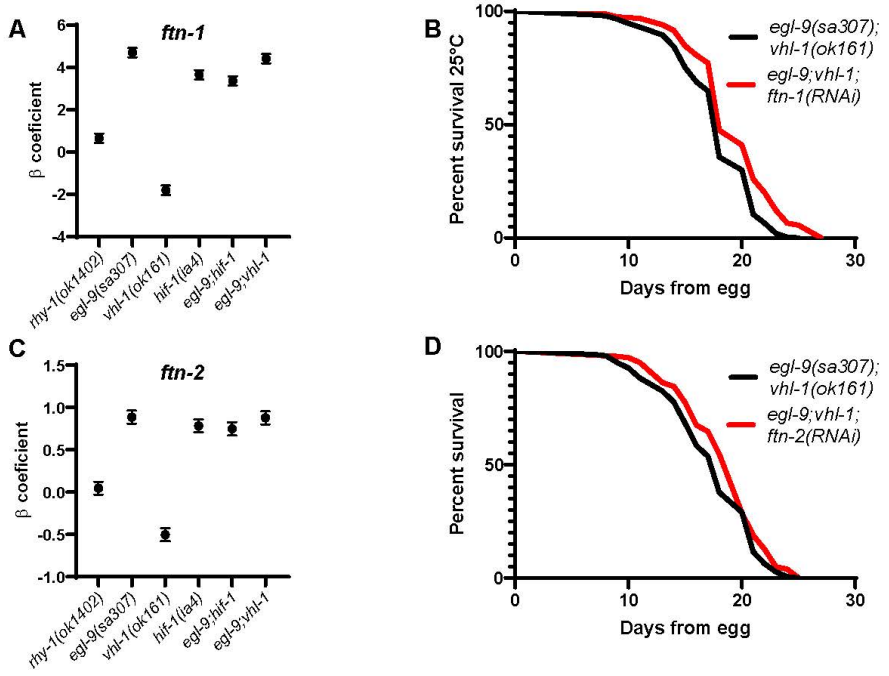

Figure 4.3. Effects of additional VHL-1/EGL-9 antagonistic HIF-1 targets on lifespan. A, C) expression levels of selected transcripts from RNA-seq analyses. B-D) Treatment with *ftn-1(RNAi),* and *ftn-2(RNAi)* increases lifespan of *egl-9(sa307);vhl-1(ok161)* mutants ($p<.05$ by log-rank). Lifespan data are aggregated from at least three experiments, and are significant ($p<.05$ by log-rank with Bonferroni correction) in 2 out of 4 individual trials (Table 4.3).

Discussion

Collectively, our results show that, while reduction in RHY-1 and EGL-9 activity can increase lifespan via the hypoxic response, RHY-1 and EGL-9 activity also promote longevity downstream of HIF-1 stabilization by *vhl-1* mutation. We further demonstrate that RHY-1 and EGL-9 activity are required to control the direction of differential expression of numerous transcripts in *vhl-1* mutants and that EGL-9-dependent suppression of *nlp-31*, *lys-7*, *lys-10*, and *lips-10* promotes longevity in *vhl-1* mutants.

Genetic interactions of *vhl-1*, *egl-9*, and *rhy-1*.

While HIF has emerged as a key regulator of longevity, it was previously unknown how hypoxic signaling pathway components interact to influence longevity. HIF-1 hydroxylation is required for its interaction with VHL-1, so in theory we might expect *egl-9* mutant phenotypes to be epistatic to *vhl-1* mutant phenotypes. However, reports that 1) EGL-9 and RHY-1 have VHL-1-independent roles in the expression and tissue distribution of hypoxic response genes, 2) EGL-9 interacts with other proteins through proline-hydroxylase-activity-dependent and -independent mechanisms to influence phenotype, and 3) EGL-9 and RHY-1 are transcriptionally upregulated when HIF-1 is stabilized, make these phenotypic interactions difficult to predict (*231, 235-238*).

We found that *rhy-1(ok1402)* blocked lifespan extension by *vhl-1(RNAi)* and *vhl-1(ok161)*, while *egl-9(sa307)* blocked lifespan extension by *vhl-1(RNAi)* and partially blocked lifespan extension by *vhl-1(ok161)*. While these results are broadly consistent with a model where RHY-1 regulates lifespan through its known EGL-9 modulating activity, it is interesting that *rhy-1* mutation has a stronger effect on the longevity of *vhl-1(ok161)* mutants than the *egl-9(sa307)* mutation. This could be explained by the reportedly more robust HIF-1 stabilization and upregulation of pro-longevity HIF-1 target genes in *egl-9(sa307)* relative to *rhy-1(ok1402)*, or by an additional, HIF-1-independent role for RHY-1 in longevity determination (*231*).

We confirmed the surprising, previously reported, result that the *rhy-1(ok1402)* mutation does not extend lifespan, despite stabilizing HIF-1. However, interestingly, *rhy-1(RNAi)*

extends lifespan through a mechanism that is partially dependent on its established interactions with CYSL-1 and HIF-1. While off-target effects of RNAi are a concern when mutant and RNAi phenotypes differ, the observation that the *rhy-1(RNAi)*-mediated lifespan increase is fully abrogated in a *rhy-1(ok1402)* mutant background strongly suggests that modulation of RHY-1 is the primary factor influencing lifespan in this context. It is worth noting that, while *cysl-1(ok762)* and *hif-1(ia4)* mutations reduce the longevity promoting effect of *rhy-1(RNAi)*, neither completely abrogates it. This suggests that RHY-1 may have secondary, HIF-1-independent roles that influence longevity. Published reports showing that *rhy-1;hif-1* compound mutants have a synthetic deleterious effect on fertility and that RHY-1 modulates hydrogen sulfide resistance in a HIF-1-independent manner also suggest interesting HIF-1-independent roles for RHY-1 (*231, 239*).

A published mechanism explaining the interaction between RHY-1 and HIF-1 suggests that *rhy-1* mutants should largely phenocopy *egl-9* mutants (*230*). While interpretation of *egl-9* phenotypes is complicated by the lack of a viable *egl-9* null mutant, published results do suggest that *egl-9(n571*), a point mutant that is predicted to affect splicing, and *egl-9(RNAi)* have more robust longevity promoting phenotypes than the strong loss-of-function mutant, *egl-9(sa307)*, a deletion in the EGL-9 catalytic domain (*233, 236, 250, 251*). These results are consistent with EGL-9 also having longevity promoting and limiting functions, with the mutant phenotype depending on the severity of the loss in activity. These data are consistent with a model in which EGL-9 and RHY-1 act in the same pathway to both limit wild-type longevity by destabilizing HIF-1 and increase longevity when HIF-1 is stabilized.

VHL-1-independent EGL-9 targets modulate lifespan.

Along with other groups, we identified a substantial subset of targets that are transcriptionally regulated in opposite directions by EGL-9 and VHL-1 (*240, 248*). This suggests that upregulation of EGL-9 and RHY-1 when HIF-1 is stabilized has substantial effects on the hypoxic transcriptome in addition to possible feedback regulation of HIF-1. Previous publications have established that EGL-9 has VHL-1-

independent activities that can increase or reduce resistance to various pathogens (*237, 238*). Here, we find that several RNAi clones targeting genes with reported or likely functions in innate immunity, *nlp-31(RNAi), lys-7(RNAi)*, *lys-10(RNAi)*, and *lips-10(RNAi)*, extend lifespan in *egl-9(sa307);vhl-1(ok161)* mutants, suggesting that EGL-9-dependent downregulation of these genes promotes longevity in *vhl-1(ok161)* mutants.

The mechanisms underlying VHL-1-independent transcriptional regulation by EGL-9 have not been fully established. Previous studies report that *egl-9(sa307)* and *hif-1(ia4)* loss of function mutants cause transcriptional upregulation of the direct HIF-1 transcriptional target *ftn-1*, while *vhl-1* loss of function mutants and overexpression of non-hydroxylatable HIF-1 (P621A) suppress *ftn-1* expression (*248, 249*). These results are consistent with a model in which binding of hydroxylated and non-hydroxylated HIF-1 may have opposite effects on the *ftn-1* promoter region, with *vhl-1(ok161)* mutation causing increases in hydroxylated HIF-1 while *hif-1(ia4)* and *egl-9(sa307)* mutation both eliminate hydroxylated HIF-1 (*248, 249*). A recent analysis from the Sternberg group showed expression patterns consistent with a role for hydroxylated HIF-1 in expression of a larger set of transcripts that are oppositely affected by VHL-1 and EGL-9 (*240*).

Other reports suggest that EGL-9 may trigger VHL-1-independent transcriptional responses through more complex mechanisms. Multiple labs report that EGL-9 affects gene expression through mechanisms that are independent of its hydroxylation activity (*236, 237*). One study suggests that EGL-9 represses HIF-1 activity through a mechanism that requires physical interaction between EGL-9/PHD and the WD repeat containing protein SWAN-1 (*238*). EGL-9 might also affect gene expression via hydroxylation of substrates other than HIF-1, with one study indicating that LIN-10 is a target of EGL-9 hydroxylation (*252*). Mechanistic biochemical studies to 1) identify EGL-9 hydroxylation targets and protein-protein interaction partners, and 2) establish whether hydroxylated and non-hydroxylated HIF-1 interact with distinct transcriptional complexes, will be needed to fully understand the complex biological function of EGL-9/PHD.

Constitutive sterile activation of the innate immune response increases during mammalian aging and is a key driver of many age-related pathologies (*253*). A trade-off between constitutive immune activation and longevity has also been established in *Drosophila* (*254*). In *C. elegans*, immune-related signaling genes contribute to the longevity phenotypes of long-lived insulin signaling mutants; however, to our knowledge, this is the first evidence of antagonism between immune activation and non-pathogen exposed survival in *C. elegans* (*243*). Further mechanistic studies of the connection between pathogen resistance genes and accelerated aging-related phenotypes in tractable model systems may yield insights and interventions that can be translated to mammalian inflammatory aging pathologies.

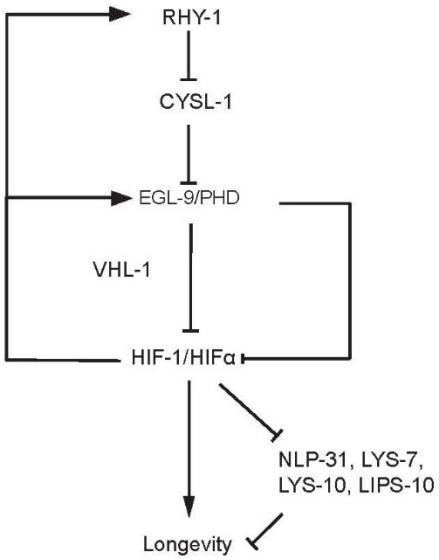

Figure 4.4. Epistatic model of lifespan regulation by VHL-1, RHY-1, and EGL-9.
RHY-1 and EGL-9 act in the same pathway to inhibit HIF-1 activity through both VHL-1-dependent and VHL-1-independent mechanisms. When HIF-1 is stabilized through loss of VHL-1, expression of RHY-1 and EGL-9 is increased, driving reductions in expression of longevity reducing target genes including, NLP-31, LYS-7, LYS-10 and LIPS-10 through a HIF-dependent and VHL-1-independent mechanism. Inhibition of EGL-9 activity causes upregulation of genes including NLP-31, LYS-7, LYS-10 and LIPS-10, inhibiting longevity.

A role for SCP-like extracellular proteins in C. elegans aging

Abstract

Metabolic adaptation to changes in food availability is a critical aspect of healthy physiology. Indeed, one consequence of dietary restriction (DR) in the laboratory is increased lifespan. In *C. elegans*, the physiological changes associated with increased lifespan rely on the induction of a xenobiotic enzyme, flavin-containing monooxygenase-2 (*fmo-2).* Manipulating *fmo-2* expression leads to systemic changes in metabolism, stress resistance and longevity, but how it does so remains unknown. Here, we use RNA-seq analyses on animals with elevated *fmo-2* to find key downstream changes associated with *fmo-2* induction and improved health and longevity. Our resulting data show that *fmo-2* expression leads to down-regulation of three members of the SCP-like extracellular (*scl*) protein family. The function and expression patterns of these secreted proteins is largely unknown. However, studies show elevated expression during aging. Here we show knockdowns of subset of *scl* proteases, *scl-3* and *scl-5,* significantly extend lifespan. Additionally, we find they are non-additive with FMO-2 OE and DR-mediated longevity. Upon further evaluation of the gene family, we find that *scl* genes frequently modify longevity and may represent an understudied gene family with an impact on the aging process. Similarly, the mammalian SCL homologs, CRISPs, are thought to play an integral role in embryogenesis but their function in adult animals is uncertain. Together, our results demonstrate the value of unbiased exploratory analyses to derive novel hypotheses and identify new regulators of the aging process.

Introduction

Flavin-containing monooxygenases (FMOs) are enzymes that play an important role in xenobiotic metabolism in the mammalian liver and nematode intestine. FMOs were first discovered by Ziegler's group in 1972 in a sample of purified porcine liver microsomes as distinct but related activity from cytochrome p450s (CYPs) (*255*). Ziegler and others showed that FMOs carry out the oxygenation of nucleophilic metabolites, commonly amines and sulfur groups, by utilizing electrons from NADPH and molecular oxygen and producing water as a byproduct (*256*).

Importantly, unlike CYPs, FMOs are self-priming and consequently can be extremely enzymatically active in the presence of a substrate, oxygen, and NADPH. Recent studies have implicated a novel role for FMOs in several endogenous processes outside xenobiotic metabolism. Trimethylamine N-oxide (TMAO), a byproduct of mammalian FMO3 activity, is linked to cardiovascular disease and atherosclerosis in both mice and humans, suggesting that FMO activity may be modified in response to disease states (*257*). Several publications also present compelling evidence that modifying FMO expression can cause dramatic changes in systemic metabolism (changes in resting energy expenditure) and stress (changes in liver stress levels) in mice, supporting a major role for FMOs in still unknown, endogenous processes (*258-260*). Compelling evidence also links FMOs to longevity. mFMO3 is upregulated in the liver of seven distinct long-lived mouse models (*76*). In C elegans, *fmo-2* overexpression (OE) is sufficient to extend lifespan downstream of multiple longevity-promoting pathways (*12*). From these data it can be concluded manipulating FMOs expression leads to systemic changes in metabolism, stress resistance and longevity, but how FMOs induce these changes remains unknown.

Our data presented in this study support a model where FMO-2 activity or dietary restriction (DR) downregulate two SCP-like extracellular (*scl*) proteases, *scl-3* and *scl-5,* to causatively impact worm lifespan. We also find compelling information that these *scls* are secreted into the pharynx and intestinal lumen. Collectively, these data suggest complex metabolic rearrangement occurs, potentially by shunting amino acid availability, during times and conditions when FMO-2 activity is elevated.

RNA-seq analyses of two genetically distinct FMO-2 OE animals

To address how FMOs improve healthy aging, we first analyzed the worm transcriptome by RNA-seq to investigate what changes occur when FMO-2 levels are elevated. By focusing first on transcriptional changes, we hoped to understand how the increased expression, and presumably activity, of a single enzyme, would result in feedback through downstream changes in gene expression. We also hypothesized that one or more of these transcriptional changes may be important for *fmo-2*-mediated longevity benefits. As previous studies show that *fmo-2* is downstream of multiple longevity pathways (*12, 261*), each of which affects metabolism, we hypothesized that metabolic-related genes may be affected by *fmo-2* expression.

Our resulting transcriptomic data show consistent and overlapping expression changes between multiple lines of *fmo-2* overexpressing animals with some variability in overexpression (**Figure 4.5A**). Using a stringent selection criteria (see materials and methods), we identified 143 genes differentially regulated by increased expression of *fmo-2,* including 25 genes that were identified in both strains, which we defined as consistent *fmo-2* effected genes. Since *fmo-2* is not a transcription factor, we expect that this concise list of genes represents genes whose expression is modified in response to the effects of FMO-2 enzymatic activity. Focusing on the 25 genes common to both FMO-2 OE strains, we immediately noticed that 3 of the 25 genes (12%) modified by FMO-2 OE belong to the same family of genes, SCP-like extracellular proteins (SCLs). We also noticed that all three of these *scl* genes were similarly significantly down-regulated in fmo-2 over-expressor samples (**Figure 4.5A-B**). These cysteine-rich secretory protein (CRISP) homologs are a large family of proteins highly conserved from invertebrates to mammals. 26 genes have been classified *as scls* in nematodes (*262*) (**Figure 4.5C**), while mice possess 33 homologs and humans 30 (*263*). Most mammalian CRISPs are highly expressed in reproductive organs (*264*), but CRISP3 and peptidase inhibitor 16 (PI16) transcripts are found in the prostate, pancreas, colon, and thymus (*265-267*) and have been found in over-abundant quantities in some age-related diseases. Serum collected from those suffering from chronic pancreatitis show elevated levels of CRISP3 and PI16 (*268, 269*). In a mouse

model of heart failure, PI16 is highly up-regulated, and a similar increase was observed in damaged human heart tissue (*270*). Similarly, CRISP3 has been found to be the most highly up-regulated protein, with a 21-fold over-expression, in cancerous prostate tissue compared with matched control tissue (*271*). Taken together, these data are supportive of SCL/CRISP proteins playing a larger, still unknown, role in organismal health outside of embryogenesis.

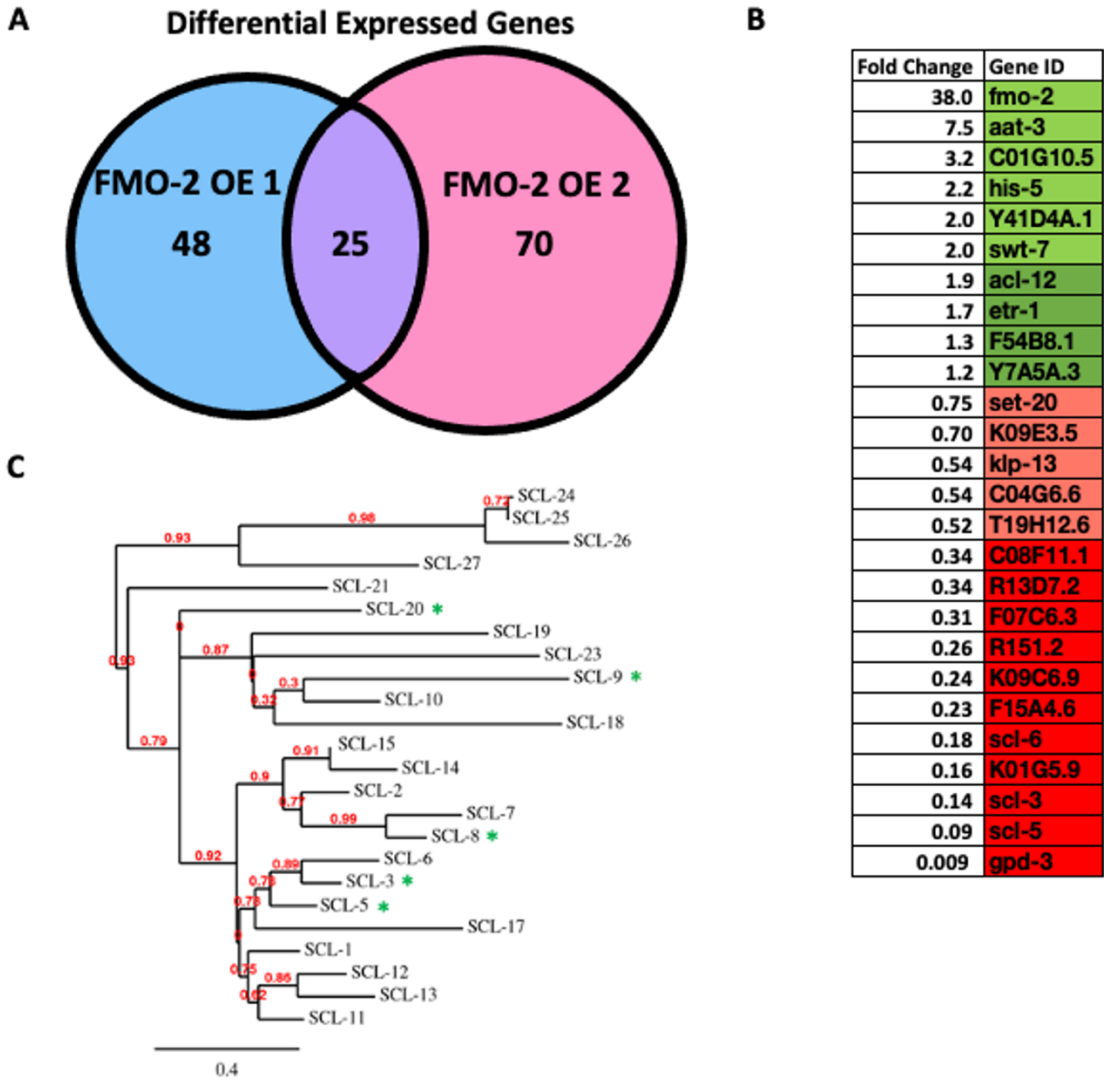

Fold Change	Gene ID
38.0	fmo-2
7.5	aat-3
3.2	C01G10.5
2.2	his-5
2.0	Y41D4A.1
2.0	swt-7
1.9	acl-12
1.7	etr-1
1.3	F54B8.1
1.2	Y7A5A.3
0.75	set-20
0.70	K09E3.5
0.54	klp-13
0.54	C04G6.6
0.52	T19H12.6
0.34	C08F11.1
0.34	R13D7.2
0.31	F07C6.3
0.26	R151.2
0.24	K09C6.9
0.23	F15A4.6
0.18	scl-6
0.16	K01G5.9
0.14	scl-3
0.09	scl-5
0.009	gpd-3

Figure 4.5. Several differentially expressed genes are present in both FMO-2 OE transgenic lines.
(A) Overlap between genes that are differentially expressed in two independent FMO-2 OE lines. (B) Summary table of shared DE genes and averaged fold-change (Gene IDs in green are up-regulated, red are down-regulated). (C) Cladogram of s*cl* protein family made using *phylogeny.fr (272)*.

Knockdown of *scl-3* and *scl-5* increases stress resistance and longevity.
Data from tissue culture experiments and model organisms show longevity interventions share a positive correlation with increased stress resistance to a myriad of stressors (*76, 187, 273, 274*) . We therefore hypothesized that knockdown (KD) of *scl-3, scl-5* and/or *scl-6* would lead to enhanced stress resistance and longevity if their knockdown was at least partially responsible for the FMO-2 OE longevity. Interestingly, our results do not perfectly follow these predicted trends. KD of all three *scls* increases survivability to high levels of the ROS producer paraquat (**Figure 4.6A**), whereas only *scl-3* KD confers resistance to the heavy metal cadmium chloride (**Figure 4.6B**) and *scl-5* and *scl-6* KD to heat stress (**Figure 4.6C**). These data suggest the type of stress resistance may be separable depending on the function of these three predicted proteases. Similarly, we find that *scl-3* and *scl-5* KD each significantly increases lifespan (**Figure 4.6D-E**) while *scl-6* KD recapitulates wild-type lifespan on the vector control (**Figure 4.6F**). Together, these findings suggest down-regulating *scl* activity can improve health and longevity outcomes.

Using the MosSCI system, we created a stably expressed *scl-5* transcriptional reporter (scl-5p::GFP) to confirm SCL expression patterns. Colocalization assays will reveal SCLs are expressed throughout the animal, but primarily in the pharynx and intestine (**Figure 4.6G**). SCL-3, SCL-5 and SCL-6 share the most sequence identity (>60%) between the 26 nematode SCL proteins, therefore it is plausible that they will also overlap in biological function and localization, but translational reporters will confirm or disprove this hypothesis.

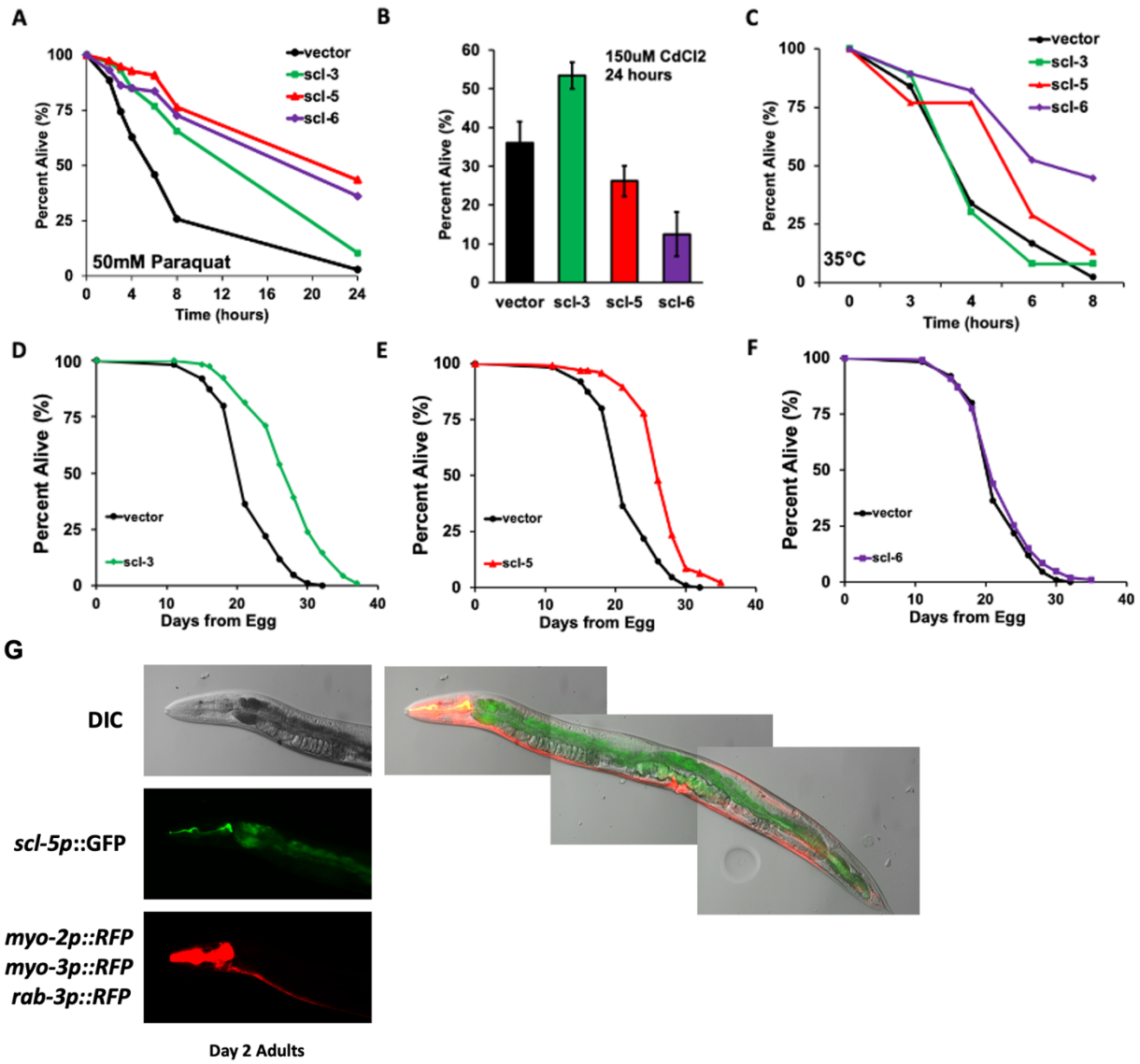

Figure 4.6. Knockdown of *scl-3* and *scl-5* increases stress resistance and longevity. Short-term stress resistance assays comparing wild-type (N2) animals on vector (black), *scl-3* (green), *scl-5* (red), and *scl-6* (purple) RNAi exposed to 150mM paraquat (A), 150μM cadmium chloride (B) and 35°C heat stress (C). Survival curves of wild-type animals on vector (black), *scl-3* (D), *scl-5* (E), and *scl-6* (F) RNAi. (G) *scl-5p*::GFP expression pattern points to release in the pharynx**.** Lifespan statistics can be found in Table 4.4.

Additional screening finds mixed results of scl knockdown effect on lifespan. We next wondered whether down-regulating other *scls* would results in increased lifespan. As previously stated, genomic annotation algorithms recognize 26 coding regions as members of the *scl* protein family. Due to the high level of conserved sequence identity and clustering on chromosome IV and V (**Figure 4.5C**), it is likely these genes arose from duplication events (*275*) bolstering the likelihood that this family of proteins could produce similar effects as we see with *scl-3* and *scl-5.*

To better understand the interplay between *scl* KD and longevity, we measured the lifespans of worms on 15 of the 26 *scl* ORFS that are present in the Vidal RNAi library (**Table 5.2,** Figure 4.7). **Figure 4.8** illustrates four examples of how longevity can be impacted representing conditions that:

- robustly increase median and maximum lifespan (*scl-9* RNAi)
- robust increase maximum lifespan (*scl-14* RNAi)
- robustly decrease median and maximum lifespan (*scl-19* RNAi)
- do not alter lifespan at any temperature (*scl-17* RNAi)

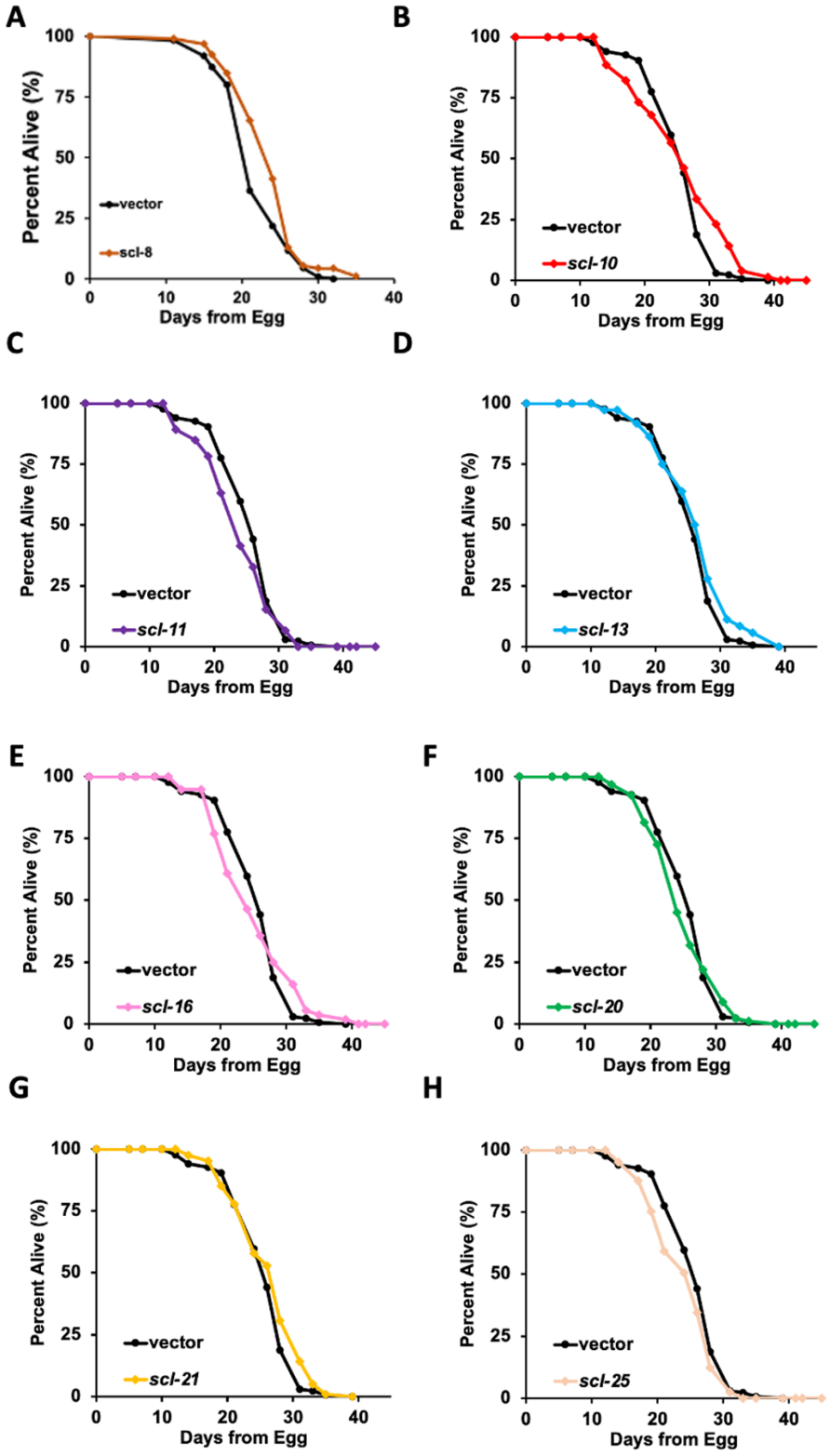

Figure 4.7. Additional *scl* knockdown replicates.
Survival curves of wild-type animals on vector (black), *scl-8* (A), *scl-10* (B), *scl-11* (C), *scl-13* (D), *scl-16* (E), *scl-20* (F), *scl-21* (G), and *scl-25* (H) RNAi. Lifespan statistics can be found in Table 4.4.

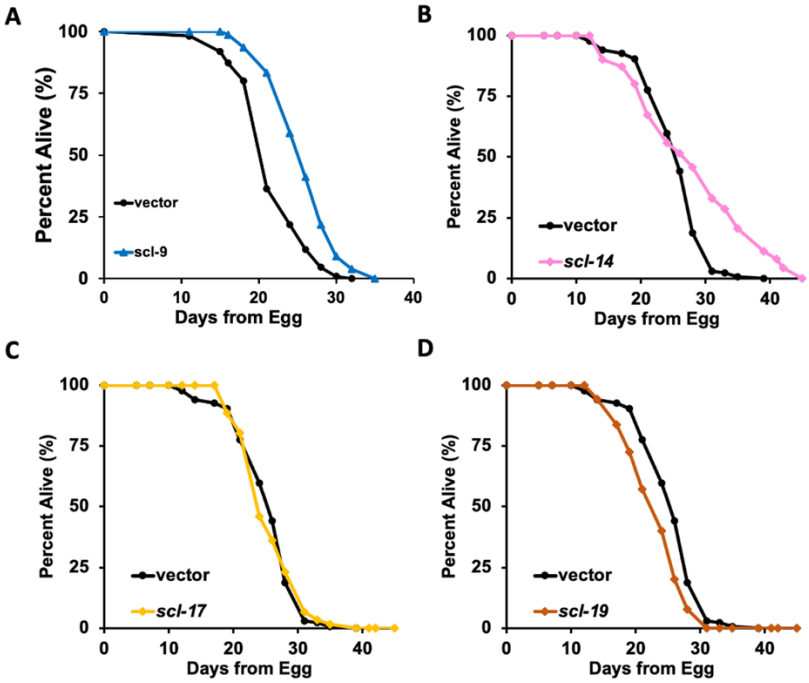

Figure 4.8. Example effects of *scl* knockdown on lifespan.
Survival curves of wild-type animals on vector (black), *scl-9* (A), *scl-14* (B), *scl-17* (C), and *scl-19* (D) RNAi. Lifespan statistics can be found in Table 4.4.

	RNAi	% change
Increased median LS	*scl-3* *scl-5* *scl-8* *scl-9* *scl-20*	+ 25% + 20% + 10% + 20% + 10%
Increased maximum LS	*scl-10* *scl-14*	+ 20% + 50%
Decreased median LS	*scl-11* *scl-19* *scl-25*	- 10% - 10% - 5%
Comparable LS	*scl-13* *scl-16* *scl-17* *scl-21*	N.S. N.S. N.S. N.S.
Untested	*scl-1* *scl-2* *scl-7* *scl-12* *scl-15* *scl-18* *scl-23* *scl-27*	- - - - - - - -

Table 4.2. Lifespan summary statistics.

***scl-3* and *scl-5* act downstream of DR-mediated *fmo-2* induction.**

Finding only a handful of *scls* that extend lifespan when knocked down, we next asked which, if any, act downstream of DR- and FMO-2-mediated longevity. To test these two questions, we subjected WT and FMO-2 OE animals to RNAi of the pro-longevity *scls* in both fed conditions and in combination with DR. Strikingly, we find only *scl-3* and *scl-5* KD extend lifespan in a DR-dependent manner (**Figure 4.9A-B**) while *scl-9* and *scl-20* KD extend lifespan in a DR-independent manner (**Figure 4.9C-D**). Knockdown of *scl-6* recapitulates the effects of WT animals on DR (Figure 4.10A) and *scl-8* KD synergistically enhances DR-mediated longevity (Figure 4.10B). These findings suggest the differential expression analyses from our RNA-seq studies correctly identified a relationship between the pro-longevity effects of *scl-3* and *scl-5* KD.

Since *scl-3* and *scl-5* KD acts downstream of DR-mediated longevity, we hypothesized their knockdown will not further extend FMO-2 OE. Congruent with this hypothesis, we find *scl-3* and *scl-5* KD confers no additional benefit for FMO-2 OE longevity (**Figure 4.9E-F**) while *scl-9* and *scl-11* KD abrogate its longevity phenotype (**Figure 4.9G-H**). While it is critical to validate these results, they suggest that *scl-9* and *scl-11* activity are required for the fmo-2 longevity phenotype.

Together, these data support a model where DR conditions up-regulate FMO-2 expression which, in turn, down-regulates proteasomal degradation via SCL-3 and SCL-5 during the metabolic rewiring that occurs and subsequently promotes longevity.

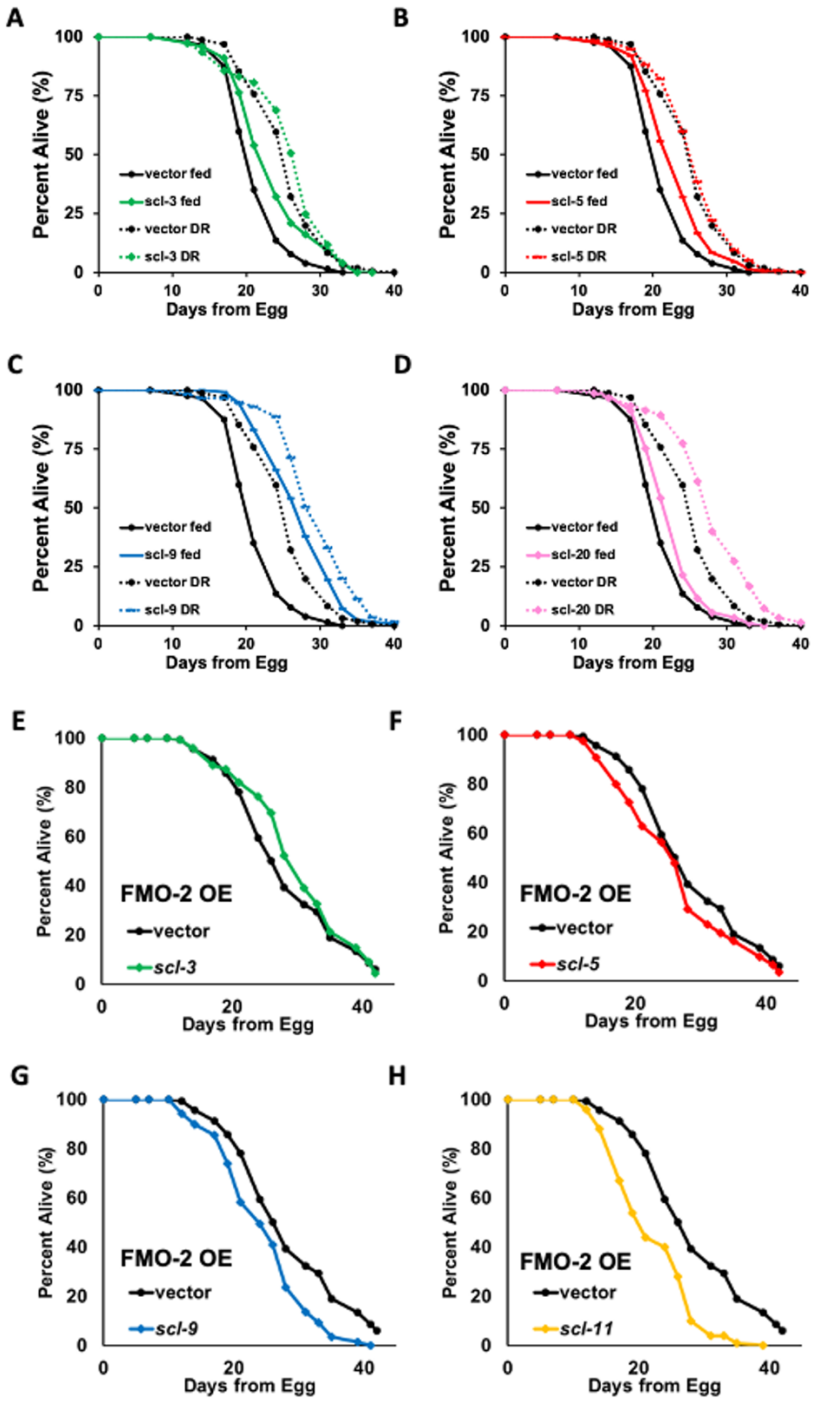

Figure 4.9. *scl-3* and *scl-5* act downstream of FMO-2 OE and DR-mediated longevity. Survival curves comparing vector, *scl-3* (A), *scl-5* (B), *scl-9* (C), or *scl-20* (D) RNAi on fed (solid line) and DR (dotted lines). Survival curves comparing vector, *scl-3* (E), *scl-5* (F), *scl-9* (G), and *scl-11* (H) RNAi in FMO-2 OE animals. Lifespan statistics can be found in Table 4.4.

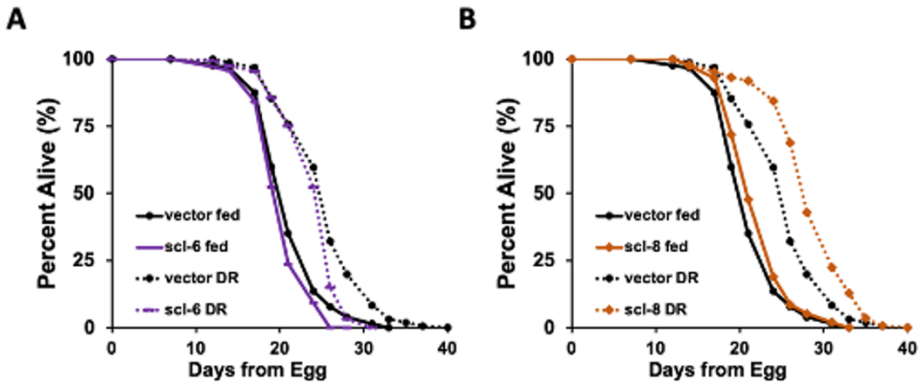

Figure 4.10. Additional effects of *scl* knockdown on DR lifespan.
Survival curves comparing vector (black), *scl-6* (A) and *scl-8* (B) RNAi on fed (solid line) and DR (dotted lines). Lifespan statistics can be found in Table 4.4.

Discussion

In this study we employed a transcriptional strategy to prioritize genes downstream of FMO-2 OE for functional analysis. The results led us to explore a family of under-characterized proteins homologous to mammalian CRISPs. Our data suggest that down-regulating *scl-3* and *scl-5* can extend nematode lifespan, and these genes acquired a specific pro-longevity function, as they were the only genes shown to act downstream of DR signaling and FMO-2 OE. We also find that two additional *scls* extend lifespan when knocked down, suggesting a conserved role of multiple members of the gene family in limiting longevity. To test whether *scl-3* and *scl-5* down-regulation plays a necessary role downstream of the metabolic rewiring that occurs during DR and FMO-2, we can overexpress SCL-3 and SCL-5 and see if their activity is sufficient to abrogate FMO-2 OE and DR-mediated longevity.

It is interesting that *scl* genes have been superficially implicated in modulating nematode aging. Proteomic analyses of young (day 4) and old (day 10) nematodes found SCL-12 to be one of the few proteins upregulated in elderly animals (*276*). An RNAi screen showed *scl-4* knock-down (KD) leads to long-lived animals (*277*). Counter to these data, knocking out *scl-1* completely blocks the long-lived *daf-2(e1370)* mutant animal's lifespan extension (*278*). With these seemingly conflicting pieces of data and little known about this family of proteins endogenous function, this study aims to characterize their potential role downstream of FMO-2-mediated nematode health and longevity. Our resulting data support a model where FMO-2 upregulation recapitulates a DR-like state that, in-turn, down-regulates predicted proteases *scl-3* and *scl-5* potentially by driving the worms to rely on fat-metabolism.

We expected animals with depleted *scl-3, scl-5* and *scl-6* would survive stressful conditions better than control animals. Surprisingly, we find stress resistance is not always a direct correlation with longevity. While *scl-6* KD promoted robust survivability to paraquat and heat stress, this did not translate to longevity. These results suggest stress resistance and longevity are separable phenotypes that cannot always be used as a proxy for the other, in agreement with other studies (*279, 280*).

The substantial shared sequence homology between *scl-3, scl-5* and *scl-6* (>60%) is both beneficial and detrimental when interpreting our findings. From a mechanistic standpoint, it adds relevance to our RNA-seq data and suggests they are likely to be performing similar biological functions. Moreover, the online bioinformatics tool SignalP (*281*) shows that the SCL-3 and SCL-5 amino acid sequence contains the same secretion signal (Q18), unlike SCL-6 (E19*).* However, this potential for functional redundancy also means we may not see a lifespan extension when we knockout a single SCL protein since RNAi treatment on similar sequences can knock down multiple gene family members simultaneously. RNAi is prone to off-target effects that could lead to false positives (i.e. RNAi alters lifespan but mutation does not). Furthermore, RNAi may result in incomplete knockdown of mRNA and protein levels, especially in neurons and pharynx that are refractory to RNAi, resulting in false negatives (i.e. mutation alters lifespan but RNAi does not). Thus, critical longevity genes may be missed by using only RNAi or mutants. It is worth exploring in future studies whether genetic knockouts recapitulate the data presented here.

Epistasis experiments show FMO-2 OE animals received no additional benefits to their lifespan when we KD *scl-3* and *scl-5*. These data are consistent with *scls* being detrimental to nematode health and longevity in an FMO-2-dependent manner. Similarly, we find *scl-3* and *scl-5* KD are non-additive with DR longevity. There are several potential mechanisms worth exploring in future studies. Long-term stressors, like DR, are known to decrease protein translation in order to conserve nutrients (*282*). Additionally, SILAC proteomics experiments find long-lived *daf-2* mutants have decreased protein turnover as they age (*283*). Since some *scls* are hypothesized proteases and we find *scl-5* is likely released into the pharyngeal lumen, it is logical to hypothesize these long-lived environmental and genetic conditions down-regulate proteases to shunt their energy from protein decomposition potentially towards fat metabolism. It will be interesting to perform fat staining and measure protein translation levels across *scl-3* and *scl-5* KD and OE animals. We'd expect *scl* KD to result in leaner worms with decreased protein translation while OE results in the opposite phenotype.

Materials and Methods

Strains and growth conditions

See chapter 2.

RNAi knockdown

See chapter 2.

Lifespan measurements

See chapter 2. Additional information in Tables 4.3-4 includes statistics.

Statistical analyses

See chapter 2.

Stress resistance assays

Paraquat (Methyl viologen dichloride hydrate from Sigma-Aldrich) was used to induce oxidative stress. Worms were synchronized from eggs on RNAi plates seeded with *E. coli* HT115 strain expressing RNAi for a particular gene and at L4 stage 40 worms were transferred on RNAi-FUDR plates containing 50 mM paraquat. Similar conditions were prepared with the heavy metal stressor, 150μM cadmium chloride (Sigma-Aldrich). A minimum of two plates per strain per condition were used per replicate experiment. Worms were scored every hour for the first eight hours and considered dead when they did not move in response to prodding under a dissection microscope. Worms that crawled off the plate were not considered, but ruptured worms were noted but considered as previously described (*213*).

RNA isolation, sequencing, and analysis

Worm strains were synchronized by treating gravid adult worms with sodium hypochlorite and collecting ~1000 offspring per genetic condition. Once the offspring reached young adulthood, they were collected in M9 buffer and immediately flash-frozen in liquid nitrogen. RNA was extracted following Invitrogen's TRIZOL RNA extraction protocol. Before library preparation the samples were analyzed on an Agilent 2100 BioAnalyzer. Only samples with an RNA integrity numbers (RIN) equal to or greater than 9.0 were used in downstream analyses. Single-strand

reverse transcription, library preparation, and sequencing were performed on an Illumina machine. Read alignments were mapped using Kallisto and differential expression analyses was performed using Sleuth. We used a q-value cutoff of <.05 for downstream comparisons across conditions as it's adjusted for multiple hypothesis testing (*241, 242*). Additionally, in project 2, we required shared directionality (enrichment or depletion) between FMO-2 OE strains to be classified as a hit.

Experiment number	genotype	deaths	median survival (days)	Comparison	P value(log rank) * Bonferonni corrected for multiple comparions
1 (Figure 5.2B,D,F,H S5.1)	*N2*	57	14		
1 (not shown)	*egl-9(sa307)*	74	17	*N2*	<0.0001
1 (not shown)	*vhl-1(ok161)*	106	21	*N2*	<0.0001
1 (Figure 5.2B,D,F,H S5.1)	*egl-9;vhl-1*	131	18	*egl-9(sa307)*	0.0002
1 (Figure 5.2B)	*egl-9;vhl-1;nlp-31(RNAi)*	135	18	*egl-9;vhl-1*	0.06*
1 (Figure 5.2D)	*egl-9;vhl-1;lys-7(RNAi)*	150	18	*egl-9;vhl-1*	<0.0001*
1 (Figure 5.2F)	*egl-9;vhl-1; lys-10(RNAi)*	120	18	*egl-9;vhl-1*	0.01*
1 (Figure 5.2H)	*egl-9;vhl-1; lips-10(RNAi)*	113	21	*egl-9;vhl-1*	0.0014*
1 (Figure S5.1B)	*egl-9;vhl-1;ftn-1(RNAi)*	162	18	*egl-9;vhl-1*	1*
2 (Figure 5.2B,D,F,H S5.1)	*N2*	98	15		
2 (not shown)	*egl-9(sa307)*	64	16	*N2*	<0.0001
2 (not shown)	*vhl-1(ok161)*	98	22	*N2*	<0.0001
2 (Figure 5.2B,D,F,H S5.1)	*egl-9;vhl-1*	93	18	*egl-9(sa307)*	<0.0001
2 (Figure 5.2B)	*egl-9;vhl-1;nlp-31(RNAi)*	55	23	*egl-9;vhl-1*	<0.0001*
2 (Figure 5.2D)	*egl-9;vhl-1;lys-7(RNAi)*	72	23	*egl-9;vhl-1*	<0.0001*
2 (Figure 5.2F)	*egl-9;vhl-1; lys-10(RNAi)*	58	23	*egl-9;vhl-1*	<0.0001*
2 (Figure 5.2H)	*egl-9;vhl-1; lips-10(RNAi)*	96	23	*egl-9;vhl-1*	<0.0001*
2 (Figure S5.1B)	*egl-9;vhl-1;ftn-1(RNAi)*	55	21	*egl-9;vhl-1*	0.0005*
2 (Figure S5.1D)	*egl-9;vhl-1;ftn-2(RNAi)*	83	20	*egl-9;vhl-1*	0.037*
3 (Figure 5.2B,D,F,H S5.1)	*N2*	87	16		
3 (not shown)	*egl-9(sa307)*	38	16	*N2*	0.97
3 (not shown)	*vhl-1(ok161)*	56	16	*N2*	0.0003
3 (Figure 5.2B,D,F,H S5.1)	*egl-9;vhl-1*	40	16	*egl-9(sa307)*	0.53
3 (Figure 5.2B)	*egl-9;vhl-1;nlp-31(RNAi)*	42	18	*egl-9;vhl-1*	0.0001*
3 (Figure 5.2D)	*egl-9;vhl-1;lys-7(RNAi)*	47	16	*egl-9;vhl-1*	0.86*
3 (Figure 5.2F)	*egl-9;vhl-1; lys-10(RNAi)*	51	16	*egl-9;vhl-1*	0.56*
3 (Figure 5.2H)	*egl-9;vhl-1; lips-10(RNAi)*	54	18	*egl-9;vhl-1*	0.0005*
3 (Figure S5.1D)	*egl-9;vhl-1;ftn-2(RNAi)*	33	16	*egl-9;vhl-1*	0.17*

Table 4.3. Survival statistics for project 1.

CHAPTER 5

Conclusions and Future Directions

Foreword

The overarching goal of this dissertation was to understand how stressful stimuli, like dietary restriction, can rewire a worm's metabolism to extend lifespan. Much work has been done in the past thirty years exploring this question. While there is extensive research implicating the nervous system plays a critical role in this metabolic rewiring, little progress has been made to map the individual cells or signals involved in these processes. Chapter 2 detailed how serotonin and dopamine signaling work in concert to signal "times are good" when food is present and vice versa during DR. Additionally, we identify a subset of essential neurons and receptors through selective genetic knockout and rescue experiments. Despite these discoveries, there remains some strange and ambiguous results left to disentangle. Luckily, one particularly enjoyable facet of research is that it has a compounding effect. Meaning some results are only interpretable in hindsight with the development of new assays, more information, etc.

To that end, this chapter encompasses the 1) loose ends that arose from the data generated in the previous chapters and 2) data that could not be incorporated seamlessly into previous stories. By chasing down concrete answers to the open questions presented in this chapter, we can further shape our understanding of the complex signaling events that occur during stressful stimuli. While none of this work is currently undergoing peer-review, the hope is future scientists will find value in these data when interpreting their own.

Can we link or separate DR longevity to behavioral changes?

In chapter 2, we began to map the neuronal circuitry of DR-mediated longevity. An interesting phenomenon we qualitatively noticed during our studies was worms on fed, DR, and DR-mimetics (like mianserin) all interacted quite differently with their environment. Bolstering these observations, it's been shown food deprived worms undergo periods of enhanced foraging and increased dwelling once they encounter food (*184, 284*). Because of this we asked whether changes in foraging could be detected with the addition of food smell.

To answer this question, we extracted x-y coordinate data for individual worms using the wrMTrck program (*285*) and plotted their movement over the course of a two-minute video after 3 hours on fed or DR +/- food smell. As expected, DR worms move farther from their origin when compared to fed (**Figure 5.1A** to **1C**, summary in **Figure 5.1I**), but remarkably the addition of food smell significantly enhances the distance travelled by DR (**Figure 5.1A** to **1B**) but not fed worms (**Figure 5.1C** to **1D**). This is consistent with the data presented in Chapter 2 suggesting that worms are seeking out a compound secreted by the bacteria. It remains unknown whether this enhanced foraging plays a causative role in the lifespan suppression we see when DR worms are exposed to food smell.

Since serotonin-null mutants (*tph-1*) are epistatic to DR, but required for food smell to blunt DR longevity, we hypothesized *tph-1* mutants foraging behavior would not be changed by DR or food smell. Indeed, we see no significant change in foraging across all four conditions (**Figure 5.1E-H**, summary in **Figure 5.1J**) while there does seem to be a trend towards hyperactivity when comparing basal WT to *tph-1* movement, consistent with what has been purported in the literature (*177*). Interestingly, we find that food smell alone does not increase pumping on DR conditions in either N2 or *tph-1* worms (**Figure 5.1K).**

Note: The raw data was collected by Elizabeth Dean (Figure 5.1A-H) and Dr. Safa Beydoun (Figure 5.1K), but we designed and analyzed the experiments together.

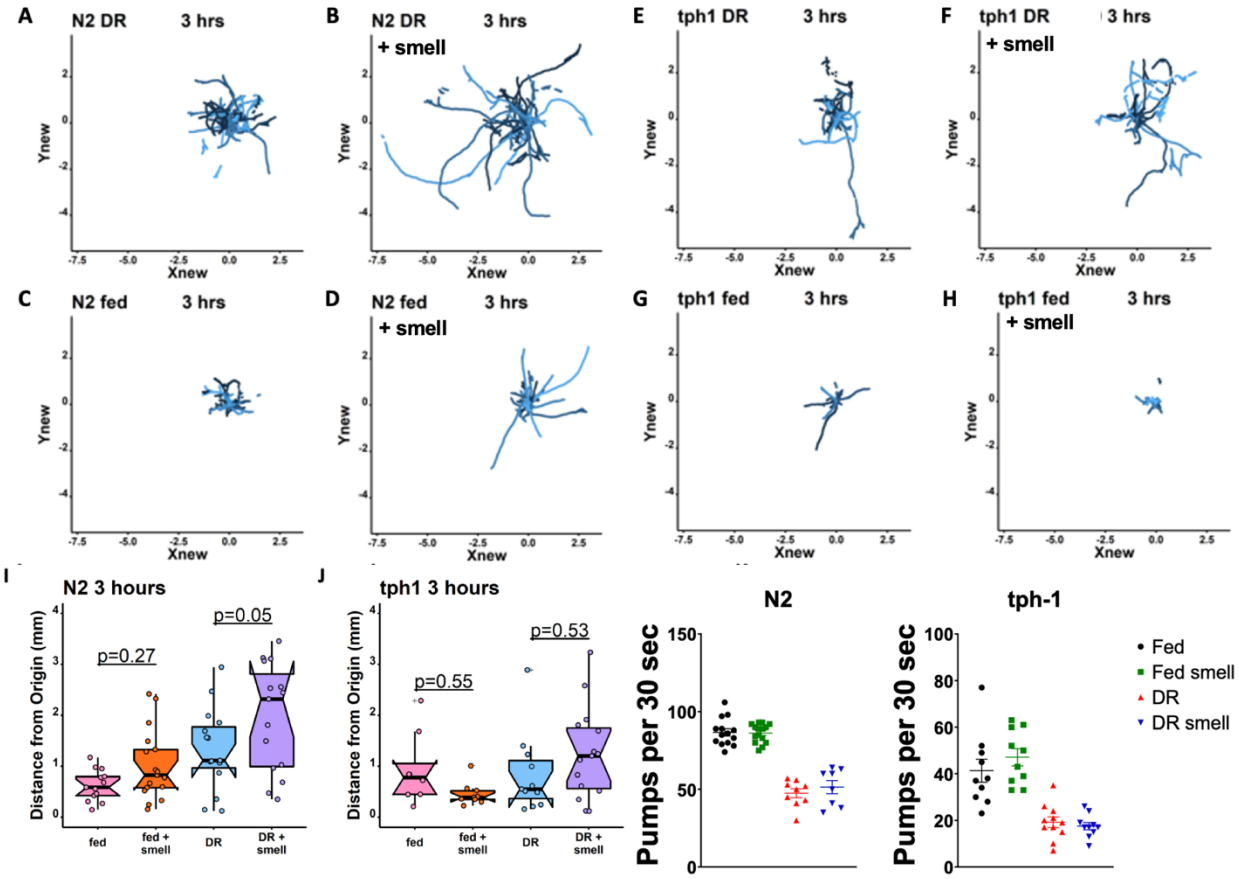

Figure 5.1. Food smell enhances foraging but not pumping in a 5-HT-dependent manner. Wild-type worm positions tracked from 2' videos taken after 3 hours on DR (A), DR + food smell (B), fed (C), and fed + food smell (D). *tph-1* worm positions tracked from 2' videos taken after 3 hours on DR (E), DR + food smell (F), fed (G), and fed + food smell (H). (I) Quantification of A-D. (J) Quantification of E-H. (K) Pumping rates of n=8-15 worms/condition.

These data along with findings in **Figure 2.1** led us to wonder if mianserin treatment could rescue the reduction in DR-mediated longevity caused by the perception of food. Unfortunately, this experiment proved more challenging than we anticipated since the combination of DR and mianserin leads to excessive fleeing (**Figure 5.2**) making long-term tracking assays like survival currently impossible. Future iterations on the palmitic acid barrier will need to be made before this assay is feasible.

Taken together, these data support a model where the initial perception of food leads to behavioral changes that, in turn, can function as indicators of accelerated aging. Whether this is true warrants further investigation.

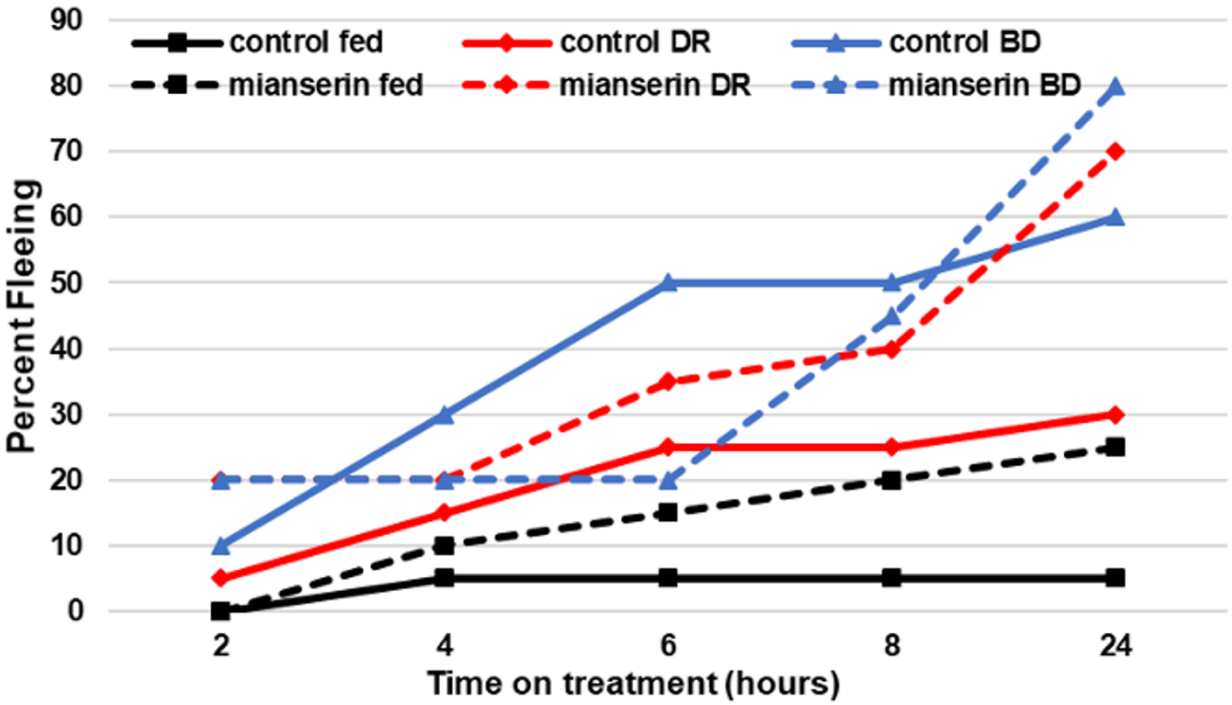

Figure 5.2. DR fleeing is enhanced by the addition of mianserin.
Quantified fleeing rates (n=50/condition) along a 24-hour time-course where fed control (black), DR (red) or BD (blue) animals are combined with water (solid lines) or mianserin (dashed lines).

Another open question surrounds neuronal function during aging. Would a DR-mimetic like mianserin enhance neuronal excitability and protect against proteotoxic aggregation? Since exogenous treatment with DR-mimetic N-acetyl-l-cysteine (NAC) is shown to be protective against neuronal protein aggregation and paralysis (*286*) ,and mianserin treatment increases neurotransmission in aged *C. elegans* (*158, 287*) we wondered whether it may be protective against paralysis from Aβ-aggregation. To test this question, we utilized an Aβ strain GMC101 that causes paralysis when shifted from the permissive temperature of 20ºC to 25ºC (*288*). After 24 hours of exposure to mianserin, DR, or mianserin and DR, we placed the animals at 25ºC. To measure movement and paralysis, videos were taken at 36-, 50-, and 72-hours post-temperature shift (**Figure 5.3A**) and analyzed using Wormlab software.

Interestingly, mianserin and DR modify worm behavior at both temperatures. *C. elegans* when deprived of food alter their foraging behavior by increasing the distance and speed traveled when compared to their fed counterparts (**Figure 5.3B**) and mianserin and DR can effectively rescue GMC101 worms from paralysis and aggregation at 25ºC (**Figure 5.3C**). Our data also suggest this behavior is seen for a transient period of time (<72 hours) (**Figure 5.3D**), and mianserin follows a similar trend as DR. These results support the hypothesis that mianserin acts downstream of DR signaling and partially recapitulates DR-mediated phenotypes.

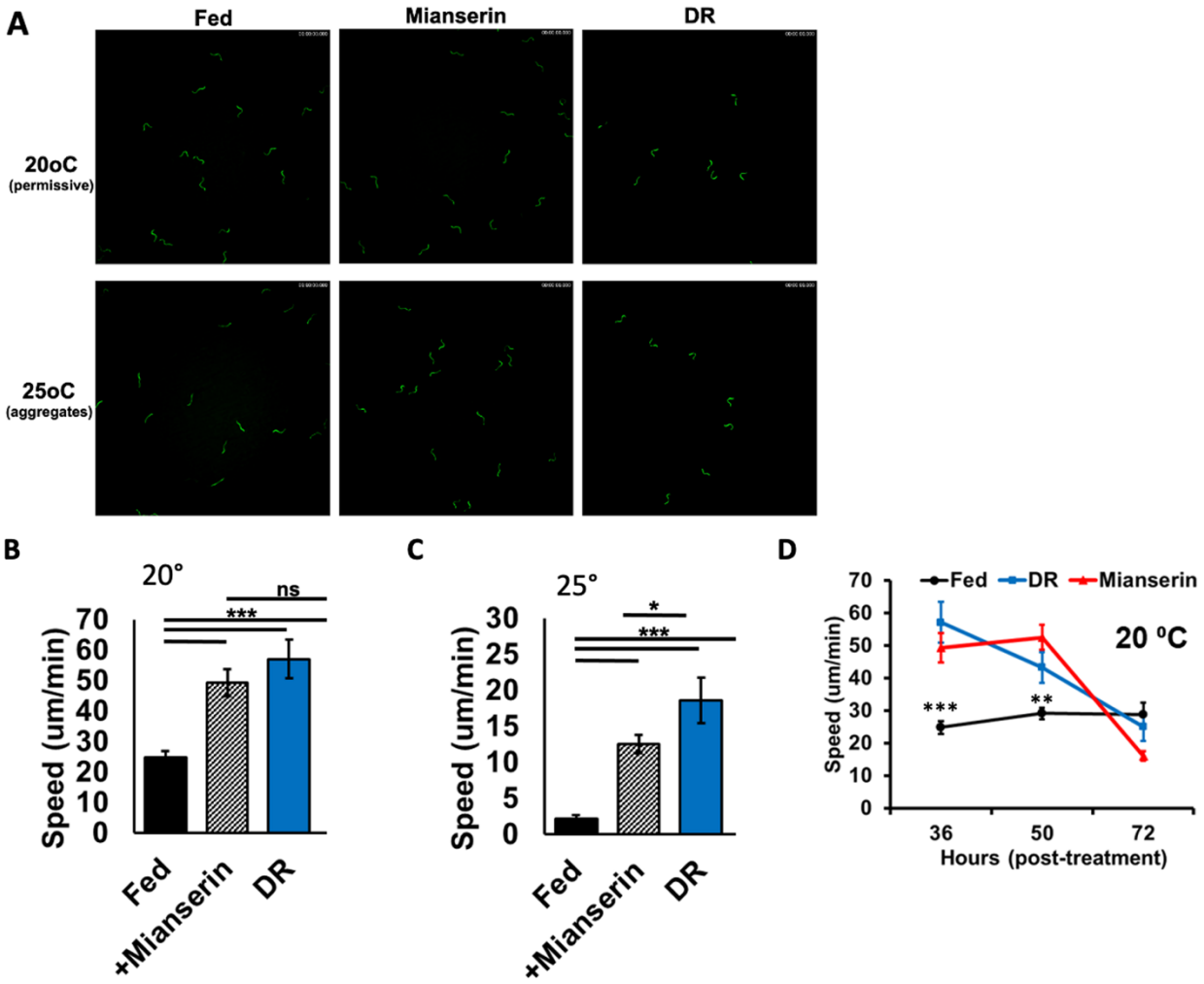

Figure 5.3. DR-mimetics modify foraging behavior and enhance resistance to Aβ-toxicity. Representative still images from 1' videos taken after 36, 50 and 72 hours left at 20ºC (permissive) or transferred to 25ºC (aggregate) temperature. Wormlab quantification of movement speed on fed (black), + 50μM mianserin (hatched), or DR (blue) after 36 hours at the permissive 20ºC (B) or aggregate 25ºC (C) temperature. Line graphs summarizing the change in movement when subjected to fed (black), 50μM mianserin (red), and DR (blue) at the permissive 20ºC (B) and aggregate 25ºC temperature (H).** denotes P<.01, *** denotes P<.001.

Can we identify additional signals downstream of serotonin release?

An effective method often used in worm labs to discover novel genetic mechanisms is an RNAi screen. For screening purposes, we chose *fmo-2* induction in a *vhl-1* mutant background (genetic mimetic for hypoxia) and under DR as our read-out. From here, we knocked down 263 neuropeptide and receptor clones from the Ahringer RNAi library. Our screening criteria was three consecutive experiments where *fmo-2* induction was blunted by >50% in *vhl-1* mutants (**Figure 5.4A**) or DR (**Figure 5.4B**). Interestingly, we find five shared signaling components that may act downstream of both hypoxic and DR signaling (**Table 5.1**). It is worth exploring whether these five signaling components are consequential in a pro-longevity context. We have considered two hypotheses; (i) one or more may be acting as the most downstream signaling event before *fmo-2* is induced in the intestine or, (ii) less interestingly, they could be necessary for normal physiological function.

Our screen also identified several signaling components that are necessary for hypoxia- or DR-mediated induction of *fmo-2.* Our hypothesis is the location of these signals and receptors acts as an intermediary between serotonin release and one of the shared signaling events in **Table 5.1**.

If we find inconclusive data on the necessity of these signaling components identified in **Table 5.1**, we can pursue the causative mutations from an unbiased EMS forward-genetic screen we performed. Using a 50% threshold for loss of fluorescence induction, we identified and validated nine independent strains where *fmo*-2 induction is significantly blunted during DR. Subjecting these hits to mianserin allowed us to place the causative mutation(s) either up- or downstream of serotonin signaling. If the mutagenized strain induced *fmo-2* on mianserin, the causative mutation(s) is upstream (class I – 3 mutants) whereas the causative mutation(s) acts downstream (class II – 6 mutants) for those that block mianserin and DR induction of *fmo*-2. Returning to these mutants would provide multiple benefits including (1) increased coverage of the genome since ~100 neuropeptides/receptors are not present in the RNAi libraries and (2) validation of components already implicated in food perception.

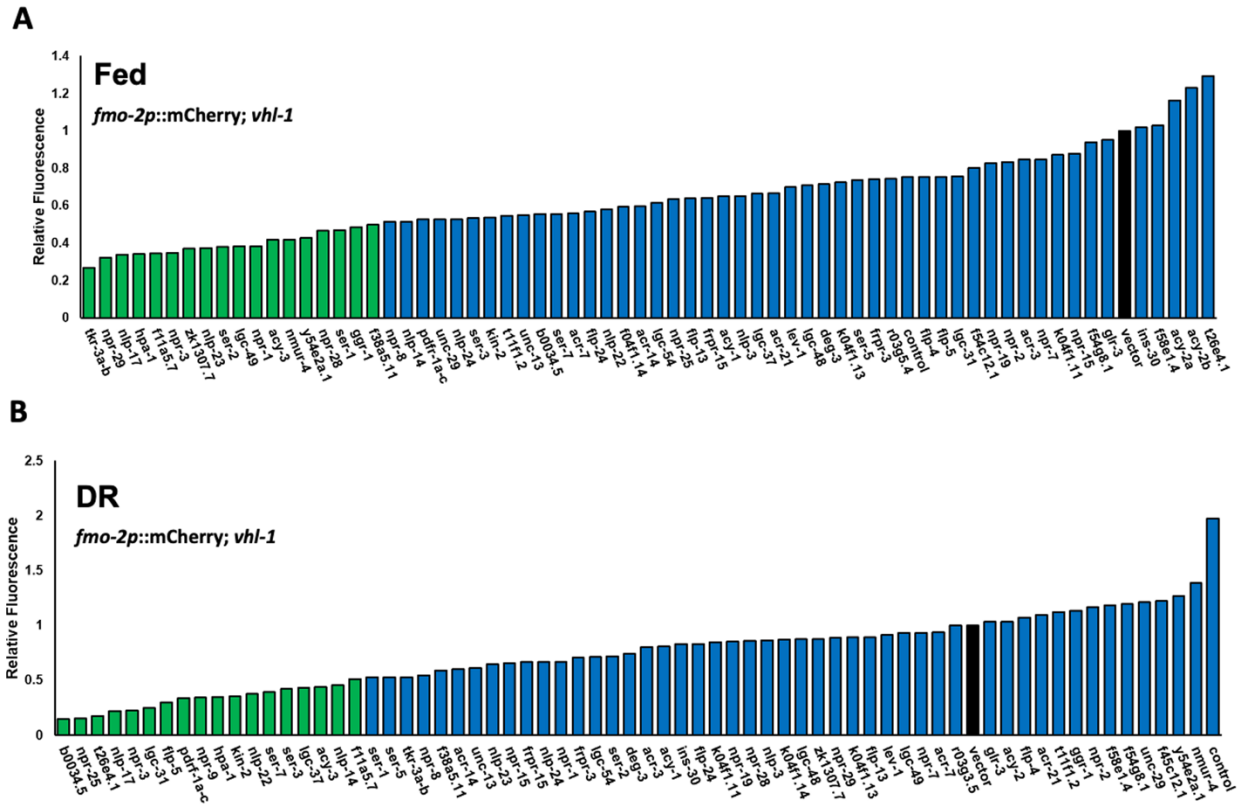

Figure 5.4. RNAi screen uncovers several neuronal signaling components to investigate. Results from validation screen of neuropeptides and receptors that blunt *fmo-2* induction under HIF-1 stabilization (A) and DR (B) when knocked down via RNAi. Green bars represent "hits" classified as >50% reduction in *fmo-2p*::mCherry expression.

HIF-1 pathway	shared	DR pathway
tkr-3	*acy-3*	B0034.5
npr-29	F11A5.7	*npr-25*
ZK1307.7	*flp-5*	*irld-52*
nlp-23	*hpa-1*	*lgc-31*
ser-2	*nlp-17*	*pdfr-1*
lgc-49	*npr-3*	*npr-9*
npr-1		*kin-2*
nmur-4		*nlp-22*
Y45E2A.1		*ser-7*
npr-28		*ser-3*
ser-1		*lgc-37*
ggr-1		*nlp-14*
F38A5.11		

Table 5.1. Hits from Neuropeptide RNAi screen.

Is there a retrograde signal released from the intestines during hypoxia or DR?

As mentioned in Chapter 1, most aging studies ask how the nervous system communicates with peripheral tissues, but recent data from invertebrates supports the idea that peripheral tissues use a retrograde signal back to the nervous system to maintain or further modify physiology (*105, 161-163*). This type of signaling seems logical, as organisms require feedback from individual tissues to monitor homeostasis, but the role of retrograde signaling in regulation of aging is not well understood.

When testing *fmo-2* induction in a neuronally sensitized strain TU3311 (see Table 5.2 for more information) and neuronal-specific RNAi strain MAH677, we discovered MAH677 does not recapitulate the effects of TU3311. Knockdown (KD) of neuropeptide-containing dense core vesicles (DCVs) formation via *unc-31* and synaptic vesicle release via *unc-13* showed inconsistent results. Our data suggest *sid-1* expression is required for unc-13/unc-31 KD to suppress DR fmo-2 induction (**Figure 5.5A-F**). These surprising results led us to wonder whether *unc-13/31* KD in the MAH677 background would have similar effects on fmo-2-mediated longevity. To test this hypothesis, we chose to expose long-lived *vhl-1*, MAH677, and *vhl-1; MAH677* (dKO) animals to *unc-31* RNAi and measured their lifespan. Since serotonin signaling is necessary for *vhl-1*-mediated longevity (*12*), we'd expect *unc-31* KD would abrogate its enhanced longevity. This is what we observed in the *vhl-1* background (**Figure 5.5G**). More surprisingly, we find neuron-only KD of *unc-31* does not abrogate *vhl-1*-mediated longevity (**Figure 5.5H**) suggesting that there are necessary long-range signals that are released from both neurons and distal tissues.

These data present an interesting case for future studies to investigate the signaling events that occur from the downstream metabolic tissues back to the nervous system. It also provides an opportunity to better understand how cells at the interface of forward and retrograde signaling (i.e. the hypothalamus) make decisions that affect both upstream and downstream physiology.

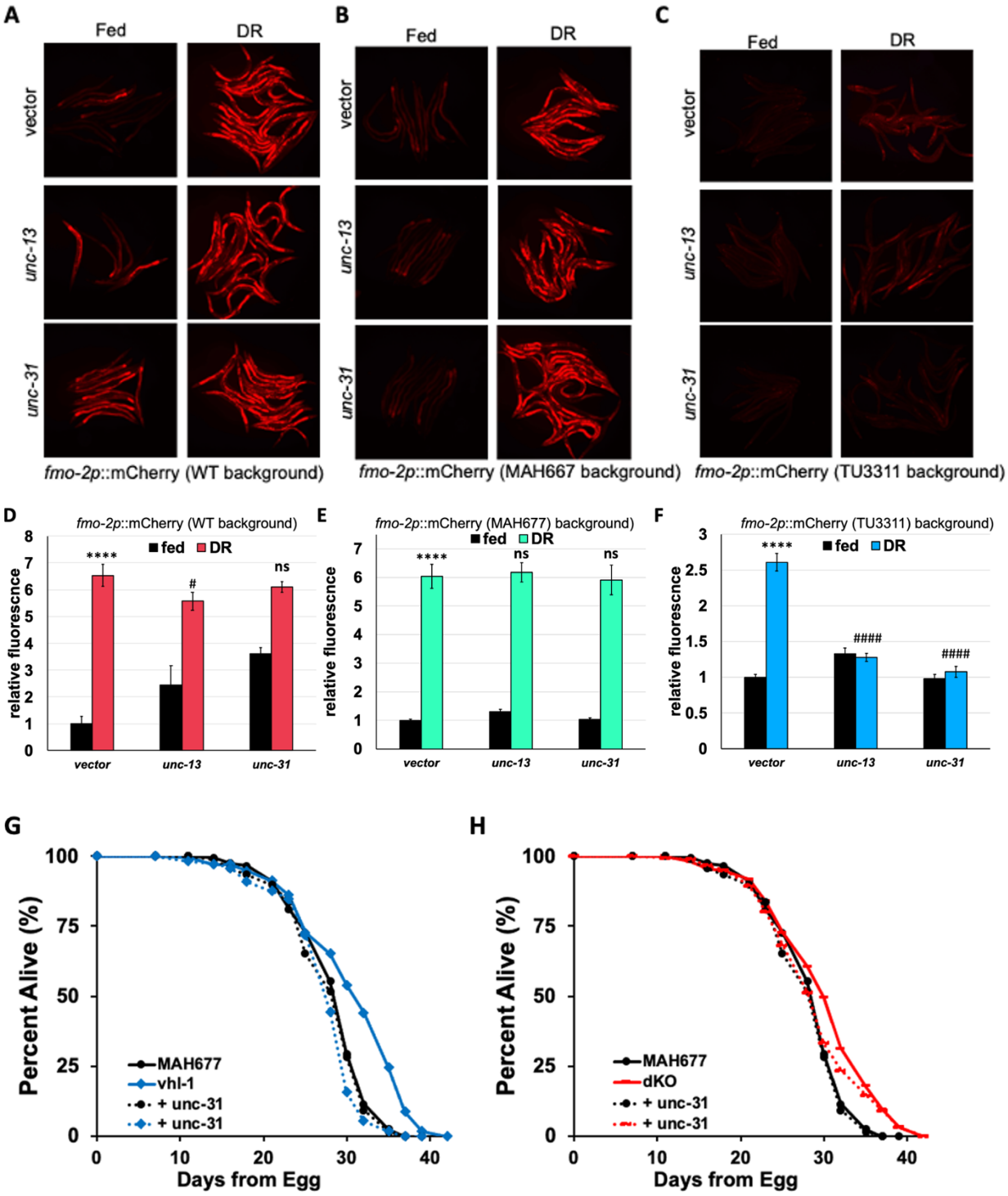

Figure 5.5. *unc-31* enhances DR signaling from the intestine to the nervous system. Images of *fmo-2p*::mCherry animals in the wild-type (A), MAH677 (B), and TU3311 (C) background on *unc-13* and *unc-31* RNAi exposed to DR. Quantification of wild-type (D), MAH677 (E), and TU3311 (F) images. Survival curves of MAH677 (black), vhl-1 (blue, G), and dKO (red, H) on vector (solid lines) or unc-31 RNAi (dotted lines). **** denotes P<.0001 when compared to fed (Tukey's HSD) ### #denotes P < 0.001 when compared to DR (Tukey's HSD).

We next exposed our three mutant animals to several RNAis from the shared and HIF-1 pathway hit lists (**Table 5.1**). Importantly, we find that none of the RNAis tested affect our control MAH677 lifespan (representative data in **Figure 5.6**) and of the RNAi screened, two neuropeptides produce convincing, if not slightly confusing results. Concurrent with our hypothesis, we find neuropeptides *nlp-17* and *nlp-23* necessary for *vhl-1*-mediated longevity (**Figure 5.6A-B**). Incongruous with our hypothesis, we see that *nlp-17*, but not *nlp-23*, is necessary for *vhl-1*; MAH677 longevity (**Figure 5.6C-D**).

If these results are not a strange artifact of our genetic crosses, what could this mean? It could be that neurons expressing and releasing *nlp-17* are not refractory to RNAi which would explain why *vhl-1*, with its endogenous *sid-1* locus, and *vhl-1*; MAH677 show similar results. This information could help us subset the neurons releasing *nlp-17* in our pathway by targeting the neurons that respond more aptly to RNAi. Similarly, if the inverse is true for *nlp-23,* there are two plausible hypotheses: 1) only a small subset of neurons are shown not to express *unc-119* (*289*), the promoter used to drive *sid-1* expression in MAH677, are responsible for *nlp-23* release or 2) some other non-neuronal tissue produces and releases nlp-23 downstream of HIF-1 stabilization. Since the intestine expresses neuropeptides and *nlp*-23 is proposed to be expressed in the hypodermis and tail (*246*), we favor the latter as the simplest explanation. To test this, we can cross tissue-specific RNAi strain into the *vhl-1* background and measure the effects of *nlp-13* and *nlp-23* KD on lifespan.

Are glial cells involved across stress-induced longevity pathways?

A population of cells that has gone mostly ignored by biogerontologists are glial cells. Unlike in mammalian brains, neurons outnumber glial cells 4:1 in nematodes (*290*). Only recently have scientists begun to explore glial cells potential role in longevity. The Dillon lab provides compelling data that glial cells play a critical modulating the effects of UPR activation on longevity (*48*). Could these cells be necessary for DR-mediated longevity? Could their absence in the neuron-specific RNAi strain explain the differences we see in our two *sid-1* mutants? Retesting these experiments using a glia-specific RNAi strain would help answer this question.

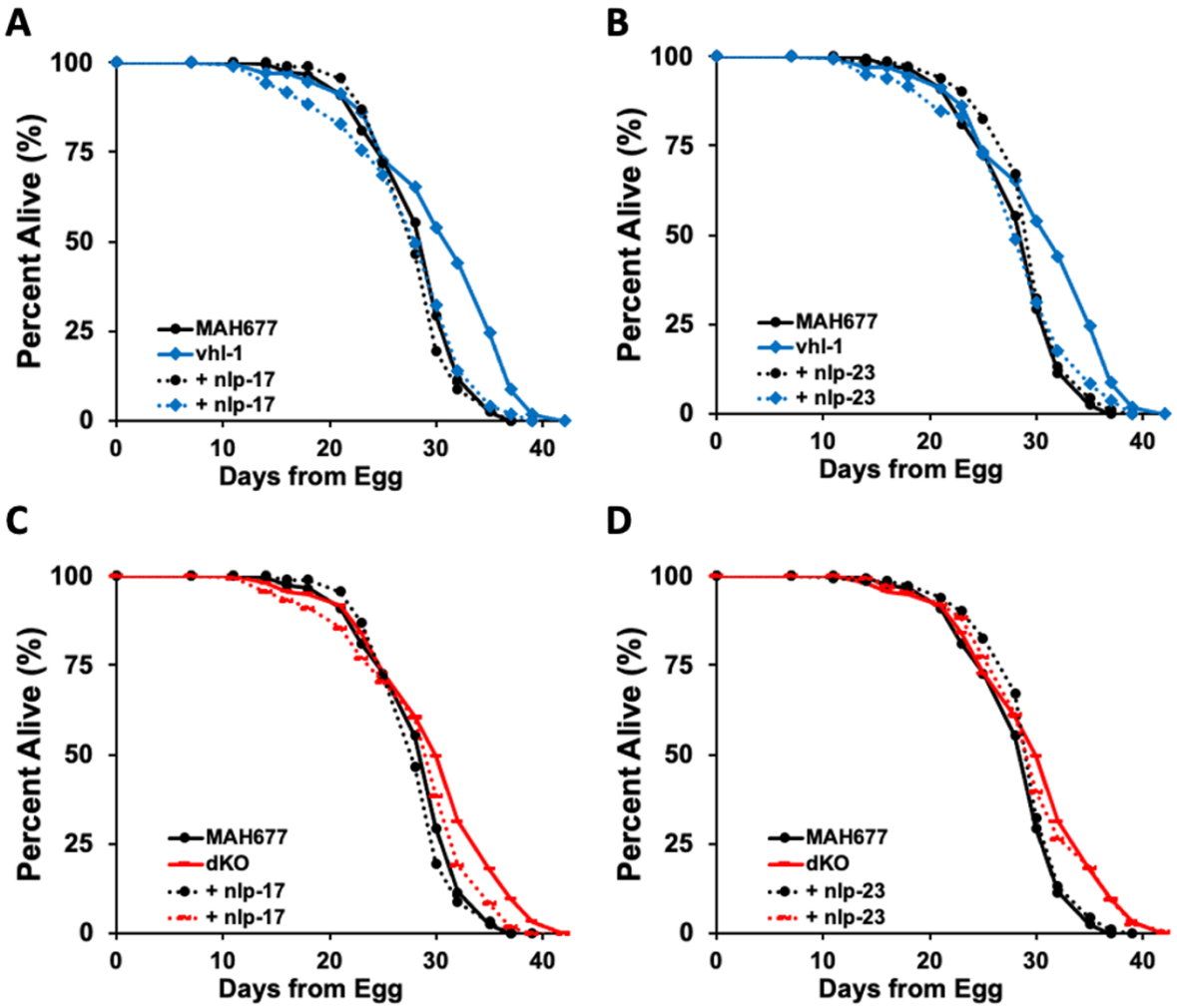

Figure 5.6. *nlp-23* functions as a necessary intestinal signal while *nlp-17* functions as a necessary neuronal signal to promote *vhl-1* longevity.
Survival curves of MAH677 (black) and *vhl-1* (blue) mutants on vector (solid lines), nlp-17 (A) or nlp-23 (B) RNAi (dotted lines). Survival curves of MAH677 (black) and dKO (red) mutants on vector (solid lines), nlp-17 (C) or nlp-23 (D) RNAi (dotted lines).

What transcription factors regulate intestinal FMO-2 expression?

Another important question worth exploring is how *fmo-2* is induced once the nervous system alerts the intestines about an on-going stressor. Utilizing publicly available modENCODE ChIP-seq data (*291*), we find 26 transcription factors (TFs) peaks in the 5' region upstream of *fmo-2's* ORF (MDL-1 and PHA-4 examples shown in **Figure 5.7A**). For our initial screen, we measured *fmo-2* induction under DR when we knocked down 17 clones present in the Ahringer library. We found several blunt *fmo-2* induction while two TFs*, nhr-49* and *mdl-1*, robustly block *fmo-2* induction (**Figure 5.7B-C**). Moreover, we find *nhr-49* is necessary for DR-mediated longevity (**Figure 5.8**). It's predicted NHR-49 is a functional PPARα ortholog (*292, 293*) while MDL-1 is a MAD-Like MXD3 ortholog (*294*). Both TFs have been implicated in modifying longevity (*32, 35, 36, 295-297*). However, *mdl-1's* role in longevity is thought to function, at least partially, through inhibition of oocyte formation (*296*) while *nhr-49* has been shown to drive metabolic rearrangement in distal tissues downstream of neuronal perception of stressors (*35*). While it is worth testing whether *mdl-1* is necessary for DR-mediated longevity, we would hypothesize any potential abolishment of longevity is a global trend of germline dysregulation not specific to DR signaling or food perception.

An important caveat to consider when interpreting these data is that the Waterson lab collects modENCODE samples during larval development not during adulthood or under stressful stimuli. Validating these results would require exposing NHR-49::GFP worms to DR and hypoxia and performing additional ChIP-seq experiments. That said, compounding evidence from the literature and our preliminary data suggest NHR-49 drives *fmo-2* transcription and it is worth exploring further whether these effects are specific to hypoxia and DR.

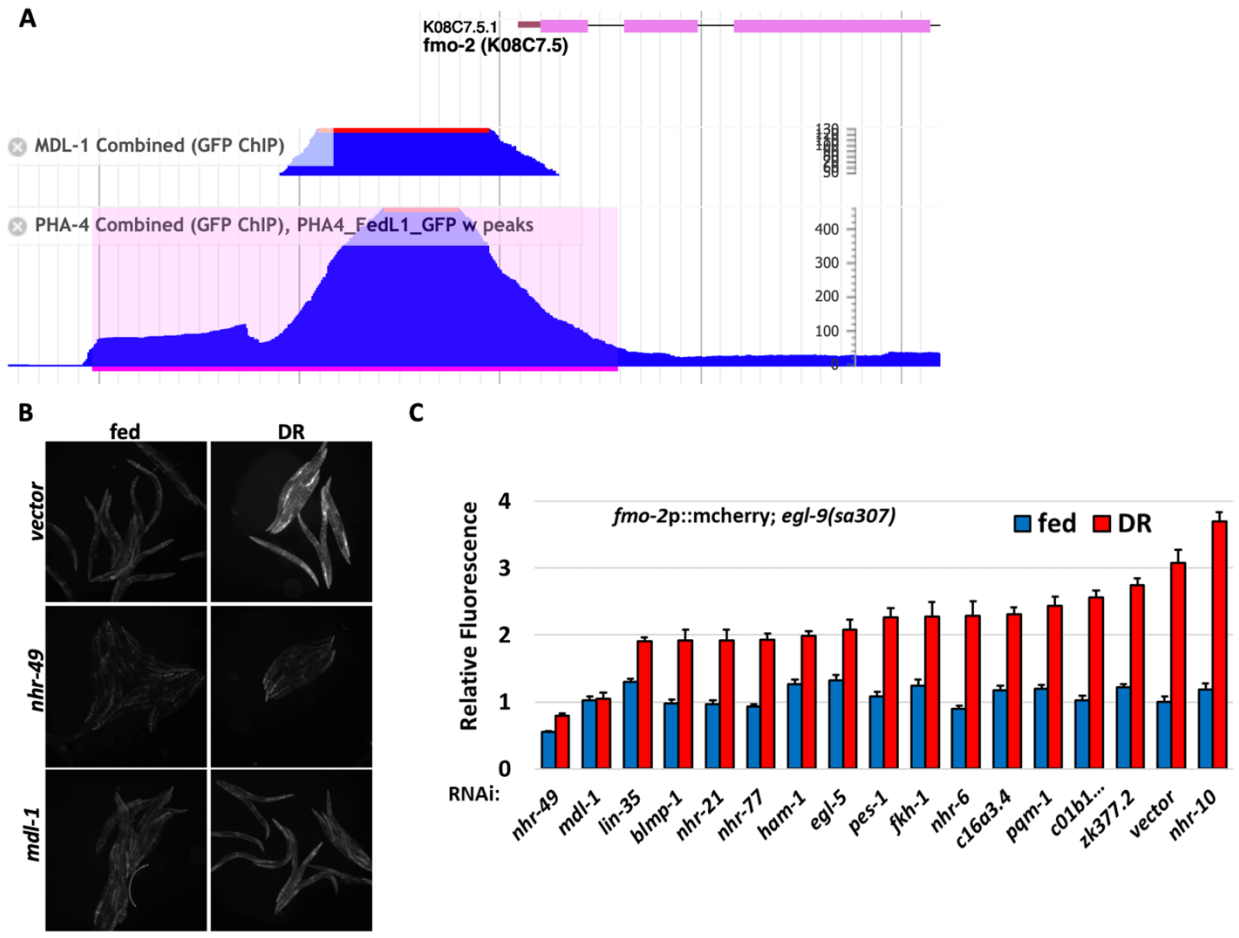

Figure 5.7. TFs *nhr-49* and *mdl-1* are required for DR-mediated *fmo-2* induction. Example ChIP-seq peaks called in *fmo-2* 5'UTR (A). Representative images (B) and quantification (C) of fmo-2p::MC; egl-9 animals screened TF RNAi on fed (blue) and DR (red)

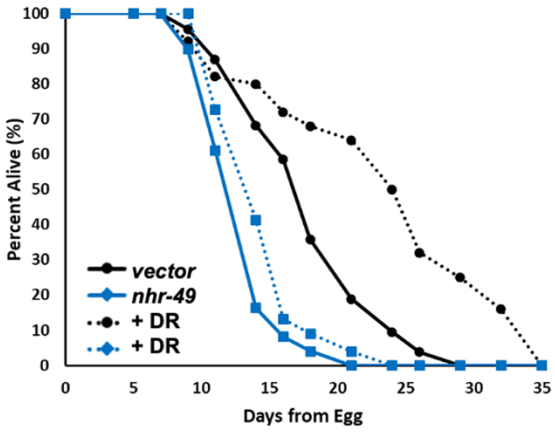

Figure 5.8. PPARα ortholog *nhr-49* is required for DR-mediated longevity. Survival curves of WT animals on vector (black) and *nhr-49* (blue) RNAi on fed (solid lines) or DR (dotted lines).

Models, speculation, and implications

The guiding principle of this thesis was to stand on the shoulders of the many great scientists before me to discover new insights into the highly orchestrated, multi-organ response to stressful stimuli since many of these ancient and complex signaling events are found to modulate aging.

In chapter 2, we present compelling evidence that reward circuitry, namely NTs serotonin and dopamine release, are tied to the perception of food smell and that these signals suppress pro-longevity genes like *fmo-2*. As similar results have been shown in flies, it's worth considering the potential conservation of these signaling events in mammals. With greater resolution into the specific cells involved in invertebrates, will we be able to modify NTs release within a subpopulation of neurons in higher organisms? Will these results recapitulate what we see in worms and flies? We hypothesize reward circuitry plays a similar role in mammalian aging but testing this hypothesis in mice remains quite challenging. Fortunately, with the advent of CRISPR and cerebral organoids, future scientists can alter, test, and measure neuronal function in an expedited fashion before moving their studies into whole organisms.

Moreover, it may be possible to mimic these signaling pathways with small molecules to abate mammalian aging through the DR pathway, without restricting the diet. This is crucial since it is likely humans will not willingly choose a DR diet despite its potential benefits. By better understanding the molecular and signaling mechanisms downstream of DR, these processes can be targeted directly, attaining benefits to human health while circumventing the challenges of implementing population-scale DR. Additional studies need to be performed across taxa to parse out the pro-longevity effects from the side effects. This is particularly important since it seems antidepressants have a small range of efficacy and can lead to numerous side effects in a sub-population of patients at different doses. Ideally, we would find the lowest dose of serotonin or dopamine modulators that can consistently increase lifespan in heterogenous drosophila backgrounds and HET3 mice to recapitulate the variability we see in the human population. In addition to providing the potential for long-term health benefits, this

knowledge will benefit our understanding of serotonin and dopamine signaling networks that affect numerous human processes and diseases outside of aging.

Research in chapter 3 explores temperatures' interaction with longevity interventions and genotypes. These data shed light on the complex interplay of stress responses and suggest some act in a temperature dependent or independent manner. As additional mechanistic studies on the factors that control differences in the comparative lifespan vs. temperature axis are completed, we expect that probable links will be made between temperature-specific longevity in nematodes and specific diseases of aging in mammals. Nevertheless, we must remain cautious of over-interpreting these data as the connection between cellular stress resistance and increased longevity remains correlative rather than causative in mammals. While it seems plausible that increased cellular stress resistance could prevent the damage that leads to the onset of age-related diseases in the elderly, mechanistic studies are required to conclusively connect stress resistance and longevity.

Finally, we utilized my bioinformatics training to analyze two RNA-seq datasets generated by the Leiser lab in chapter 4. Both projects have led to initial discoveries in HIF-1 regulation and FMO-2 mechanisms of action. However, we should remain cautious and agnostic about the functions of these downstream genes until more conclusive analyses are carried out. By testing the sufficiency of *flp-10* and *scl-5* OE to abrogate the lifespan effects of HIF-1 and FMO-2 activation, respectively, we will know whether these genes play an active role in accelerating aging in *C. elegans*. Additionally, it is critical we discover whether these genes have homologs that also modulate mammalian aging.

Materials and Methods

Strains and Growth Conditions

See chapter 2. Additional information in Table 5.2 includes a list of the strains and RNAi conditions used in this study.

Lifespan measurements

See chapter 2. Additional information in Table 5.3 includes statistics.

RNAi knockdown

See chapter 2.

Drug treatments

See chapter 2.

Dietary restriction (DR) treatment

See chapter 2.

Aβ-toxicity paralysis

Worm synchronization and induction of paralysis was performed as previously described (*288*). Instead of manually scoring paralysis, videos were taken in the GFP channel to measure aggregation and paralysis using Wormlab software.

Behavioral measurements

Videos were taken with the LASx software and Leica scope and >30 worms/treatment at 1x magnification. We analyzed the videos using wrMTrck ImageJ plugin (*285*). We used this tutorial (http://www.phage.dk/plugins/download/wrMTrck.pdf) to learn the software.

Statistical analyses

See chapter 2.

Description	Source	Identifier
wild-type	CGC	N2
tph-1(mg280)	CGC	MT15434
dvIs100 [unc-54p::A-beta-1-42::unc-54 3'-UTR + mtl-2p::GFP]	CGC	GMC101
vhl-1(ok161)	CGC	CB5602
uIs60 [unc-119p::YFP + unc-119p::sid-1]	CGC	TU3311
sid-1(qt1); sqIs71[rgef-1p::sid-1::GFP]	Malene Hansen	MAH677
[(pCF150) (fmo-2p::mCherry + H2B::GFP) + Cbr-unc-119(+)] II	chapter 2	LZR1
[(pCF150) (fmo-2p::mCherry + H2B::GFP) + Cbr-unc-119(+)] II; uIs60 [unc-119p::YFP + unc-119p::sid-1]	this study	LZR13
[(pCF150) (fmo-2p::mCherry + H2B::GFP) + Cbr-unc-119(+)] II; sid-1(qt1); sqIs71[rgef-1p::sid-1::GFP]	this study	LZR14
uIs60 [unc-119p::YFP + unc-119p::sid-1]; vhl-1(ok161)	this study	LZR15
sid-1(qt1); sqIs71[rgef-1p::sid-1::GFP] ; vhl-1(ok161)	this study	LZR16

Table 5.2. *C. elegans* strains used in this chapter.

data	strain	Mean lifespan	comparison	Mean lifespan	p-value
Fig. 5.5G-H	vhl-1 vector	30.86	MAH677 vector	28.54	0
	MAH677 unc-31	28.03	MAH677 vector	28.54	1
	vhl-1 unc-31	27.3	vhl-1 vector	30.86	0
	dKO vector	30.2	MAH677 vector	28.54	0.00004
	dKO unc-31	29.17	dKO vector	30.2	1
Fig. 5.6A-D	MAH677 nlp-17	28.4	MAH677 vector	28.54	1
	vhl-1 nlp-17	27.75	vhl-1 vector	30.86	0.0001
	dKO nlp-17	28.6	dKO vector	30.2	0.0381
	MAH677 nlp-23	29.49	MAH677 vector	28.54	0.7512
	vhl-1 nlp-23	28.38	vhl-1 vector	30.86	0.000022
	dKO nlp-23	30.19	dKO vector	30.2	1
Fig. 5.8	fed nhr-49 RNAi	12.85	fed vector RNAi	20.29	0
	DR nhr-49 RNAi	13.84	fed vector RNAi	20.29	0
	DR nhr-49 RNAi	13.84	DR vector RNAi	27.21	0

Table 5.3. Survival statistics for Figures 5.5-8.

References

1. D. B. Friedman, T. E. Johnson, A Mutation in the age-1 Gene in Caenorhabditis elegans Lengthens Life and Reduces Hermaphrodite Fertility. *Genetics* **118**, 75-86 (1988).
2. C. Kenyon, J. Chang, E. Gensch, A. Rudner, R. Tabtiang, A C. elegans mutant that lives twice as long as wild type. *Nature* **366**, 461-464 (1993).
3. K. D. Kimura, H. A. Tissenbaum, Y. Liu, G. Ruvkun, daf-2, an insulin receptor-like gene that regulates longevity and diapause in Caenorhabditis elegans. *Science* **277**, 942-946 (1997).
4. S. Libert *et al.*, Regulation of Drosophila life span by olfaction and food-derived odors. *Science* **315**, 1133-1137 (2007).
5. T. L. Kaeberlein *et al.*, Lifespan extension in Caenorhabditis elegans by complete removal of food. *Aging Cell* **5**, 487-494 (2006).
6. R. Mehta *et al.*, Proteasomal regulation of the hypoxic response modulates aging in C. elegans. *Science* **324**, 1196-1198 (2009).
7. A. H. Maehle, "Receptive substances": John Newport Langley (1852-1925) and his path to a receptor theory of drug action. *Med Hist* **48**, 153-174 (2004).
8. S. Cohen, The stimulation of epidermal proliferation by a specific protein (EGF). *Dev Biol* **12**, 394-407 (1965).
9. W. D. Paton, H. P. Rang, THE UPTAKE OF ATROPINE AND RELATED DRUGS BY INTESTINAL SMOOTH MUSCLE OF THE GUINEA-PIG IN RELATION TO ACETYLCHOLINE RECEPTORS. *Proc R Soc Lond B Biol Sci* **163**, 1-44 (1965).
10. R. Nusse, Wnts and Hedgehogs: lipid-modified proteins and similarities in signaling mechanisms at the cell surface. *Development* **130**, 5297-5305 (2003).
11. R. Schinzel, A. Dillin, Endocrine aspects of organelle stress—cell non-autonomous signaling of mitochondria and the ER. *Curr Opin Cell Biol* **33**, 102-110 (2015).
12. S. F. Leiser *et al.*, Cell nonautonomous activation of flavin-containing monooxygenase promotes longevity and health span. *Science*, (2015).
13. Y. Zhang *et al.*, Neuronal TORC1 modulates longevity via AMPK and cell nonautonomous regulation of mitochondrial dynamics in. *Elife* **8**, (2019).
14. G. Zhang *et al.*, Hypothalamic programming of systemic ageing involving IKK-β, NF-κB and GnRH. *Nature* **497**, 211-216 (2013).
15. C. E. Riera *et al.*, TRPV1 pain receptors regulate longevity and metabolism by neuropeptide signaling. *Cell* **157**, 1023-1036 (2014).
16. J. Ro *et al.*, Serotonin signaling mediates protein valuation and aging. *Elife* **5**, (2016).
17. J. Apfeld, C. Kenyon, Cell nonautonomy of C. elegans daf-2 function in the regulation of diapause and life span. *Cell* **95**, 199-210 (1998).
18. S. Gottlieb, G. Ruvkun, daf-2, daf-16 and daf-23: genetically interacting genes controlling Dauer formation in Caenorhabditis elegans. *Genetics* **137**, 107-120 (1994).
19. N. Libina, J. R. Berman, C. Kenyon, Tissue-specific activities of C. elegans DAF-16 in the regulation of lifespan. *Cell* **115**, 489-502 (2003)

20. M. McCormick, K. Chen, P. Ramaswamy, C. Kenyon, New genes that extend Caenorhabditis elegans' lifespan in response to reproductive signals. *Aging Cell* **11**, 192-202 (2012).
21. C. A. Wolkow, K. D. Kimura, M. S. Lee, G. Ruvkun, Regulation of C. elegans life-span by insulinlike signaling in the nervous system. *Science* **290**, 147-150 (2000).
22. J. Apfeld, C. Kenyon, Regulation of lifespan by sensory perception in Caenorhabditis elegans. *Nature* **402**, 804-809 (1999).
23. J. Alcedo, C. Kenyon, Regulation of C. elegans longevity by specific gustatory and olfactory neurons. *Neuron* **41**, 45-55 (2004).
24. R. Kaletsky *et al.*, The C. elegans adult neuronal IIS/FOXO transcriptome reveals adult phenotype regulators. *Nature* **529**, 92-96 (2016).
25. M. C. Silva, M. D. Amaral, R. I. Morimoto, Neuronal reprograming of protein homeostasis by calcium-dependent regulation of the heat shock response. *PLoS Genet* **9**, e1003711 (2013).
26. M. J. De Rosa *et al.*, The flight response impairs cytoprotective mechanisms by activating the insulin pathway. *Nature* **573**, 135-138 (2019).
27. H. Hsin, C. Kenyon, Signals from the reproductive system regulate the lifespan of C. elegans. *Nature* **399**, 362-366 (1999).
28. T. M. Yamawaki *et al.*, The somatic reproductive tissues of C. elegans promote longevity through steroid hormone signaling. *PLoS Biol* **8**, (2010).
29. B. J. Reinhart *et al.*, The 21-nucleotide let-7 RNA regulates developmental timing in Caenorhabditis elegans. *Nature* **403**, 901-906 (2000).
30. K. Boulias, H. R. Horvitz, The C. elegans microRNA mir-71 acts in neurons to promote germline-mediated longevity through regulation of DAF-16/FOXO. *Cell Metab* **15**, 439-450 (2012).
31. M. J. Steinbaugh *et al.*, Lipid-mediated regulation of SKN-1/Nrf in response to germ cell absence. *Elife* **4**, (2015).
32. R. Ratnappan *et al.*, Germline signals deploy NHR-49 to modulate fatty-acid β-oxidation and desaturation in somatic tissues of C. elegans. *PLoS Genet* **10**, e1004829 (2014).
33. J. Apfeld, G. O'Connor, T. McDonagh, P. S. DiStefano, R. Curtis, The AMP-activated protein kinase AAK-2 links energy levels and insulin-like signals to lifespan in C. elegans. *Genes Dev* **18**, 3004-3009 (2004).
34. W. Mair *et al.*, Lifespan extension induced by AMPK and calcineurin is mediated by CRTC-1 and CREB. *Nature* **470**, 404-408 (2011).
35. K. Burkewitz *et al.*, Neuronal CRTC-1 governs systemic mitochondrial metabolism and lifespan via a catecholamine signal. *Cell* **160**, 842-855 (2015).
36. E. Moreno-Arriola, M. El Hafidi, D. Ortega-Cuéllar, K. Carvajal, AMP-Activated Protein Kinase Regulates Oxidative Metabolism in Caenorhabditis elegans through the NHR-49 and MDT-15 Transcriptional Regulators. *PLoS One* **11**, e0148089 (2016).
37. M. J. Alkema, M. Hunter-Ensor, N. Ringstad, H. R. Horvitz, Tyramine Functions independently of octopamine in the Caenorhabditis elegans nervous system. *Neuron* **46**, 247-260 (2005).
38. S. Suo, Y. Kimura, H. H. Van Tol, Starvation induces cAMP response element-binding protein-dependent gene expression through octopamine-Gq signaling in Caenorhabditis elegans. *J Neurosci* **26**, 10082-10090 (2006).
39. H. Mills *et al.*, Monoamines and neuropeptides interact to inhibit aversive behaviour in Caenorhabditis elegans. *EMBO J* **31**, 667-678 (2012).
40. C. Y. Wu *et al.*, Enhancing GABAergic Transmission Improves Locomotion in a. *eNeuro* **5**, (2018).

41. M. A. Schreiber, J. T. Pierce-Shimomura, S. Chan, D. Parry, S. L. McIntire, Manipulation of behavioral decline in Caenorhabditis elegans with the Rag GTPase raga-1. *PLoS Genet* **6**, e1000972 (2010).
42. E. J. Calabrese, G. Dhawan, R. Kapoor, I. Iavicoli, V. Calabrese, What is hormesis and its relevance to healthy aging and longevity? *Biogerontology* **16**, 693-707 (2015).
43. J. Durieux, S. Wolff, A. Dillin, The cell-non-autonomous nature of electron transport chain-mediated longevity. *Cell* **144**, 79-91 (2011).
44. Q. Zhang *et al.*, The Mitochondrial Unfolded Protein Response Is Mediated Cell-Non-autonomously by Retromer-Dependent Wnt Signaling. *Cell* **174**, 870-883.e817 (2018).
45. B. C. Prasad, S. G. Clark, Wnt signaling establishes anteroposterior neuronal polarity and requires retromer in C. elegans. *Development* **133**, 1757-1766 (2006).
46. R. C. Taylor, A. Dillin, XBP-1 is a cell-nonautonomous regulator of stress resistance and longevity. *Cell* **153**, 1435-1447 (2013).
47. S. Imanikia, N. P. Özbey, C. Krueger, M. O. Casanueva, R. C. Taylor, Neuronal XBP-1 Activates Intestinal Lysosomes to Improve Proteostasis in C. elegans. *Curr Biol* **29**, 2322-2338.e2327 (2019).
48. A. E. Frakes *et al.*, Four glial cells regulate ER stress resistance and longevity via neuropeptide signaling in. *Science* **367**, 436-440 (2020).
49. J. R. Daniele *et al.*, UPR. *Sci Adv* **6**, eaaz1441 (2020).
50. S. Imanikia, M. Sheng, C. Castro, J. L. Griffin, R. C. Taylor, XBP-1 Remodels Lipid Metabolism to Extend Longevity. *Cell Rep* **28**, 581-589.e584 (2019).
51. C. Li, K. Kim, L. S. Nelson, FMRFamide-related neuropeptide gene family in Caenorhabditis elegans. *Brain Res* **848**, 26-34 (1999).
52. C. Li, L. S. Nelson, K. Kim, A. Nathoo, A. C. Hart, Neuropeptide gene families in the nematode Caenorhabditis elegans. *Ann N Y Acad Sci* **897**, 239-252 (1999).
53. H. Miller *et al.*, Genetic interaction with temperature is an important determinant of nematode longevity. *Aging Cell*, (2017).
54. D. M. Walther *et al.*, Widespread Proteome Remodeling and Aggregation in Aging C. elegans. *Cell* **161**, 919-932 (2015).
55. J. Labbadia, R. I. Morimoto, Repression of the Heat Shock Response Is a Programmed Event at the Onset of Reproduction. *Mol Cell* **59**, 639-650 (2015).
56. M. Santra, K. A. Dill, A. M. R. de Graff, Proteostasis collapse is a driver of cell aging and death. *Proc Natl Acad Sci U S A* **116**, 22173-22178 (2019).
57. V. Prahlad, T. Cornelius, R. I. Morimoto, Regulation of the cellular heat shock response in Caenorhabditis elegans by thermosensory neurons. *Science* **320**, 811-814 (2008).
58. M. C. Tatum *et al.*, Neuronal serotonin release triggers the heat shock response in C. elegans in the absence of temperature increase. *Curr Biol* **25**, 163-174 (2015).
59. S. J. Lee, C. Kenyon, Regulation of the longevity response to temperature by thermosensory neurons in Caenorhabditis elegans. *Curr Biol* **19**, 715-722 (2009).
60. P. M. Douglas *et al.*, Heterotypic Signals from Neural HSF-1 Separate Thermotolerance from Longevity. *Cell Rep* **12**, 1196-1204 (2015).
61. C. Kumsta *et al.*, Integrin-linked kinase modulates longevity and thermotolerance in C. elegans through neuronal control of HSF-1. *Aging Cell* **13**, 419-430 (2014).
62. B. Zhang *et al.*, Brain-gut communications via distinct neuroendocrine signals bidirectionally regulate longevity in. *Genes Dev* **32**, 258-270 (2018).
63. M. Artan *et al.*, Food-derived sensory cues modulate longevity via distinct neuroendocrine insulin-like peptides. *Genes Dev* **30**, 1047-1057 (2016).
64. R. Xiao *et al.*, A genetic program promotes C. elegans longevity at cold temperatures via a thermosensitive TRP channel. *Cell* **152**, 806-817 (2013).

65. C. McCay, M. Crowell, L. Maynard, The effect of retarded growth upon the length of life span and upon the ultimate body size. *J Nutr.* **10**, 63-79 (1935).
66. L. Fontana, L. Partridge, Promoting health and longevity through diet: from model organisms to humans. *Cell* **161**, 106-118 (2015).
67. N. A. Bishop, L. Guarente, Two neurons mediate diet-restriction-induced longevity in C. elegans. *Nature* **447**, 545-549 (2007).
68. Y. J. You, J. Kim, D. M. Raizen, L. Avery, Insulin, cGMP, and TGF-beta signals regulate food intake and quiescence in C. elegans: a model for satiety. *Cell Metab* **7**, 249-257 (2008).
69. R. J. McCloskey, A. D. Fouad, M. A. Churgin, C. Fang-Yen, Food responsiveness regulates episodic behavioral states in. *J Neurophysiol* **117**, 1911-1934 (2017).
70. L. E. Waggoner, G. T. Zhou, R. W. Schafer, W. R. Schafer, Control of alternative behavioral states by serotonin in Caenorhabditis elegans. *Neuron* **21**, 203-214 (1998).
71. S. Srinivasan *et al.*, Serotonin regulates C. elegans fat and feeding through independent molecular mechanisms. *Cell Metab* **7**, 533-544 (2008).
72. S. Zheng *et al.*, A functional study of all 40. *J Biol Chem* **293**, 16912-16922 (2018).
73. M. Petrascheck, X. Ye, L. B. Buck, A high-throughput screen for chemicals that increase the lifespan of Caenorhabditis elegans. *Ann N Y Acad Sci* **1170**, 698-701 (2009).
74. S. F. Leiser, M. Fletcher, A. Begun, M. Kaeberlein, Life-span extension from hypoxia in Caenorhabditis elegans requires both HIF-1 and DAF-16 and is antagonized by SKN-1. *J Gerontol A Biol Sci Med Sci* **68**, 1135-1144 (2013).
75. W. R. Swindell, Genes and gene expression modules associated with caloric restriction and aging in the laboratory mouse. *BMC Genomics* **10**, 585 (2009).
76. M. J. Steinbaugh, L. Y. Sun, A. Bartke, R. A. Miller, Activation of genes involved in xenobiotic metabolism is a shared signature of mouse models with extended lifespan. *Am J Physiol Endocrinol Metab* **303**, E488-495 (2012).
77. D. H. A. Fitch. (Wormbook, WormBook, ed. The C.elegans Research Community, 2005).
78. D. S. Hwangbo *et al.*, Drosophila dFOXO controls lifespan and regulates insulin signalling in brain and fat body. *Nature* **429**, 562-566 (2004).
79. K. Kannan, Y. W. Fridell, Functional implications of Drosophila insulin-like peptides in metabolism, aging, and dietary restriction. *Front Physiol* **4**, 288 (2013).
80. D. J. Clancy *et al.*, Extension of life-span by loss of CHICO, a Drosophila insulin receptor substrate protein. *Science* **292**, 104-106 (2001).
81. M. Tatar *et al.*, A mutant Drosophila insulin receptor homolog that extends life-span and impairs neuroendocrine function. *Science* **292**, 107-110 (2001).
82. M. E. Giannakou *et al.*, Long-lived Drosophila with overexpressed dFOXO in adult fat body. *Science* **305**, 361 (2004).
83. D. S. Hwangbo, B. Gershman, M. P. Tu, M. Palmer, M. Tatar, Drosophila dFOXO controls lifespan and regulates insulin signalling in brain and fat body. *Nature* **429**, 562-566 (2004).
84. W. Brogiolo *et al.*, An evolutionarily conserved function of the Drosophila insulin receptor and insulin-like peptides in growth control. *Curr Biol* **11**, 213-221 (2001).
85. J. Colombani, D. S. Andersen, P. Leopold, Secreted peptide Dilp8 coordinates Drosophila tissue growth with developmental timing. *Science* **336**, 582-585 (2012).
86. S. Gronke, D. F. Clarke, S. Broughton, T. D. Andrews, L. Partridge, Molecular evolution and functional characterization of Drosophila insulin-like peptides. *PLoS Genet* **6**, e1000857 (2010).
87. H. Bai, P. Kang, M. Tatar, Drosophila insulin-like peptide-6 (dilp6) expression from fat body extends lifespan and represses secretion of Drosophila insulin-like peptide-2 from the brain. *Aging Cell* **11**, 978-985 (2012).

88. S. J. Broughton *et al.*, DILP-producing median neurosecretory cells in the Drosophila brain mediate the response of lifespan to nutrition. *Aging Cell* **9**, 336-346 (2010).
89. S. J. Broughton *et al.*, Longer lifespan, altered metabolism, and stress resistance in Drosophila from ablation of cells making insulin-like ligands. *Proc Natl Acad Sci U S A* **102**, 3105-3110 (2005).
90. A. Haselton *et al.*, Partial ablation of adult Drosophila insulin-producing neurons modulates glucose homeostasis and extends life span without insulin resistance. *Cell Cycle* **9**, 3063-3071 (2010).
91. L. E. Enell, N. Kapan, J. A. Söderberg, L. Kahsai, D. R. Nässel, Insulin signaling, lifespan and stress resistance are modulated by metabotropic GABA receptors on insulin producing cells in the brain of Drosophila. *PLoS One* **5**, e15780 (2010).
92. M. C. Wang, D. Bohmann, H. Jasper, JNK extends life span and limits growth by antagonizing cellular and organism-wide responses to insulin signaling. *Cell* **121**, 115-125 (2005).
93. S. Post *et al.*, Drosophila insulin-like peptide dilp1 increases lifespan and glucagon-like Akh expression epistatic to dilp2. *Aging Cell* **18**, e12863 (2019).
94. A. Bednarova, D. Kodrik, N. Krishnan, Unique roles of glucagon and glucagon-like peptides: Parallels in understanding the functions of adipokinetic hormones in stress responses in insects. *Comp Biochem Physiol A Mol Integr Physiol* **164**, 91-100 (2013).
95. M. J. Waterson *et al.*, Water sensor ppk28 modulates Drosophila lifespan and physiology through AKH signaling. *Proc Natl Acad Sci U S A* **111**, 8137-8142 (2014).
96. M. J. Waterson, T. P. Chan, S. D. Pletcher, Adaptive Physiological Response to Perceived Scarcity as a Mechanism of Sensory Modulation of Life Span. *The Journals of Gerontology: Series A* **70**, 1088-1091 (2015).
97. M. E. Giannakou, M. Goss, L. Partridge, Role of dFOXO in lifespan extension by dietary restriction in Drosophila melanogaster: not required, but its activity modulates the response. *Aging Cell* **7**, 187-198 (2008).
98. R. Yamamoto, M. Tatar, Insulin receptor substrate chico acts with the transcription factor FOXO to extend Drosophila lifespan. *Aging Cell* **10**, 729-732 (2011).
99. M. Ulgherait, A. Rana, M. Rera, J. Graniel, D. W. Walker, AMPK modulates tissue and organismal aging in a non-cell-autonomous manner. *Cell Rep* **8**, 1767-1780 (2014).
100. J. M. Copeland *et al.*, Extension of Drosophila life span by RNAi of the mitochondrial respiratory chain. *Curr Biol* **19**, 1591-1598 (2009).
101. E. Owusu-Ansah, W. Song, N. Perrimon, Muscle mitohormesis promotes longevity via systemic repression of insulin signaling. *Cell* **155**, 699-712 (2013).
102. J. Feng, F. Bussière, S. Hekimi, Mitochondrial electron transport is a key determinant of life span in Caenorhabditis elegans. *Dev Cell* **1**, 633-644 (2001).
103. Y. W. Fridell, A. Sánchez-Blanco, B. A. Silvia, S. L. Helfand, Targeted expression of the human uncoupling protein 2 (hUCP2) to adult neurons extends life span in the fly. *Cell Metab* **1**, 145-152 (2005).
104. D. M. Humphrey, J. M. Toivonen, M. Giannakou, L. Partridge, M. D. Brand, Expression of human uncoupling protein-3 in Drosophila insulin-producing cells increases insulin-like peptide (DILP) levels and shortens lifespan. *Exp Gerontol* **44**, 316-327 (2009).
105. F. Demontis, N. Perrimon, FOXO/4E-BP signaling in Drosophila muscles regulates organism-wide proteostasis during aging. *Cell* **143**, 813-825 (2010).
106. A. Rallis *et al.*, Hedgehog Signaling Modulates Glial Proteostasis and Lifespan. *Cell Rep* **30**, 2627-2643.e2625 (2020).
107. N. J. Linford, J. Ro, B. Y. Chung, S. D. Pletcher, Gustatory and metabolic perception of nutrient stress in Drosophila. *Proc Natl Acad Sci U S A* **112**, 2587-2592 (2015).

108. I. Ostojic *et al.*, Positive and negative gustatory inputs affect Drosophila lifespan partly in parallel to dFOXO signaling. *Proc Natl Acad Sci U S A* **111**, 8143-8148 (2014).
109. S. M. Solon-Biet *et al.*, The ratio of macronutrients, not caloric intake, dictates cardiometabolic health, aging, and longevity in ad libitum-fed mice. *Cell Metab* **19**, 418-430 (2014).
110. W. Mair, M. D. Piper, L. Partridge, Calories do not explain extension of life span by dietary restriction in Drosophila. *PLoS Biol* **3**, e223 (2005).
111. D. A. Skorupa, A. Dervisefendic, J. Zwiener, S. D. Pletcher, Dietary composition specifies consumption, obesity and lifespan in Drosophila melanogaster. *Aging Cell*, (2008).
112. S. J. Simpson, D. Raubenheimer, Caloric restriction and aging revisited: the need for a geometric analysis of the nutritional bases of aging. *J Gerontol A Biol Sci Med Sci* **62**, 707-713 (2007).
113. K. Steck *et al.*, Internal amino acid state modulates yeast taste neurons to support protein homeostasis in Drosophila. *Elife* **7**, (2018).
114. Q. Liu *et al.*, Branch-specific plasticity of a bifunctional dopamine circuit encodes protein hunger. *Science* **356**, 534-539 (2017).
115. C. M. Gendron *et al.*, Drosophila life span and physiology are modulated by sexual perception and reward. *Science* **343**, 544-548 (2014).
116. Z. M. Harvanek *et al.*, Perceptive costs of reproduction drive ageing and physiology in male Drosophila. *Nat Ecol Evol* **1**, 152 (2017).
117. T. S. Chakraborty *et al.*, Sensory perception of dead conspecifics induces aversive cues and modulates lifespan through serotonin in Drosophila. *Nat Commun* **10**, 2365 (2019).
118. G. S. Suh *et al.*, Light activation of an innate olfactory avoidance response in Drosophila. *Curr Biol* **17**, 905-908 (2007).
119. P. C. Poon, T. H. Kuo, N. J. Linford, G. Roman, S. D. Pletcher, Carbon dioxide sensing modulates lifespan and physiology in Drosophila. *PLoS Biol* **8**, e1000356 (2010).
120. H. M. Brown-Borg, K. E. Borg, C. J. Meliska, A. Bartke, Dwarf mice and the ageing process. *Nature* **384**, 33 (1996).
121. K. Flurkey, J. Papaconstantinou, D. E. Harrison, The Snell dwarf mutation Pit1(dw) can increase life span in mice. *Mech Ageing Dev* **123**, 121-130 (2002).
122. K. Flurkey, J. Papaconstantinou, R. A. Miller, D. E. Harrison, Lifespan extension and delayed immune and collagen aging in mutant mice with defects in growth hormone production. *Proc Natl Acad Sci U S A* **98**, 6736-6741 (2001).
123. K. T. Coschigano *et al.*, Deletion, but not antagonism, of the mouse growth hormone receptor results in severely decreased body weights, insulin, and insulin-like growth factor I levels and increased life span. *Endocrinology* **144**, 3799-3810 (2003).
124. M. Holzenberger *et al.*, IGF-1 receptor regulates lifespan and resistance to oxidative stress in mice. *Nature* **421**, 182-187 (2003).
125. L. Kappeler *et al.*, Brain IGF-1 receptors control mammalian growth and lifespan through a neuroendocrine mechanism. *PLoS Biol* **6**, e254 (2008).
126. J. M. Zullo *et al.*, Regulation of lifespan by neural excitation and REST. *Nature* **574**, 359-364 (2019).
127. M. De Luca *et al.*, Sex-specific longevity associations defined by Tyrosine Hydroxylase-Insulin-Insulin Growth Factor 2 haplotypes on the 11p15.5 chromosomal region. *Exp Gerontol* **36**, 1663-1671 (2001).
128. T. Nagatsu, Tyrosine hydroxylase: human isoforms, structure and regulation in physiology and pathology. *Essays Biochem* **30**, 15-35 (1995).
129. D. L. Grady *et al.*, DRD4 genotype predicts longevity in mouse and human. *J Neurosci* **33**, 286-291 (2013).

130. A. Taguchi, L. M. Wartschow, M. F. White, Brain IRS2 signaling coordinates life span and nutrient homeostasis. *Science* **317**, 369-372 (2007).
131. R. de Cabo, D. Carmona-Gutierrez, M. Bernier, M. N. Hall, F. Madeo, The search for antiaging interventions: from elixirs to fasting regimens. *Cell* **157**, 1515-1526 (2014).
132. D. E. Harrison *et al.*, Rapamycin fed late in life extends lifespan in genetically heterogeneous mice. *Nature* **460**, 392-395 (2009).
133. A. Bitto *et al.*, Transient rapamycin treatment can increase lifespan and healthspan in middle-aged mice. *Elife* **5**, (2016).
134. N. V. Bobkova *et al.*, Exogenous Hsp70 delays senescence and improves cognitive function in aging mice. *Proc Natl Acad Sci U S A* **112**, 16006-16011 (2015).
135. D. A. N. Barbosa *et al.*, The hypothalamus at the crossroads of psychopathology and neurosurgery. *Neurosurg Focus* **43**, E15 (2017).
136. B. Conti *et al.*, Transgenic mice with a reduced core body temperature have an increased life span. *Science* **314**, 825-828 (2006).
137. K. Taniguchi, M. Karin, NF-κB, inflammation, immunity and cancer: coming of age. *Nature Reviews Immunology* **18**, 309-324 (2018).
138. A. Satoh *et al.*, Sirt1 extends life span and delays aging in mice through the regulation of Nk2 homeobox 1 in the DMH and LH. *Cell Metab* **18**, 416-430 (2013).
139. J. N. Rea, A. Carvalho, S. E. McNerlan, H. D. Alexander, I. M. Rea, Genes and life-style factors in BELFAST nonagenarians: Nature, Nurture and Narrative. *Biogerontology* **16**, 587-597 (2015).
140. F. L. Spadafora *et al.*, Aspects of sleep in centenarians. *Arch Gerontol Geriatr* **22 Suppl 1**, 419-422 (1996).
141. E. M. Simonsick, H. C. S. Meier, N. C. Shaffer, S. A. Studenski, L. Ferrucci, Basal body temperature as a biomarker of healthy aging. *Age (Dordr)* **38**, 445-454 (2016).
142. P. Carmeliet *et al.*, Plasminogen activator inhibitor-1 gene-deficient mice. I. Generation by homologous recombination and characterization. *J Clin Invest* **92**, 2746-2755 (1993).
143. M. Eren, C. A. Painter, J. B. Atkinson, P. J. Declerck, D. E. Vaughan, Age-dependent spontaneous coronary arterial thrombosis in transgenic mice that express a stable form of human plasminogen activator inhibitor-1. *Circulation* **106**, 491-496 (2002).
144. M. Eren *et al.*, PAI-1-regulated extracellular proteolysis governs senescence and survival in Klotho mice. *Proc Natl Acad Sci U S A* **111**, 7090-7095 (2014).
145. K. Yamamoto, K. Takeshita, T. Kojima, J. Takamatsu, H. Saito, Aging and plasminogen activator inhibitor-1 (PAI-1) regulation: implication in the pathogenesis of thrombotic disorders in the elderly. *Cardiovasc Res* **66**, 276-285 (2005).
146. J. Campisi, L. Robert, Cell senescence: role in aging and age-related diseases. *Interdiscip Top Gerontol* **39**, 45-61 (2014).
147. M. Demaria *et al.*, An essential role for senescent cells in optimal wound healing through secretion of PDGF-AA. *Dev Cell* **31**, 722-733 (2014).
148. J. Campisi, Aging, cellular senescence, and cancer. *Annu Rev Physiol* **75**, 685-705 (2013).
149. J. Campisi *et al.*, From discoveries in ageing research to therapeutics for healthy ageing. *Nature* **571**, 183-192 (2019).
150. A. S. Kulkarni, S. Gubbi, N. Barzilai, Benefits of Metformin in Attenuating the Hallmarks of Aging. *Cell Metab* **32**, 15-30 (2020).
151. I. M. Conboy *et al.*, Rejuvenation of aged progenitor cells by exposure to a young systemic environment. *Nature* **433**, 760-764 (2005).
152. F. S. Loffredo *et al.*, Growth differentiation factor 11 is a circulating factor that reverses age-related cardiac hypertrophy. *Cell* **153**, 828-839 (2013).

153. L. Katsimpardi *et al.*, Vascular and neurogenic rejuvenation of the aging mouse brain by young systemic factors. *Science* **344**, 630-634 (2014).
154. J. Rebo *et al.*, A single heterochronic blood exchange reveals rapid inhibition of multiple tissues by old blood. *Nat Commun* **7**, 13363 (2016).
155. M. J. Yousefzadeh *et al.*, Heterochronic parabiosis regulates the extent of cellular senescence in multiple tissues. *Geroscience* **42**, 951-961 (2020).
156. M. Sinha *et al.*, Restoring systemic GDF11 levels reverses age-related dysfunction in mouse skeletal muscle. *Science* **344**, 649-652 (2014).
157. D. Shytikov, O. Balva, E. Debonneuil, P. Glukhovskiy, I. Pishel, Aged mice repeatedly injected with plasma from young mice: a survival study. *BioResearch open access* **3**, 226-232 (2014).
158. D. Bazopoulou, A. R. Chaudhury, A. Pantazis, N. Chronis, An automated compound screening for anti-aging effects on the function of C. elegans sensory neurons. *Sci Rep* **7**, 9403 (2017).
159. T. D. Admasu *et al.*, Drug Synergy Slows Aging and Improves Healthspan through IGF and SREBP Lipid Signaling. *Dev Cell* **47**, 67-79.e65 (2018).
160. J. I. Castillo-Quan *et al.*, A triple drug combination targeting components of the nutrient-sensing network maximizes longevity. *Proc Natl Acad Sci U S A* **116**, 20817-20819 (2019).
161. A. N. Minniti *et al.*, Temporal pattern of neuronal insulin release during Caenorhabditis elegans aging: Role of redox homeostasis. *Aging Cell* **18**, e12855 (2019).
162. A. D. Bouagnon *et al.*, Intestinal peroxisomal fatty acid β-oxidation regulates neural serotonin signaling through a feedback mechanism. *PLoS Biol* **17**, e3000242 (2019).
163. M. Ulgherait, A. Rana, M. Rera, J. Graniel, D. W. Walker, AMPK modulates tissue and organismal aging in a non-cell-autonomous manner. *Cell Rep* **8**, 1767-1780 (2014).
164. C. López-Otín, M. A. Blasco, L. Partridge, M. Serrano, G. Kroemer, The hallmarks of aging. *Cell* **153**, 1194-1217 (2013).
165. Y. Medkour, V. Svistkova, V. I. Titorenko, Cell-Nonautonomous Mechanisms Underlying Cellular and Organismal Aging. *Int Rev Cell Mol Biol* **321**, 259-297 (2016).
166. H. A. Miller, E. S. Dean, S. D. Pletcher, S. F. Leiser, Cell non-autonomous regulation of health and longevity. *Elife* **9**, (2020).
167. M. Berger, J. A. Gray, B. L. Roth, The expanded biology of serotonin. *Annu Rev Med* **60**, 355-366 (2009).
168. O. Arias-Carrión, M. Stamelou, E. Murillo-Rodríguez, M. Menéndez-González, E. Pöppel, Dopaminergic reward system: a short integrative review. *Int Arch Med* **3**, 24 (2010).
169. K. Saharia, R. Kumar, K. Gupta, S. Mishra, J. R. Subramaniam, Reserpine requires the D2-type receptor,. *J Biosci* **41**, 689-695 (2016).
170. J. A. Yin, X. J. Liu, J. Yuan, J. Jiang, S. Q. Cai, Longevity manipulations differentially affect serotonin/dopamine level and behavioral deterioration in aging Caenorhabditis elegans. *J Neurosci* **34**, 3947-3958 (2014).
171. R. Peters, Ageing and the brain. *Postgrad Med J* **82**, 84-88 (2006).
172. L. Fontana, L. Partridge, V. D. Longo, Extending Healthy Life Span--From Yeast to Humans. *Science* **328**, 321-326 (2010).
173. M. I. Petalcorin, G. W. Joshua, P. M. Agapow, C. T. Dolphin, The fmo genes of Caenorhabditis elegans and C. briggsae: characterisation, gene expression and comparative genomic analysis. *Gene* **346**, 83-96 (2005).
174. C. I. Bargmann, E. Hartwieg, H. R. Horvitz, Odorant-selective genes and neurons mediate olfaction in C. elegans. *Cell* **74**, 515-527 (1993).

175. S. E. Worthy *et al.*, Identification of attractive odorants released by preferred bacterial food found in the natural habitats of C. elegans. *PLoS One* **13**, e0201158 (2018).
176. W. M. Nuttley, K. P. Atkinson-Leadbeater, D. Van Der Kooy, Serotonin mediates food-odor associative learning in the nematode Caenorhabditiselegans. *Proc Natl Acad Sci U S A* **99**, 12449-12454 (2002).
177. S. W. Flavell *et al.*, Serotonin and the neuropeptide PDF initiate and extend opposing behavioral states in C. elegans. *Cell* **154**, 1023-1035 (2013).
178. R. J. Marshall, The pharmacology of mianserin--an update. *Br J Clin Pharmacol* **15 Suppl 2**, 263S-268S (1983).
179. K. F. Shana M. Feinberg , Abdolreza Saadabadi, in *Thioridazine*. (Stat Pearls, 2020).
180. M. Petrascheck, X. Ye, L. B. Buck, An antidepressant that extends lifespan in adult Caenorhabditis elegans. *Nature* **450**, 553-556 (2007).
181. H. Murakami, S. Murakami, Serotonin receptors antagonistically modulate Caenorhabditis elegans longevity. *Aging Cell* **6**, 483-488 (2007).
182. J. Y. Sze, M. Victor, C. Loer, Y. Shi, G. Ruvkun, Food and metabolic signalling defects in a Caenorhabditis elegans serotonin-synthesis mutant. *Nature* **403**, 560-564 (2000).
183. C. Trent, N. Tsung, H. R. Horvitz, Egg-laying defective mutants of the nematode Caeenorhabditis Elegans. *Genetics* **104**, 619-647 (1983).
184. J. L. Rhoades *et al.*, ASICs Mediate Food Responses in an Enteric Serotonergic Neuron that Controls Foraging Behaviors. *Cell* **176**, 85-97.e14 (2019).
185. M. A. Churgin, R. J. McCloskey, E. Peters, C. Fang-Yen, Antagonistic Serotonergic and Octopaminergic Neural Circuits Mediate Food-Dependent Locomotory Behavior in Caenorhabditis elegans. *J Neurosci* **37**, 7811-7823 (2017).
186. . (2020).
187. S. Murakami, A. Salmon, R. A. Miller, Multiplex stress resistance in cells from long-lived dwarf mice. *FASEB J* **17**, 1565-1566 (2003).
188. J. M. Harper, A. B. Salmon, S. F. Leiser, A. T. Galecki, R. A. Miller, Skin-derived fibroblasts from long-lived species are resistant to some, but not all, lethal stresses and to the mitochondrial inhibitor rotenone. *Aging Cell* **6**, 1-13 (2007).
189. J. Ro, Z. M. Harvanek, S. D. Pletcher, FLIC: high-throughput, continuous analysis of feeding behaviors in Drosophila. *PLoS One* **9**, e101107 (2014).
190. E. R. Sawin, R. Ranganathan, H. R. Horvitz, C. elegans locomotory rate is modulated by the environment through a dopaminergic pathway and by experience through a serotonergic pathway. *Neuron* **26**, 619-631 (2000).
191. N. Cermak *et al.*, Whole-organism behavioral profiling reveals a role for dopamine in state-dependent motor program coupling in. *Elife* **9**, (2020).
192. T. Hills, P. J. Brockie, A. V. Maricq, Dopamine and glutamate control area-restricted search behavior in Caenorhabditis elegans. *J Neurosci* **24**, 1217-1225 (2004).
193. K. S. Lee *et al.*, Serotonin-dependent kinetics of feeding bursts underlie a graded response to food availability in C. elegans. *Nat Commun* **8**, 14221 (2017).
194. Z. Li, J. Ichikawa, J. Dai, H. Y. Meltzer, Aripiprazole, a novel antipsychotic drug, preferentially increases dopamine release in the prefrontal cortex and hippocampus in rat brain. *Eur J Pharmacol* **493**, 75-83 (2004).
195. R. A. Bantick, M. H. De Vries, P. M. Grasby, The effect of a 5-HT1A receptor agonist on striatal dopamine release. *Synapse* **57**, 67-75 (2005).
196. D. Bang *et al.*, Sub-second Dopamine and Serotonin Signaling in Human Striatum during Perceptual Decision-Making. *Neuron*, (2020).
197. D. H. A. Fitch. (Wormbook, WormBook, ed. The C.elegans Research Community, 2005).
198. C. Frokjaer-Jensen *et al.*, Single-copy insertion of transgenes in Caenorhabditis elegans. *Nat Genet* **40**, 1375-1383 (2008).

199. L. A. Berkowitz, A. L. Knight, G. A. Caldwell, K. A. Caldwell, Generation of stable transgenic C. elegans using microinjection. *J Vis Exp*, (2008).
200. G. L. Sutphin, M. Kaeberlein, Measuring Caenorhabditis elegans life span on solid media. *J Vis Exp*, (2009).
201. K. Zarse, M. Ristow, Antidepressants of the serotonin-antagonist type increase body fat and decrease lifespan of adult Caenorhabditis elegans. *PLoS One* **3**, e4062 (2008).
202. N. J. Linford, C. Bilgir, J. Ro, S. D. Pletcher, Measurement of lifespan in Drosophila melanogaster. *J Vis Exp*, (2013).
203. B. Conti, Considerations on temperature, longevity and aging. *Cell Mol Life Sci* **65**, 1626-1630 (2008).
204. R. Hosono, Y. Mitsui, Y. Sato, S. Aizawa, J. Miwa, Life span of the wild and mutant nematode Caenorhabditis elegans. Effects of sex, sterilization, and temperature. *Exp Gerontol* **17**, 163-172 (1982).
205. J. Loeb, J. H. Northrop, Is There a Temperature Coefficient for the Duration of Life? *Proc Natl Acad Sci U S A* **2**, 456-457 (1916).
206. M. J. Lamb, Temperature and lifespan in Drosophila. *Nature* **220**, 808-809 (1968).
207. B. Zhang *et al.*, Environmental Temperature Differentially Modulates C. elegans Longevity through a Thermosensitive TRP Channel. *Cell Rep* **11**, 1414-1424 (2015).
208. S. F. Leiser, A. Begun, M. Kaeberlein, HIF-1 modulates longevity and healthspan in a temperature-dependent manner. *Aging Cell* **10**, 318-326 (2011).
209. M. Horikawa, S. Sural, A. L. Hsu, A. Antebi, Co-chaperone p23 regulates C. elegans Lifespan in Response to Temperature. *PLoS Genet* **11**, e1005023 (2015).
210. C. Y. Ewald, J. N. Landis, J. Porter Abate, C. T. Murphy, T. K. Blackwell, Dauer-independent insulin/IGF-1-signalling implicates collagen remodelling in longevity. *Nature* **519**, 97-101 (2015).
211. Y. C. Chen *et al.*, A C. elegans Thermosensory Circuit Regulates Longevity through crh-1/CREB-Dependent flp-6 Neuropeptide Signaling. *Dev Cell* **39**, 209-223 (2016).
212. K. Seo *et al.*, Heat shock factor 1 mediates the longevity conferred by inhibition of TOR and insulin/IGF-1 signaling pathways in C. elegans. *Aging Cell*, (2013).
213. S. F. Leiser *et al.*, Age-associated vulval integrity is an important marker of nematode healthspan. *Age* **38**, 419-431 (2016).
214. V. Singh, A. Aballay, Regulation of DAF-16-mediated Innate Immunity in Caenorhabditis elegans. *J Biol Chem* **284**, 35580-35587 (2009).
215. D. Garigan *et al.*, Genetic analysis of tissue aging in Caenorhabditis elegans: a role for heat-shock factor and bacterial proliferation. *Genetics* **161**, 1101-1112 (2002).
216. E. M. Fawcett, J. W. Horsman, D. L. Miller, Creating defined gaseous environments to study the effects of hypoxia on C. elegans. *J Vis Exp*, e4088 (2012).
217. G. L. Sutphin, E. Bishop, M. E. Yanos, R. M. Moller, M. Kaeberlein, Caffeine extends life span, improves healthspan, and delays age-associated pathology in Caenorhabditis elegans. *Longev Healthspan* **1**, 9 (2012).
218. T. Lenoir, E. Giannella, The emergence and diffusion of DNA microarray technology. *J Biomed Discov Collab* **1**, 11 (2006).
219. A. C. Epstein *et al.*, C. elegans EGL-9 and mammalian homologs define a family of dioxygenases that regulate HIF by prolyl hydroxylation. *Cell* **107**, 43-54 (2001).
220. S. K. Ramakrishnan, Y. M. Shah, Role of intestinal HIF-2α in health and disease. *Annual review of physiology* **78**, 301-325 (2016).
221. A. Pezzuto, E. Carico, Role of HIF-1 in cancer progression: Novel insights. A review. *Current molecular medicine* **18**, 343-351 (2018).
222. K. Balamurugan, HIF-1 at the crossroads of hypoxia, inflammation, and cancer. *International journal of cancer* **138**, 1058-1066 (2016).

223. M. E. Cockman *et al.*, Hypoxia inducible factor-α binding and ubiquitylation by the von Hippel-Lindau tumor suppressor protein. *Journal of Biological Chemistry* **275**, 25733-25741 (2000).
224. R. Mehta *et al.*, Proteasomal regulation of the hypoxic response modulates aging in C. elegans. *Science* **324**, 1196-1198 (2009).
225. Y. Zhang, Z. Shao, Z. Zhai, C. Shen, J. A. Powell-Coffman, The HIF-1 hypoxia-inducible factor modulates lifespan in C. elegans. *PloS one* **4**, (2009).
226. S. F. Leiser, M. Kaeberlein, The hypoxia-inducible factor HIF-1 functions as both a positive and negative modulator of aging. *Biological chemistry* **391**, 1131-1137 (2010).
227. R.-U. Müller *et al.*, The von Hippel Lindau tumor suppressor limits longevity. *Journal of the American Society of Nephrology* **20**, 2513-2517 (2009).
228. M. Treinin *et al.*, HIF-1 is required for heat acclimation in the nematode Caenorhabditis elegans. *Physiological genomics* **14**, 17-24 (2003).
229. H. Jiang, R. Guo, J. A. Powell-Coffman, The Caenorhabditis elegans hif-1 gene encodes a bHLH-PAS protein that is required for adaptation to hypoxia. *Proceedings of the National Academy of Sciences* **98**, 7916-7921 (2001).
230. D. K. Ma, R. Vozdek, N. Bhatla, H. R. Horvitz, CYSL-1 interacts with the O2-sensing hydroxylase EGL-9 to promote H2S-modulated hypoxia-induced behavioral plasticity in C. elegans. *Neuron* **73**, 925-940 (2012).
231. C. Shen, Z. Shao, J. A. Powell-Coffman, The Caenorhabditis elegans rhy-1 gene inhibits HIF-1 hypoxia-inducible factor activity in a negative feedback loop that does not include vhl-1. *Genetics* **174**, 1205-1214 (2006).
232. S. F. Leiser, A. Begun, M. Kaeberlein, HIF-1 modulates longevity and healthspan in a temperature-dependent manner. *Aging cell* **10**, 318-326 (2011).
233. H. Miller *et al.*, Genetic interaction with temperature is an important determinant of nematode longevity. *Aging cell* **16**, 1425-1429 (2017).
234. E. L. T. Di Chen, P. Kapahi, HIF-1 modulates dietary restriction-mediated lifespan extension via IRE-1 in Caenorhabditis elegans. *PLoS genetics* **5**, (2009).
235. C. Shen, D. Nettleton, M. Jiang, S. K. Kim, J. A. Powell-Coffman, Roles of the HIF-1 hypoxia-inducible factor during hypoxia response in Caenorhabditis elegans. *Journal of Biological Chemistry* **280**, 20580-20588 (2005).
236. Z. Shao, Y. Zhang, J. A. Powell-Coffman, Two distinct roles for EGL-9 in the regulation of HIF-1-mediated gene expression in Caenorhabditis elegans. *Genetics* **183**, 821-829 (2009).
237. L. G. Luhachack *et al.*, EGL-9 controls C. elegans host defense specificity through prolyl hydroxylation-dependent and-independent HIF-1 pathways. *PLoS pathogens* **8**, (2012).
238. Z. Shao, Y. Zhang, Q. Ye, J. N. Saldanha, J. A. Powell-Coffman, C. elegans SWAN-1 Binds to EGL-9 and regulates HIF-1-mediated resistance to the bacterial pathogen Pseudomonas aeruginosa PAO1. *PLoS pathogens* **6**, (2010).
239. J. W. Horsman, F. I. Heinis, D. L. Miller, A Novel Mechanism To Prevent H2S Toxicity in Caenorhabditis elegans. *Genetics* **213**, 481-490 (2019).
240. D. Angeles-Albores, C. P. Robinson, B. A. Williams, B. J. Wold, P. W. Sternberg, Reconstructing a metazoan genetic pathway with transcriptome-wide epistasis measurements. *Proceedings of the National Academy of Sciences* **115**, E2930-E2939 (2018).
241. N. L. Bray, H. Pimentel, P. Melsted, L. Pachter, Near-optimal probabilistic RNA-seq quantification. *Nature biotechnology* **34**, 525-527 (2016).
242. H. Pimentel, N. L. Bray, S. Puente, P. Melsted, L. Pachter, Differential analysis of RNA-seq incorporating quantification uncertainty. *Nature methods* **14**, 687 (2017).

243. C. T. Murphy *et al.*, Genes that act downstream of DAF-16 to influence the lifespan of Caenorhabditis elegans. *Nature* **424**, 277-283 (2003).
244. T. W. Harris *et al.*, WormBase: a comprehensive resource for nematode research. *Nucleic acids research* **38**, D463-D467 (2010).
245. C. Couillault *et al.*, TLR-independent control of innate immunity in Caenorhabditis elegans by the TIR domain adaptor protein TIR-1, an ortholog of human SARM. *Nature immunology* **5**, 488-494 (2004).
246. A. N. Nathoo, R. A. Moeller, B. A. Westlund, A. C. Hart, Identification of neuropeptide-like protein gene families in Caenorhabditis elegans and other species. *Proceedings of the National Academy of Sciences* **98**, 14000-14005 (2001).
247. E. K. Marsh, M. C. van den Berg, R. C. May, A two-gene balance regulates Salmonella typhimurium tolerance in the nematode Caenorhabditis elegans. *PloS one* **6**, (2011).
248. D. Ackerman, D. Gems, Insulin/IGF-1 and hypoxia signaling act in concert to regulate iron homeostasis in Caenorhabditis elegans. *PLoS genetics* **8**, (2012).
249. L. Romero-Afrima *et al.*, Ferritin is regulated by a neuro-intestinal axis in the nematode Caenorhabditis elegans. *Redox biology* **28**, 101359 (2020).
250. C. Trent, N. Tsung, H. R. Horvitz, Egg-laying defective mutants of the nematode Caenorhabditis elegans. *Genetics* **104**, 619-647 (1983).
251. C. Darby, C. L. Cosma, J. H. Thomas, C. Manoil, Lethal paralysis of Caenorhabditis elegans by Pseudomonas aeruginosa. *Proceedings of the National Academy of Sciences* **96**, 15202-15207 (1999).
252. E. C. Park *et al.*, Hypoxia regulates glutamate receptor trafficking through an HIF-independent mechanism. *The EMBO journal* **31**, 1379-1393 (2012).
253. C. Franceschi, J. Campisi, Chronic inflammation (inflammaging) and its potential contribution to age-associated diseases. *Journals of Gerontology Series A: Biomedical Sciences and Medical Sciences* **69**, S4-S9 (2014).
254. S. Libert, Y. Chao, X. Chu, S. D. Pletcher, Trade-offs between longevity and pathogen resistance in Drosophila melanogaster are mediated by NFκB signaling. *Aging cell* **5**, 533-543 (2006).
255. D. M. Ziegler, C. H. Mitchell, Microsomal oxidase. IV. Properties of a mixed-function amine oxidase isolated from pig liver microsomes. *Arch Biochem Biophys* **150**, 116-125 (1972).
256. S. Eswaramoorthy, J. B. Bonanno, S. K. Burley, S. Swaminathan, Mechanism of action of a flavin-containing monooxygenase. *Proc Natl Acad Sci U S A* **103**, 9832-9837 (2006).
257. M. Warrier *et al.*, The TMAO-Generating Enzyme Flavin Monooxygenase 3 Is a Central Regulator of Cholesterol Balance. *Cell Rep*, (2015).
258. B. J. Bennett *et al.*, Trimethylamine-N-oxide, a metabolite associated with atherosclerosis, exhibits complex genetic and dietary regulation. *Cell Metab* **17**, 49-60 (2013).
259. S. Veeravalli *et al.*, The phenotype of a flavin-containing monooyxgenase knockout mouse implicates the drug-metabolizing enzyme FMO1 as a novel regulator of energy balance. *Biochem Pharmacol* **90**, 88-95 (2014).
260. R. C. Schugar *et al.*, The TMAO-Producing Enzyme Flavin-Containing Monooxygenase 3 Regulates Obesity and the Beiging of White Adipose Tissue. *Cell Rep* **19**, 2451-2461 (2017).
261. C. F. Bennett *et al.*, Transaldolase inhibition impairs mitochondrial respiration and induces a starvation-like longevity response in Caenorhabditis elegans. *PLoS Genet* **13**, e1006695 (2017).

262. D. D. Shaye, I. Greenwald, OrthoList: a compendium of C. elegans genes with human orthologs. *PLoS One* **6**, e20085 (2011).
263. G. M. Gibbs, K. Roelants, M. K. O'Bryan, The CAP superfamily: cysteine-rich secretory proteins, antigen 5, and pathogenesis-related 1 proteins--roles in reproduction, cancer, and immune defense. *Endocr Rev* **29**, 865-897 (2008).
264. G. M. Gibbs, M. K. O'Bryan, Cysteine rich secretory proteins in reproduction and venom. *Soc Reprod Fertil Suppl* **65**, 261-267 (2007).
265. J. R. Reeves *et al.*, Identification, purification and characterization of a novel human blood protein with binding affinity for prostate secretory protein of 94 amino acids. *Biochem J* **385**, 105-114 (2005).
266. J. R. Reeves, H. Dulude, C. Panchal, L. Daigneault, D. M. Ramnani, Prognostic value of prostate secretory protein of 94 amino acids and its binding protein after radical prostatectomy. *Clin Cancer Res* **12**, 6018-6022 (2006).
267. J. Krätzschmar *et al.*, The human cysteine-rich secretory protein (CRISP) family. Primary structure and tissue distribution of CRISP-1, CRISP-2 and CRISP-3. *Eur J Biochem* **236**, 827-836 (1996).
268. H. Friess *et al.*, Identification of disease-specific genes in chronic pancreatitis using DNA array technology. *Ann Surg* **234**, 769-778; discussion 778-769 (2001).
269. Q. Liao *et al.*, Preferential expression of cystein-rich secretory protein-3 (CRISP-3) in chronic pancreatitis. *Histol Histopathol* **18**, 425-433 (2003).
270. R. J. Frost, S. Engelhardt, A secretion trap screen in yeast identifies protease inhibitor 16 as a novel antihypertrophic protein secreted from the heart. *Circulation* **116**, 1768-1775 (2007).
271. T. Ernst *et al.*, Decrease and gain of gene expression are equally discriminatory markers for prostate carcinoma: a gene expression analysis on total and microdissected prostate tissue. *Am J Pathol* **160**, 2169-2180 (2002).
272. A. Dereeper *et al.*, Phylogeny.fr: robust phylogenetic analysis for the non-specialist. *Nucleic Acids Res* **36**, W465-469 (2008).
273. H. D. Wang, P. Kazemi-Esfarjani, S. Benzer, Multiple-stress analysis for isolation of Drosophila longevity genes. *Proc Natl Acad Sci U S A* **101**, 12610-12615 (2004).
274. G. J. Lithgow, G. A. Walker, Stress resistance as a determinate of C. elegans lifespan. *Mech Ageing Dev* **123**, 765-771 (2002).
275. S. Magadum, U. Banerjee, P. Murugan, D. Gangapur, R. Ravikesavan, Gene duplication as a major force in evolution. *J Genet* **92**, 155-161 (2013).
276. N. Copes *et al.*, Metabolome and proteome changes with aging in Caenorhabditis elegans. *Exp Gerontol* **72**, 67-84 (2015).
277. B. Hamilton *et al.*, A systematic RNAi screen for longevity genes in C. elegans. *Genes Dev* **19**, 1544-1555 (2005).
278. S. Ookuma, M. Fukuda, E. Nishida, Identification of a DAF-16 transcriptional target gene, scl-1, that regulates longevity and stress resistance in Caenorhabditis elegans. *Curr Biol* **13**, 427-431 (2003).
279. D. J. Dues *et al.*, Uncoupling of oxidative stress resistance and lifespan in long-lived isp-1 mitochondrial mutants in Caenorhabditis elegans. *Free Radic Biol Med* **108**, 362-373 (2017).
280. D. J. Dues, E. K. Andrews, M. M. Senchuk, J. M. Van Raamsdonk, Resistance to Stress Can Be Experimentally Dissociated From Longevity. *J Gerontol A Biol Sci Med Sci* **74**, 1206-1214 (2019).
281. T. N. Petersen, S. Brunak, G. von Heijne, H. Nielsen, SignalP 4.0: discriminating signal peptides from transmembrane regions. *Nat Methods* **8**, 785-786 (2011).

282. L. M. Margolis *et al.*, Prolonged Calorie Restriction Downregulates Skeletal Muscle mTORC1 Signaling Independent of Dietary Protein Intake and Associated microRNA Expression. *Front Physiol* **7**, 445 (2016).
283. M. Visscher *et al.*, Proteome-wide Changes in Protein Turnover Rates in C. elegans Models of Longevity and Age-Related Disease. *Cell Rep* **16**, 3041-3051 (2016).
284. K. Shimizu, K. Ashida, K. Hotta, K. Oka, Food deprivation changes chemotaxis behavior in. *Biophys Physicobiol* **16**, 167-172 (2019).
285. C. I. Nussbaum-Krammer, M. F. Neto, R. M. Brielmann, J. S. Pedersen, R. I. Morimoto, Investigating the spreading and toxicity of prion-like proteins using the metazoan model organism C. elegans. *J Vis Exp*, 52321 (2015).
286. S. I. Oh, S. K. Park, N-acetyl-l-cysteine mimics the effect of dietary restriction on lifespan and reduces amyloid beta-induced toxicity in. *Food Sci Biotechnol* **26**, 783-790 (2017).
287. M. Kim, D. Knoefler, E. Quarles, U. Jakob, D. Bazopoulou, Automated phenotyping and lifespan assessment of a. *Transl Med Aging* **4**, 38-44 (2020).
288. G. McColl *et al.*, Utility of an improved model of amyloid-beta ($A\beta_{1-42}$) toxicity in Caenorhabditis elegans for drug screening for Alzheimer's disease. *Mol Neurodegener* **7**, 57 (2012).
289. J. Cao *et al.*, Comprehensive single-cell transcriptional profiling of a multicellular organism. *Science* **357**, 661-667 (2017).
290. A. Singhvi, S. Shaham, Glia-Neuron Interactions in. *Annu Rev Neurosci* **42**, 149-168 (2019).
291. M. B. Gerstein *et al.*, Integrative analysis of the Caenorhabditis elegans genome by the modENCODE project. *Science* **330**, 1775-1787 (2010).
292. J. M. Maglich *et al.*, Comparison of complete nuclear receptor sets from the human, Caenorhabditis elegans and Drosophila genomes. *Genome Biol* **2**, RESEARCH0029 (2001).
293. A. E. Sluder, S. W. Mathews, D. Hough, V. P. Yin, C. V. Maina, The nuclear receptor superfamily has undergone extensive proliferation and diversification in nematodes. *Genome Res* **9**, 103-120 (1999).
294. J. Yuan, R. S. Tirabassi, A. B. Bush, M. D. Cole, The C. elegans MDL-1 and MXL-1 proteins can functionally substitute for vertebrate MAD and MAX. *Oncogene* **17**, 1109-1118 (1998).
295. A. Folick *et al.*, Aging. Lysosomal signaling molecules regulate longevity in Caenorhabditis elegans. *Science* **347**, 83-86 (2015).
296. M. Riesen *et al.*, MDL-1, a growth- and tumor-suppressor, slows aging and prevents germline hyperplasia and hypertrophy in C. elegans. *Aging (Albany NY)* **6**, 98-117 (2014).
297. M. R. Van Gilst, H. Hadjivassiliou, A. Jolly, K. R. Yamamoto, Nuclear hormone receptor NHR-49 controls fat consumption and fatty acid composition in C. elegans. *PLoS Biol* **3**, e53 (2005).